A Geostatistical Study of the Uranium Deposit at Kvanefjeld, The Ilimaussaq Intrusion, South Greenland

Lund Clausen, Flemming

Publication date:
1982

Document Version
Publisher's PDF, also known as Version of record

Risø-R-468

RISØ

Risø-R-468

A Geostatistical Study of the Uranium Deposit at Kvanefjeld, The Ilímaussaq Intrusion, South Greenland

Flemming Lund Clausen

Risø National Laboratory, DK-4000 Roskilde, Denmark

RISØ-R-468

A GEOSTATISTICAL STUDY OF THE URANIUM DEPOSIT AT KVANEFJELD, THE ILÍMAUSSAQ INTRUSION, SOUTH GREENLAND

Flemming Lund Clausen
Department of Mineral Industry, Technical University of Denmark

Abstract. The uranium deposit at Kvanefjeld within the Ilímaussaq intrusion in South Greenland has been tested by 70 diamond drill holes. In total 5658 drill core samples were selected and analysed by various methods. A data base containing all the analytical data, geological information and characteristic drill hole parameters was constructed.

Based on different types of spatially distributed samples the uranium variation within the deposit was studied. The spatial variation, which comprises a large random component, was modelled, and the intrinsic function was used to establish grade-tonnage curves by the best linear unbiased estimator of geostatistics (kriging).

From data obtained by a ground surface gamma-spectrometric survey it is shown that the uranium variation is possibly subject to a spatial anisotropy consistent with the geology. It is also shown that, although anisotropy exists, the uranium variation has a second-order stationarity.

(Continue on next page)

May 1982
Risø National Laboratory, DK 4000 Roskilde, Denmark

A global estimation of the total reserves shows that single block grade values are always estimated with high errors. This is mainly caused by the poor spatial structure and the very sparse sampling pattern. The best way to solve this problem appears to be a selective type of kriging. The overall uranium reserves are estimated as approx. 23600 tons with a mean grade of 297 ppm using a cutoff grade of 250 ppm U. The effect of using different block sizes/bench heights is studied.

Studies of data from the Kvanefjeld tunnel show that local geostatistical estimation can be done with acceptably small errors provided that a close sampling pattern is used. Geostatistics is therefore regarded as a useful tool for the estimation of this deposit. A regression relationship is established to correct field gamma-spectrometric measures of bulk grades towards truer values.

Multivariate cluster and discriminant analyses were used to classify lujavrite samples based on their trace element content. A number of mis-labelled samples were discovered. Misclassification is due to a possibly continuous transition between naujakasite lyjavrite and arfvedsonite lujavrite which was not recognized by the geologists. Some of the main mineralogical differences between the geolcgical units are identified by the discriminating effect of the individual variable.

INIS descriptors: URANIUM ORES; RESERVES; GEOLOGICAL DEPOSITS; GREENLAND; STATISTICAL MODELS; SPATIAL DISTRIBUTION; DATA ACQUISITION SYSTEMS; DRILL CORES; SAMPLING; EXPLORATION.

UDC 553.495(988)

ISBN 87-550-0846-1
ISSN 0106-2840

Risø Repro 1982

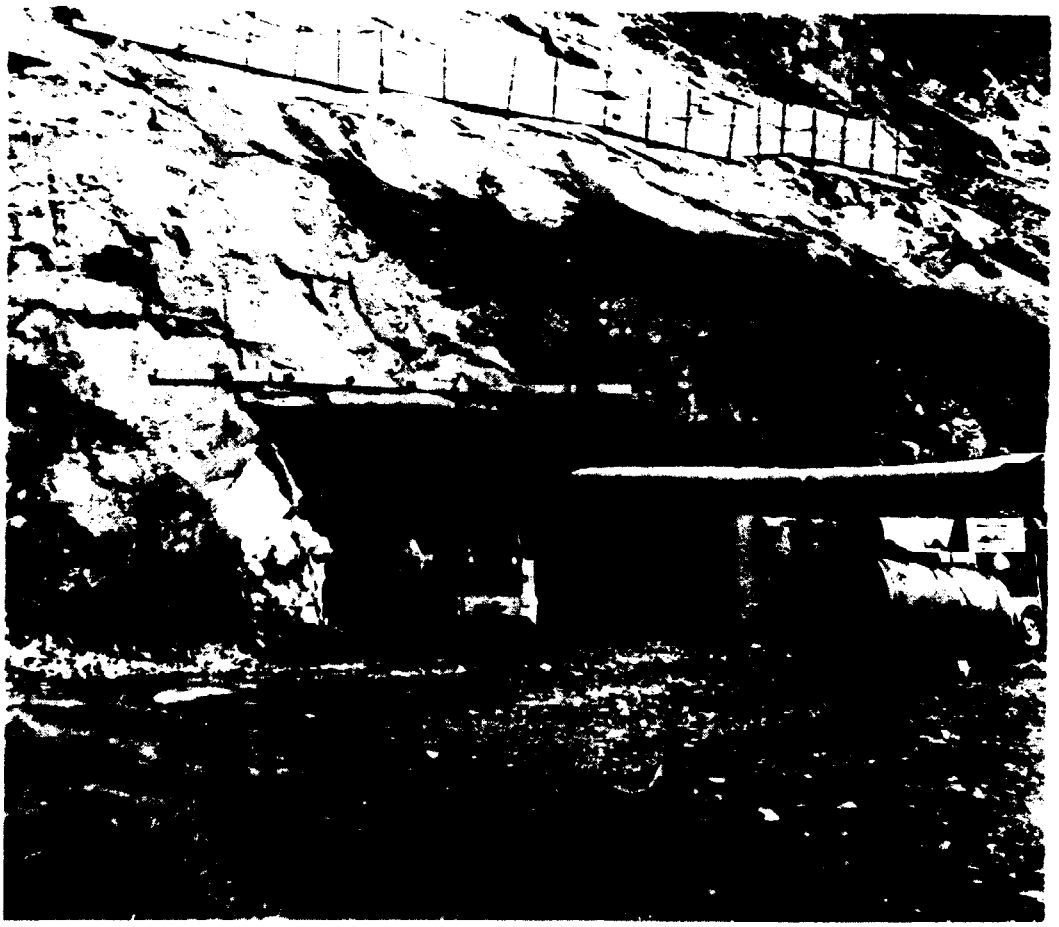

Entrance of the Kvanefjeld tunnel.
(Photo: P. Nyegaard)

The present thesis has been submitted in partial fulfilment of the requirements for the degree of Licentiatus Technices in Department of Mineral Industry, The Technical University of Denmark.

TABLE OF CONTENTS

1 INTRODUCTION

This thesis represents the documentation of a PhD project initiated in the summer of 1978 following a proposal made by the Geological Survey of Greenland. At that time the primary aims of the project were to 1) collect the existing analytical, geological and geographical data from the drilling campaign at Kvanefjeld and organize these on a structured data base, 2) study the uranium and thorium mineralisations by means of the 'Theory of Regionalised Variables' - also known as 'Geostatistics', 3) make global geostatistical ore reserve calculations of uranium and 4) make geostatistical ore reserve estimations of other (economic) elements present in the deposit.

After the completion of items 1, 2 and 3 it became obvious that the geostatistical estimation of elements other than uranium and thorium could not be possible without new information, mainly because of the complex structure of the deposit and the low number of analyses for these elements. It was therefore decided to concentrate further on the uranium values. Justifiable (conventional) reserve estimates of Zr, Nb, Zn, Pb, Y, La, Ce, Nd, Sm, Li, Ga, Rb and F are found in Nyegaard (1979). As shall be demonstrated it appeared that due to the high correlation between U and Th, thorium behaves spatially in the same way as uranium. Th can therefore be estimated using the techniques described in this thesis. During the project period plans for a pilot plant to test a new extraction technique, the Carbonate Pressure Leaching (CPL) process, were elaborated at the National Laboratory RISØ. In order to obtain approx. 5000 tons of ore for this plant a test adit (known as the Kvanefjeld tunnel) was driven through the mineralisation. Based on the geostatistical results from the drill hole information a chip sampling programme within the tunnel was designed by the author. Furthermore, it was decided that the data from the tunnel should be included in the present study.

The Kvanefjeld uranium deposit is a magmatic (syngenetic) porphyritic mineralisation formed at the latest stages of an alkaline intrusion. Although the deposit's genesis is considerably different from the more well-known sedimentary uranium deposits, the spatial variation of the uranium shows remarkable similarities to structures discovered in other types of uranium occurrences, such as roll front deposits. However, the present study is the first attempt to apply geostatistics to this type of mineralisation. Due to the complex nature of the deposit geological prediction is difficult. The work presented in this thesis includes the mathematical models established in order to make prediction possible, and the methods to quantify the confidence of prediction - provided the geology is reflected in the uranium values.

1.1 Why geostatistics?

The name 'geostatistics' was given to the application of the 'Theory of Regionalized Variables' (Matheron, 1971) to problems in geology and mining. While its most common applications have been to solving ore reserve estimation problems it has also found use in other areas such as forestry (Poissonnet et al., 1970), meteorology (Delhomme and Delfiner, 1973) and contour mapping (Royle et al., 1981). Czubek (pers.comm.) has used the theory for the calibration of nuclear well-logs.

The application of statistical methods to ore-reserve problems was first attempted some 30 years ago in South Africa. Studies by e.g. Krige (1951), DeWijs (1972) and Sichel (1966), have made significant contributions to the current art of ore reserve estimation. In the United States and Canada much effort has been put into the field of Trend Surface Analysis (Agterberg, 1968). However, the method developed by Matheron has special appeal to geologists and mining engineers for several reasons. One is that it is the only method that explicitly takes into account the spatial correlation between the samples. Another is that it makes better use of the available data and provides confidence limits for the estimates.

Let us briefly review what ore reserve estimation is about. Consider the three dimensional situation in figure 1-1, where the mean grade of the block A is to be estimated from a set of samples in and around it (g_i). What all estimation methods tend to do, both the conventional (such as the polygonal, inverse distance weighting and the method of triangles) and the geostatistical, is to form an estimator which is a linear combination of the sample values. The estimators differ in the way the samples are weighted. This is usually a function of the distance of the sample from the centre of the block. The problems are: which combination of sample weights is optimal and when does sampling cease? Or, in other words, how many samples are needed to estimate the block and where should they be located?

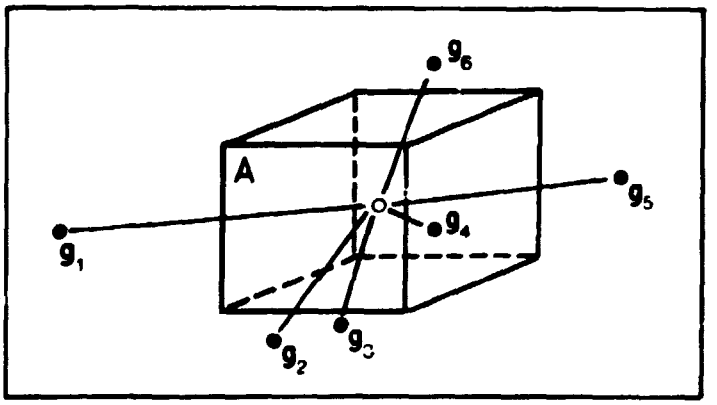

FIGURE 1-1: The general prediction problem in ore reserve estimation. The block A is to be estimated from the samples g_i.

The theory of regionalized variables was developed to solve these problems. By establishing the spatial correlation between grade values (or any other regionalized variable) it is possible to estimate the block grade with minimum standard error, by taking only the relevant samples into account. Furthermore, geostatistics considers the fact that grade values might be on different supports of samples and that the estimation of a large block presents a different problem from the estimation of a small one. During estimation the geostatistical estimator,

known as kriging, considers not only the relation between the samples and the block, but also the relation between the samples themselves. In this way clusters of samples are not over-weighted. Kriging finds the optimal combination of sample weights during minimisation of the estimation error. There is no reason to believe that a porphyry copper deposit should be evaluated in the same way as a vein-type scheelite occurrence. It is therefore emphasised that kriging is totally dependent on the spatial structure (correlation) of the phenomenon studied.

Other advantages of geostatistics are that sampling (drilling) and valuation programs can be designed economically and geostatistics can help to optimize sampling patterns. Grade-control problems are amenable to geostatistical treatment because the number of working stopes needed to keep mill-feed grade fluctuations within predetermined limits can be easily determined. The unbiased nature of geostatistical estimation is of prime importance for the control of valuation and mining operations. It does not create compensating errors that mask other deficiencies in ore estimation, mining and milling.

1.2 Exploration history

It is hoped that the work presented in this thesis may contribute to a better understanding of the Kvanefjeld mineralisation and to decisions about possible future mining operations. On the other hand, this study is only a small part of the overall exploration of the Kvanefjeld deposit.

The exploration history of the Kvanefjeld uranium deposit dates back to the middle fifties; during the subsequent 25 years the deposit has been investigated with varying intensity. An excellent presentation of the exploration history is found in Nielsen (1980), from which the following is taken. A more general resume is found in Nielsen (1977).

The Kvanefjeld uranium deposit was discovered in 1956 one year after a regional exploration programme for uranium was initiated within the Ilimaussaq intrusion. Since then the exploration of the deposit has comprised geological methods, mineralogical, geochemical and leaching studies, geophysical surveys (mainly radiometric investigations), drilling, borehole logging and minor bulk mining projects. Main exploration programmes are listed in Table 1-1.

Numerous people have contributed to the geological as well as the mineralogical/geochemical understanding of the Kvanefjeld area. Detailed geological mapping was initiated in 1964 (1:2000) and the results were published by Sørensen et al.

TABEL 1-1: Sequence of events in the exploration of the Kvanefjeld uranium deposit. From Nielsen (1980).

Year	Exploration activity
1955-1956	Regional radiometric exploration within the Ilímaussaq intrusion. The Kvanefjeld uranium deposit is discovered.
1957	Field radiometric survey.
1958	First core drilling programme in the Kvanefjeld Mine area. Total core length 3728 metres.
1958-1961	Regional mapping of the Ilímaussaq intrusion (1:20.000). Laboratory tests on uranium extraction.
1962	Test mining of 180 tons of ore and deepening of the 1958 drill holes.
1964-1967	Detailed geological mapping of Kvanefjeld (1:2000). Continuous metallurgical tests.
1969	Third core drilling programme in the Mine area. Total core length 1621 metres.
1970-1976	Metallurgical work and feasibility studies. Environmental study on the geochemistry in the Ilímaussaq area.
1977	Fourth drilling programme. Total core length 5103 metres. Extensive field gamma-spectrometric survey on a 10 by 10 metre grid. Drill hole logging. Small pilot plant for extraction study (sulphatising roasting).
1978-1981	New extraction technique applied (carbonate pressure leaching). The Kvanefjeld tunnel opened for the mining of 5000 tons of ore for new pilot plant. Further environmental studies.

(1969). After the completion of this map only limited geological field work was carried out except for the guidance of the drilling projects. A brief geological description of the area with relevant references is given in the following chapter. Field radiometric surveys have played an important role in the investigation of the deposit. The first radiometric survey carried out in 1955-1956 led to the discovery of the deposit. Later, in 1957, a survey based on geiger readings on 50 metre and 5 metre grids formed the basis of the first drilling programme. Since 1957 several field programmes based on gamma-ray spectrometry have been completed (Løvborg et al., 1968, 1971, Nyegaard et al., 1977). The data from the extensive survey performed in 1977 on a 10 by 10 metre grid in the norther part of the area ('the Plateau') are investigated in the present study.

The drilling campaign at Kvanefjeld comprises four programmes carried out in 1958, 1962, 1969 and 1977. The result of all the diamond drilling programmes was 70 holes with a total core length of 10730 metres (table 1-2). The locations of drill holes can be seen in Plate I. Among these holes 4 were drilled at the adjacent Steenstrup fjeld area. Most of the 70 holes, all drilled from the surface, are vertical and only a few are inclined with varying dips. A full listing of azimuth, dip and other drill hole parameters is found in appendix E.

It can be seen from table 1-2 that drilling falls into three main groups: the Mine area, the Northern area and the Steenstrup fjeld area. Another five holes (34, 35, 36, 38 and 41) are located outside these areas, but since no analytical data are available from them they will not be considered in this study. The Mine area and the Northern area are indicated on Plate I as well (see also fig. 2-4). All holes located in the Northern area, except 45 and 47, were logged gamma-spectrometrically. The drill core samples have been intensely analysed as described in chapter 3.

Ore processing studies have been concentrated on two different leaching methods which, due to the complexity of the ore, differ substantially from the classical techniques of acid

TABLE 1-2: Available core drilling at Kvanefjeld and Steenstrup fjeld. Based on data from Sørensen et al. (1971), Nyegaard et al. (1977) and Nielsen (1980).

Area	No.of holes	Core length	Hole numbers
Mine area	36	4670	1-33, 37, 42, 43
Northern area	25	4608	39, 40, 45-50, 54-70
Steenstrup fjeld	4	855	44, 51-53
Kvanefjeld outside Northern and Mine areas	5	597	34-36, 38, 41
Total	70	10730	

leaching and carbonate leaching. For a long period of time, about 15 years, a sulphatising roast was the most effective extraction technique. The recovery of uranium by this method was 40 to 70% depending of the type of mineralised rock (Asmund, 1971, Gamborg-Hansen, 1977). It was the mining of a bulk ore sample of 180 tons for the purpose of testing this technique which gave the name 'Mine area' to the southern part of the Kvanefjeld area. After 1978 a new process, the CPL process, was developed and the recovery is at present of the order of 70 to 90% uranium. A 960 metre test adit, the Kvanefjeld tunnel, was driven through the orebody in order to provide 5000 tons of ground for a pilot plant based on the CPL-method. Data from this tunnel are included in the study.

1.3 Previous grade/tonnage calculations at Kvanefjeld

The uranium tonnage and mean grade of the Kvanefjeld ore have been estimated by conventional (i.e. non-statistical) methods. A preliminary geostatistical study has also been carried out.

In the Mine area estimation was performed in a triangular block pattern where the sample values at the triangle corners were

averaged to form the block value (Sørensen et al., 1974). The reasonably-assured resources obtained by this method included 5670 tons of uranium with a mean grade of 339 ppm U. A cutoff value at 300 ppm U was used and the total ore tonnage was approx. 16.7 million tons. Geostatistical estimation carried out at the Royal School of Mines gave the following figures: 7353 tons of uranium in approx. 21.5 million tons of ore. The mean grade above a 300 ppm cutoff value was estimated at 342 ppm U (Pryor Report, 1974).

In the Northern area three conventional estimates are available. Based on accumulations of one-metre thick horizontal ore slices (approx. 140x140 metres), allocated grade values equal to the assay value of the intersecting drill core sample, the uranium tonnage was estimated at 21413(16447) tons at a cutoff of 250(300) ppm U. Mean grade was estimated at 346(375) ppm and the total amount of ore was estimated at approx. 43.3 million tons (Nyegaard et al., 1977). Another estimate, also based on the assay data but using accumulations of minimum five-metre thick ore slices, gave a uranium tonnage of 22219 tons with a mean grade of 338 ppm using a cutoff at 250 ppm. Only samples inside each block were used to calculate the block means (Nyegaard, 1979).

The third estimate of the resources in the Northern area was based on the drill hole logging data. When the logging results were calibrated in each hole by individual constants the grade and tonnage calculations resulted in a 10% increase of the uranium tonnage to 22757 tons with a mean grade at 354 ppm U (cutoff 250 ppm). Here also estimation was performed by accumulations of one-metre thick ore slices (Løvborg et al., 1980).

1.4 Structure of the thesis

The work presented in this thesis is regarded as a study of the application of some advanced statistical methods to the different data collected from the Kvanefjeld deposit. The statistical theory is presented as it was used, rather than in a single theoretical chapter. In all cases final results are discussed

instead of rigorous mathematical derivations. It is felt that a full introduction to geostatistics is outside the scope of this thesis, as such are available elsewhere. Many introductory works and application papers are given in the list of references or can be found in the useful bibliographies of Pauncz (1978), Alldredge and Alldredge (1978) and Bell and Reeves (1979).

The next part of the thesis contains seven chapters of which the first two are of a descriptive character. The following four chapters contain results and discussions whereas the last chapter summarises the conclusions. In chapter 2 the geology of the investigated area is briefly reviewed. Chapter 3 gives a detailed description of the data used in the study, the different coordinate systems and the drill core database which was established. Chapter 4 describes the geostatistical work on the uranium values from the drill holes. Since the Kvanefjeld area can be divided into two main areas (the Mine area and the Northern area, see Plate I) based on geography, differences in sample density (i.e. drill hole spacing), sampling methods, analytical method and, as shall be shown, also on differences in the spatial correlation, results are presented accordingly (sections 4.2 and 4.3). A third section of chapter 4 contains the results from the geostatistical treatment of the logging data. In chapter 4 emphasis is put on the grade/tonnage calculations but more academic studies, such as the stability of the experimental semi-variogram, testing of Krige's relationship, test of semi-variogram model and effects of the scale of estimation are presented.

The uranium and to some extent the thorium values from samples taken in the Kvanefjeld tunnel are considered in chapter 5. The main object is to make a comparative study of different conventional and geostatistical methods in order to determine the mean grade in the bulk samples selected for the pilot plant. The tunnel data are not used in the estimation of the global reserves. In chapter 6 the uranium values from the field gamma-spectrometric survey are examined. Second-order stationarity, one of the basic assumptions of geostatistics, is studied by a

non-stationary estimation method and the horizontal spatial variation is investigated for isotropic/anisotropic conditions. The data are mapped by an automatic contouring method.

Finally, in chapter 7, multivariate statistical analyses are used to classify selected lujavrite samples from drill holes. Different classifying methods are discussed and the importance of the individual elements in discrimination is studied.

It is noted that, due to the spatial distribution of the samples, the results in chapter 4 (drill hole calculations) are based on models for the vertical spatial variation whereas the results in chapter 5 and 6 are based on horizontal models. As will be noted in chapter 8 these features can hardly be linked together into a single three-dimensional model. Despite this fact three-dimensional estimation was performed assuming that isotropical conditions exist although this is probably not true. However, this assumption is necessary because of the lack of data.

The mathematical symbols used in the text are listed and explained in appendix D. Most of the computer programs used are written in standard FORTRAN. Exceptions are those concerning data handling (sorting, storing and merging of data sets etc.) and database creation, for which the Statistical Analysis System is used (appendix A).

2 GEOLOGY OF THE INVESTIGATED AREA.

2.1 Introduction

The magmatic U/Th mineralisation in the Kvanefjeld area is part of the Ilimaussaq alkaline complex (fig. 2-1). This complex belongs to the Precambrian Gardar igneous province of South Greenland (Emeleus and Upton, 1976).

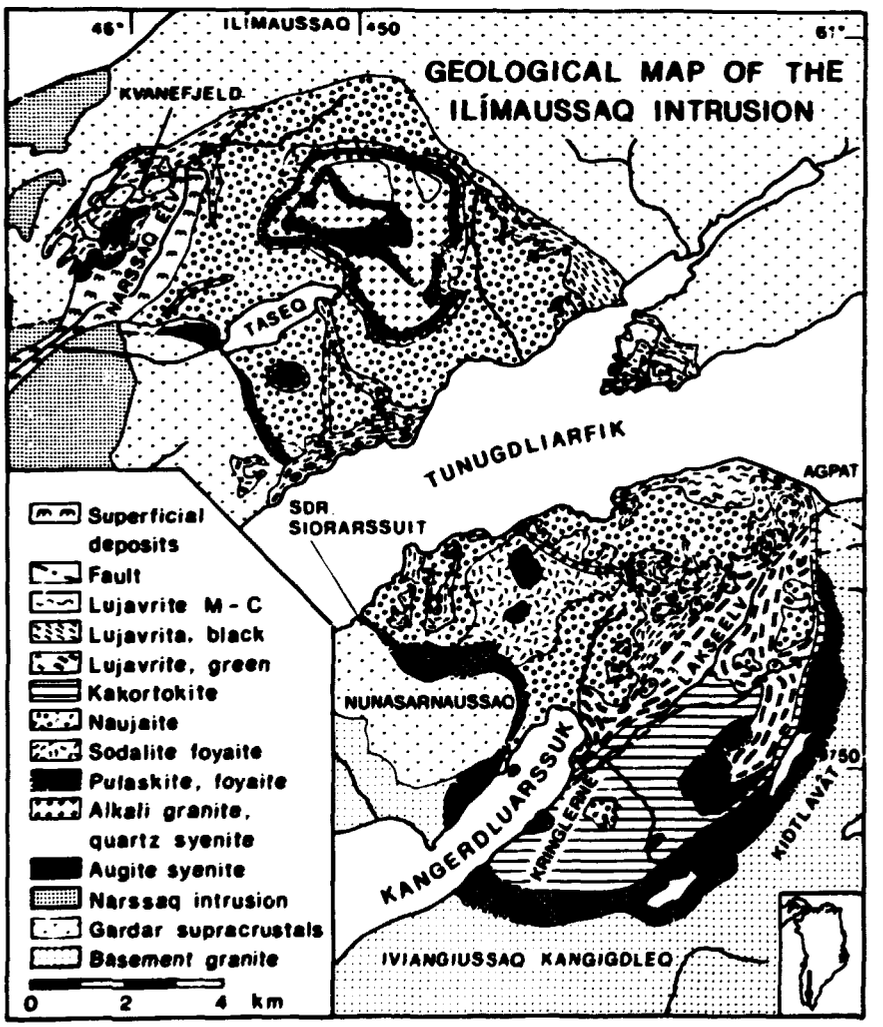

FIGURE 2-1: Simplified geological map of the Ilímaussaq intrusive complex. After Ferguson (1964).

The Gardar province is a cratogenic rift province with similarities to the East African rift system and the Oslo igneous province (Sørensen, 1966). It consists of SW-NE dyke swarms and central intrusions emplaced into a basement granite of the Ketilidian mobile belt and an overlying series of continental sandstones interlayered with basaltic lavas and sills. The province contains a great variety of alkalic volcanic and plutonic igneous rocks. The transitional alkaline basalts of the province show fractionation trends towards both Si-rich rocks such as comendites and alkali granites and Si-poor rocks such as phonolites and nepheline syenites. The U/Th mineralisation is associated with the extreme differentials of the Si-undersaturated trend.

2.2 Geology of the Ilimaussaq intrusion (summary)

The geological and petrological evolution of the Ilimaussaq intrusion is discussed by Ussing (1912), Sørensen (1958, 1962, 1970, 1978), Hamilton (1964), Ferguson (1964, 1970a, 1970b) and Engell (1973). The following summary is mainly taken from Nyegaard (1979).

The intrusion (fig. 2-1) which covers about 156 km^2 was emplaced at 1168 +/- 2[illegible] m.y. (Blaxland et al., 1976). The intrusion is situated in the eastern part of the province and is the youngest of several plutonic centres in that area (fig. 2-2). The position of the intrusion seems related to the intersection of major ESE and ENE faults. The oval shape of the intrusion and the steeply faulted margins suggest that the intrusion was largely emplaced by block subsidence. Locally in the roof zone there are signs of piecemeal stoping. The intrusion is believed to have been emplaced in several pulses. At least three phases can be distinguished: 1) an augite syenite forming a discontinuous margin around and at the top of the intrusion. 2) a small unit of quartz syenite and alkali granite, which also occurs at the top of the intrusion, and 3) a

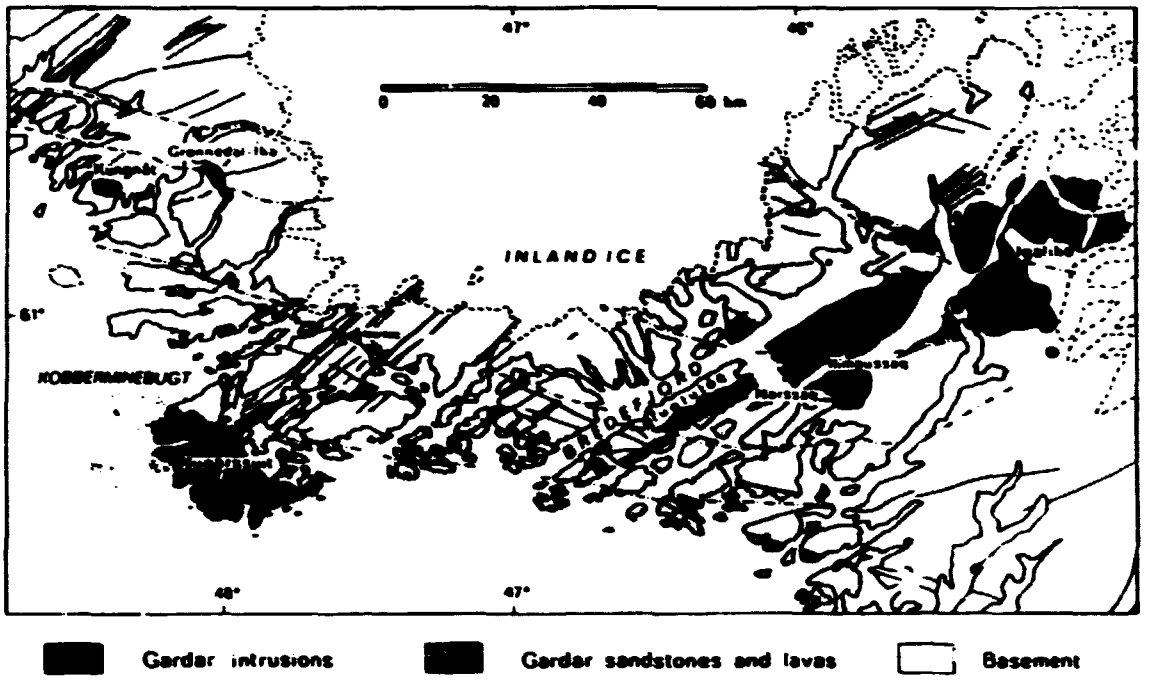

FIGURE 2-2: Sketch map of part of South Greenland showing the main intrusions and dyke swarms in the Gardar igneous province. (After Watt, 1966).

layered sequence of nepheline syenites which shows differentiation along an agpaitic trend.

The layered sequence consists of pulaskite, foyaite, sodalite foyaite, naujaite, kakortokite and lujavrites. The sequence from pulaskite to naujaite crystallized downwards from the roof. The kakortokites were formed by bottom accumulation (fig 2-3). Upwards the kakortokite changes into lujavrites (Bohse et al., 1971). The lujavrites represent the end product of an agpaitic magma. From its position between the kakortokite and the naujaite the lujavritic magma intruded and brecciated the overlaying syenite, as well as the surrounding country rock, as repeated injections at short intervals accompanied by hydrothermal veins. The U/Th-mineralizations at Kvanefjeld are related to such intrusive lujavrites.

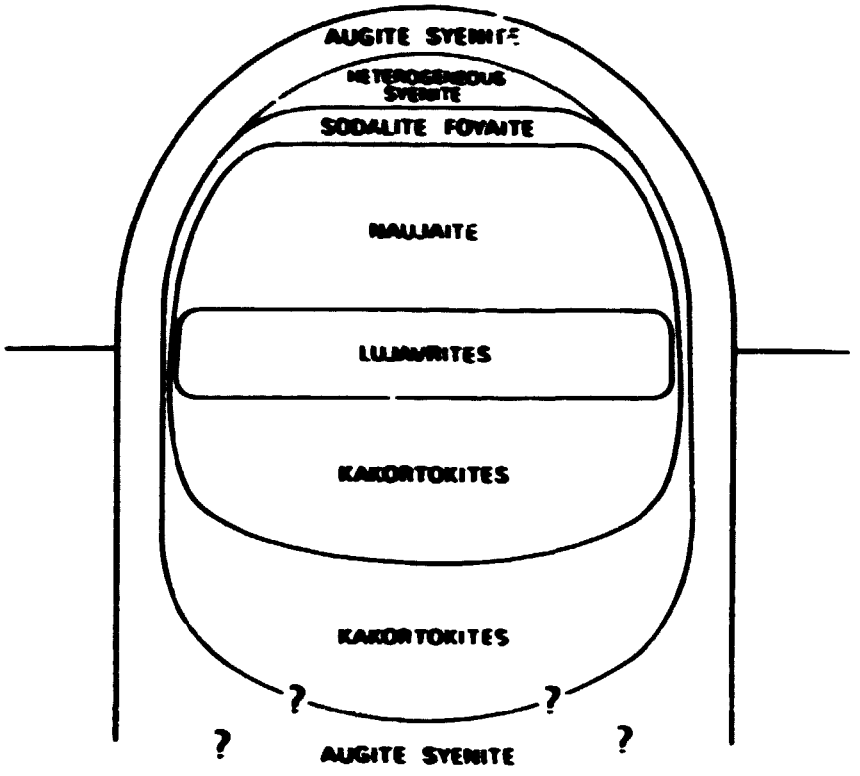

FIGURE 2-3: Schematic representation of the evolution of the Ilimaussaq intrusion. (After Ferguson, 1964).

2.3 Geology of the Kvanefjeld area (summary)

General descriptions of the geology and evolution of the Kvanefjeld area are found in Sørensen et al. (1969), Sørensen et al. (1971), Sørensen et al. (1974) and Nielsen and Steenfelt (1979).

The Kvanefjeld area is situated at the northwestern contact of the Ilimaussaq intrusion (fig. 2-1). A simplified geological map is given in fig. 2-4. It forms a 2.5 km^2 hilly plateau at an elevation of 500-700 metres. The area is a megabreccia in which various types of volcanic and sedimentary rocks, together with rocks from early phases of the intrusion, form blocks and sheets within the later in rusive lujavrite. It is bounded to the north by the volcanic rocks of the roof, consisting of lava, dykes and sills together with minor

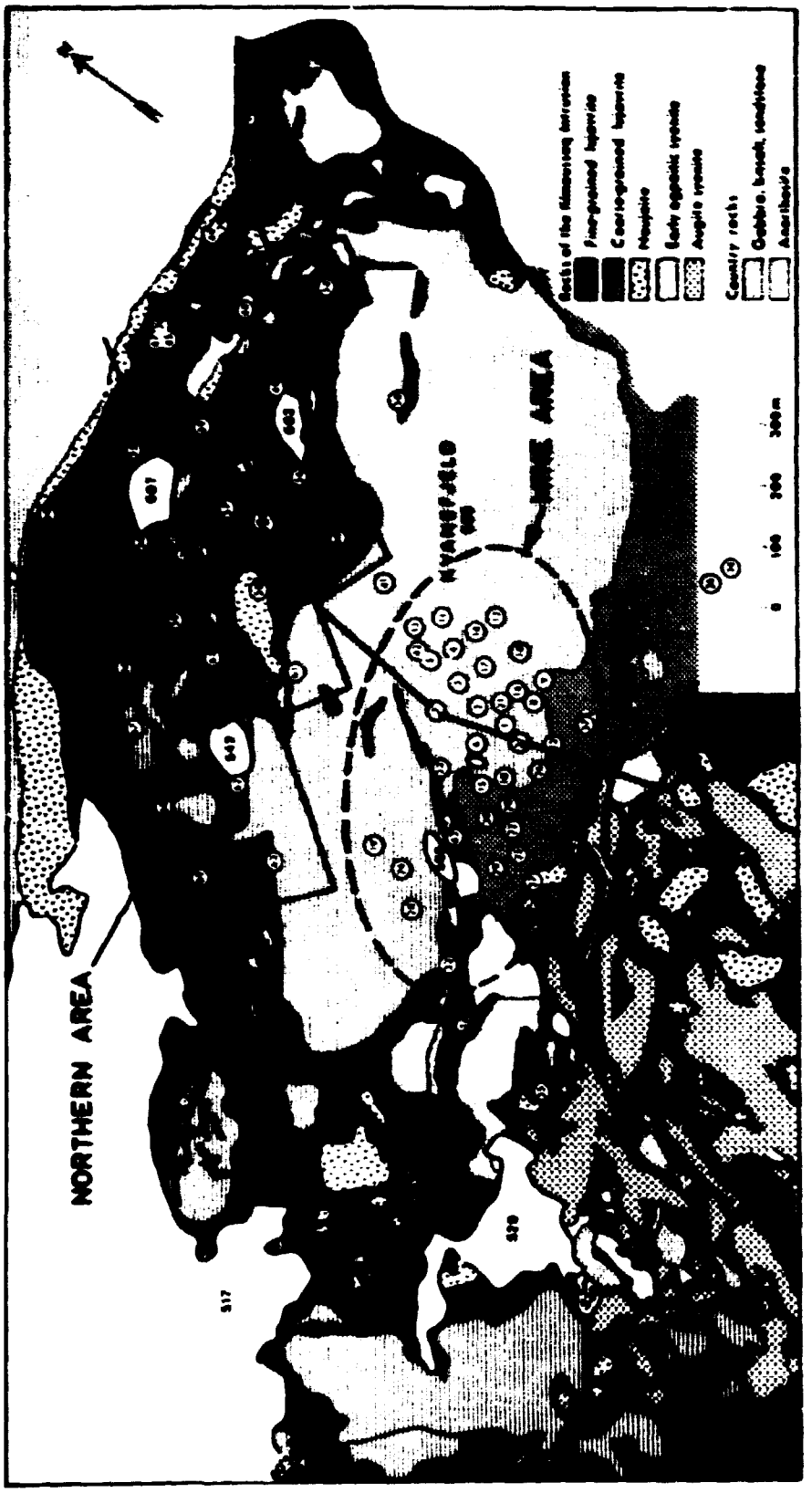

FIGURE 2-4: Simplified map of the geology of the Kvanefjeld area showing location of diamond drilling. The Mine area, the Northern area and the Kvanefjeld tunnel are indicated. (After Nielsen and Steenfelt, 1978).

sandstones. Towards the south and the southeast the plateau is bounded by the valley of Narssaq Elv.

Outcrop account for some 50% of the surface, of which the lujavrites occupy 30-40%.

In the multiple, complex lujavrite intrusion at Kvanefjeld three types of lujavrite are of principal importance. The first two types comprise the fine-grained lujavrites arfvedsonite lujavrite and naujakasite lujavrite. These belong, apparently, to the older, magmatic phases. The third type is the mc-lujavrite which represents a locally important, later formed rock of a presumably pegmatitic-metasomatitic character. Other types of lujavrites like acmite lujavrite are of secondary importance and are not considered in this study.

Macroscopic discrimination between arfvedsonite lujavrite and naujakasite lujavrite is based on the presence of naujakasite which occurs as 1/2-2 mm rhombohedral flakes (Per Nyegaard, pers. comm.). Microscopically, the naujakasite lujavrite carries naujakasite but never eudialyte (Zr-silicate) as a main constituent. On the other hand, eudialyte is often found in arfvedsonite lujavrite either as a main constituent or accessory mineral. However, eudialyte-free arfvedsonite lujavrite is also common (Makovicky et al., 1980). If eudialyte is the main constituent steenstrupine is generally absent. In general a greater number of accessory minerals are found in arfvedsonite lujavrite than in naujakasite lujavrite.

In the central part of the plateau a gabbroic sill is underlain by a sheet-like intrusion of medium- to coarse-grained lujavrite (mc-lujavrite) which cuts all the other rocks of the area, including the fine-grained lujavrites. This area is referred to as the 'Mine Area' because small amounts of ground have been mined south of drill-holes 23 and 26 for uranium-extraction experiments (fig. 2-3).

2.4 Geology of the Kvanefjeld tunnel

Part of the present study is based on data from the Kvanefjeld tunnel driven in 1980-81. A geological description of the tunnel is found in Nyegaard (1980a) and a detailed map at 1:100 is presented in Nyegaard (1980b). Extracts from these studies combined with a geostatistical study on uranium-thorium data from the tunnel will be presented in Clausen et al. (in prep.).

A simplified geological profile of the tunnel is given in figure 2-5. The projected location of the tunnel is indicated in figure 2-4. The actual location is plotted on plate 1. All three main types of lujavrite are found in the tunnel. Over the first 40 metres arfvedsonite lujavrite predominates, but xenoliths of augite syenite are present. After a 25 m. section of augite syenite the next section of 65-220 metres comprises mc-lujavrite in which xenoliths of augite syenite and lava, as well as lamprophyric dykes and pegmatite veins, are found. From 220 metres to 880 metres the tunnel is dominated by naujakasite lujavrite which is divided into sub-sections by xenoliths, mainly lava and naujaite, of different lengths. From 880 to 960 metres the tunnel is in lava.

The uranium content of the arfvedsonite lujavrite and the mc-lujavrite is generally low, about 150-200 ppm, and these rocks are not considered in the leaching study. In contrast the naujakasite lujavrite contains several zones with fairly high uranium values (300-500 ppm U). The bulk samples shipped to RISØ were taken solely from naujakasite lujavrite where the uranium content exceeded 350 ppm.

2.5 Uranium potential

Occurrences of uranium in Kvanefjeld are associated with the youngest nepheline syenite, the lujavrite, which is generally dark and fine-grained with a pronounced magmatic lamination (Sørensen et al., 1974, Nielsen and Steenfelt, 1979). This rock

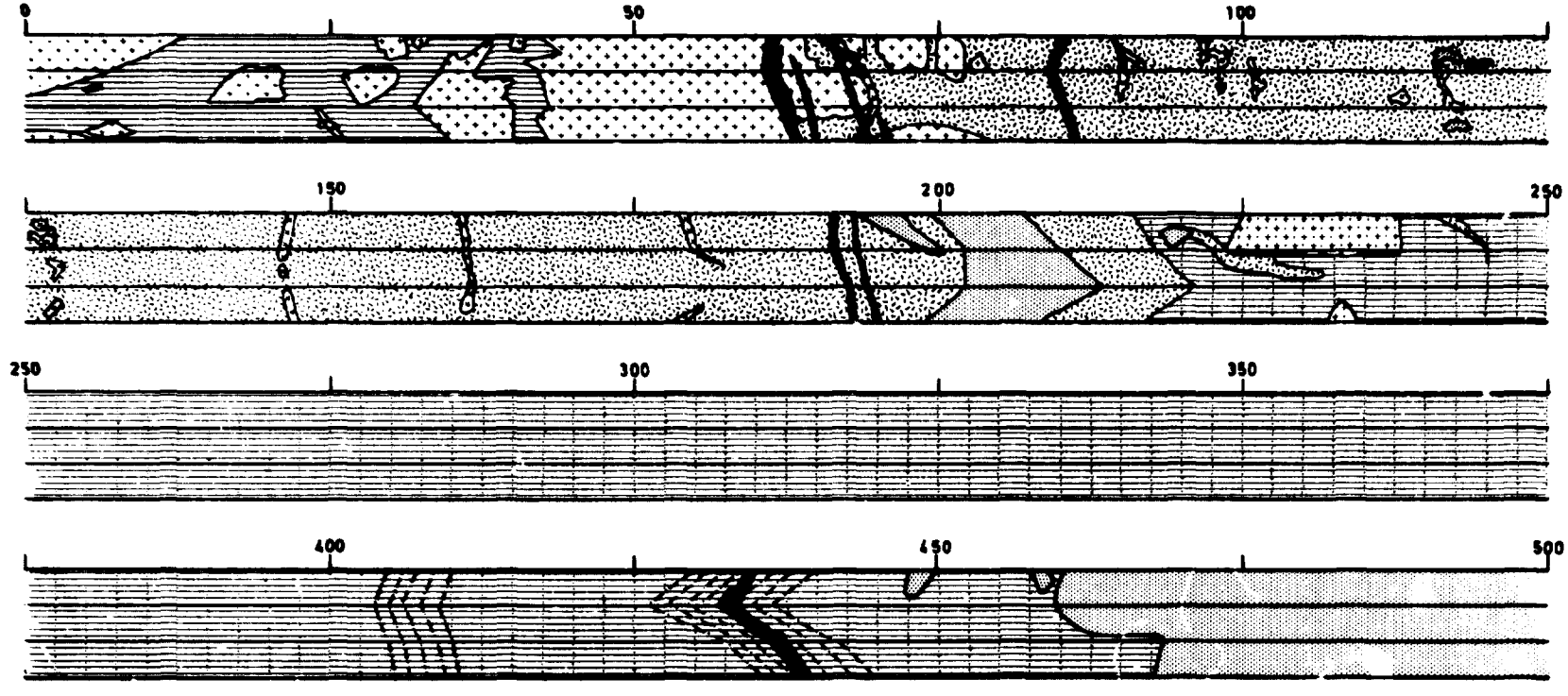

FIGURE 2-5: Simplified map of the geology in the Kvanefjeld tunnel. (After Nyegaard, 1980a).

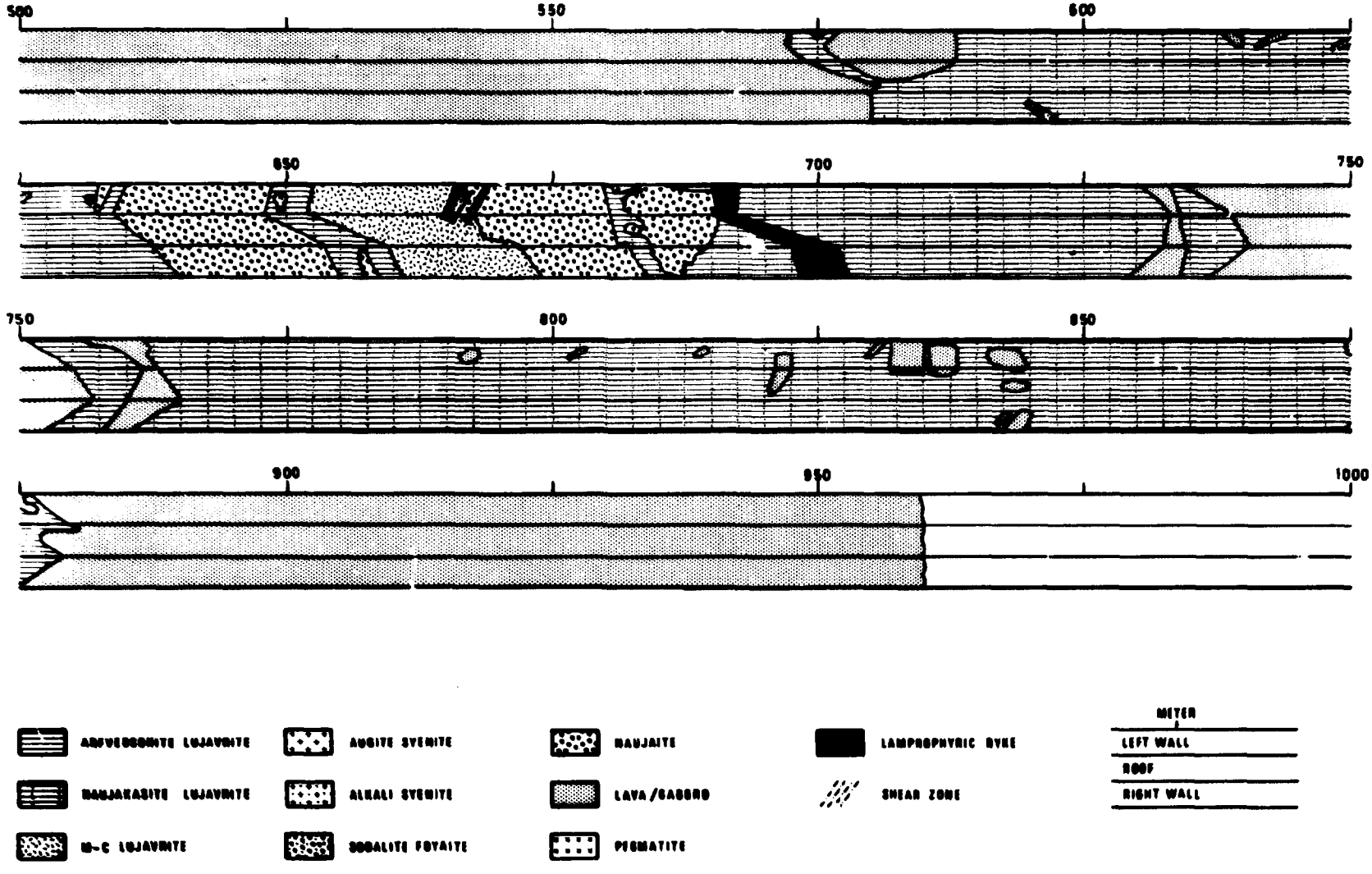
500
550
600
650
700
750
750
800
850
900
950
1000
ARFVEDSONITE LUJAVRITE
RANJAKASITE LUJAVRITE
M-C LUJAVRITE
AUGITE SYENITE
ALKALI SYENITE
SODALITE FOYAITE
NAUJAITE
LAVA/GABBRO
PEGMATITE
LAMPROPHYRIC DYKE
SHEAR ZONE
METER
LEFT WALL
ROOF
RIGHT WALL

type is enriched in both uranium and thorium as well as niobium, zirconium, beryllium, lithium, fluorine and rare earths. It was concluded by Makovicky et al. (1980) that the bulk of 'ore' is represented by various types (generations) of lujavrite. The xenoliths may be considered to be of no interest as a source of radioactive raw material. However, additions to the 'ore' mass can also be gained from the metasomatically altered volcanic rocks interleaved with, or overlying, lujavrites. The average ratio of lujavrite to xenoliths is estimated at 2:3 (Nielsen, 1980).

The radioactivity of the lujavrite arises mainly from disseminated crystals of steenstrupine, a uranium-thorium-bearing rare-earth phosphosilicate (Makovicky et al., 1980, Makovicky and Karup-Møller, 1981, Sørensen, 1962). The uranium content of the steenstrupine varies from 0.2% to 1.4% and the thorium content from below 1% up to 5%. High grade veins and pegmatites are not of economic importance because of their small volume.

The overall radioactivity of lujavrite corresponds typically at Kvanefjeld to uranium contents between 200 and 400 ppm U. As will be shown later, the uranium content varies over a wide range (0-1000 ppm) in different types of sample.

Homogeneous sections of lujavrite show a trend in element content with depth. The main ones are uranium, thorium, yttrium and rare earths, which appear to decrease at depth. Zirconium, however, seems to increase with depth (Kunzendorff et al., 1981 and Nyegaard, 1979).

3 THE DATA.

This chapter describes the data available for the present study. Special emphasis is laid on sampling procedures, analytical methods and on the coordinate systems by which each sample was located. The three main types of data are:

(1) From drill holes.

(2) From the Kvanefjeld tunnel

(3) From a gamma-spectrometric survey of surface exposures.

The drill hole data comprised both assay and log values. All the assay data from drill holes were, together with the drilling parameters, stored on a major database called KVANE (Clausen, 1980a). The creation and structure of this database will be described. Examples of input format for all types of data are given in appendix C.

3.1 Coordinate systems

There is a not inconsiderable confusion about geographical locations in the Kvanefjeld area. The main reason for this is that surveys conducted at various times have not been standardised, so different coordinate systems have been used, especially for drill hole locations. In order to overcome this impasse all available information was referred to a single, well-defined coordinate system which, according to Bjarne Wallin (pers. comm.), is reliable. The system is defined as follows. The origin of the coordinate system coincides with drill hole 39 (fig. 3-1) which is located in the north-eastern corner of the Kvanefjeld plateau. The axes have the directions shown in figure 3-1. The X-axis is positive through drill hole 45, while the positive Y-axis forms an angle of 12^{o} with the magnetic north. In what follows, this global system is referred to as Coordinate System I (CSI). Distances are in all cases given in metres. Since, however, most plotting routines and programs for geostatistical calculations require that the spatial data are located on a proper X,Y-coordinate system, a new system CSII was formed from CSI. In CSII, shown in figure 3-2, the condition that all drill holes should have positive coordinates in both the X- and Y-direction is fulfilled. The connexion between CSI and CSII is given by

$$X_{CSII} = 1100 - X_{CSI}$$

$$Y_{CSII} = 1100 + Y_{CSI}$$

The positive Y-axis in CSII is in a direction magnetic north + 12^{o}.

As will be demonstrated in chapter 4, global estimates of the uranium tonnages in the Mine area and in the Northern area were made separately. The block patterns used for these estimates are constructed so as to fit the drilling pattern, and hence have to be referred to local coordinate systems with axes par-

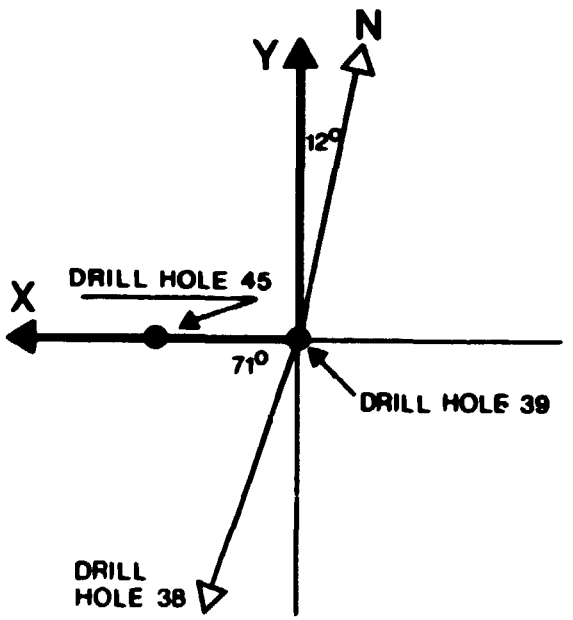

FIGURE 3-1: Orientation of the coordinate system CSI in relation to magnetic north and the drill holes 39 and 45. (After Nyegaard et al., 1977).

allel to the actual block pattern. These systems were fixed according to CSII and were defined as follows. In the Mine area the coordinate system for block estimation (CSmine) uses the transformation:

$$X_{mine} = (X_{II}-392)\cos 46 + (Y_{II}+29)\sin 46$$

$$Y_{mine} = -(X_{II}-392)\sin 46 + (Y_{II}+29)\cos 46$$

In the Northern area CSnorth is given by the transformation:

$$X_{north} = (X_{II}-510)\cos 46 + (Y_{II}-195)\sin 46$$

$$Y_{north} = -(X_{II}-392)\sin 46 + (Y_{II}-195)\cos 46$$

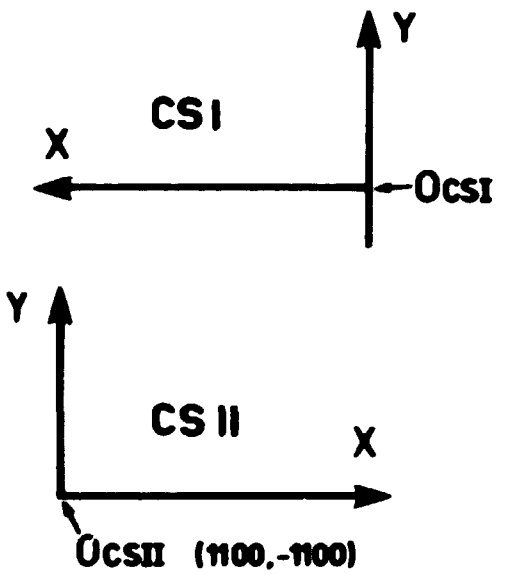

FIGURE 3-2: Relationship between the coordinate systems CSI and CSII. (See also Plate I).

The two coordinate systems are indicated on plate I. Finally, a third global coordinate system, CSIII, was used for the data from the gamma-spectrometric survey in order to use the simplest transformations (section 3.4.1). The axes of CSIII coincide with the axes of CSI and the two systems are:

$$X_{CSIII} = X_{CSI}$$

$$Y_{CSIII} = -Y_{CSI}$$

Hence the Y-axis of CSIII is negative towards the magnetic north.

3.2 Drill hole data

3.2.1 Sampling procedure and drill hole coordinates.

70 drill holes were available at Kvanefjeld and Steenstrup fjeld (fig. 2-3). From the holes drilled in 1977 (i.e. in the 'Northern area') core samples of 1 metre length have been taken every second metre (fig. 3-3). In some holes a few samples were taken every metre. Each sample was split into two halves, one of which was crushed and homogenized. The powder was then split into minor portions which were analysed by different laboratories. Drill cores prior to 1977 (i.e. from the 'Mine area') were analysed by a non-destructive drill core scanning device (Løvborg et al., 1972) (sec. 3.2.2.1.) at one metre intervals (fig. 3-3), and no actual samples were taken. Neighbouring sections so scanned generally overlap each other by a few centimetres, but this was ignored for the purposes of the present analysis.

Drill hole coordinates and elevations (i.e. Z-coordinates) from the 1977 holes were available from Nyegaard et al. (1977). These were referred to CSI. Coordinates (in a coordinate system of uncertain location) and elevations for holes prior to 1977 were estimated from a 1:2000 topographic map produced by Geodætisk Institut and Aerokort A/S (sheets 60 V2-H11 I1, 60 VII-H11 H1 and 60 V1-H10 H10) and from internal GGU notes. By combining information from these two sources Mine area holes were referenced to the CSI grid as well.

The orientations of the drill holes (dip and azimuth) were determined for the 1977 holes. These were carried out by

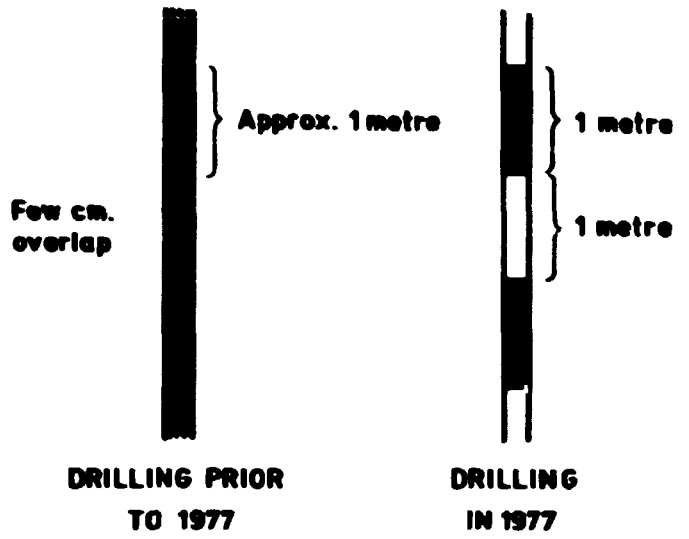

FIGURE 3-3: Schematic representation of the sampling procedure used for drill core samples. Shaded sections indicate the samples.

Geoteknisk Institut and were available in internal GGU notes. The same data have not been determined from the Mine area drill holes, and information about the dip and azimuth of inclined holes in this area is only available from scattered references in internal reports and field diaries (Sørensen et al., 1971, Henning Sørensen and Bjarne Leth Nielsen, pers. comm.). A full listing of coordinates, elevations, orientations, numbers of samples and types of analyses are given in appendix E.

It is the opinion of the author that the determination of coordinates and orientation of drill holes is subject to errors. This is especially the case for the early drill holes, as seen in table 3-1 where the possible accuracy of drill hole parameters is listed. These deviations may cause large errors, especially of the X and Y coordinates at the bottom of a drill hole. However, the effect of coordinate errors on the estimates of the global reserves is regarded as negligible.

X, Y and Z coordinates were calculated for the top of each sample in CSI. Holes with inclinations of less than 1^{o} were considered vertical because of the inaccuracy of the parameters (table 3-1). The algorithm used for inclined holes was:

$$X = X_{start} - \sin\rho(D1\cos\alpha)$$

$$Y = Y_{start} + \cos\rho(D1\cos\alpha)$$

$$Z = Z_{start} - D1\sin\alpha$$

where D1 is the depth to the top of the sample, ρ the azimuth plus 12^{o} (the deviation between the magnetic north and the Y-axis) and α the dip.

TABLE 3-1: Possible accuracy of drill hole parameters as estimated by the author. Z is the elevation above sea level.

Drilling area	X,Y	Z	Azimuth	Dip
Mine area	±2 m	±3 m	$\pm 3\text{-}10^{o}$	$\pm 5\text{-}10^{o}$
Northern area	±0.5 m	±1 m	$\pm 1^{o}$	$<\pm 1^{o}$

3.2.2 Assay data.

An intense analytical programme was carried out on the drill core samples. All samples were analysed for uranium, thorium and potassium by gamma-spectrometry and a large number of samples from the 1977 drill holes were analysed for a wide spectrum of elements by different laboratories. In the following sections these methods are described and the accuracy of the methods discussed. In appendix E a listing of the analytical methods used on the samples from each individual drill core is given.

3.2.2.1. Gamma-ray spectrometry (GAM-SPEC). 3444 samples from holes prior to 1977 have been analysed by a non-destructive drill core scanning device (Løvborg et al., 1972) for uranium,

thorium and potassium. The accuracy of the method depends on comparisons against standards of known content. The total error to which uncertainty of the standard, instrument calibration and counting time contribute, varies with the properties of the drill core. Examples of sources of errors are: missing core material, variations in the core density and heterogeneously distributed radioactive veinlets or inclusions.

The relative standard deviation of the method is estimated at 2-10%, the highest uncertainty being present in low grade material (≃10 ppm U). The analyses, which were provided by RISØ, were accompanied by their individual standard errors.

Samples from the 1977 holes, in total 2214, were also analysed in an automatic gamma-ray spectrometer at RISØ (Løvborg, 1972) for U, Th and K. About 250 grammes of material were placed in a metal container, which was sealed and stored for three weeks to allow radon-222 to build up to radioactive equilibrium. About 30 samples were analysed during one spectrometer run lasting 20 hours. The accuracy of the method, which is affected by the uncertainties of the standard and the counting time, is much better than the method of core scanning. The average standard error is estimated at 0.5 to 2%, but for low element concentrations (e.g. 2 ppm U) the error is much bigger.

Both analytical methods are influenced by the U/Th-ratio. Furthermore, satisfactory determinations of potassium cannot be made where there is a high content of uranium and thorium (several hundred ppm).

3.2.2.2. X-ray fluorescence (XRF). 614 samples were analysed by X-ray fluorescence at the Institute for Petrology in the University of Copenhagen. The following elements were determined by the method: Zn, Ga, Rb, Sr, Y, Zr, Nb, Pb and Th. The precision (reproducibility) and detection limits normally range between 5-10 ppm. The accuracy of the method is uncertain since analyses were made on too coarsely-grained material, but was probably +/- 20-40%. A single South African lujavrite standard is used for calibration (NIM-L).

3.2.2.3. Energy dispersive X-ray fluorescence (EDX-CD,EDX-PLU). A selection of 234 samples containing Nb-bearing minerals was analysed by radioisotope energy dispersive X-ray fluorescence with a Cd^{109}-source (EDX-CD). Seven USGS standards were used for assaying and the following elements were obtained: Fe, Rb, Sr, Y, Zr, Nb, Mo, Pb, Th, U.

The accuracy is uncertain, but is estimated at +/- 10%, except for uranium and thorium where the accuracy is greater.

The core samples analysed by XRF were also analysed by EDX, but using a Pu^{238}-source (EDX-PLU). In total 573 samples were analysed for the following elements: K, Ca, Ti, V, Cr, Mn, Fe, Ni,Cu, Zn, Ga, Sr and Pb. The same 7 standards as used for the EDX-CD were also used for EDX-PLU. The accuracy is probably +/- 10% except for V and Cr, where analytical figures must be considered unreliable. Both types of EDX assaying were done at RISØ.

3.2.2.4. Fluorine analyses (FLUOR). 570 samples were analysed for water soluble fluorine (fluorine from villiaumite, NaF) using a fluoride specific ion-electrode. The method is described in Nyegaard (1979) who also took charge of the analytical work. The accuracy is estimated at +/- 5%, and the detection limit is 100 ppm F.

3.2.2.5. Optical spectrometry (OP-SPEC). Optical spectrometry was used to analyse lithium and beryllium in 107 lujavrite samples. The assaying was done at the Institute for Petrology, University of Copenhagen. The analytical results are only semi-quantitative and the accuracy lies between +/- 50-100%.

3.2.2.6. Instrumental neutron activation analysis (ENAA). Instrumental neutron activation analyses were done on a total of 833 samples. The method is described by Jørgart (1977) and

Nyegaard (1979). 33 elements were measured, out of which only 26 can be considered reliable because of high detection limits. These elements are: Na, K, Sc, Cr, Mn, Mn, Fe, Co, Zn, Rb, Zr, Sn, Sb, Cs, Ba, La, Ce, Nd, Sm, Eu, Gd, Tb, Yb, Lu, Hf, Ta and Th. The accuracy of the determinations varies from sample to sample, and no limits of precision can be stated. In general, the values of K, Co, Zn, Zr, Sn and Sb are subject to high errors.

The equipment used for the ENAA analyses is available at RISØ.

3.2.3 Logging data.

Gamma spectrometric logging of drill holes was done both in the Mine area (Løvborg et al., 1972) and in the Northern area (Løvborg et al., 1980a). Only the logging results from the Northern area were considered in the present study, mainly because the values of gamma radiation measured in this area have been converted into element concentrations of U, Th and K. The Mine area logs (14 holes) provided a measure of the total gamma radiation which was used only to compare drill core scanning results.

Logging results were available from all the 1977 drill holes at Kvanefjeld, except for holes 45 and 47, and holes 39 and 40 drilled in 1969. The logging equipment included a 19 x 76 mm sodium iodide gamma-ray detector, a GAD-6 four channel gamma-ray spectrometer and a digital printer. The holes were logged in steps of 25 cm from top to bottom, and at each position counts were accumulated for 100 seconds in four energy windows (total gamma, potassium, uranium and thorium). The calibration constants of the spectrometer were determined by calculating the average number of U and Th counts per meter of borehole and comparing these with the U-Th concentrations in the corresponding 1 m sections of analyzed drill cores. Two types of calibration were performed: one using an overall calibration, and one in which each hole was calibrated individually. The latter method, which compensates for hole-to-hole variations in

sensitivity and background count rate (probably due to variations in the emanation of radon from the borehole walls), was used to calibrate the data in the present study.

The data, (borehole number, depth, U and Th values), which were provided by RISØ on magnetic tape, were read and stored on a disk file as card images. Each record represented one sample. The X, Y and Z coordinates (CSnorth) for each of these were assigned by merging the file with a similar file containing assay data and coordinates, cross-referenced by sample number (see section 3.2.4.).

The main advantages of the logging data compared with the assay data are that data were available for every meter of borehole and that no 'gaps' were present (barren inclusions were also logged). As the assay data were used to calibrate the logging data the accuracy of the latter is considerably lower than the assays with maybe as much as a 50% error in unfavourable circumstances.

3.2.4 The database KVANE.

A database containing all the drill hole information, except for the logging results, was constructed using the Statistical Analysis System (SAS) at NEUCC. The information comprised the sample number, a code describing the geology of the sample, coordinates according to CSI and CSII and the assay values described in section 3.2.2. A description of the database KVANE and examples of its use can be found in Clausen (1980a) from which the following is extracted. The SAS system is documented in Helwig and Council (1979).

The assay data from the seven different analytical methods (table 3-2) were read from punched cards and magnetic tape, (examples of data format are given in appendix C) by individual programs. This was necessary since data formats have not been standardised. Later the files were merged by sample number to form the master file KVANE (fig. 3-4). A listing of the computer program illustrated in figure 3-4 is found in Appendix A.

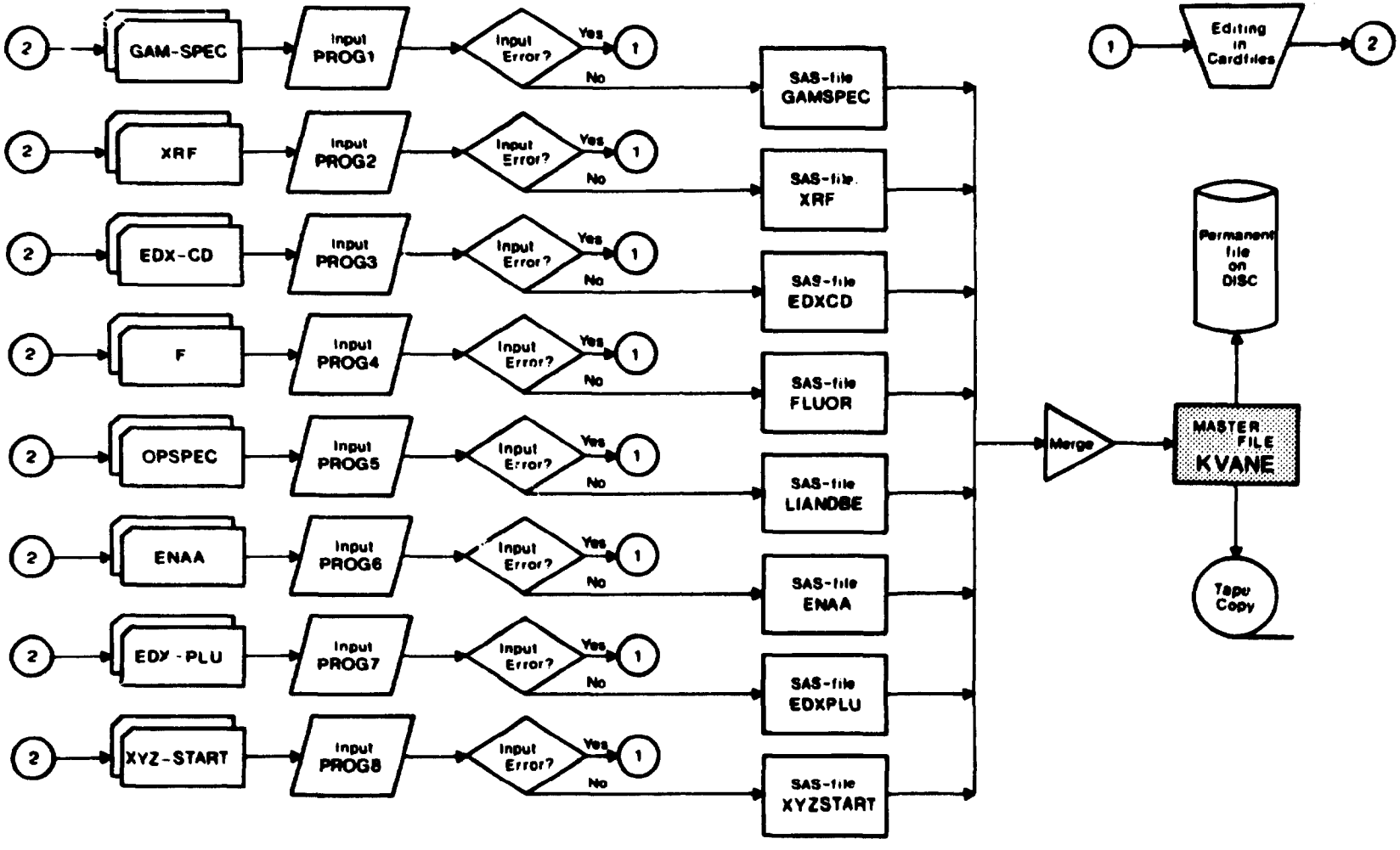

FIGURE 3-4: Flow chart showing the main programming phases during development of the database KVANE.

The sample number as used in KVANE has the form

PR_NR = DDMMM.CC

where DD is the drill hole number and MMM.CC the depth below surface to the top of the sample in metres. Both the drill hole number and the sample number were stored as numerical variables, which makes sorting possible by logic expressions.

A self-explanatory way of naming analytical variables was used as follows:

EL_UNIn

where EL is the element symbol (e.g. LA for La), UNI the value unit (PPM or PCT) and n the analysis method index as defined in table 3-2. Hence, discrimination between the same element obtained from different analytical methods is possible.

TABLE 3-2: Summary table showing the analytical work on drill core samples. Abbreviations used for analytical method and the method Index are explained in the text. N_c is the number of cores involved. N_s is the number of samples analysed by the method concerned.
†): Unreliable elements have been rejected.

Analytical method	Elements obtained	N_s	Index	N_c
GAM-SPEC	U, Th, K	5663	1	63
XRF	Zn, Ga, Rb, Sr, Y, Zr, Nb, Pb, Th	614	2	7
EDX-CD	Fe, Rb, Sr, Y, Zr, Nb, Mo, Pb, Th, U	234	3	18
F	F	570	4	23
OP-SPEC	Li, Be	107	5	13
ENAA †)	Na, K, Sc, Cr, Mn, Fe, Co, Zn, Rb, Zr, Sn, Sb, Cs, Ba, La, Ce, Nd, Sm, Eu, Gd, Tb, Yb, Lu, Hf, Ta, Th	833	6	13
EDX-PLU †)	K, Ca, Ti, Mn, Fe, Ni, Cu, Zn, Ga, Pb, Sr	573	7	7

Error checking was built into the reading programs if more than one input record was necessary to define one observation. This was the case for EDX-CD (10 cards/obs.), EDX-PLU (13 cards/obs.) and ENAA (16 cards/obs). Editing was especially necessary on the ENAA input files as a large number of mis-punchings occurred and several input records were missing. If it was not possible to recover the missing data the variable, or even the whole record, was deleted.

The variable describing the geology of the sample is a three digit code where each digit defines the main rock type, the secondary rock type (if any) and other characteristics (if any), respectively. A geological coding table provided by the Geological Survey of Greenland is listed in appendix E.

3.3 Tunnel data.

The data from the Kvanefjeld tunnel comprised:

(1) U, Th (and K) values from different types of sample within the tunnel.

(2) U, Th (and K) values in batch samples (of excavated material).

As to (1), two types of 'sample' were available a) chip samples taken at two metre intervals in each tunnel wall, and b) in-situ determinations of U and Th by a portable gamma-spectrometer at 5 metre intervals in the first section of the tunnel (310 m).

3.3.1 Sample coordinates.

As the study of the tunnel data was of a local nature there was no need to relate samples to the global coordinate systems. Although the tunnel was not straight (see plate I) it was considered to be so for computational convenience. The X-axis of the local pseudo-coordinate system was then 'parallel' to and

coincident with the right-hand tunnel wall, and hence samples have X-coordinates equal to the distance from the tunnel entrance. The Y-coordinate is zero if the sample was taken in the right wall and equal to the tunnel width if it came from the left.

3.3.2 Analytical data.

3.3.2.1. Gamma-spectrometric survey. A gamma-spectrometric survey was done along part of the tunnel (0-310 m) using a portable four channel Geometrics/Exploranium GR-410 gamma-spectrometer with a 3 x 3" NaI(Tl) detector.

Readings were taken at every 5 metres, but because of the 'view' of the detector (5 metres) and because of the uncertainty of measuring geometrics, sensivity and stripping constants, results must be viewed with some reservation. The calibration of the equipment is described by Sørensen (1979).

3.3.2.2. Chip samples. The chip sampling programme which is described by the author (Clausen, 1979, 1980b and Clausen et al., in prep.), was completed in two periods of a fortnight each. Each chip sample of approx. 1.3 kg. material measured 2 metre vertically, and had a horizontal dimension of about 1/2 m. The samples, each of which comprised 15-25 chips, were taken at two metre intervals in each tunnel wall (fig. 3-5). Only lujavrite sections or contacts with lujavrite were sampled. GGU numbers for the samples were coded as follows:

Sample in right wall at X-distance NNN: Number = 294NNN

Sample in left wall at X-distance MMM : Number = 295MMM

At each sample site information about tunnel width, sample length, number, geology and X-distance was recorded on specially designed coding sheets (Appendix C), which were later used directly for card punching.

In the laboratory the samples were dried, crushed and homogenized before 250 g portions were selected and analysed for U, Th and K by the gamma-spectrometer at RISØ. A total of 674 chip samples was available.

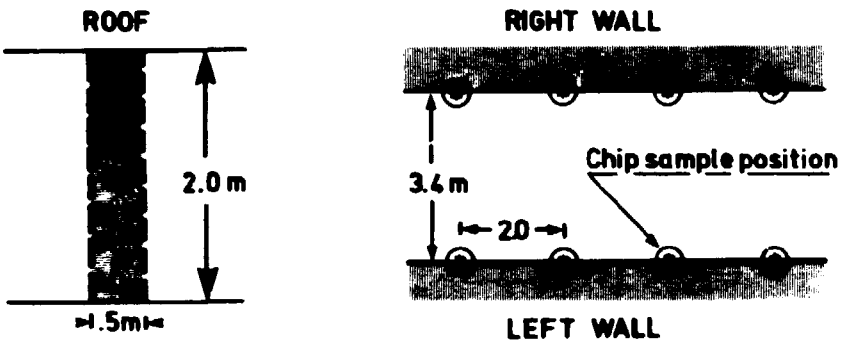

FIGURE 3-5: Schematic representation of the chip sampling procedure within the Kvanefjeld tunnel. The sampling interval is 2 metres. Each chip sample consists of 15-25 chips (indicated as crosses).

3.3.2.3. Batch samples. In order to discriminate between 'ore' and waste (cutoff 250 ppm U) the uranium and thorium contents were measured of each batch sample of exavated material from two tunnel blasts (approx. 140 metric tons). Because of the high radioactive background in the area, a concrete screen was built (fig. 3-6). The screen reduced the background count by a factor of 20. Approx. 15-20 kg. of material varying in size from cobbles to sand were collected at random from the blast material and placed in a pail with a detector at the centre. The instrument was a GR 410 gamma-spectrometer. Counting took place over 30 sec. periods and the average counts after correcting for background, were converted into element concentrations. Descriptions of calibration and instrument arrangement are found in Sørensen (1979) and in Clausen et al., (in prep.). The geographical location, geometry and geology were recorded for each of the 58 batch samples (appendix E). Some of these were later merged to give a final total of 53 batch samples.

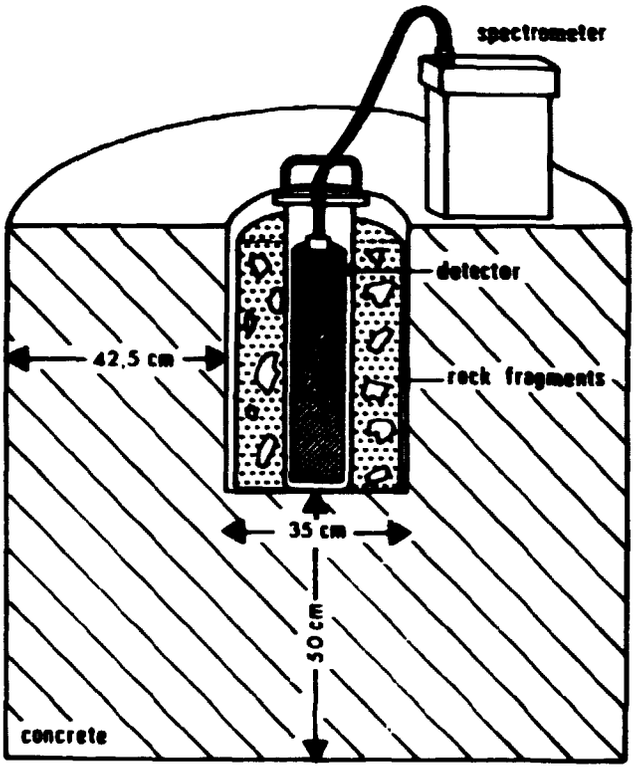

FIGURE 3-6: Gamma-spectrometer apparatus used for measuring the uranium concentration in batch samples.

3.4 Surface data.

A detailed gamma-spectrometric survey was completed on a 10 by 10 metre grid on the Kvanefjeld plateau and at Steenstrup fjeld. The area of investigation, which can be seen from plate I, covers most of the area drilled in 1977 (the Northern area).

3.4.1 Sample coordinates.

The area of investigation was divided into 5 sub-areas as shown in figure 3-7. Two other areas at Steenstrup fjeld were not considered. The coordinates of the sample points in the sub-areas were transformed into the CSIII system as follows:

Area 1: Unchanged

Area 2: $X_{CSIII} = 1000 + X_2$

$Y_{CSIII} = Y_2$

Area 3: $X_{CSIII} = X_3$

$Y_{CSIII} = -Y_3$

Area 4: $X_{CSIII} = -X_4$

$Y_{CSIII} = -Y_4$

Area 5: $X_{CSIII} = -X_5$

$Y_{CSIII} = Y_5$

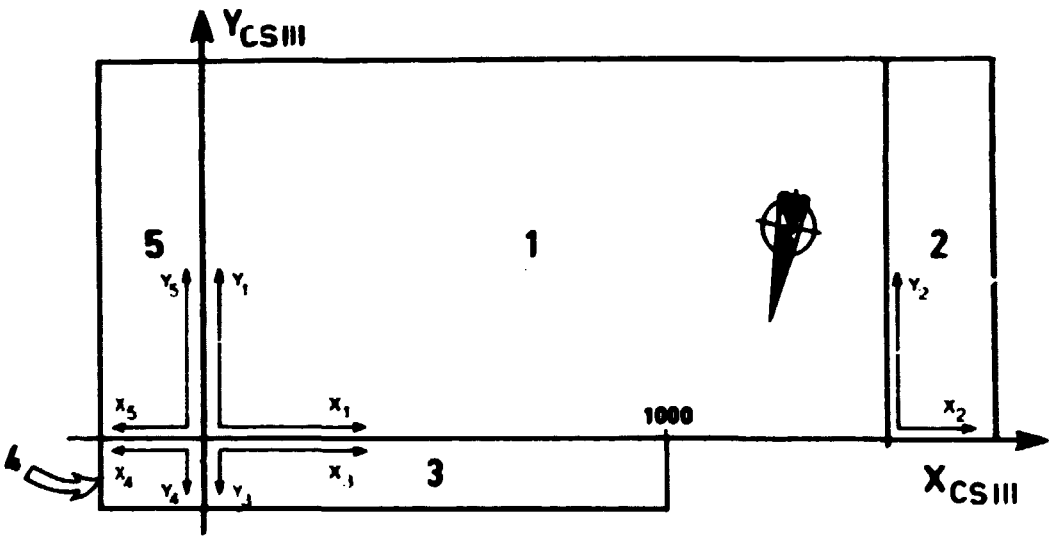

FIGURE 3-7: Sub-division of the ground gamma-spectrometer survey area and its relation to coordinate system CSIII.

3.4.2 Analytical data.

3028 determinations of the radioelement concentrations were made within the test area (Kvanefjeld). Gamma-ray counting was done with a portable four channel Geometrics/Exploranium GR-410 gamma-spectrometer equipped with a NaI(Tl) scintillation detector. The instruments, which were installed in a specially designed rucksack, were calibrated at RISØ in a concrete calibration facility (Løvborg et al., 1978).

Counts were converted to concentrations of U and Th as described in Nyegaard et al., (1977), where other details of the actual survey can be found. General descriptions of monitoring natural radioactivity by gamma-ray spectrometry are given by Løvborg et al., (1979) and Løvborg et al., (1980b).

Although sample determinations were considered as being on 'points', samples occupy a certain volume. The detector was situated approx. 1.5 metre abcve the surface in which case 90% of the count contribution in the U-channel was emitted within a circular area with a radius of 5 metres. 50% of the detected gamma-radiation was emitted from an area with a radius of 2.95 metres. These observations on the 'effective' sample were used when the grid spacing was selected.

At each grid point counts were made over periods of 20 to 120 seconds depending on the radioactivity. The amounts of outcrop, sand, stone, soil, vegetation, snow and water were estimated within a circle of 2.5 metres in radius. A standard GGU geology code (appendix E) was also recorded. The approximate standard deviation of the individual measure varies between 20 and 30%.

The data file was edited for duplicate samples and for samples outside the grid points. The resulting data file contained 2848 sample points.

4 URANIUM IN DRILL HOLES.

4.1 Introduction

In this chapter all the investigations of the uranium values from drill holes, that is, both assay values and logging data, will be presented. The investigation was mainly based on the 'Theory of Regionalized Variables' developed by Matheron (1963, 1971), and its main object was to produce a global estimate of the uranium resources and a confidence interval for this estimate. It is considered out of scope of this presentation to give a full account of the theory. Instead, comprehensive references are given throughout the text and the main results are mentioned. The interested reader is referred to several introductory works on the subject, e.g. those by Clark (1979a), David (1977), Rendu (1978), Journel and Huijbregts (1978), Royle (1977a) and Knudsen and Kim (1978). Summaries of the theory are described elsewhere by the author (Clausen, 1980c, 1981).

The basic concept in regionalized variable theory (RV theory or just 'geostatistics') is the intrinsic hypothesis. This hypothesis implies that a random function, known as the intrinsic function, describes the spatial behaviour of the RV within the space, and that this function is an intrinsic feature of the regionalization. In this study the uranium values are regarded as being a RV, and the spatial behaviour is modelled by the empirical function called the semi-variogram.

If two samples at positions (x,y,z) and (x,y,z-1) are considered, the grade of each sample can be denoted by Z(x,y,z) and Z(x,y,z-1). These samples can, for example, be two adjacent drill cores of one metre length. Each of these measures will be a sample of some random distribution depending on the location. If the difference in grade is calculated, D(x,y,z,1) = Z(x,y,z)-Z(x,y,z-1), this value will also follow a distribution (e.g. Clark, 1978). Now, consider another pair of samples,

$Z(x_1,y_1,z_1)$ and $Z(x_1,y_1,z_1-1)$, and their difference $D(x_1,y_1,z_1,1)$. This too will have a distribution. If the 'continuity', or 'structure', of the deposit is consistent then these two distributions will be the same. That is, the differences between values one metre apart in drill cores will be 'stationary'. This does not mean that they will have the same values, but only that they can be considered to be from the same distribution.

Next, consider samples two metres apart. If the above mentioned stationarity is present, it can again be assumed that the differences between such samples belong to the same distribution. However, this distribution is not necessarily the same as in the 1 metre case, since it can be expected that samples two metres apart are less alike than samples one metre apart. To generalise, it is assumed that any pair of samples a given distance, say h, apart (in a given direction) can be assumed to be taken from a probability distribution, and that the form of this distribution depends only on the distance (and perhaps direction) separating the samples.

Each of these distributions will have a mean and a variance which can be calculated. If there is no local trend in the data, the expected values of the two samples will be the same, and hence the expected value of their difference will be zero. Accepting this, the variance of the distribution is calculated as the mean square of the differences in grade:

$$\text{Variance} = E\{(Z(x,y,z) - Z(x,y,z+h))^2\} = 2\gamma(h)$$

The variance is denoted by $2\gamma(h)$ since it depends only on the distance (and direction) between the samples. $2\gamma(h)$ is called the variogram, whereas $\gamma(h)$ is the semi-variogram. The semi-variogram measures the 'size' of the variance of expected differences between any two samples at some given distance h apart, and is usually presented as a graph of $\gamma(h)$ versus h. It may take any form, but as will be shown later there are only a few models in general use.

The semi-variogram is closely related to the covariance (cf. fig. 4-10) and they can both be regarded as equally useful tools for characterizing the auto-correlation between two variables Z(X) and Z(X+h) separated by the distance h. The relationship is given by

$$\gamma(h) = \sigma^2 - \mathrm{cov}(h)$$

where σ^2 is the a priori variance of Z(X) and cov(h) the covariogram. A full derivation of this relationship is found in Clausen (1980).

Having defined the basic tool of geostatistics, i.e. the semivariogram, practical examination may commence. The following presentation is divided into three major parts; namely, work on assay data from two areas, the Mine area and the Northern area, and work on the logging data. Among the reasons for considering the two areas separately are the differences in analytical methods, and hence accuracy of the values, and different sampling methods and drill hole spacings. A priori, the geology of the two areas also seems to support such a division. As will be shown, geostatistics reveal that the two areas differ considerably in the spatial correlations of their uranium content (caused in fact by the geology).

4.2 Uranium in the Mine area.

4.2.1 Uranium distribution.

The statistical distribution of uranium in 3107 core samples is illustrated by the histogram of fig. 4-1. It is highly skewed and markedly bimodal, or even multimodal. It is obvious that the complex form of the histogram is caused by the compound nature of the geology of the area. The histogram can be interpreted two ways. Firstly, histograms of uranium within a priori defined geological units can be compared with the compound one,

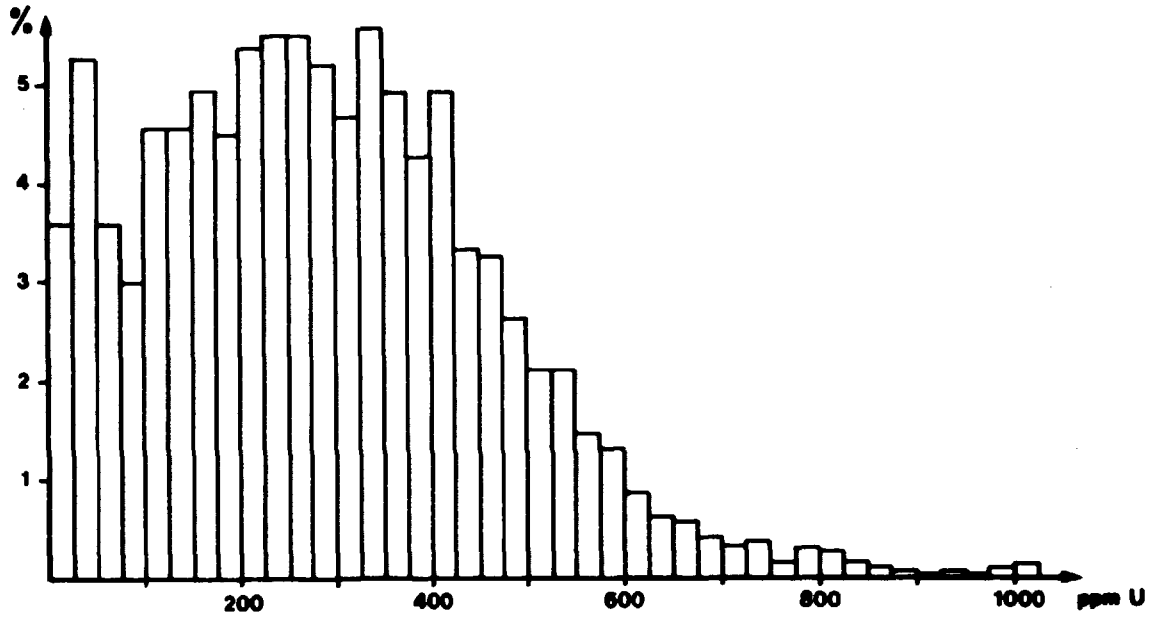

FIGURE 4-1: Histogram of uranium content in drill core samples from the Mine area. The number of samples is 3107.

and different modes perhaps explained. Secondly, each unit in the compound distribution may be identified and quantified by a numerical decomposition of the mixed of distribution. The latter was done by a modified version of the interactive program ROKE (Clark, 1977a) during a visit to the the Royal School of Mines by the author. Case studies on the decomposition of mixtures of distributions by nonlinear least-squares methods are discussed in Clark and Garnett (1974) and in Clark (1976).

Histograms of the uranium content of drill-core sections, classified geologically, are presented in fig. 4-2. The following units are considered: mc-lujavrite 944 samples, naujakasite lujavrite 340, arfvedsonite lujavrite 644, pure fine-grained lujavrite + (i.e. excluding samples of mixed geology) 303, fine-grained lujavrite + (incl. mixture samples) 1021, and finally the inclusions 1103. It is easily seen that the first peak (0-50 ppm U) in the histogram of fig. 4-1, can be explained by the very low-grade samples from barren inclusions (fig. 4-2f). However, inclusion samples do also represent areas of high grades. The next peak of the histogram (125-175 ppm) seems related to the mode of the mc-lujavrite distribution

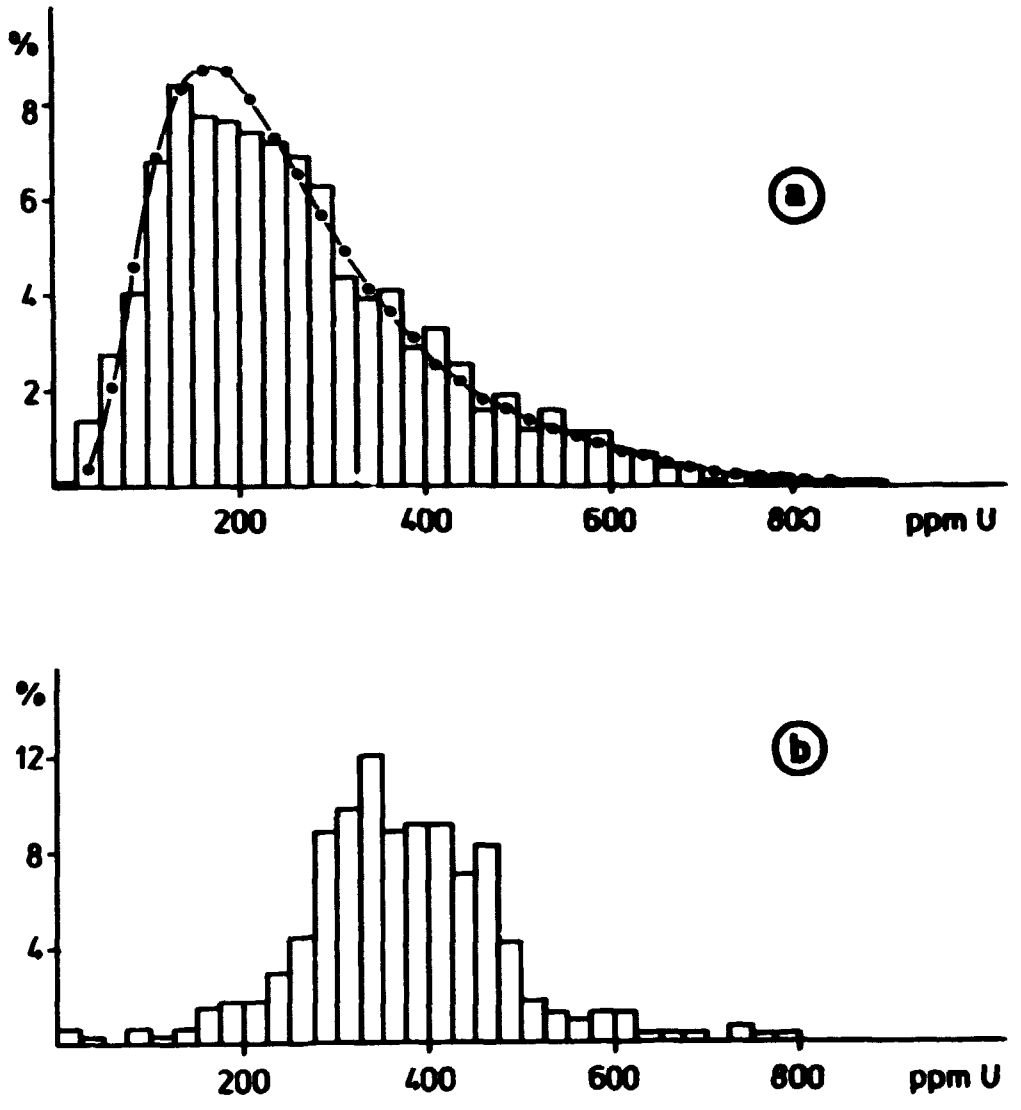

FIGURE 4-2: Histograms of uranium content in drill core samples sorted by geology. a) MC-lujavrite (944 samples), b) naujakasite lujavrite (340), c) arfvedsonite lujavrite (644), d) fine-grained lujavrite + mixted samples (1021), e) fine-grained lujavrite + mixted samples (303) and f) inclusions. Fits of distributions to a) and e) is shown (in table 4-2).

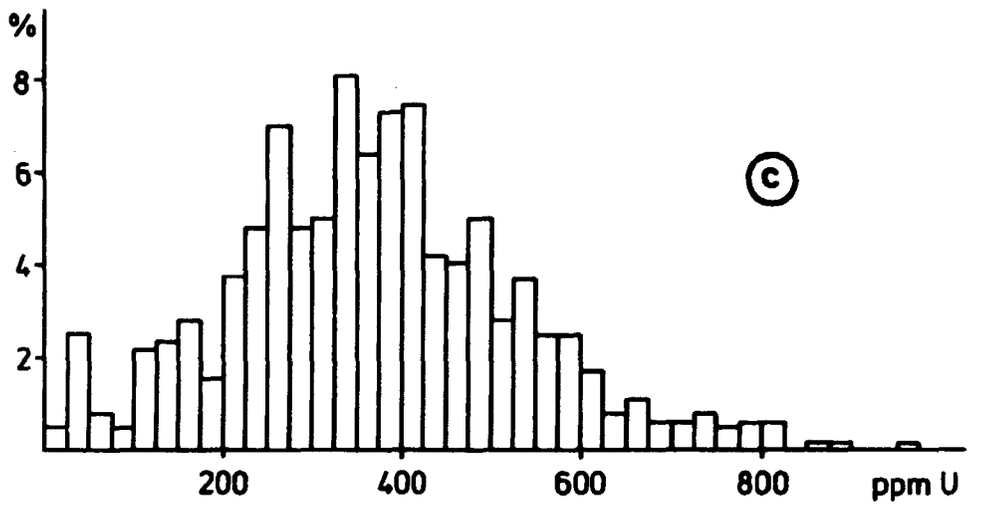

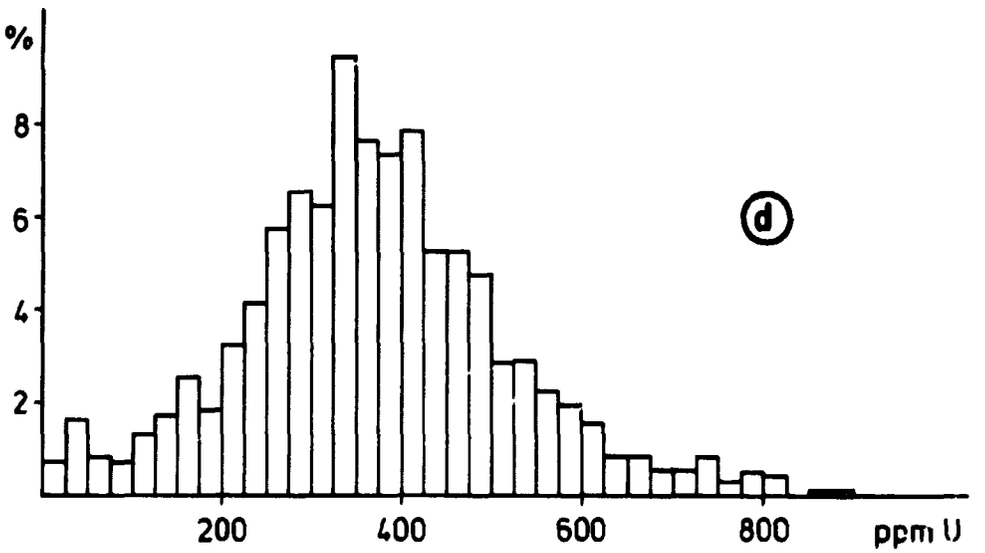

4-2

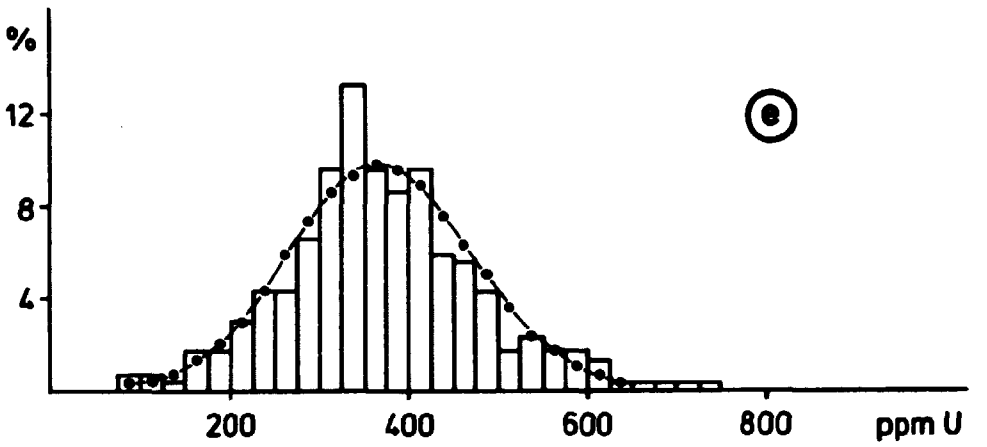

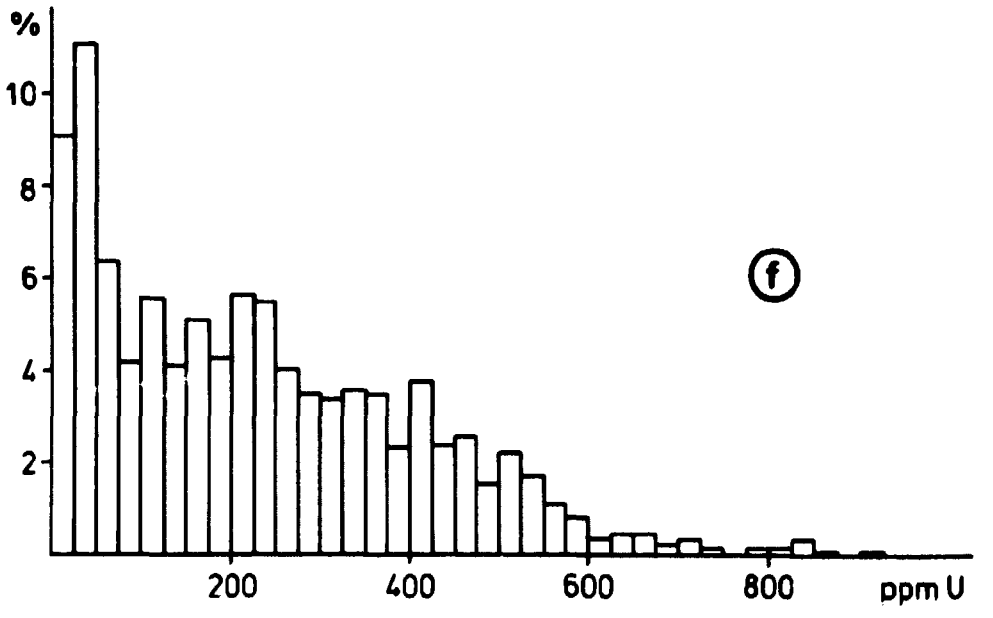

4-2

(fig. 4-2a). The histogram of these samples seems to be of the lognormal type, whereas the fine-grained lujavrites (fig. 4-2b-e), give the impression of more normal distributions. The peak(s) between 200 and 400 ppm are mainly caused by the fine-grained lujavrites, which can also be seen from the overall parameters of the distributions presented in table 4-1. A measure of the spread of the distributions is given by the coefficient of variation ($\sqrt{V(X)}/E(X)$). It can be seen from table 4-1 that the uranium distributions in the two types of fine-grained lujavrites (naujakasite/arfvedsonite) only differ in their standard deviations. This difference may perhaps be explained by the different numbers of samples. The difference between the distributions of uranium in mc-lujavrite and the two fine-grained lujavrites possibly reflect the effects of the magmatic as well as the post-magmatic processes that have taken place at Kvanefjeld.

TABLE 4-1: Simple statistics for uranium (ppm) in the Mine area. + and ÷ means that 'mixted samples' are included and excluded respectively.

Type of data	N_s	Mean	Std. dev.	Coeff. of var.
Total sample set	3107	286.9	176.1	0.61
MC-lujavrite	944	269.1	156.1	0.58
Naujakasite lujavrite	340	371.2	123.5	0.33
Arfvedsonite lujavrite	644	369.7	162.8	0.44
Fine-grained lujavrite +	1021	370.6	150.5	0.41
Fine-grained lujavrite ÷	303	371.6	113.9	0.31
Inclusions	1103	230.0	184.6	0.80

Different types of model were fitted to the distributions of the total data set, fine-grained lujavrites (+ and +), mc-lujavrite and the inclusions, using ROKE. ROKE fits the best

model comprising a mixture of up to four normal or lognormal distributions to a given histogram. Fitting is based on a non-linear least-squares method of matching the cumulative probability curve of a model having a specified number of component distributions with the observed cumulative curve from the data (the root mean square deviation, e.g. Kennedy and Neville, 1976). The user initiates the number and type of components, and the mode, spread and proportion of each of them. The program then returns a better fit after a certain number of iterations. This process is repeated with different initial parameters and the best fit is selected. Results are presented in table 4-2. The goodness of fit is illustrated by the root mean square deviation of estimated probabilities from the observed proportions:

$$RMS = \sqrt{\frac{1}{N_{int.}} \sum (\text{Expected probability} - \text{Obs.cum.proportion})^2}$$

and a chi-square test:

$$\chi^2 = \frac{(\text{observed} - \text{expected})^2}{\text{expected}}$$

TABLE 4-2: Final estimates of components from nonlinear least-squares fitting of distributions to different groups of data. N_s is the number of samples, N_i the number of iterations and N_{cp} the number of components. RMS is the root mean square deviation (see text).

Type of data	N_s	N_i	N_{cp}	Type of distrib.	Mean	Std. dev.	%	RMS	χ^2	DF
Total sample set	3107	24	2	lognormal	148.3 367.8	156.9 147.0	35.6 64.4	$0.82 \cdot 10^{-2}$	154.7	32
MC-lujavrite	944	5	1	lognormal	274.9	172.5	100.0	$0.95 \cdot 10^{-2}$	33.7	28
Fine-grained lujavrite +	1021	7	2	lognormal	247.5 398.1	243.2 121.3	17.1 82.9	$0.44 \cdot 10^{-2}$	50.2	26
Fine-grained lujavrite ÷	303	5	1	normal	366.8	102.0	100.0	$0.13 \cdot 10^{-1}$	24.6	16
Inclusions	1103	11	3	lognormal	58.8 300.0 460.4	60.0 167.2 77.3	34.6 56.7 8.8	$0.27 \cdot 10^{-2}$	25.0	22

From the test of significance, it can be seen that the models fitted to the distributions of mc-lujavrite, fine-grained lujavrite (+) and the inclusions, can be accepted. The models of the fine-grained lujavrite (+), and especially of the total population, cannot be accepted. In figure 4-3 the histogram of the total sample set is compared with the best model comprising a mixture of two components. It is obvious that this fit is useless for identifying the individual components since the fits to some of these tend to imply a large number of components e.g. the model fitted to the inclusions comprises three components. However, the fit is reasonably good at the upper tail of the distribution and can therefore be used to calculate theoretical grade/tonnage curves for blocks of a given size (sec. 4.2.13). Not surprisingly, the best model fitted to the histogram of inclusions is complex, since it contains many types of geological units. On the other hand, it seems to be the case that the distributions of the coarse-grained and the fine-grained lujavrites can be described by simple one-component lognormal and normal models respectively.

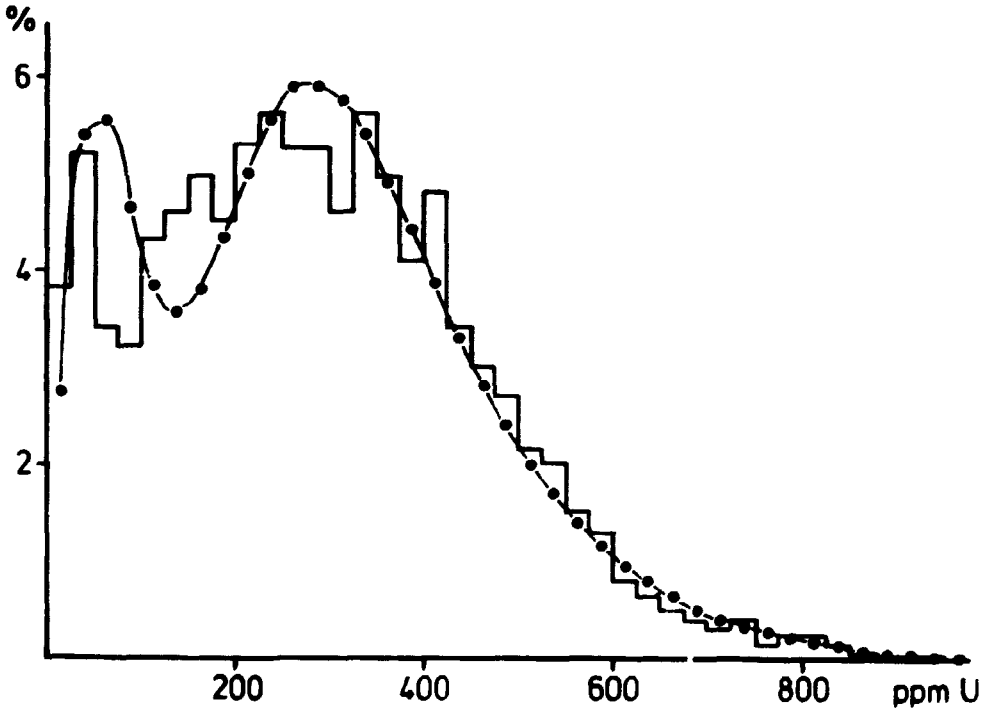

FIGURE 4-3: Best fit of a two component (lognormal) distribution to the histogram of the total Mine area drill core sample values.

4.2.2 Proportional effect.

If the mean and variance (or standard deviation) of groups of samples taken at several locations are correlated the deposit is said to be influenced by a proportional effect. Examples of proportional effects are given by Stanley (1976) and Clark (1979d). This means that if the 'local mean' shifts, the variance will also shift accordingly. Some authors (David, 1977, Guarascio, 1976) have suggested that the effect is due to values following a log-normal distribution. It has been further suggested (op. cit.) that the spatial variation represented by the semi-variogram should be corrected by dividing it by the square of the local mean before it is used for estimation. According to Clark (1979) this correction is not necessary to produce reliable estimates by geostatistics.

The local variance versus local mean is plotted in figure 4-4. 'Local' is here defined as the individual drill hole, and the

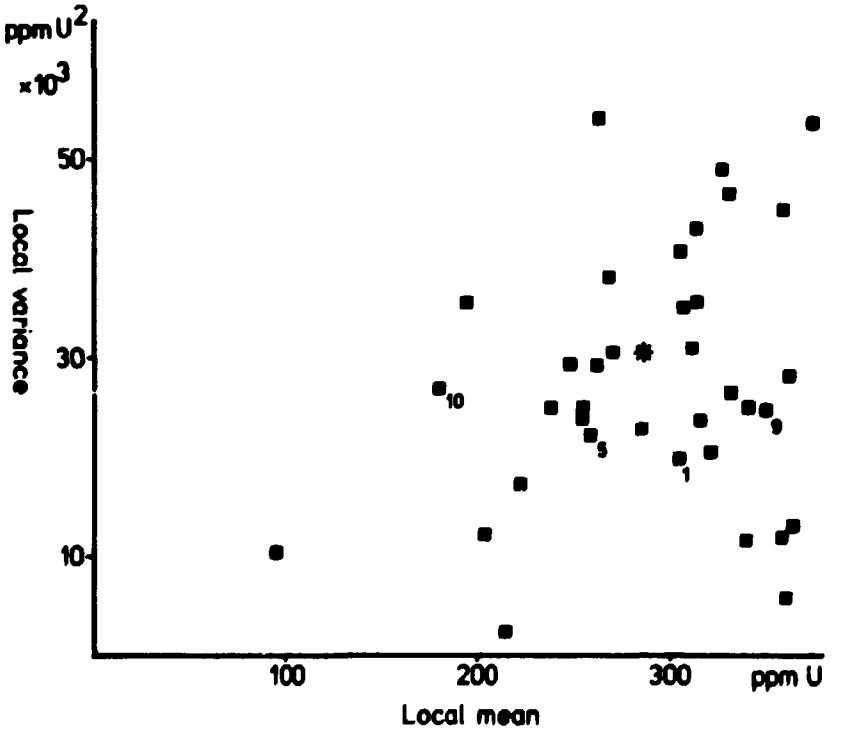

FIGURE 4-4: Testing for proportional effect in the Mine area. Each value represents one drill hole. The overall mean and variance are indicated by the star. Drill holes 1, 5, 9 and 10 are shown as they will be referred to later.

mean and variance in each of these are shown. The overall mean and variance are indicated by a star. Although the histogram of the data is highly skewed and influenced by log-normal components no significant proportional effect seems to be present. It was therefore decided to neglect this effect during the study.

4.2.3 Spatial structure, semi-variograms.

The spatial structure of the uranium values was investigated by experimental semi-variograms. It can be shown (Journel and Huijbregts, 1978) that, under the intrinsic hypothesis, an unbiased estimator of the semi-variogram $\gamma(h)$ is:

$$\hat{\gamma}(h) = \sum_{i=1}^{n(h)} \left[Z(x_i) - Z(x_i+h) \right]^2$$

where n(h) is the number of sample pairs at lag h. Calculations were carried out by the program SEMI developed at the Royal School of Mines, London (Clark, 1979b). SEMI calculates experimental semi-variograms along each individual drill hole (disregarding dip and azimuth). Secondly, vertical and horizontal semi-variograms were calculated. The horizontal ones were determined in the directions of the coordinate axes. SEMI was run on both the total set of data and on data sorted into geological units: mc-lujavrite, arfvedsonite lujavrite and naujakasite lujavrite.

As most of the drill holes in the area were vertical and because the drill hole spacing caused sample values to be independent of one another in horizontal directions (as shall be shown), only 'vertical' semi-variograms were considered. Hence, the deposit had to be considered isotropic, although strictly this is probably not the case (see chapter 6). Results are presented in figure 4-5, where experimental $\gamma^*(h)$ values are plotted versus the distance h. The curve from the total sample set shows an initial rapid increase with pronounced 'levelling

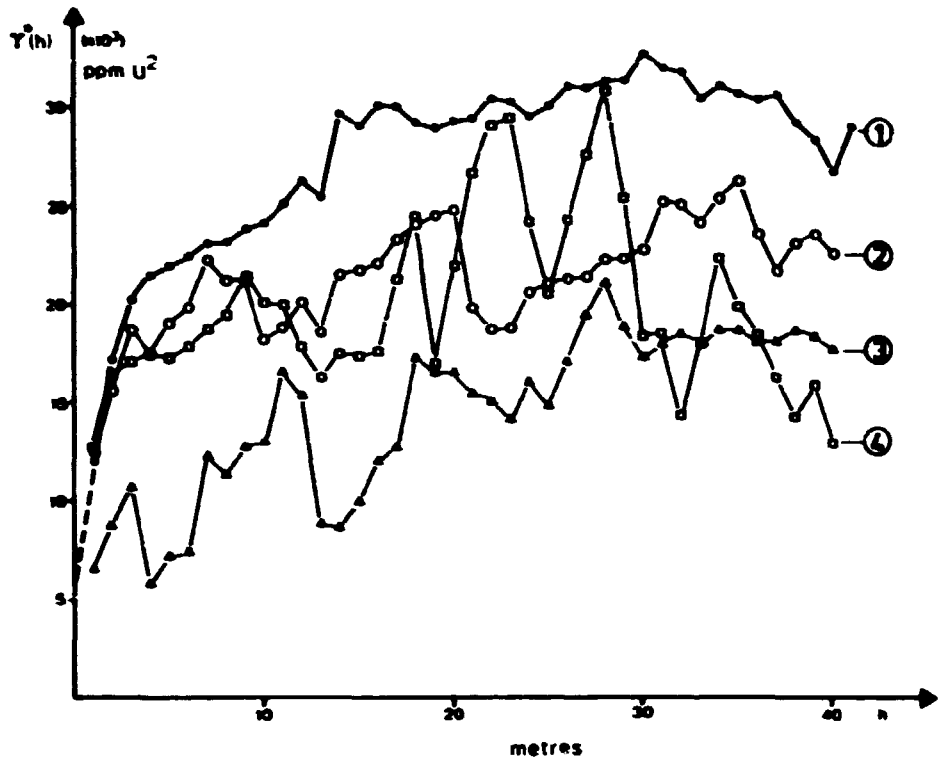

FIGURE 4-5: Experimental semi-variograms for drill hole samples in the Mine area. 1) Total sample set, 2) MC-lujavrite, 3) naujakasite lujavrite and 4) arfvedsonite lujavrite.

offs' at distances of about four metres and about thirty metres. The semi-variograms of the lujavrite types look very 'noisy' but a distinct levelling off can still be recognized after very short distances. The graph also shows an absence of drift (Journel, 1969, sec. 6.2.). As would be intuitively expected, the 'single-rock' type semi-variograms have lower values than the overall one. This is because the material within one geological unit is more homogeneous, so its values will have a lower variance. It is believed that the noisy aspect of the single rock type semi-variograms is caused by the low number of sample pairs available (figure 4-6).

In figure 4-7 the overall vertical semi-variogram is compared with semi-variograms calculated on data sets from which the mc-lujavrite samples, and then the mc-lujavrite plus inclusion samples, have been removed. Removing mc-lujavrite samples

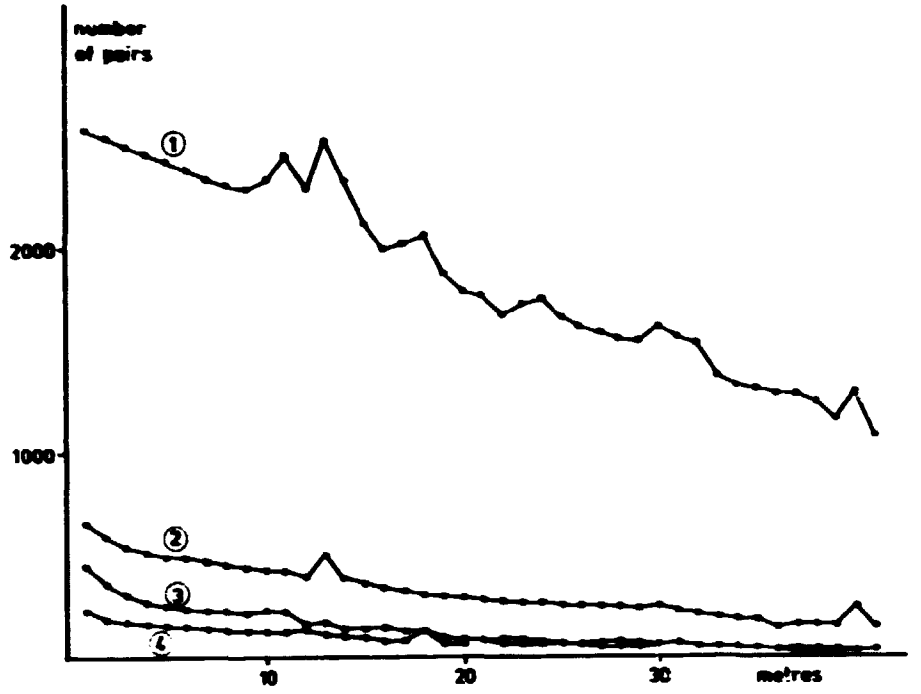

FIGURE 4-6: The number of sample pairs on which the experimental semi-variograms in figure 4-5 are based. 1) Total sample set, 2) MC-lujavrite, 3) arfvedsonite lujavrite and 4) naujakasite lujavrite.

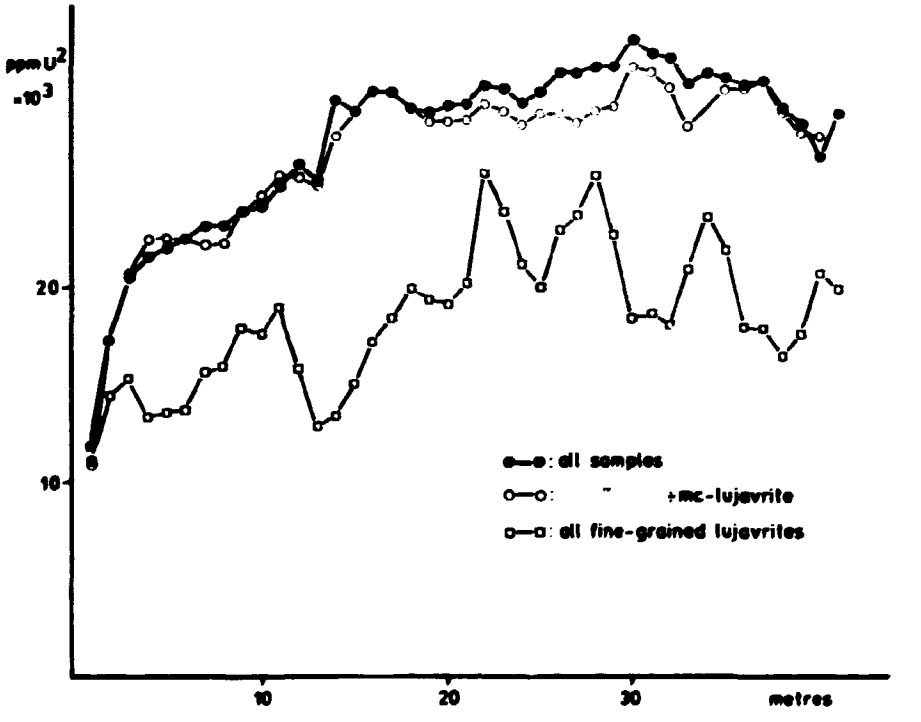

FIGURE 4-7: Experimental semi-variograms from drill hole samples in the Mine area compared with the overall semi-variogram.

hardly affects the experimental semi-variogram, indicating a very poor spatial structure for these samples. It can also be seen that if in addition the inclusions are removed the spatial structure is almost lost. This is probably due to both the low number of sample pairs and the displacement of concentration levels.

As examples, the semi-variograms from drill holes 1, 5, 9 and 10 are compared with the overall vertical semi-variogram in figure 4-8. Apart from drill hole 10, in which a strong drift seems to be present, the individual hole semi-variograms display similar features as those found in the total data set. The deviation displayed in hole 10 is probably, once again, caused by a low number of samples (34). Holes 1, 5 and 9 have lower variances than the average, as can also be seen in figure 4-4.

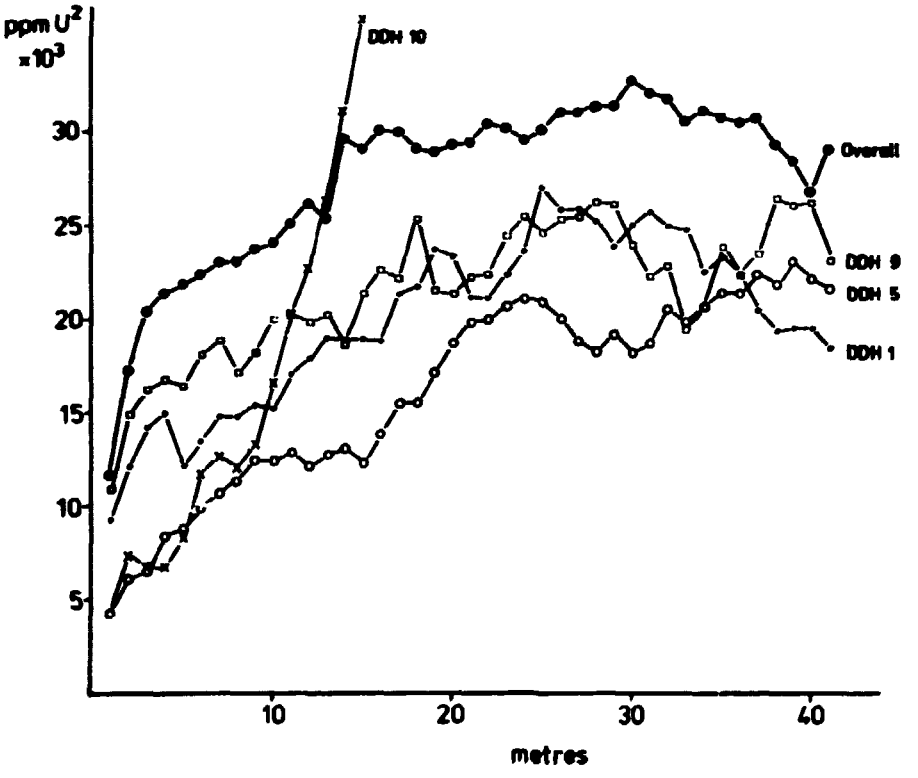

FIGURE 4-8: Experimental semi-variograms from drill holes 1, 5, 9 and 10 compared with the overall semi-variogram of the Mine area.

4.2.4 Semi-variogram modelling.

As stated earlier, the semi-variogram may take any form, but only few practical models exist (Clark, 1979a). Intuitively, if the distance h is zero the difference in grades must be zero; at small distances h there will be a finite difference in the values between samples, and at larger distances this difference tends to be greater. It is usually the case that at some distance the rate of increase in the differences tends to decrease. Then, sample values become independent of one another and their mean squared difference becomes constant. Most models of $\gamma(h)$ reflect this behaviour to some extent.

There are two main types of model - those which do not level off or reach a 'sill', and those which do. Of the former category the simplest one is the linear model (fig. 4-9) given by the formula:

$$\gamma(h) = ph$$

where p is the slope of the line. A more generalized version is the model:

$$\gamma(h) = ph^{\lambda}, \qquad 0 \leq \lambda < 2$$

but no applications of this model seem to have been published to date. The other commonly used model without a sill is the de Wijsian model, in which $\gamma(h)$ gives a straight line when plotted against $\log_e(h)$. There are only two common models with a sill (fig. 4-9), the exponential model:

$$\gamma(h) = C(1 - \exp(-h/a)), \qquad h \geq 0$$

and the spherical or Matheron model:

$$\gamma(h) = C\left[\frac{3h}{2a} - \frac{h^3}{2a^3}\right] \qquad 0 \leq h \leq a$$

$$= C \qquad h \geq a$$

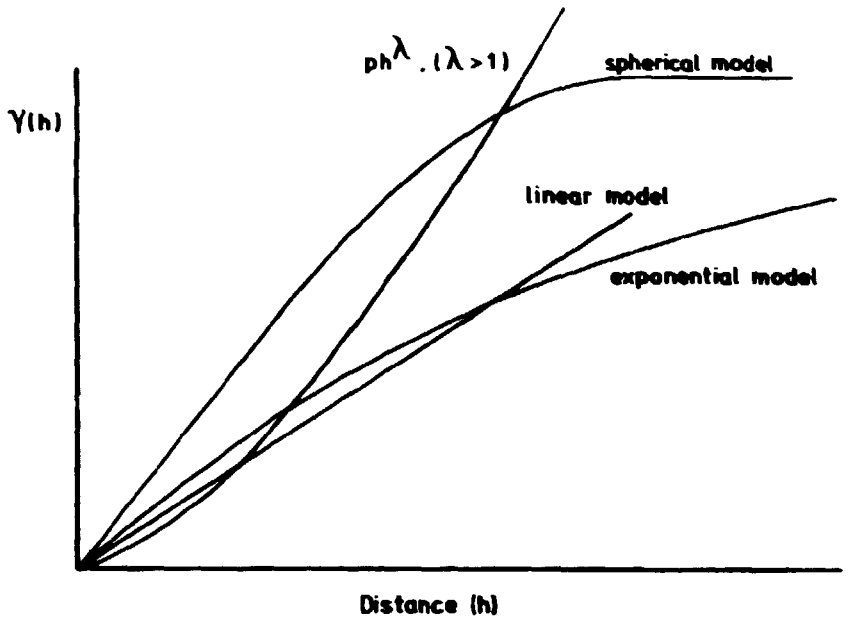

FIGURE 4-9: Different possible semi-variogram models.

In both equations C represents the value at which the graph levels off, and is termed the sill. It can be shown mathematically (Matheron, 1971) that in a truly stationary deposit C is equal to the ordinary variance of independent random samples. In the spherical model, the distance represented by 'a' is the distance at which samples become independent of one another (fig. 4-10), and it is termed the 'range of influence' of the variable. It should be mentioned that although the same symbol is used in the exponential model, the intuitive meaning is less clear. Secondly, it can be noted that the exponential model never actually reaches the sill value, but instead approaches it asymptotically.

In addition to these models, which represent idealised descriptions of continuity, there is one which represents completely random behaviour. That is, no matter how closely samples are taken they are deemed to be independent and the semi-variogram to have reached its sill:

$$\gamma(0) = 0$$

$$\gamma(h) = C \qquad h > 0$$

This model is generally called the pure nugget effect. Most semi-variograms in practice are comprised of mixtures of these models (Clark, 1979a), and this is the case for the semi-variograms modelled in the present study.

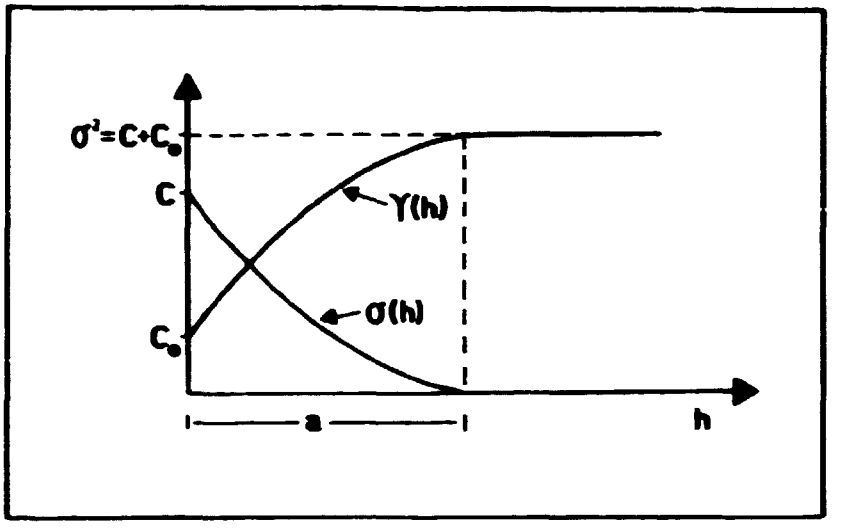

FIGURE 4-10: Relationship between the spherical semi-variogram $\gamma(h)$ and the covariogram $\sigma(h)$, C_0 is the nugget effect and C the sill value. a is called the range of influence.

Applications of the exponential model have been given by Singh (1976). An example of the De Wijsian model is found in Royle (1977b). Applications of the spherical model are legion, and seem to embrace many different types and structures of orebodies (cf. Clark, 1978, Journel, 1973, Sinclair and Deraisme, 1974). With the present study in mind, it is noteworthy that several uranium deposits have already been described by this model (Blais and Carlier, 1968, Kim and Knudsen, 1977, Guarascio, 1976, Sandefur and Grant, 1980).

The practice of semi-variogram modelling is found in Clark (1979a). Only the overall semi-variogram was modelled and used in the present study, because of the difficulties in fitting stable models to the individual geological types due to low numbers of samples available for each type. It can be seen from figure 4-5 that the overall semi-variogram has a high nugget effect, of $\simeq 5.6 \times 10^3$ ppm U^2. There appears to be an intermedi-

ate sill at 22 x 10^3 ppm U^2 and a final sill at 31 x 10^3 ppm U^2. Consequently, the semi-variogram is expected to comprise two spherical components and a nugget effect (C_o). Trial and error, using program FGAM2 (Appendix A), was used to estimate the parameters of this model and a first approximation is given by:

$$C_o = 5600 \text{ ppm } U^2$$

$$a_{1\ell} = 3.5 \text{ metres}, \quad C_{1\ell} = 13600 \text{ ppm } U^2$$

$$a_{2\ell} = 30.0 \text{ metres}, \quad C_{2\ell} = 11800 \text{ ppm } U^2$$

The subscript ℓ is used to emphasize that the model is only an approximation, since the 'samples' used to calculate the experimental semi-variogram were actually drill core sections of length ℓ (1 metre). The full (core) model can be written mathematically as follows:

For distances h less than 3.5 metres:

$$\gamma^*_\ell(h) = 5600 + 13600\left(\frac{3h}{7} - \frac{h^3}{2(3.5)^3}\right) + 11800\left(\frac{3h}{60} - \frac{h^3}{2(30)^3}\right)$$

for distances between 3.5 metres and 30.0 metres:

$$\gamma^*_\ell(h) = 19200 + 11800\left(\frac{3h}{60} - \frac{h^3}{2(30)^3}\right)$$

and for distances greater than 30.0 metres:

$$\gamma^*_\ell(h) = 31000$$

The model can be seen in figure 4-11.

The same type of nested model was used by Guarascio (1976) to describe a stratiform uranium deposit. High nugget effects within a roll front uranium deposit have been mentioned by Sandefur and Grant (1980).

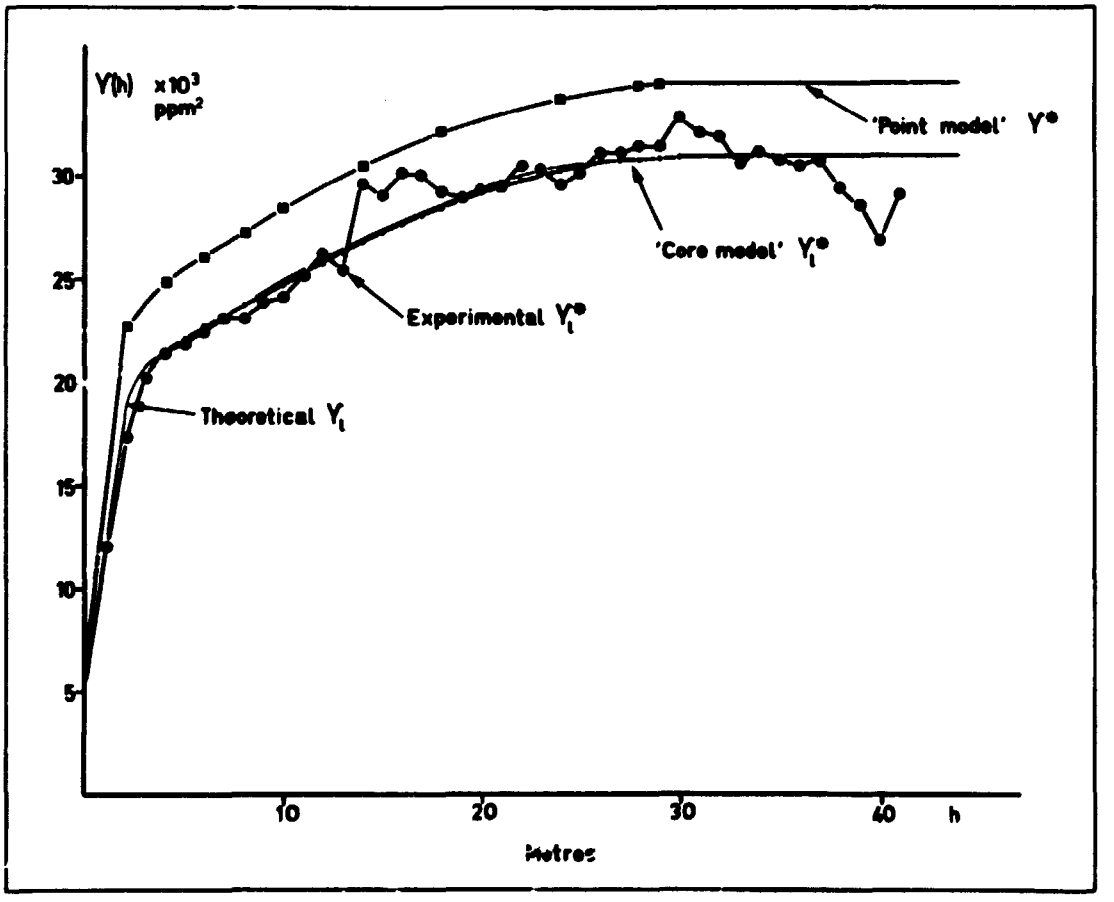

FIGURE 4-11: Semi-variogram models for drill core samples in the Mine area. Two component spherical models (+ nugget effect) are used.

4.2.5 Testing the semi-variogram model, point kriging.

The question which may arise after fitting three components to the model semi-variogram is: 'What happens if this model is used to describe the local spatial behaviour although in fact it has been estimated globally?'. One way to answer this question is simply to compare local semi-variograms with the overall one as has been done in figure 4-8. However, it is

necessary to quantify the comparison. Before this can be done, the final goal of geostatistics, namely estimation, is reviewed briefly.

The estimation procedure used in RV theory is called 'kriging' to honour Danie Krige and his work on weighted moving averages. Kriging assumes the intrinsic hypothesis to be satisfied and gives the best linear unbiased estimator (BLUE) for an unknown volume, area, or point A, given a set of samples g_i with known values $Z(x_i)$.

It can be shown that the estimation variance of the general unbiased linear estimator is given by (Brooker, 1979):

$$\sigma_\varepsilon^2 = 2\sum_{i=1}^{n} w_i \bar{\gamma}(g_i,A) - \sum_{i=1}^{n}\sum_{j=1}^{n} w_i w_j \bar{\gamma}(g_i,g_j) - \bar{\gamma}(A,A)$$

where w_i is the i'th weight given to the i'th sample and $\bar{\gamma}(g_i,A)$ is the mean semi-variogram value between g_i and V_i. The first term of the expression is the estimation error introduced when <u>all</u> points within A are estimated from the g_i's. Since it is the <u>mean</u> of A, and not all points within A, which is estimated, the variance between all points within A ($\bar{\gamma}(A,A)$) must be subtracted. The actual estimator has the form:

$$Z^*(A) = \sum_{i=1}^{n} w_i Z(x_i)$$

i.e., it is a weighted <u>average</u> of the samples. Since the first term of the variance expression takes the <u>individual</u> samples into account the variance between samples has to be subtracted (second term). The optimal weights are obtained by minimizing the expression for σ_ε^2 under the non-bias condition $\Sigma w_i - 1 = 0$ using the Lagrangian Multiplier:

$$\frac{\delta}{\delta w_i}(\sigma_\varepsilon^2 - \lambda(\sum w_i - 1)) = 0$$

which yields a set of equations of the form:

$$w_j\bar{\gamma}(g_i,g_j) + w_{i+1}\bar{\gamma}(g_i,g_{j+1}) + \ldots + w_n\bar{\gamma}(g_i,g_n) + \lambda = \bar{\gamma}(g_i,A)$$

The complete kriging system, which has to be solved to obtain the weights $w_1,w_2\ldots,w_n$, can be expressed as the matrix shown in figure 4-12. It can be shown that the minimum estimation variance, called the kriging variance, can be written as:

$$\sigma_k^2 = w_i\bar{\gamma}(g_i,A) + \lambda - \bar{\gamma}(A,A)$$

A fully worked out example of kriging using the overall semi-variogram model from the Mine area is given in appendix B.

Having defined kriging one may return to the question of how putative semi-variogram models can be compared. If the models are used to estimate known values it is possible to get a measure of the error of estimation by comparing the true values

$$\begin{bmatrix} \bar{\gamma}(g_1,g_1) & \bar{\gamma}(g_1,g_2) & \ldots & \bar{\gamma}(g_1,g_n) & 1 \\ \bar{\gamma}(g_2,g_1) & \bar{\gamma}(g_2,g_2) & \ldots & \bar{\gamma}(g_2,g_n) & 1 \\ \vdots & \vdots & & \vdots & \vdots \\ \bar{\gamma}(g_n,g_1) & \bar{\gamma}(g_n,g_2) & \ldots & \bar{\gamma}(g_n,g_n) & 1 \\ 1 & 1 & \ldots & 1 & 0 \end{bmatrix} \cdot \begin{bmatrix} w_1 \\ w_2 \\ \vdots \\ w_n \\ \lambda \end{bmatrix} = \begin{bmatrix} \bar{\gamma}(g_1,A) \\ \bar{\gamma}(g_2,A) \\ \vdots \\ \bar{\gamma}(g_n,A) \\ 1 \end{bmatrix}$$

$$\mathbf{A} \qquad\qquad \mathbf{X} \qquad \mathbf{B}$$

FIGURE 4-12: The kriging matrix system. The A-matrix contains the inter-sample relations, while B contains the sample-block relations. w_i are the weights assigned to the samples and λ the Lagrangian Multiplier.

(the $Z(x_i)$'s) with the estimates (the $Z^*(x_i)$'s). The program PTKR has been developed at the University of Leeds for this purpose. The program, which is documented in Ahlefeldt-Laurvig (1981), reads a finite number of data points and the value of the RV at each of these. Then, the value at each point is estimated from its neighbours using a specified semi-variogram model. The point being estimated is removed from the subset of points, as kriging is an exact interpolator and leaving this point in would merely recover its value exactly.

In this study, individual models were fitted to the semi-variograms of drill holes 1, 5 and 9. The models are illustrated in figure 4-13 and the parameters are listed in table 4-3. Drill hole 5 is described by a one-component spherical model (plus nugget effect) and drill holes 1 and 9 by a two-component spherical model (plus nugget effect). For each drill hole, PTUK was run with the 'local' semi-variogram model and the overall model. The following statistics were calculated:

(a) The mean algebraic error of estimation $S1 = E\{Z-Z^*\}$.
(b) The mean absolute error of estimation $S2 = E\{|Z-Z^*|\}$.
(c) The mean squared error of estimation $S3 = E\{(Z-Z^*)^2\}$.
(d) The mean kriging variance of estimation $\bar{\sigma}_K^2$
(e) The number of points estimated N_{pts}.

TABLE 4-3: Parameters for the spherical models fitted to experimental semi-variograms. N_{spc} is the number of spherical components in the model.

Drill hole	N_{spc}	C_o	a_1	C_1	a_2	C_2	Total sill
1	2	6400	3.5	6300	30.0	11000	23700
5	1	4000	-	-	27.0	17000	21000
9	2	7000	3.0	7800	30.0	9600	24400
'Overall'	2	5600	3.5	13600	30.0	11800	31000

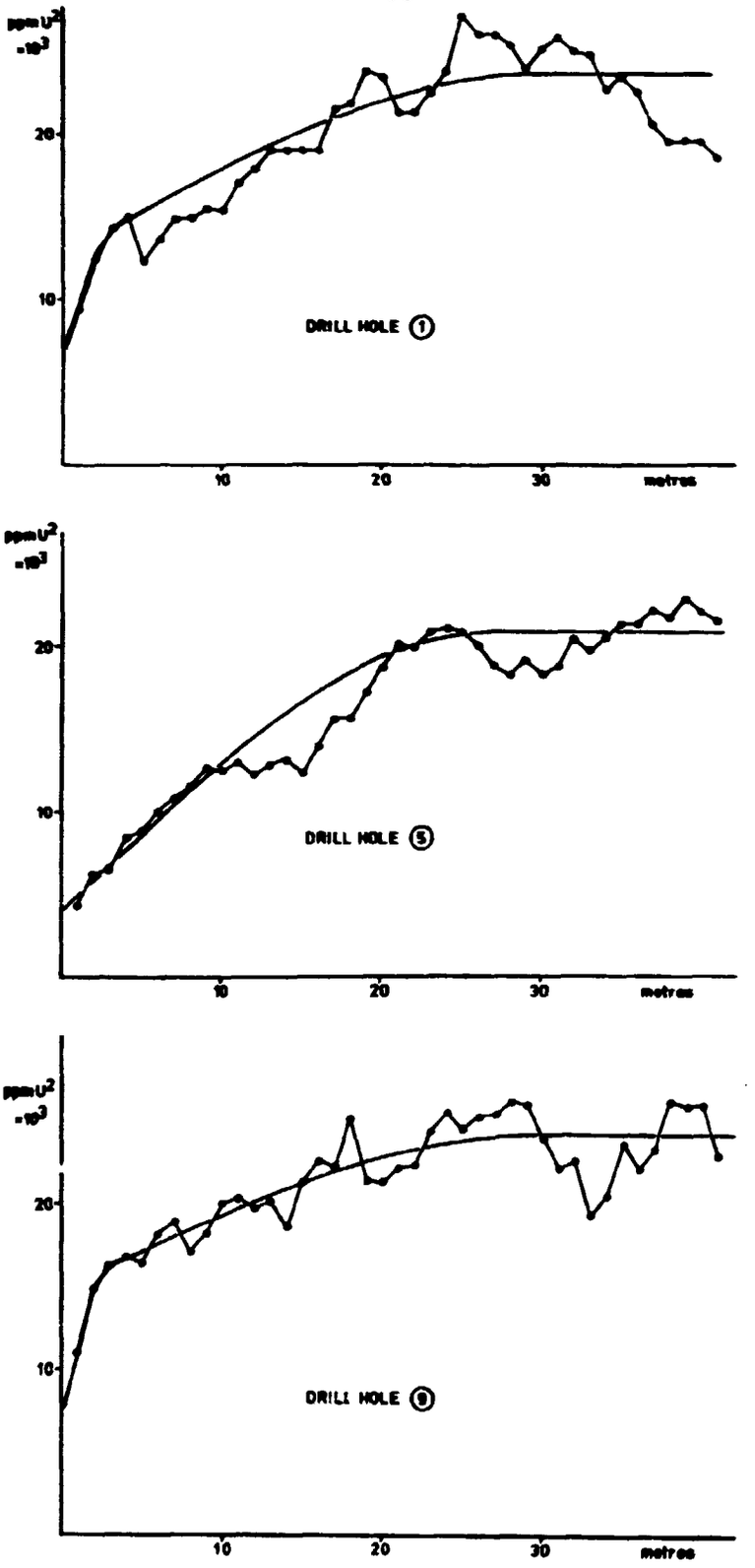

FIGURE 4-13: Models fitted to the experimental semi-variograms of individual drill holes. Drill hole 5 is modelled by a one-component spherical scheme, while 1 and 9 are modelled by two-component spherical schemes.

The following checks are made (Royle, 1977a). 1) The mean algebraic error of an unbiased estimator is zero, and the S1 statistic should therefore be acceptably small. A good criterion (A.G. Royle, pers. comm.) is that S1 is smaller than 1% of the mean value of the variable being estimated. 2) The S2 statistic is a minimum. Setting an acceptable criterion for this value is difficult and a matter of experience. Hence the usefulness of S2 is limited. 3) The S3 statistic is used directly to compare the errors produced by different models. However, the expected value of the squared error of estimation is equal to the mean kriging variance. The S3 statistic can therefore be used to check that the value of σ_K^2 is neither too optimistic nor too pessimistic. A 10% deviation is acceptable. Because the prediction of values at points is a severe test, high kriging variances can be expected and only points with at least twelve (or so) data points around them should be kriged (op. cit.). The results from PTKR are listed in table 4-4. It can be seen from the statistics S1, S2 and S3 that the estimator is unbiased and that the estimates are not sensitive to changes in the semi-variogram model. That is, kriging is a robust estimator.

TABLE 4-4: Results from point-kriging of different sets of data using a local and the overall semi-variogram model. The statistics S1, S2 and S3 are explained in the text. N_s is the number of samples estimated. S1 and S2 are given in ppm U, S3 and $\bar{\sigma}_k^2$ in ppm U^2.

Sem.-var model	Hole	N_s	N_{spc}	S1	S2	S3	$\bar{\sigma}_k^2$
Local	1	154	2	-0.315	77.86	11333	11837
Overall			2	-0.619	77.43	11512	14520
Local	5	110	1	-0.266	55.36	5640	5914
Overall			2	0.071	56.33	5748	14137
Local	9	108	2	0.294	85.94	13503	13666
Overall			2	0.121	85.97	13636	14209
Overall	All	2703	2	-0.671	80.39	14307	14333

The values of the mean kriging variance, however, display a high sensitivity to changes in the model. The magnitudes of the σ_K^2's are acceptable for all three holes if the local model is used. But, using the global model, far too high values are obtained in holes 1 and 5. It is therefore essential to use the correct semi-variogram model if a reliable measure of the estimation variance is required.

Good results were obtained when all drill core samples in the Mine area were estimated using the overall model (table 4-4). The estimator still appears to be unbiased (S1), and the S3 statistic is almost equal to σ_K^2. This again gives credibility to the fit of the overall model.

4.2.6 Stability of the experimental semi-variogram.

It is known that the estimator used to produce the experimental semi-variogram (sec. 4.2.3) is an unbiased estimator of the underlying intrinsic function. It is therefore interesting to test how stable this estimate of the intrinsic function is. For example: how does the experimental semi-variogram change if the amount of information changes? This was tested by calculating the overall semi-variogram for sample sets from which different number of samples were removed at random. With the use of a random number generator data sets from which 10%, 20%, 30%, 40%, 50%, 60% and 75% of the samples had been removed were constructed. The experimental semi-variograms of these data sets were compared with the overall semi-variogram, see figure 4-14. The semi-variogram of 75% sample deletion is marked with open circles on the graph. It can be seen that the spatial structure in the Mine area remains unchanged, although fluctuations occur, even if 60% of the samples are removed. Removing 75% of the samples caused a total loss of structure. An apparent confidence interval for the semi-variogram is subjectively indicated on the graph. Since the core model lies well within this interval it is concluded that the overall model is stable and that enough information is available to describe the spatial structure of the uranium values sufficiently well.

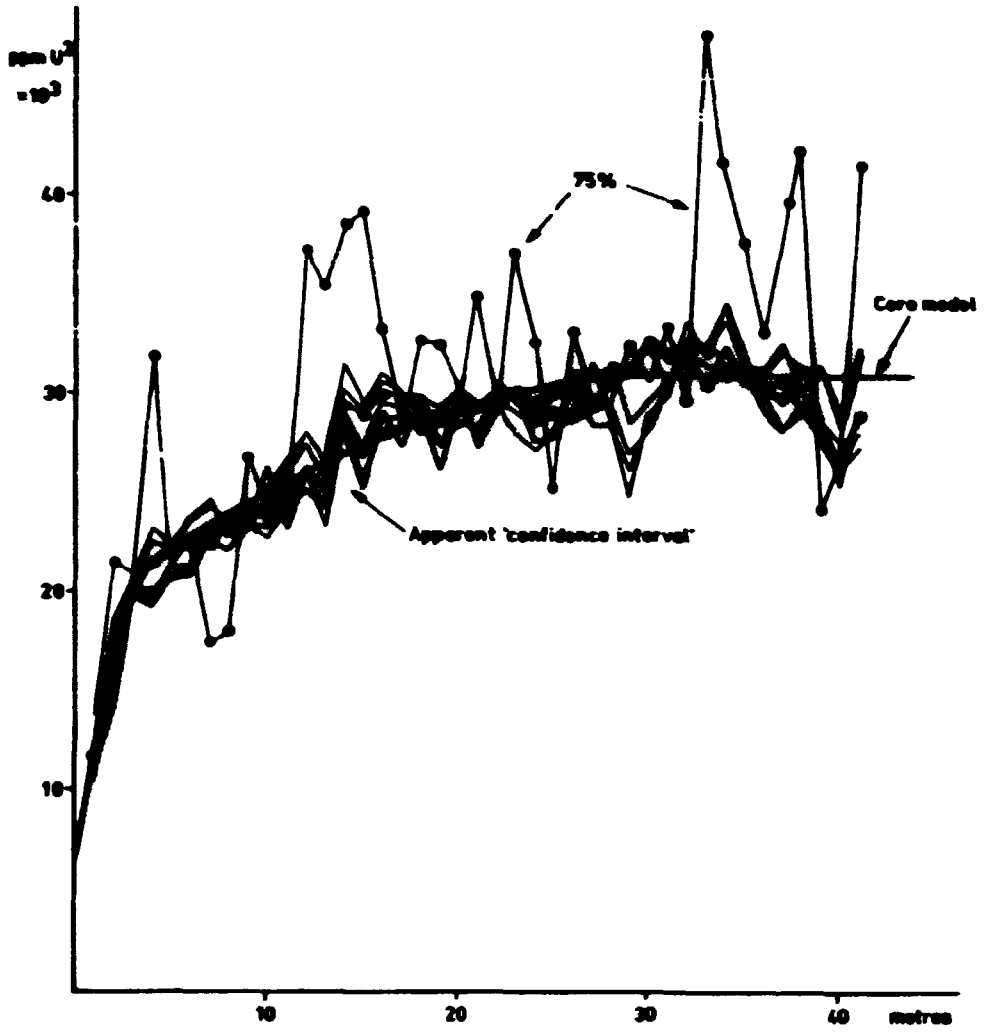

FIGURE 4-14: Experimental semi-variograms calculated on sample sets after 10%, 20%, 30%, 40%, 50%, 60% and 75% of the samples have been removed. An apparent confidence interval is shown. The overall semi-variogram (0% removed) is shown with black dots.

4.2.7 Deregularisation.

As can be seen from the kriging system in figure 4-12, kriging is based on the mean γ-values between the samples, and between the samples and the volume being estimated. The definition of 'mean γ-value' is that every point within a sample should be compared with every point in another sample or in the volume being estimated. The easiest way to proceed is to operate with simple 'supports' of data, and in practice many kriging pro-

grams assume the data are located at points. The subject which examines different sample supports and the corresponding variances is known as 'the volume-variance relationship'. Detailed descriptions of volume-variance calculations are found in Parker (1979) and in Clark (1979a) (see also appendix B). It is obvious that if the semi-variogram is based on drill core sections of length ℓ, both the range of influence and the sill value (the variance) are influenced by volume regularisation. As a rule of thumb, this effect can be disregarded if the sample length is less than 10% of the range of influence. In the present case the spatial behaviour as described by γ_ℓ^* is based on one metre core samples. Since the model comprises a spherical component with a range of influence of 3.5 metres it is necessary to correct the regularised core model to produce the deregularised needed for estimation. The regularised semi-variogram as calculated 'down-the-hole' can be written:

$$\gamma_\ell(h) = \bar{\gamma}(\ell,\ell+h) - \bar{\gamma}(\ell,\ell)$$

where $\bar{\gamma}(\ell,\ell+h)$ is the mean semi-variogram value between two core samples of length ℓ at a distance h apart:

$$\bar{\gamma}(\ell,\ell+h) = \frac{1}{\ell^2}\int_0^{\ell}\int_0^{h+\ell} \gamma(n' - n'')dn'dn''$$

n' and n'' are points located within separate cores. $\bar{\gamma}(\ell,\ell)$ is the mean semi-variogram value within one core, usually written as:

$$\bar{\gamma}(\ell,\ell) = F(\ell)$$

$$= \frac{1}{\ell^2}\int_0^{\ell}\int_0^{\ell} \gamma(n' - n'')dn'dn''$$

i.e. n' and n'' are now located within the same core. From this general expression the range of influence of the spherical deregularised model can be derived (Clark, 1977b):

$$a_{points} = a_{\ell} - \ell$$

and the sill value:

$$C_{\ell} = \frac{C}{20}\left[20 - 10\frac{\ell}{a} + \frac{\ell^3}{a^3}\right], \qquad \ell \leq a$$

$$C_{\ell} = \frac{C}{20}\,\frac{a}{\ell}\left[15 - 4\frac{a}{\ell}\right], \qquad \ell \geq a$$

Using the first approximation for the core model, a deregularised model was constructed. The theoretical regularised curve given by this model for samples of length of one metre can then be computed and compared with the experimental semi-variogram, as previously described. Using this process, the deregularised model was found to comprise two spherical components and a nugget effect with parameters:

$$C_0 = 5600 \text{ ppm } U^2$$

$$a_1 = 2.5 \text{ metres}, \quad C_1 = 16930 \text{ ppm } U^2$$

$$a_2 = 29.0 \text{ metres}, \quad C_2 = 12000 \text{ ppm } U^2$$

$$\text{Total sill: } C_1+C_2+C_0 = 34530 \text{ ppm } U^2$$

This model implies that samples up to two and a half metres apart are highly spatially correlated, and about 25% of the total variation is random. Samples up to 29 metres apart are also correlated, but to a much weaker extent as now the random component accounts for 69% of the total variation. This factor is clearly seen in the difference between the deregularised model and the regularised one (experimental or theoretical) in figure 4-11. It may be noted that the nugget effect remains unchanged during the deregularisation as no better estimate of its value can be made (Rendu, 1978).

4.2.8 Interpretation of the semi-variogram model.

The experimental semi-variograms of the individual lujavrite types (fig. 4-5) and other combinations of data (figs. 4-7, 4-8) show that a simple interpretation of the overall semi-variogram is not possible. The fact that drill hole 3 can be described by a one-component model and that mc-lujavrite is not present in this hole may indicate that this rock-type contributes significantly to a structure with a very small range of influence. The semi-variogram of the data after the removal of mc-lujavrite samples shows, however, that other geological units contribute to this structure as well.

The effect of the individual components is demonstrated when they are used alone or in different combinations for estimation. Consider the situation in figure 4-15. The aim of the study is to investigate the effect on kriging when panel A is estimated from the samples g_1 and g_{2i}, i=1,..,4, using different semi-variogram models. These models, shown in figure 4-16, are different combinations of the components which contribute to the overall Mine area deregularised model. All models have the same sill value. A full description of kriging, especially the calculation of the $\bar{\gamma}$-terms of the kriging system, is given in appendix B. As kriging weights can be calculated independently of the actual values of the samples, only the kriging

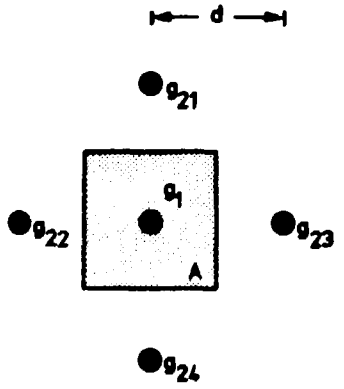

FIGURE 4-15: Pattern of samples used for two-dimensional kriging examples. The panel A is estimated from the internal sample g_1 and the external samples g_{2i}.

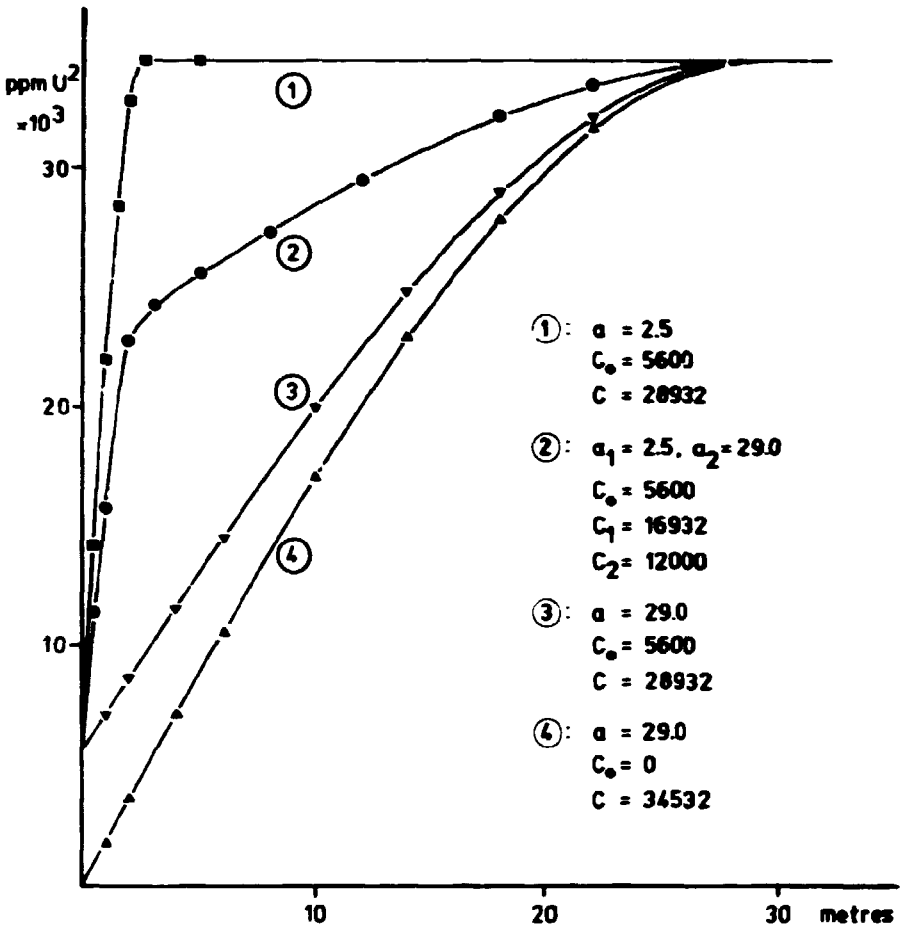

FIGURE 4-16: Semi-variogram models used in the practical kriging example.

variance and weights w_i are considered. Results from two-dimensional kriging are listed in table 4-5, where an arbitrary value of 10 metres is given to d (fig. 4-15). w_1 is the weight given to the internal sample (g_1) and w_2 the weight given to one of the external samples, which, by symmetry, are all equal. The effects of the spherical component with a short range of influence, and the nugget effect, are clearly seen. When the nugget effect and the small scale component are removed estimation is considerably improved. The small scale model is, however, nothing other than an additional nugget effect at distances exceeding 2.5 metres. It is also seen that, for this sample/block pattern, the weight given to the internal sample increases as the random variation is reduced. In fact, if the

model expresses a purely random behaviour the weights given to the samples are the same.

This example shows that even if close sampling is used, the semi-variogram model of the Mine area will always produce estimates with high estimation errors.

TABLE 4-5: Kriging weights and kriging variances using different semi-variogram models (Fig. 4-16). The panel A in Fig. 4-15 is estimated.

Semi-var. model	w_1	w_2	σ_k^2
1	0.220	0.195	7139
2	0.277	0.181	5650
3	0.454	0.137	2745
4	0.594	0.102	1246

4.2.9 Effect of the scale of estimation.

The kriging weights and errors are influenced by the scale of estimation. This can be demonstrated again using figure 4-15 where panel A is to be estimated from the available samples. What will be investigated is the behaviour of the kriging variance and the sample weights when the scale, that is the distance d, is changed. The sample/block pattern and the semi-variogram model, i.e. the overall deregularised model, are kept unchanged.

The kriging results are listed in table 4-6 and plotted on figure 4-17 using a logarithmic distance axis. Values 1, 2, 5, 10, 25, 50 and 100 were given to d. Because of the non-bias condition the graphs of w_1 and w_2 lie symmetrically about the line y = 0.5. It can be seen that the weights given to the external samples increase as the scale is enlarged. However, the relationship is not a simple one since the curves exhibit local

TABLE 4-6: Effect of the scale of estimation as demonstrated by kriging weights and the kriging variance. λ is the Lagrangian Multiplier.

d	w_1	w_2	$\bar{\sigma}_k^2$	λ
1	0.427	0.143	2746	519
2	0.489	0.128	3819	1703
5	0.316	0.171	5685	3579
10	0.277	0.181	6068	3739
25	0.327	0.168	7310	5067
50	0.258	0.185	7534	6365
100	0.214	0.197	7191	6787

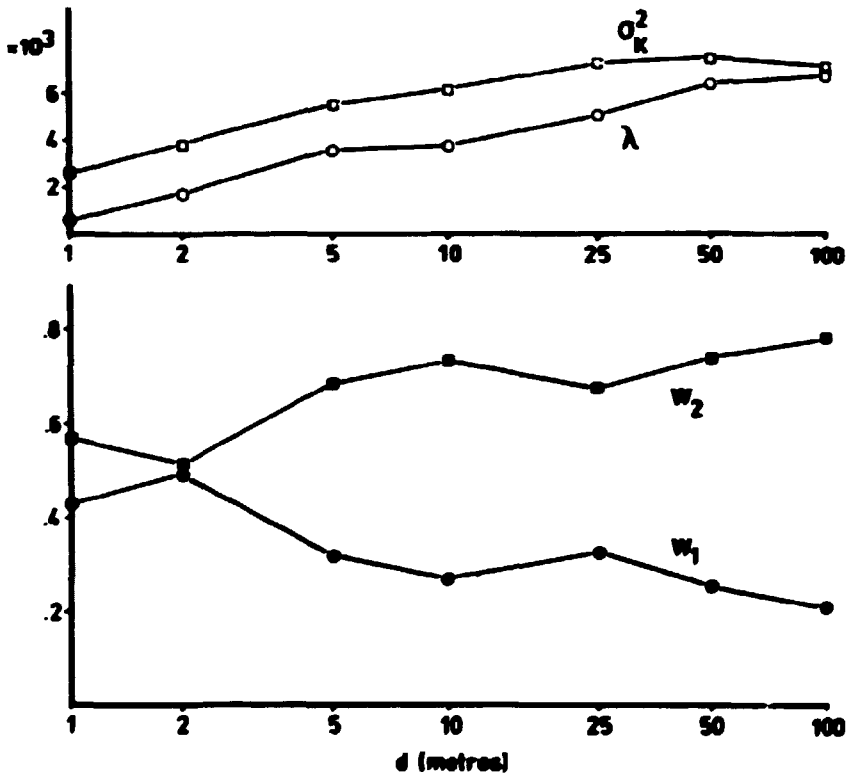

FIGURE 4-17: Curves of kriging variance (σ_k^2), the Lagrangian Multiplier (λ) and sample weights (w_i) versus the scale of estimation.

minima or maxima at distances close to the ranges of influence of the two spherical components. The kriging variance increases as the scale is enlarged, but tends to level off at distances greater than 50 metres. The reduction in the kriging variance (4.5%) between d=50 metres and d=100 metres is probably caused by small rounding off errors in the Lagrangian Multiplier during matrix operations. The magnitude of this quantity fully supports such deviations (fig. 4-17).

A clearer understanding of the behaviour of the kriging variance can be obtained when the individual terms of the equation (apart from λ) are examined:

$$\sigma_k^2 = \sum \bar{\gamma}(g_i,A)w_i + \lambda - \bar{\gamma}(A,A)$$

In figure 4-18 the contribution to the $\bar{\gamma}(g_i,A)w_i$ term and the $\bar{\gamma}(A,A)$ term are plotted for the two spherical components. The actual values are listed in table 4-7. It can be seen that although the range of influence of the first spherical component is 2.5 metres, it contributes to a reduction in the kriging variance at distances d up to 10 metres. For the second spherical component, variance reduction is present up to at least d=100 metres. This behaviour can be explained by the fact that

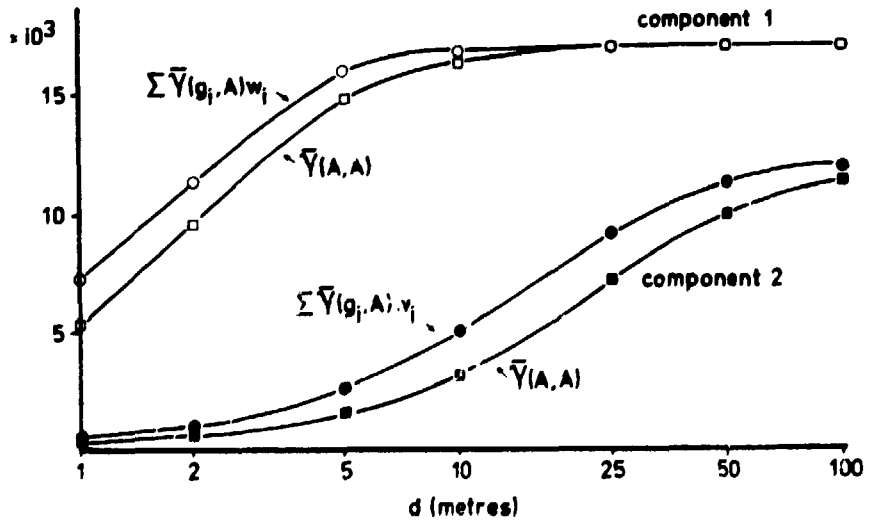

FIGURE 4-18: Curves of mean semi-variogram values versus the scale of estimation.

TABLE 4-7: Contribution to the individual terms of the kriging variance from each spherical component in the s-v model.

	$\Sigma\bar{\gamma}(g_i,A)/w_i$		$\bar{\gamma}(A,A)$	
d	Comp.1	Comp.2	Comp.1	Comp.2
1	7297	661	5164	624
2	11353	1124	9550	772
5	16091	2481	14934	1584
10	16749	5119	16356	3132
25	16899	9228	16932	7152
50	16932	11347	16932	10068
100	16932	11851	16932	11436

even at distances greater than the range of influence small parts of the panel will still either be within the range of influence of the internal sample, or within other parts of the panel (the $\bar{\gamma}(A,A)$-term). This can be illustrated if the individual $\bar{\gamma}$-terms between the samples and the panel are examined with respect to the two spherical components (figure 4-19, table 4-8). $\bar{\gamma}$-values have been standardised by their sill value in order to make comparisons easier. The curves for the first spherical component show that the external samples appear as a random variation at distances greater than 2.5 metres, whereas the internal sample still exhibits some spatial variation at distances of 10 to 25 metres. The same relationship is seen with the second spherical component at larger distances.

It is the author's opinion that the previous examples illustrate the effect of a spherical component and its contribution to kriging. Secondly, the advantage of kriging over conventional methods has been illustrated. It has been demonstrated that the variance of estimation (the kriging variance) is increased when the relationship between samples and the unknown volume is affected by an increasingly higher random variation.

If the spatial variation is not considered, estimates are only comparable with the kriging results for very large values of d.

TABLE 4-8: Sample-block semi-variogram values from each spherical component. Values are standardised by the individual sill value.

	Component 1		Component 2	
d	g_1	g_{2i}	g_1	g_{2i}
1	0.227	0.583	0.019	0.082
2	0.439	0.892	0.039	0.146
5	0.843	~1	0.098	0.257
10	0.961	~1	0.193	0.516
25	0.994	~1	0.468	0.915
50	~1	~1	0.789	~1
100	~1	~1	0.942	~1

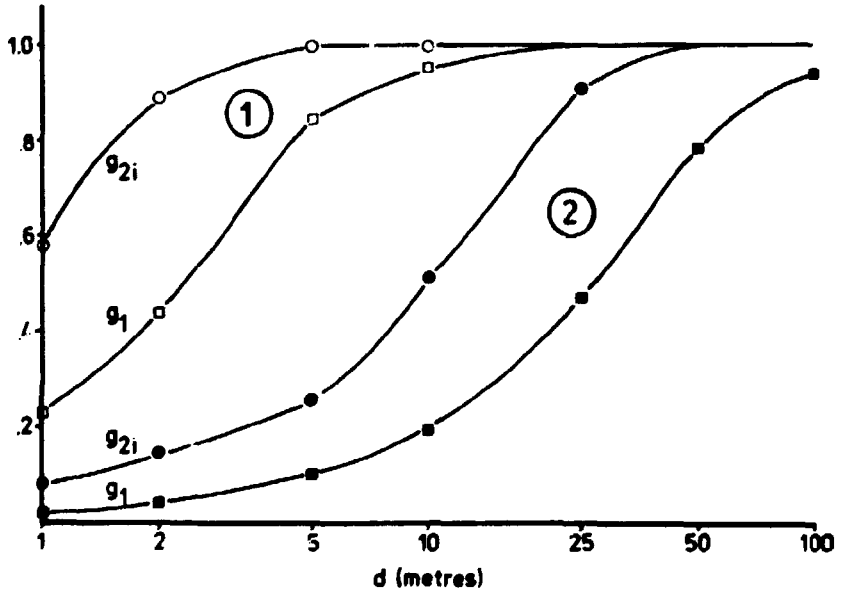

FIGURE 4-19: Mean semi-variogram values between sample and panel ($\bar{\gamma}(g_i,A)$) in the practical kriging example. 1) First spherical component (a=2.5 m), 2) second spherical component (a=29 m). Values have been standardised by their sill values.

4.2.10 Block kriging.

Having established a model for the spatial variation of deregularised values and defined the basic tool for estimation, kriging, attention is next turned to the primary aim of grade-tonnage calculations. In the estimation of any volume of ground from a given set of samples two immediate problems arise:

(a) What size and shape of blocks should be used?

(b) How should the block pattern be orientated with respect to the drill holes?

At a later stage in development, when a mine plan is being drawn up and decisions have been made about the mining method and so forth, these questions will be settled automatically. At this stage, however, the positions of the blocks and especially their size will have significant effects on the estimates of the global ore reserves. Generally, large blocks intersected by many boreholes will yield small estimation variances, i.e. give more reliable figures. On the other hand, if large blocks are chosen, only a poor distinction between ore and waste is possible. Since the Kvanefjeld uranium deposit contains a large quantity of barren inclusions, a smaller block size would be more desirable. The estimates of the values of small blocks will, however, have much larger estimation variances, eventually reaching a level where estimation is totally unreliable.

4.2.10.1. Block size determination. In view of the above considerations a random stratified grid (RSG) was fitted to the relatively sparse drilling pattern. The advantage of the RSG (Royle, 1977d) is mainly that estimation is more efficient, since equal-sized blocks are used and because each block is estimated with about the same amount of error. The first estimate for the size of the RSG is obtained by dividing the area of interest by the number of drill holes. If the distribution of drill holes is uniform in space, a square RSG will probably give a good coverage. A number of different RSG's, e.g. block sizes 50 by 50, 60 by 60, and 70 by 70 metres, were drawn on tracing paper at 1:2000 and moved over the drill hole plan. A

remarkably good fit was found for a 50 by 50 metres RSG. Most grid squares contained one hole, two contained no holes and two contained two holes each. The two grid squares with no drill hole intersection were included because they were surrounded by blocks containing drill hole information, figure 4-20. This gave a total of 39 blocks to be estimated on each bench. The location and orientation of the RSG is described in section 3.1 (CS_{mine}) and can be seen in plate 1.

4.2.10.2 3-Dimensional kriging. Many ore deposits can be considered as being two-dimensional e.g. tabular massive sulphides, sedimentary placer deposits etc. The estimation of these by block kriging is easy, since mean semi-variogram values are determined in two dimensions. Several auxiliary functions have been developed for this purpose and charts e.g. Rendu (1978), tables e.g. Royle (1977c) and subroutines Clark (1976) are available. The practice of kriging in these cases is described by David (1976).

On the other hand deposits like porphyry coppers and other large dissiminated deposits, including the Kvanefjeld uranium deposit, cannot be reduced to a two-dimensional problem. Hence, estimation has to be considered in three dimensions and the following problems are introduced:

(1) How can the semi-variogram be calculated in three dimensions?

(2) Having solved (1), how can $\bar{\gamma}$-values between samples and a 3-D block, and within the block, be calculated?

Since calculations of an experimental semi-variogram throughout the whole space are somewhat heavy on computer time, semi-variograms are often calculated one-dimensionally in each of the three main directions of the ore body i.e. north-south, east-west and vertically. If the spatial variation is isotropic only one model is considered, otherwise an anisotropy factor is introduced for each direction, (Clark, 1979a). Examples of such calculations are presented in chapter 6. As stated earlier the drill hole spacing in the Mine area frustrates calculations in

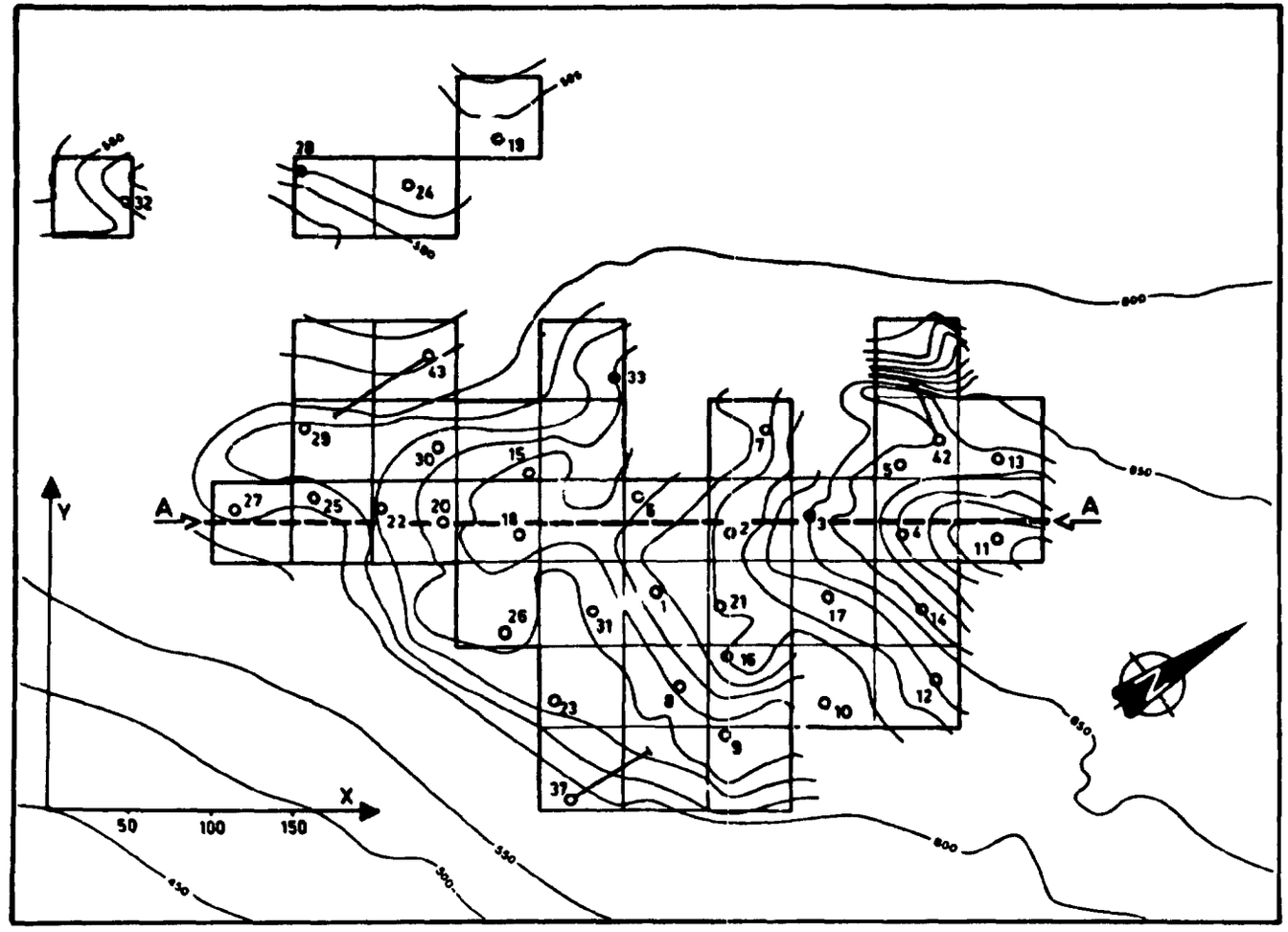

FIGURE 4-20: Random stratified grid (RSG) fitted to the drill hole pattern in the Mine area. The block size is 50 x 50 metres.

directions other than the vertical. The amount and distribution of information within the area therefore necessitates the overall vertical (deregularised) model to be used as an isotrpic three dimensional one. It is obvious that this approach must be suspect, but the sparse data do not permit any alternative.

The block kriging of the present study done by the three-dimensional program TREREG, a version of the commercial package GSTOKOS, which includes georegression calculations (sec. 4.2.14) (Clark, 1979b, 1979b). This program divides a deposit into benches and blocks one bench high are estimated from bench composites derived from the drill core samples (fig. 4-21a). The $\bar{\gamma}(g_i,A)$ terms of the kriging system (fig. 4-12) are, as these functions cannot be evaluated analytically, calculated by an approximate auxiliary function GIMEL (Clark, 1977c). It is assumed that each block can be approximated by a finite number

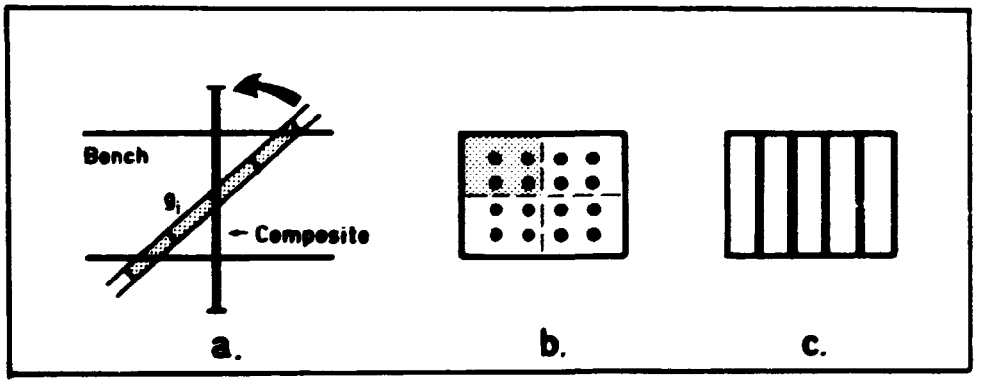

FIGURE 4-21: Approximations used in the three-dimensional kriging program GSTOKOS (TREREG). a) Bench composites are formed from the samples, b) and c) each block is approximated by an array of vertical cores.

of parallel cores (fig. 4-21b,c); GIMEL then gives the average semi-variogram value between a bench composite and the array of cores inside the block. A 4 by 4 grid of cores gives an accuracy of approx. 2-3%, while a 6 by 6 grid gives 1-2 percent and an 8 by 8 better than 1%. A 6 by 6 grid approximation was used in the present calculations. The within-block variance ($\bar{\gamma}(A,A)$) is calculated using the same approximation as that of the

$\bar{\gamma}(g_i,A)$ calculations. It may be noted that calculations are shortened since, because of symmetry, it is only necessary to relate the cores within the shaded area of the block (fig. 4-21b) to all the cores in the block (an even number of cores is chosen).

4.2.10.3. Practical estimation and block selection. Having chosen a block size of 50 by 50 metres in the plan, and selected the orientation of the blocks, it remained to chose a convenient bench height. Since samples consist of core sections one metre long, there is a lower limit for the possible bench height. Very thin benches do not, however, make much sense in a 50 metre square block. The thicknesses of the xenoliths usually range from 2 to 10 metres, and these seem in many cases to occur as lenticular bodies. With this in mind a bench height of 10 metres was selected. The kriging procedure, using the program TREREG, was carried out in three dimensions: that is, not only were samples within the bench considered, but also samples on benches above and below the block. A search volume, within which the program searched for samples to be included in the kriging system, was defined by the user. Because of the operation of TREREG this is specified in terms of the number of blocks to each side of, and above and below, the block that is to be estimated. Consideration was given to the model of the semi-variogram, which gave the largest range of influence as 29 metres. Because of this, the search area was chosen to include one block on either side and three above and below the current block (abbreviated as 1-1-3). This gave a total search area of 150 by 150 by 70 metres. It is clear that samples found on the edges of this area will be outside the range of influence as measured from the block. However, these samples will automatically receive little weight in the kriging system so no special precautions needed be taken.

Figure 4-22 shows a vertical section through the area (line A-A, fig. 4-20) and the pattern of blocks to be estimated. Drill holes within the line of blocks are shown as solid lines, and those off the section, but within the search area, as broken lines. As can be seen, the program may estimate blocks of

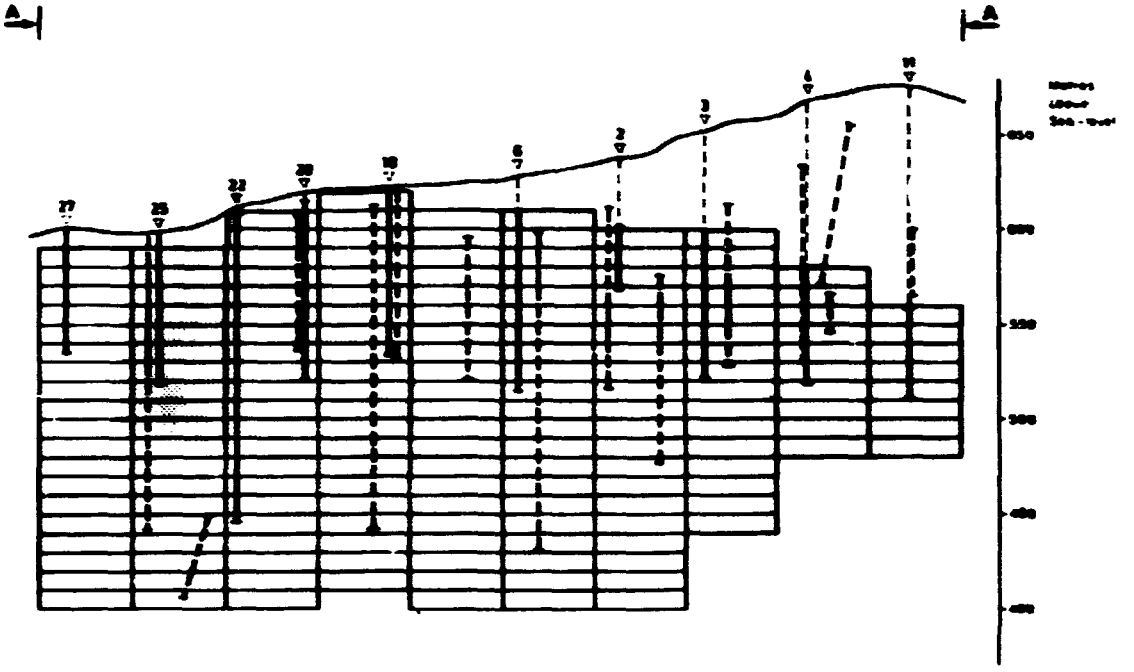

FIGURE 4-22: Typical vertical section through block plan in the Mine area. Section line is A-A in figure 4-20. The bench height is 10 metres.

air or in the barren roof zone. These blocks were eliminated by a block selection program SELMIN (appendix A). The Z-values used for selection were based on topographic maps of the area and geological drill hole profiles. It can also be seen that many blocks may be estimated at the (arbitrary) base of the deposit, from scanty information. These blocks will, of course, have very large estimation variances.

4.2.10.4. Global estimates. Grade-tonnage curves. 640 blocks remained after the block selection described in the previous section. For each block the estimated grade of uranium and the kriging standard error were available. Summary statistics for the 640 blocks are listed in table 4-9. Table 4-10 shows calculations of ore tonnage, uranium tonnage, average grade, and average kriging standard errors for various cutoff values. Grade-tonnage curves versus cutoff grade can be seen in fig. 4-23. The average kriging standard error was calculated from:

$$\bar{\sigma}_k = \frac{1}{N_{bl}} \cdot \sum_{1}^{N_{bl}} \sigma_{k_i}$$

which indicates the level of errors at which blocks are estimated. It cannot be used for a confidence interval of the global reserves, since blocks have not been estimated independently. A measure of the standard error of the global mean grade was calculated from:

$$\sigma_{\text{global mean}} = \frac{1}{N_{bl}} \sqrt{\sum_{1}^{N_{bl}} (\sigma_{k_i})^2}$$

A histogram of the 640 kriged block estimates is shown in fig. 4-24 and a scatter diagram of the estimates versus the estimation standard errors is shown in figure 4-25. When the histogram of block values is compared with the histogram of drill core values (fig. 4-1) the smoothing effect of kriging, as well as the volume-variance relationship, is clearly demonstrated. No significant correlation can be seen from the scatter diagram of figure 4-25, indicating that high grade blocks were

TABLE 4-9: Summary of block kriging of uranium in the Kvanefjeld Mine area.

Number of blocks (50×50×10 m)	:	640	
Total ore tonnage	:	$43.2 \cdot 10^6$	tons
Uranium tonnage	:	$12.04 \cdot 10^3$	tons
Mean grade of blocks	:	278.8	ppm U
Variance of block grades	:	3503	ppm U^2
Average kriging standard error	:	60.1	ppm U
Variance of kriging standard errors	:	462.4	ppm U^2
Probable average kriging variance	:	4068	ppm U^2

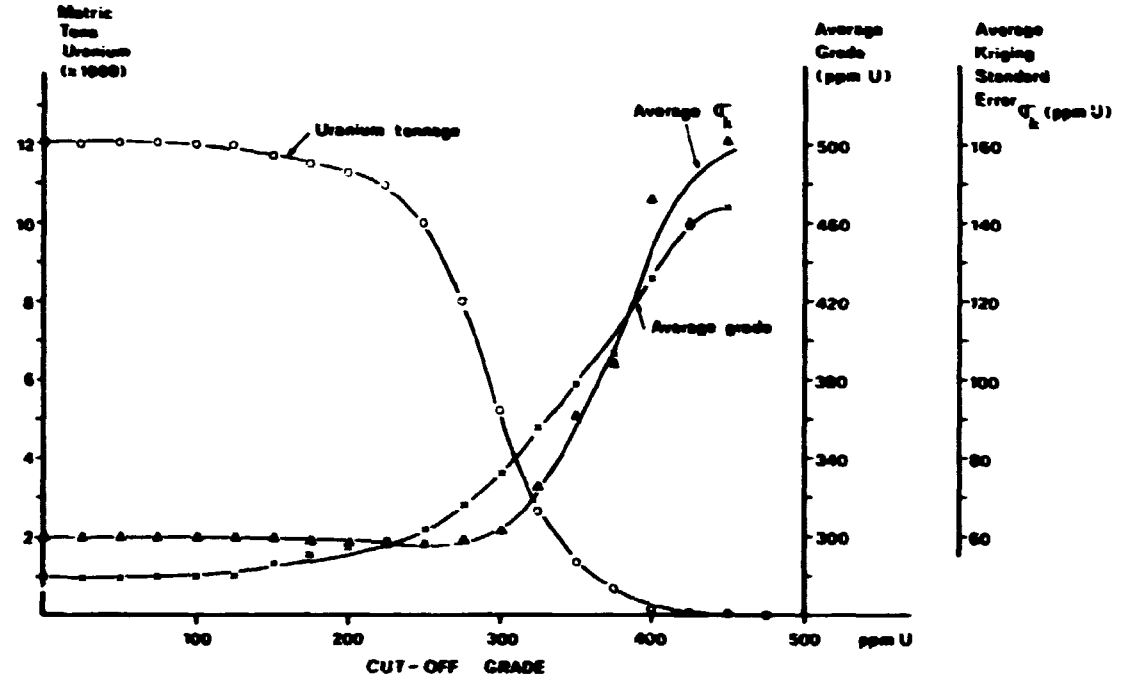

FIGURE 4-23: Grade-tonnage curves versus cutoff grade in the Mine area. The average kriging standard error is also shown.

TABLE 4-10. Grade-tonnage estimates at different cutoff values (ppm U). The ore tonnage is given in million metric tons, the uranium tonnage in tons and the mean grade and standard errors in ppm U. The block size is 50x50x10 metres.

Cutoff grade	No. of blocks	Ore tonnage	Uranium tonnage	Mean grade	Average stand.err.	Error on the global mean
0	640	43.2	12043	278.8	60.1	2.52
100	637	43.0	12030	279.9	60.0	2.53
200	571	38.5	11323	293.8	58.6	2.61
250	488	32.9	10026	304.4	58.1	2.81
300	235	15.9	5273	332.4	61.6	4.41
350	51	3.4	1300	377.5	91.3	13.5
400	5	0.3	146	431.6	146.6	65.9

estimated with about the same errors as low grade blocks. A constant density factor of 2.7 tons/m^3 was used throughout the study.

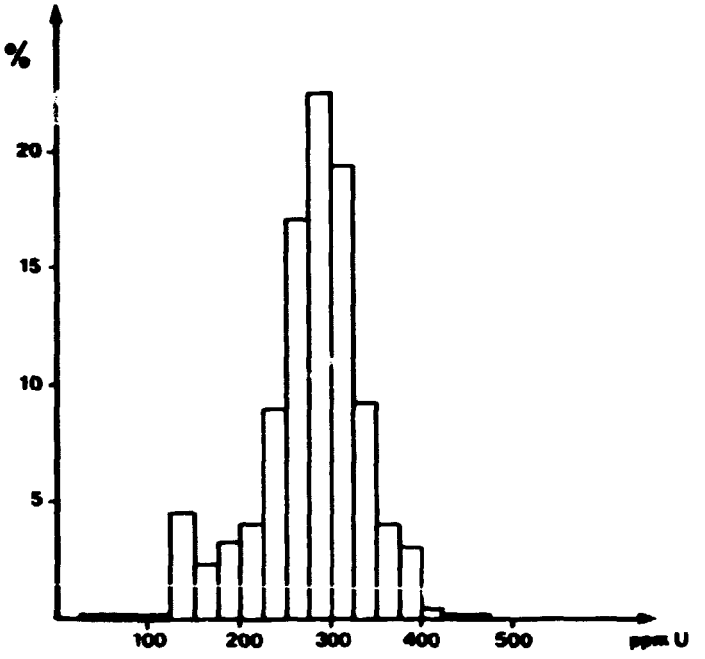

FIGURE 4-24: Histogram of 640 kriged block values in the Mine area.

4.2.10.5. Reliability of estimates. The estimates of grade and tonnage given in table 4-10 and in figure 4-23 take no account of the estimation error of each block value. If it is assumed that the errors follow a normal distribution (probably not quite so - fig. 4-25), it will be possible to obtain a, say, 95% confidence interval around the estimate by adding and subtracting two estimation standard errors from the estimate. That is, if twice the standard error is subtracted from a given block estimate, a lower 97.5% confidence limit is obtained. One can be 'almost sure' that the true block value lies above this specific limit. If this lower confidence limit is above the specific cutoff grade, one can again be 'almost sure' that the average grade of the block is above cutoff.

In the Kvanefjeld Mine area, no blocks can be said to have values above a cutoff of 300 ppm U if the 'two standard error'

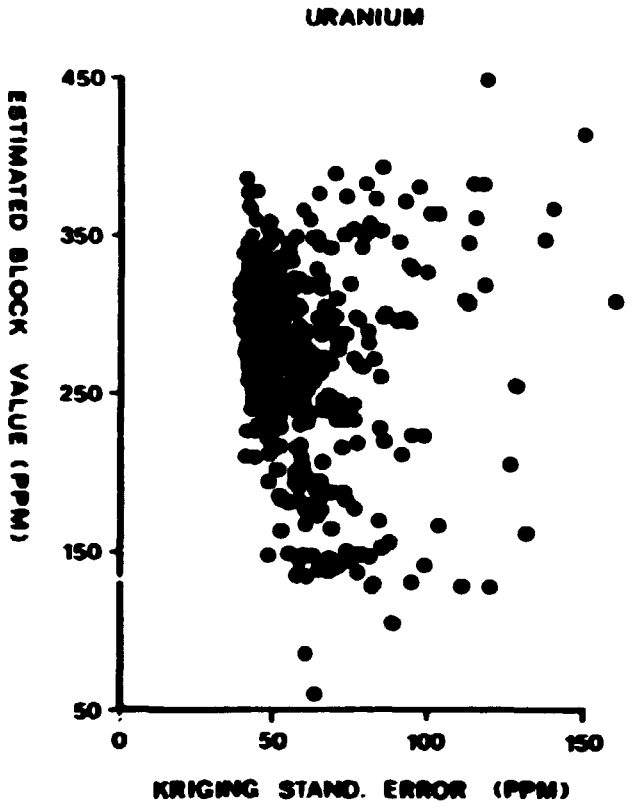

FIGURE 4-25: Scatter diagram of estimated block values versus kriging standard errors for uranium. Number of points is 640.

criterion is applied to the kriging block estimates. This process may be repeated for different (presumably lower) levels of confidence by examining the number of blocks satisfying the criterion:

$$\text{Estimated grade} - \Delta \times \text{standard error} > \text{cutoff}$$

In figure 4-26 graphs of the average grade above cutoff (300 ppm U) and the uranium tonnage versus the confidence level, Δ, are shown. The marked effect, especially on the tonnage, of the degree of 'sureness' is clearly seen.

Another way of illustrating the reliability of estimates is to produce grade-tonnage curves as functions of the kriging standard error. That is, the grades and the tonnages are calculated for blocks which have been estimated with an error below a cer-

tain value. In other words, if an individual block standard error of, say, 60 ppm U can be accepted, then the curves give the mean grade and total tonnage of the blocks passing that criterion. The curves for the 640 Mine area blocks using this technique are presented in figure 4-27.

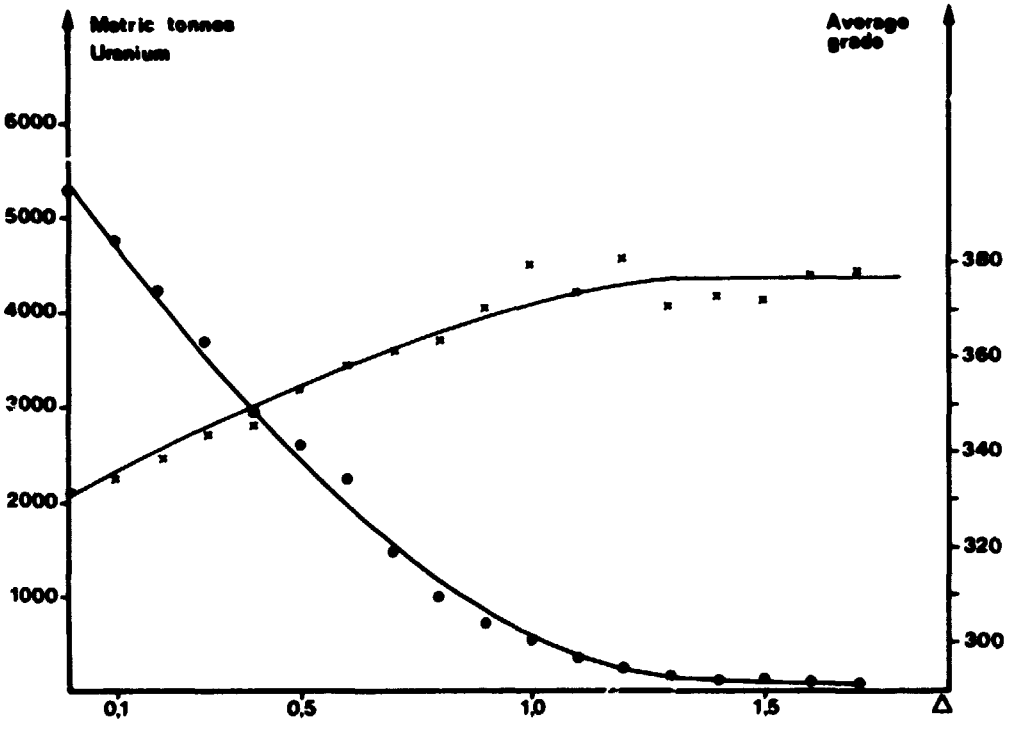

FIGURE 4-26: Grade-tonnage curves versus 'confidence level' in the Mine area.

4.2.11 Effect of the block size on grade-tonnage estimates.

As stated earlier and demonstrated during practical block estimation, distributions on different supports e.g. points, drill cores, blocks etc. have different variances. Hence, in theory the tonnage above a cutoff grade and its mean grade will differ for different sizes of blocks, except when the cutoff grade is equal to the mean grade of the deposit. To demonstrate this effect on the block estimates in the Mine area, a sub-volume was defined as:

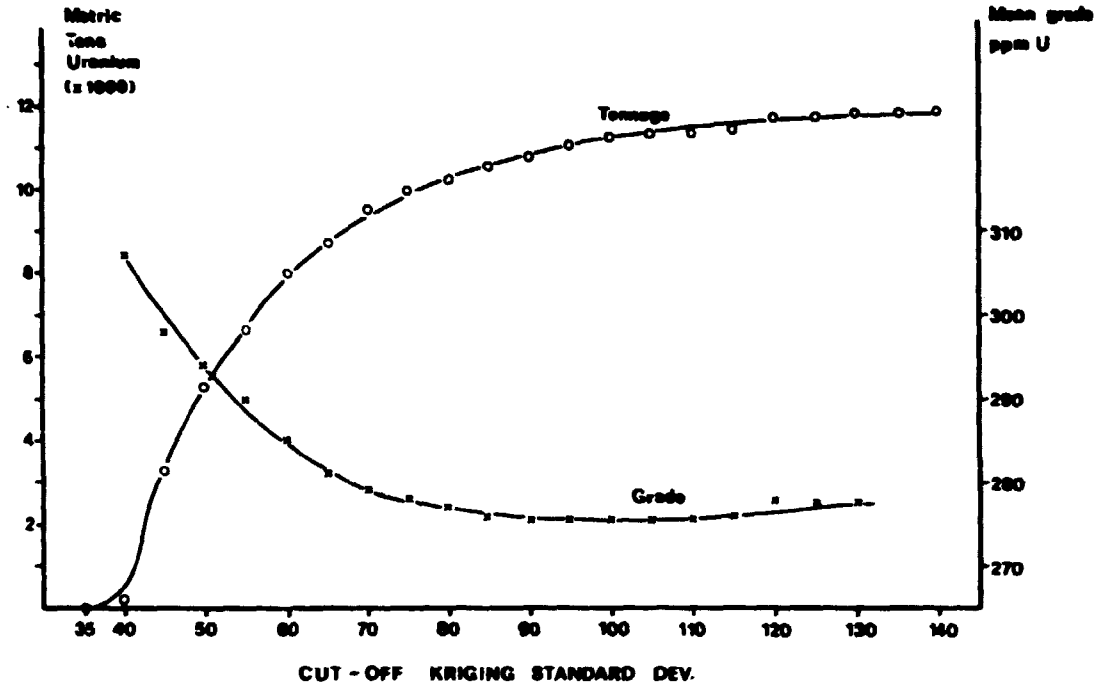

FIGURE 4-27: Grade - tonnage curves versus the kriging standard deviation σ_k.

$$150 \leq X_{CSmine} \leq 300$$

$$150 \leq Y_{CSmine} \leq 250$$

$$500 \leq Z \leq 600$$

Within this volume blocks of different sizes were estimated from the drill core samples by 3-dimensional kriging (fig. 4-28). Table 4-11 summarizes the results from 12 different block sizes ranging from 5 by 5 by 5 metres to 150 by 100 by 100 metres (the whole volume). In figure 4-29 the average kriging standard error and the standard error of the blocks are plotted against the block volume. Curves of uranium tonnage against cutoff grade are shown in figure 4-30. It can be clearly seen that small blocks, as expected, have been estimated with much higher errors than larger blocks. Secondly, the decrease in block variance as the block size is enlarged is

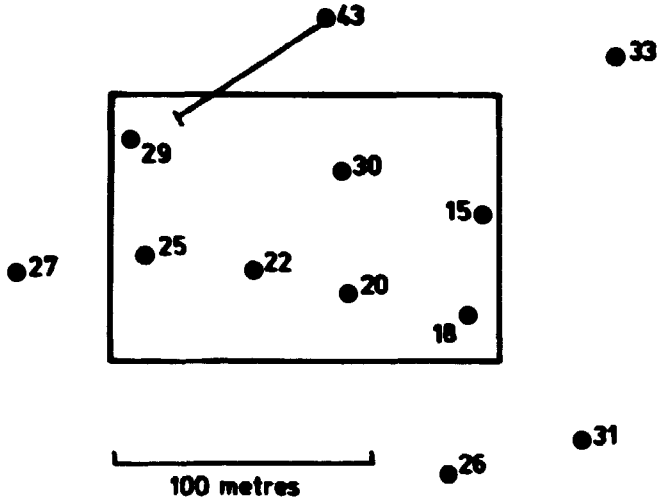

FIGURE 4-28: Sub-area used to test the effect of block size on grade-tonnage estimates. The drill holes included in the calculations are shown.

TABLE 4-11: Effects of the block size and the bench height on block kriging done in a small volume within the Mine area. The block volume is given in m^3, block mean and standard errors in ppm U. The search area is given in terms of blocks: E/W-N/S-Above/Below (see text).

Block size	No. of blocks	Block volume	Search area	Block mean	Block std.err.	$\bar{\sigma}_k$	case
5×5×5	11762	125	993	300.8	55.8	111.1	1
5×5×10	6000	250	993	299.3	46.4	100.9	2
25×25×10	240	6250	223	295.8	35.0	67.9	3
25×25×20	120	12500	222	302.1	28.5	61.3	4
50×50×10	60	25000	113	296.7	26.9	44.2	5
50×50×20	30	50000	112	301.8	19.6	39.6	6
50×50×25	24	62500	112	301.2	17.6	37.2	11
50×50×50	12	125000	111	300.6	14.4	30.5	8
75×50×10	40	37500	113	302.4	27.3	38.0	10
75×50×20	20	75000	112	306.1	18.3	33.7	7
75×100×50	4	375000	111	301.1	14.3	21.2	9
150×100×100	1	1500000	110	305.6	-	16.5	12

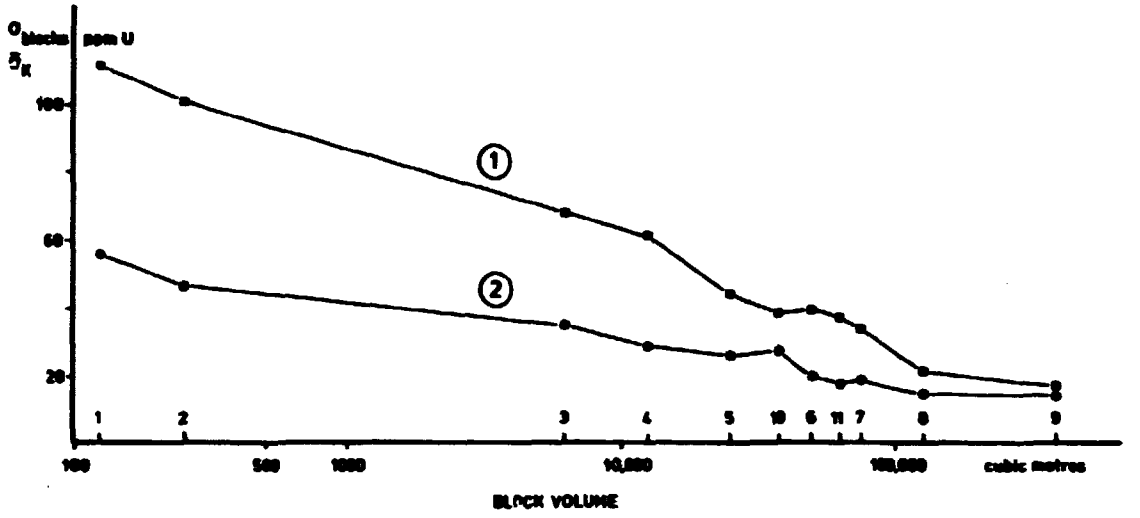

FIGURE 4-29: Curves of 1) average kriging standard errors and 2) block standard errors versus block volume. The numbers on the volume axis refer to the case in table 4-11. Mine test area.

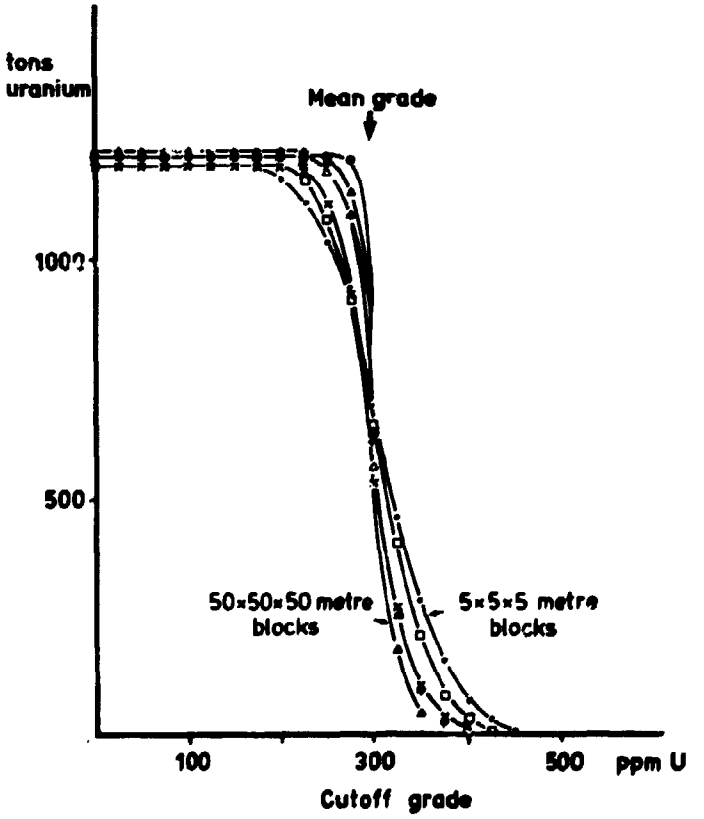

FIGURE 4-30: Tonnage curves for different block sizes versus the cutoff grade. Mine test area.

quite obvious. The tonnage curves in figure 4-30 show, although the general picture is somewhat cramped, that for cutoff grades greater than the mean value small blocks will certainly produce larger tonnages of ore than larger blocks. It is also noted that the tonnages are equal for all block sizes when the cutoff grade is equal to the overall mean of the whole volume. This is because kriging is an unbiased estimator. The volume-variance relationship can also be visualized if histograms of estimates for different block sizes are compared (fig. 4-31).

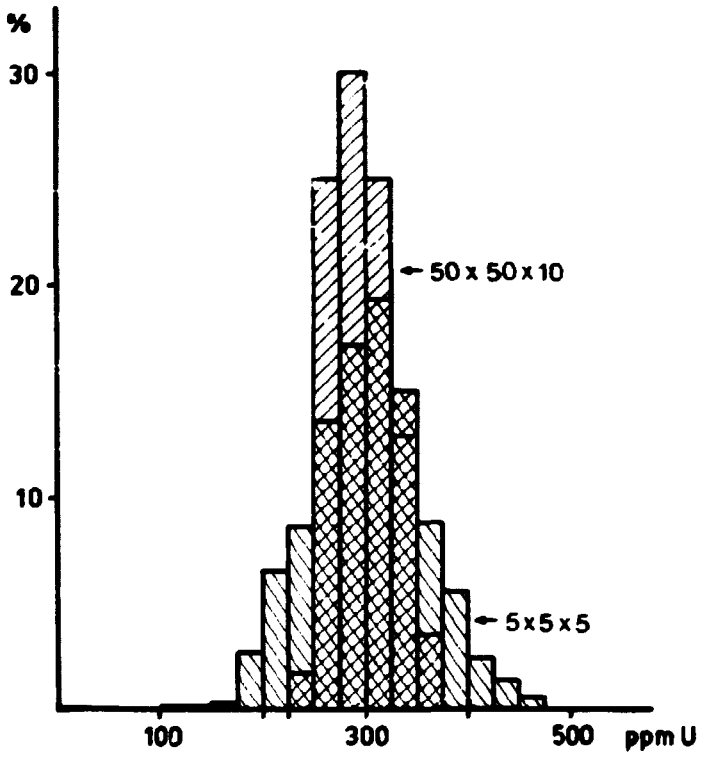

FIGURE 4-31: Histograms of kriged block estimates from the Mine test area. Block sizes of 5x5x5 metres and 50x50x10 metres are compared.

4.2.12 Testing Krige/s relationship.

The mathematical expression for the volume-variance relationship is given by Krige's relationship (e.g. David, 1977):

$$\sigma^2_{p/V} = \sigma^2_{p/v} + \sigma^2_{v/V}$$

which should be read as follows. The variance of samples on a support p within a large volume V is equal to the variance of these samples within a small volume v plus the variance of v within V. If point samples and blocks of a given size are compared, the expression can be written

$$\sigma^2_{points} = \sigma^2_{within} + \sigma^2_{blocks}$$

where σ^2_{within} is the variance of points within a block, also called the within-block variance (equal to $\bar{\gamma}(A,A)$). In the Mine area the variance of point samples was determined from the total sill of the point semi-variogram. This value was estimated to be 34530 (ppm U)^2 (sec. 4.2.7). The variance of kriged blocks of size 50 by 50 by 10 metres was found to be 3503 (ppm U)^2 (table 4-9). It is now necessary to calculate the within-block variance for a block 50 by 50 by 10 metres to check whether the relationship holds. The within-block variance is calculated by taking the mean semi-variogram value between all points within the block. The 3-dimensional auxiliary function F(L,L,B) has been developed for this purpose and tables are available for the spherical model (e.g. Clark, 1979a). In the present case:

$$\sigma^2_{within} = F(50,50,10)$$

$$= C_0 + C_1 F(50/2.5,50/2.5,10/2.5)$$

$$+ C_2 F(50/29,50/29,10/29)$$

$$= 5600 + 16930(\simeq 1) + 12000 \cdot 0.855$$

$$= 32790 \text{ ppm } U^2$$

where the individual components of the semi-variogram model are considered. The above relationship gives

$$(32790 + 3503) \text{ ppm } U^2 = 34530 \text{ ppm } U^2$$

$$36293 \text{ ppm } U^2 = 34530 \text{ ppm } U^2$$

corresponding to a difference of approx. 5%. This can be regarded as acceptable.

The relationship can also be used to compare the theoretical differences in variance, of different block sizes, with actual differences, for instance those found in the previous kriging example of sec. 4.2.11. If two distributions of blocks of sizes S1 and S2 are compared, the relationship gives:

$$(\sigma^2_{within} + \sigma^2_{blocks})_{S1} - (\sigma^2_{within} + \sigma^2_{blocks})_{S2}$$

or

$$(\sigma^2_{S1} - \sigma^2_{S2})_{within} = (\sigma^2_{S1} - \sigma^2_{S2})_{blocks}$$

In table 4-12 four comparisons of the theoretical variance difference, based on within-block variances, with the actual variance difference, based on block variances, are given. It can be seen that where S1 and S2 are not too different the differences in variance are comparable. However, comparing blocks of very different sizes gives unrealistic figures. This might be due to several reasons:

(1) The practical kriging study was done in only a part of the area and hence gives a smaller sample variance because of too few samples. The variance of the estimated blocks will therefore be too small compared with that of the whole area.

(2) The semi-variogram model used for estimation and for theoretical variance calculations was based on the whole area and not on the sub-area under consideration.

(3) No account has been taken of the 'regression effect' (sec. 4.2.14).

(4) If the block sizes are very different, the number of observations within each block will also be very different.

In a comparable way to the results presented in section 4.2.5, where local semi-variograms were compared with the overall model, testing Kriges relationship shows that if results based on global investigations are brought into local studies, these need to be regarded with some suspicion.

TABLE 4-12: The testing of Krige's relationship by comparing differences in variance (ppm U^2).

Comparison (S1 - S2)	Theoretical $(\sigma^2_{S1}-\sigma^2_{S2})_{within}$	Practical $(\sigma^2_{S2}-\sigma^2_{S1})_{blocks}$
5×5×5 - 5×5×10	1287	960
50×50×10 - 50×50×20	300	337
50×50×10 - 50×50×50	948	516
5×5×5 - 50×50×50	9949	2907

4.2.13 Calculating grade-tonnage values from the distribution of sample values.

In this section will be demonstrated how the original distribution of samples can be used directly to obtain grade-tonnage curves without any actual block estimation. Since such calculations only give the final grade and tonnage for a given cutoff, and not the values of individual blocks, they must be regarded as tools for economic planning, but not for mine planning.

It will be recalled from table 4-2 that the best fit to the histogram of the total set of drill core samples was obtained by the following two-component lognormal model:

1. component: $\bar{x}_1 = 148.3$ ppm U

$s_1 = 156.9$ ppm U

$p_1 = 0.356$

2. component: $\bar{x}_2 = 367.8$ ppm U

$s_2 = 147.0$ ppm U

$p_2 = 0.644$

where p_1 and p_2 are proportions. The fit, shown in figure 4-3, is obviously a pure artefact which does not reflect the geology. Firstly, the distribution of point samples is determined by correcting for the difference in variances; that is

$$F_1 = \frac{\sigma^2_{points}}{\sigma^2_{cores}} = \frac{34530}{31000} = 1.114$$

and hence the variances:

$$s_1(points) = s_1(cores)F_1 = 174.8 \text{ ppm U}$$

$$s_2(points) = s_2(cores)F_1 = 163.8 \text{ ppm U}$$

Next consider blocks of size 50 by 50 by 10 metres. In section (4.2.12.) the within-block variance for a block of that size was estimated at 32790. The distribution of such blocks can now be calculated. Since the block size is very large compared with the spatial structure expressed by the semi-variogram model, the two components of the distribution cannot be considered

independently of one another. Therefore, both the mean and the standard deviation of each component must be corrected when going from points to blocks (Isobel Clark, pers. comm.). The correction factor is:

$$F_2 = \frac{\sigma^2_{within}}{\sigma^2_{points}} = \frac{32790}{34530} = 0.9496$$

$$f = \sqrt{1-F_2} = 0.224$$

The corrections to the parameters of the individual components are:

$$s_i(blocks) = s_i(points)f$$

$$\bar{x}_i(blocks) = (1-f)\bar{x}_{overall} + f\bar{x}_i(points)$$

where the theoretical overall mean $\bar{x}_{overall}$ is:

$$\bar{x}_{overall} = p_1\bar{x}_1 + p_2\bar{x}_2 = 289.7 \text{ ppm U}$$

It is seen correcting the mean value tends to move it towards the overall mean. The theoretical value for the overall mean lies very close to the mean value obtained from a straight average of the samples ($\bar{x}$ = 286.9, table 4-1). Using the above correction the distribution of <u>blocks</u> is:

1. component: $\bar{x}_1 = 258.0$ ppm U

$s_1 = 39.16$ ppm U

$p_1 = 0.356$

2. component: $\bar{x}_2 = 307.2$ ppm U

$s_2 = 36.69$ ppm U

$p_2 = 0.644$

The proportion and the average grade above cutoff (COG) can now be calculated (Clark, 1979a). Let the cutoff grade COG=300 ppm U be considered. For the <u>first component</u>:

$$\beta^2 = \log_e\left(\frac{s_1^2}{\bar{x}_1^2} + 1\right)$$

$$= \log_e\left(\frac{39.16^2}{268.0^2} + 1\right) = 0.023$$

$$\beta = 0.151$$

$$\alpha = \log_e\bar{x}_1 - 0.5\beta^2$$

$$= \log_e 258.0 - 0.5 \cdot 0.023 = 5.54$$

$$Z = \frac{\log_e(COG) - \alpha}{\beta}$$

$$= \frac{\log_e 300 - 5.54}{0.151} = 1.085$$

Consulting a table of the standard Normal distribution gives the proportion above cutoff.

$$p_1 = 1 - \Phi(Z)$$

$$= 0.139$$

That is, 13.9% of the first component lies above 300 ppm. The average grade is found by the following process:

$$\bar{x}_{c1} = \frac{Q_1}{P_1} \bar{x}_1$$

where $Q = 1 - \Phi((z-\beta)$. In the present case:

$$Q = 1 - \Phi(1.085 - 0.151)$$

$$= 0.175$$

$$\bar{x}_{c1} = \frac{0.175}{0.139} 258.0$$

$$= 324.8 \text{ ppm U}$$

Repeating the calculations on the <u>second component</u> gives:

$$P = 0.554$$

$$\bar{x}_{c2} = 333.2 \text{ ppm U}$$

If the volume occupied by the 640 blocks of the kriging study (sec. 4.2.10) is regarded as being representative of the Mine area, the total ore tonnage is 43.2 mill. tons (table 4-10). The tonnage above 300 ppm is therefore:

$$43.2(P_1p_1 + P_2p_2) = 17.56 \text{ mill. tons}$$

with an average grade of:

$$\bar{x}_c = \frac{43.2}{17.56} (P_1p_1\bar{x}_{c1} + P_2p_2\bar{x}_{c2})$$

$$= 332.2 \text{ ppm U}$$

These figures correspond to approx. 5833 tons of contained U.

4.2.14 Georegression.

As mentioned in previous sections the variance of a set of samples is affected by the sample support. Generally the variance of the sampling distribution is always greater than the variance of the block mean value distribution. The difference between the two reflects that the sample distribution contains more high values and more low values than the distribution of the block grades. The means of both distributions are the same. So, for a zero cutoff value, i.e. if the whole orebody is mined, there is no bias in the estimated tonnage or mean grade of the reserves. However, due to the volume-variance relationship, any estimator, including kriging, will produce a bias in the grade-tonnage curves if the selection of blocks is based on a cutoff value not equal to zero. The bias is introduced by an overestimation of high-grade blocks and an underestimation of low-grade blocks (figure 4-32). Since blocks are selected on the basis of their estimates Z^* and not from their actual

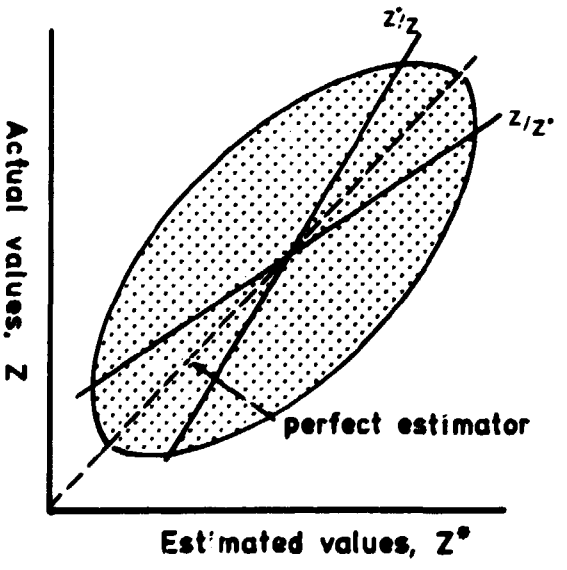

FIGURE 4-32: Theoretical illustration of the regression effect. High (actual) values tend to be over-estimated, while low values tend to be under-estimated.

values Z, it is important to be able to relate the two sets of values. Krige (1951) suggested that this bias in the estimation process can be eliminated by a regression curve which relates the linear estimator to a more accurate unbiased estimator. By comparing stope sampling from worked-out areas with the linear estimates obtained from development data, an empirical curve could be produced. This was then used to correct the linear estimator. Because of Krige's work, the bias on the estimator is known as the regression effect.

The topic appears frequently in the literature, with papers by Krige (1959, 1966), Royle and Newton (1972), Royle (1978), David et al. (1974), and many others.

The most important shortcoming of Krige's approach is of course that both estimates and true values must be available to produce the regression curve. If only samples are available corrections can made by volume-variance calculations as demonstrated above. This method, however, can only correct the bias on the global grade-tonnage curve, but not on the individual block estimates. To overcome this insufficiency, Matheron (1976) introduced a new technique, based on non-linear estimators, called disjunctive kriging. According to Journel and Huijbregts (1978) and Clark (pers. comm.) this technique cannot be considered well tried and proven and it is, in addition, difficult to use in practice.

As a simple alternative to disjunctive kriging Clark (1978, 1980) developed a new method which she called georegression which corrects for the regression effect. The method is based on the following assumptions:

(1) The overall volume under consideration is very large compared with the size of a single block.

(2) The mean of the whole volume may be estimated and the standard error of this estimate can be found. This may be done by standard kriging.

The correction is based on a simple regression-type estimator $\hat{Z}$ by assuming a linear relationship between Z^* and $\hat{Z}$:

$$\hat{Z} = \hat{a} + \hat{b}Z^*$$

where $\wedge$ denotes an estimate of the particular parameter. A full mathematical derivation of the estimation of these parameters from the model semi-variogram is found in Clark (1980). Two different types of georegression estimator are available in the program TREREG (mentioned above). These are known as 'least squares georegression' and 'perpendicular distance georegression', and correspond to two different ways of minimizing errors when the parameters of the regression line are calculated (figure 4-33).

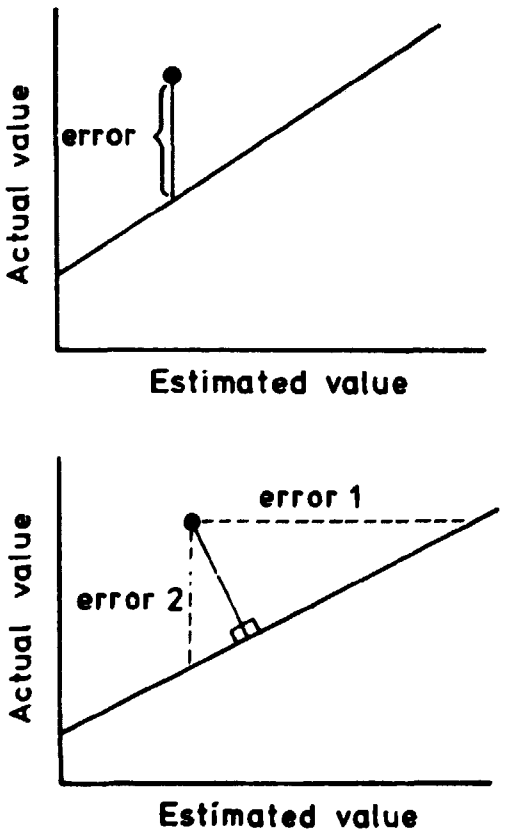

FIGURE 4-33: Possible error criteria for regression analysis: a) least squares and b) perpendicular distance. (From Clark and Clausen, 1981).

The 640 kriged block estimates from the Mine area (sec. 4.2.10) were corrected by both least-squares and perpendicular distance georegression and the results presented in Clark and Clausen (1981); the following presentation is extracted from that paper. Histograms of the corrected block values are shown in figure 4-34. When these histograms are compared with the histogram of kriged block values (fig. 4-24) the enormous smoothing

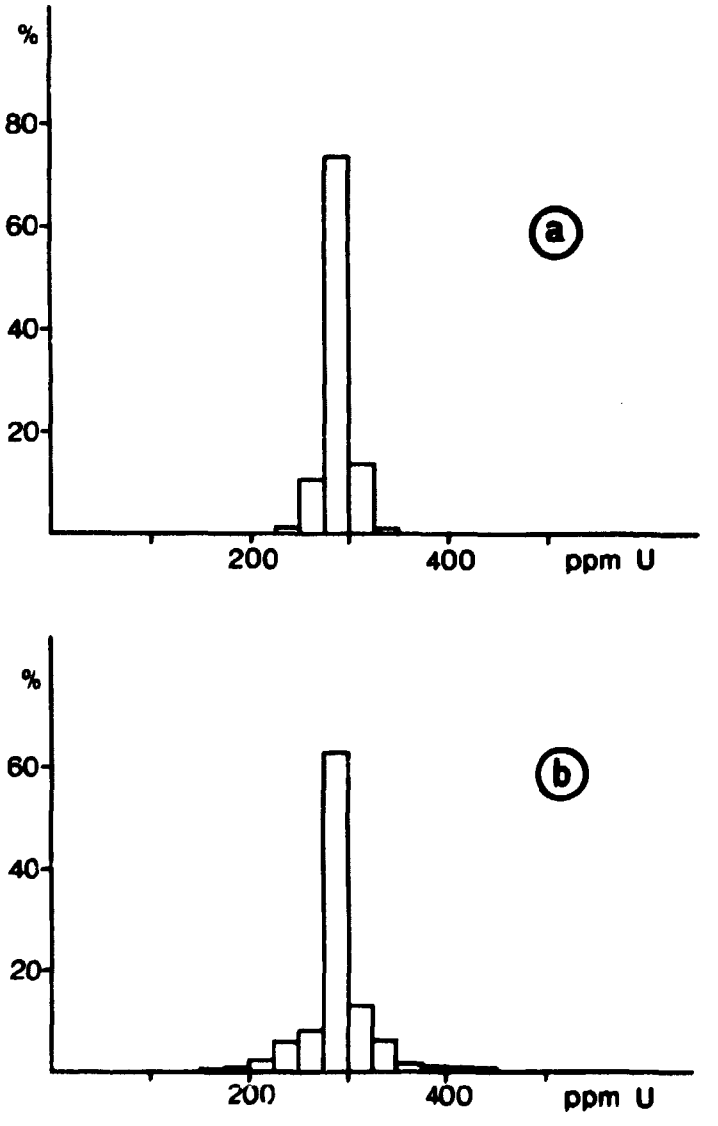

FIGURE 4-34: Histograms of kriged block estimates corrected by georegression in the Mine area. a) least squares, and b) perpendicular distance.

effect of the georegression estimator becomes immediately apparent. The least-squares histogram is obviously totally unrealistic, since almost all of the blocks are allocated the average grade of the Mine area. Royle (1978) has shown that many estimators are highly influenced by the nugget effect and this in turn tends to emphasize the bias on the grade-tonnage relationship. Some authors e.g. Marechal (1976) have shown that even kriging, which produces the best linear unbiased estimate for each individual value, produces bias on the estimated grade-tonnage curve. Since the Mine area uranium has a very poor spatial structure with a high nugget effect, the difference between a biased (kriging) estimator and an unbiased (georegression) one is very great. The individual kriged block estimates are adjusted more or less towards the mean value of the area, giving a variance much closer to that theoretically expected from such large blocks of 50 by 50 by 10 metres. If smaller blocks had been estimated the adjustment would not have been so severe.

Reliability curves for the two georegression estimators are compared with the kriging estimator in figure 4-35 (cutoff value 300 ppm U). The effect of the volume-variance relationship corrections can be clearly seen. Grade-tonnage values are listed in table 4-13 for least-squares estimates and in table 4-14 for perpendicular distance estimates. Whereas the estimation standard error varies between 40 ppm to 150 ppm when kriging is used alone (fig. 4-25), kriging plus georegression produces standard errors confined to the range 40-50 ppm. It was concluded by Clark and Clausen (1981) that some further work needs to be done to determine the criterion 'large nugget effect' since this obviously influences the choice between the two georegression methods. However, it appears that perpendicular distance georegression is more suitable when dealing with a highly erratic type of mineralisation. It is believed that the georegression estimator produces more realistic results at this early stage of analysis of the Kvanefjeld uranium deposit.

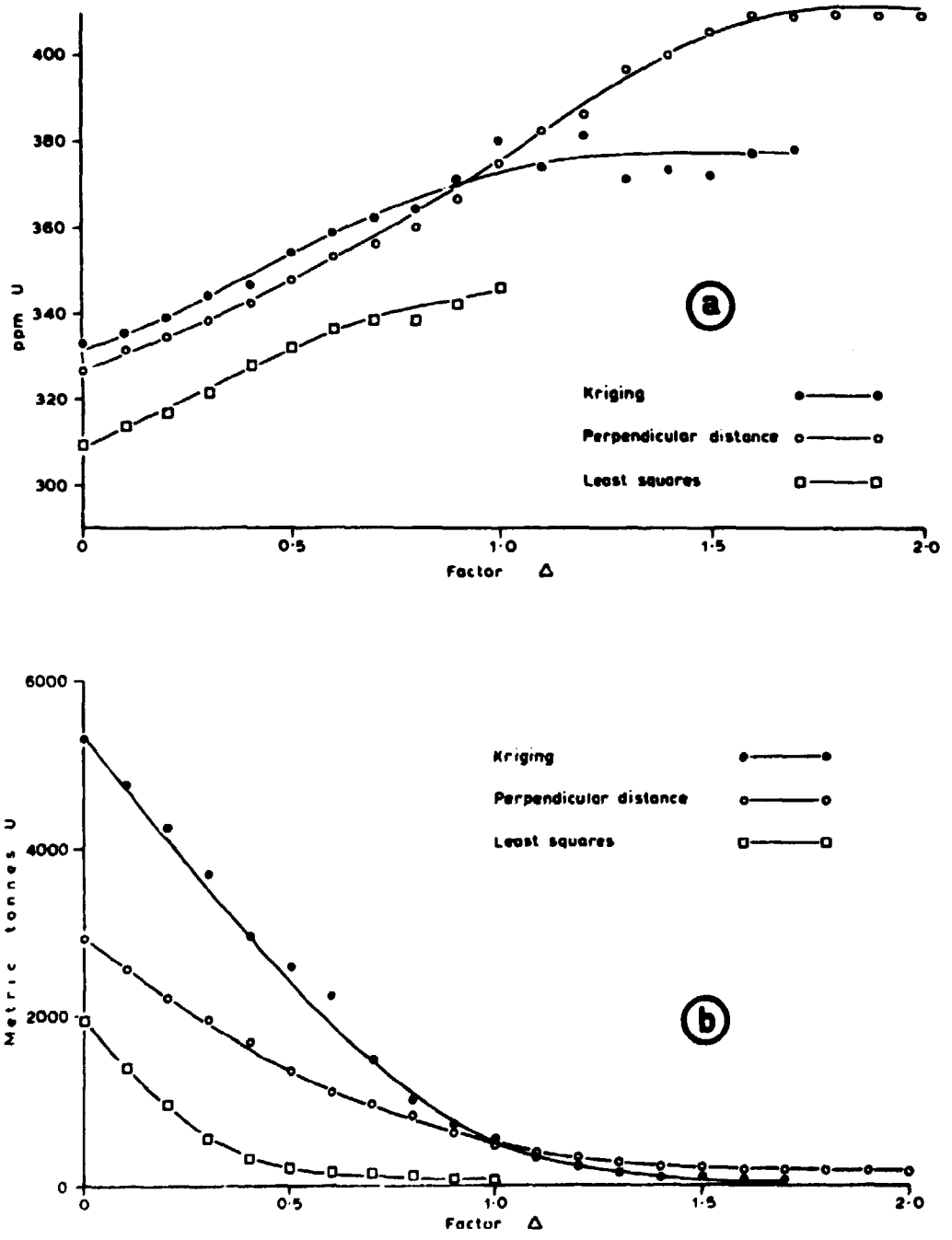

FIGURE 4-35: Estimated global reserves in the Mine area against 'confidence level'. a) average grade above cutoff (300 ppm U), and b) uranium tonnage above cutoff.

TABLE 4-13: Grade-tonnage estimates at different cutoff values (ppm U). Block estimates are corrected by least squares georegression. Units as in table 4-10. The block size is 50x50x10 metres.

Cutoff grade	No. of blocks	Ore tonnage	Uranium tonnage	Mean grade	Average stand.err.	Error on the global mean
0	640	43.2	12433	287.8	42.3	1.7
100	640	43.2	12433	287.8	42.3	1.7
200	640	43.2	12433	287.8	42.3	1.7
250	632	42.7	12302	288.4	42.3	1.7
300	94	6.3	1965	309.7	40.1	4.1
325	6	0.4	137	338.0	39.9	16.3

TABLE 4-14: Grade-tonnage estimates at different cutoff values (ppm U). Block estimates are corrected by perpendicular distance georegression. Units as in table 4-10. The block size is 50x50x10 metres.

Cutoff grade	No. of blocks	Ore tonnage	Uranium tonnage	Mean grade	Average stand.err.	Error on the global mean
0	640	43.2	12469	288.6	44.9	1.8
100	640	43.2	12469	288.6	44.9	1.8
200	635	42.9	12406	289.5	44.9	1.8
250	585	39.5	11620	294.3	44.8	1.9
300	134	9.0	2951	326.3	46.5	4.0
350	15	1.0	385	379.9	47.8	12.4
400	5	0.3	139	412.3	49.6	21.7

4.2.15 Comparison of estimates.

Table 4-15 summarizes the results of 3-dimensional block kriging, theoretical grade-tonnage calculations and georegressions, together with estimates published elsewhere (Sørensen et al., 1974, Pryor - Report , 1974). For comparison purposes a cutoff grade of 300 ppm has been chosen. This is probably higher than would be chosen in practice, although grade-tonnage calculations in the Mine area have previously been published using this figure (Sørensen et al., 1974). The estimate cited was

TABLE 4-15: Comparison of estimates in the Kvanefjeld Mine area. A cutoff value at 300 ppm uranium is used. Block volume given in m^3, rock density in tons/m^3, ore tonnage in million tons and uranium tonnage in tons. Total tonnage is the tonnage at cutoff 0 ppm U. †) from Sørensen et al. (1974), ††) from Pryor-Report (1974).

Estimation method	Block size	Block volume	Rock density	Ore tonnage	Uranium tonnage	Mean grade	Total tonnage
3D-kriging	50×50×10	25000	2.7	15.9	5273	332	43.2
Georegression (LS)	50×50×10	25000	2.7	6.3	1965	310	43.2
Georegression (PD)	50×50×10	25000	2.7	9.0	2951	326	43.2
Theoretical	50×50×10	25000	2.7	17.6	~5833	332	43.2
Triangles †	variable	~1800	2.8	18.6	5760	310	47.9
2D-kriging ††	40×40×20	32000	2.7	21.5	~7353	342	42.3

based on the classical method of triangles illustrated in figure 4-36. Within each vertical triangular prism the tonnage and grade were calculated by cumulating the average uranium content of the basic triangle when traversing the height of the prism in one metre steps. These 'blocks' must be considered small compared with the 50 by 50 by 10 metre blocks used in kriging. The block pattern gives different volumes from the RSG, which would a priori lead to a different estimate. In practice this was not the case.

Results from a preliminary geostatistical study of the uranium values from the Mine area (Pryor-Report, 1974) are also listed in table 4-15. Although the experimental semi-variogram obtained by this study was similar to the one presented here, a rather different model, comprising only one spherical component

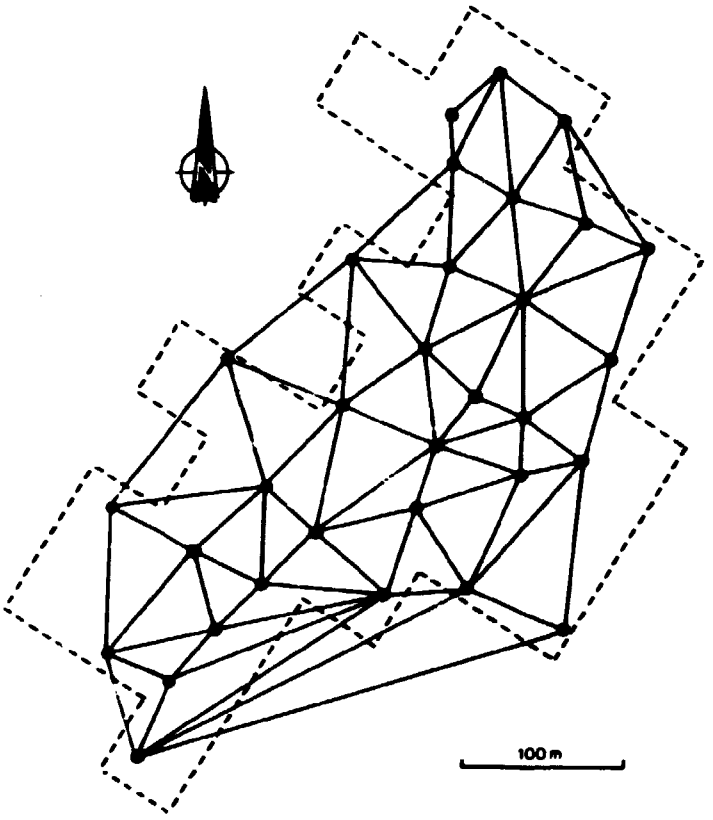

FIGURE 4-36: Triangles used for the conventional estimation of the global reserves in the Mine area. Outline of the random stratified grid used for block kriging is indicated.

with a range of influence of 30 metres and a nugget effect, was used. The block size used for this study was 40 by 40 by 20 metres, and all samples within 50 metres from the centre of the block were included in the kriging system.

It can be seen from table 4-15 that the 3D-kriging and theoretical results accord with the result given by triangles. However, the georegression results lie far below the other estimates since the cutoff value was set too high compared with the mean grade of the area. The kriging results from the Pryor report appear to be optimistic with respect to both tonnage and grade. This was probably caused by the different kriging technique (too many high grade blocks are overestimated by 2D-kriging), resulting in a severe bias on the grade-tonnage curves.

If further information were available i.e. more drill holes, smaller blocks could be estimated with acceptable errors. Such blocks would probably produce reliable figures close to the theoretical calculations and the 3D-kriging results. However, at the present stage, the perpendicular distance georegression estimator is believed to produce the most realistic figures. For lower cutoff values, i.e. near to the mean value, all the estimation methods will, of course, produce comparable results.

4.3 Uranium in the Northern area (Assay data).

4.3.1 Uranium distributions and proportional effects.

Histograms of uranium values in different groups of data from the Northern Kvanefjeld area are shown in figure 4-37 and figure 4-38a,b. Overall parameters are listed in table 4-16. The groups considered are 1) the total data set, disregarding the geology, 2) samples fulfilling the condition 200 $\leq$ geology code $\leq$ 299 (fine-grained lujavrites including mixted samples, see appendix E) and 3) fine-grained lujavrites excluding mixted samples.

The distribution of the total data set (figure 4-37) is obviously composed of several distributions. Comparing this histogram to those of the fine-grained lujavrites clearly demonstrates that the lowest mode is associated with low-grade inclusion samples. The next two modes of the histogram are apparently associated with the distribution of fine-grained lujavrite. The program ROKE (sec. 4.2.1) was used to produce an almost acceptable fit to a three component lognormal mixture of distributions which can also be recognised in figure 4-37. Parameters and proportions for the individual components are given in table 4-17.

Although the best fit to the total data set comprises a mixture of lognormal distributions the best fit to the distribution of pure fine-grained lujavrite samples comprises normal compo-

TABLE 4-16: Simple statistics for uranium (ppm) in the Northern area (assay data).

Type of data	N_s	Mean	Std. dev.	Coeff. of var.
Total sample set	2169	186.8	138.0	0.74
Fine-grained lujavrites +	1478	246.2	121.2	0.49
Fine-grained lujavrites ÷	1173	251.8	113.2	0.45

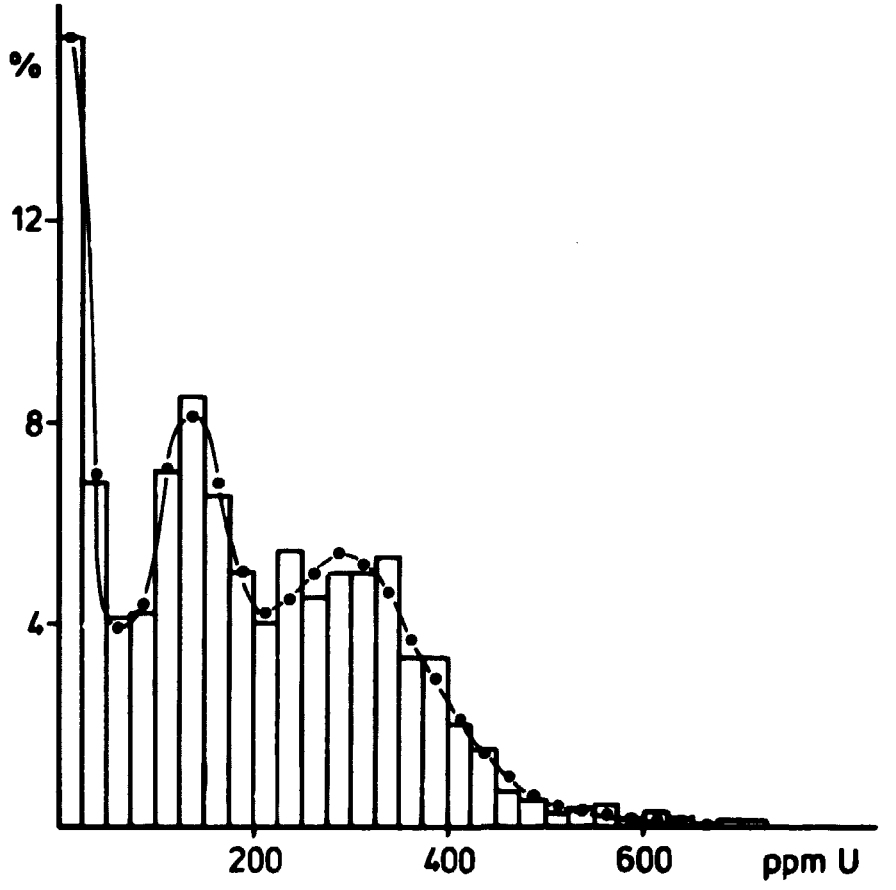

FIGURE 4-37: Histogram of uranium values in drill core samples from the Northern area. A three-component log-normal distribution was fitted as shown. The number of samples is 2169.

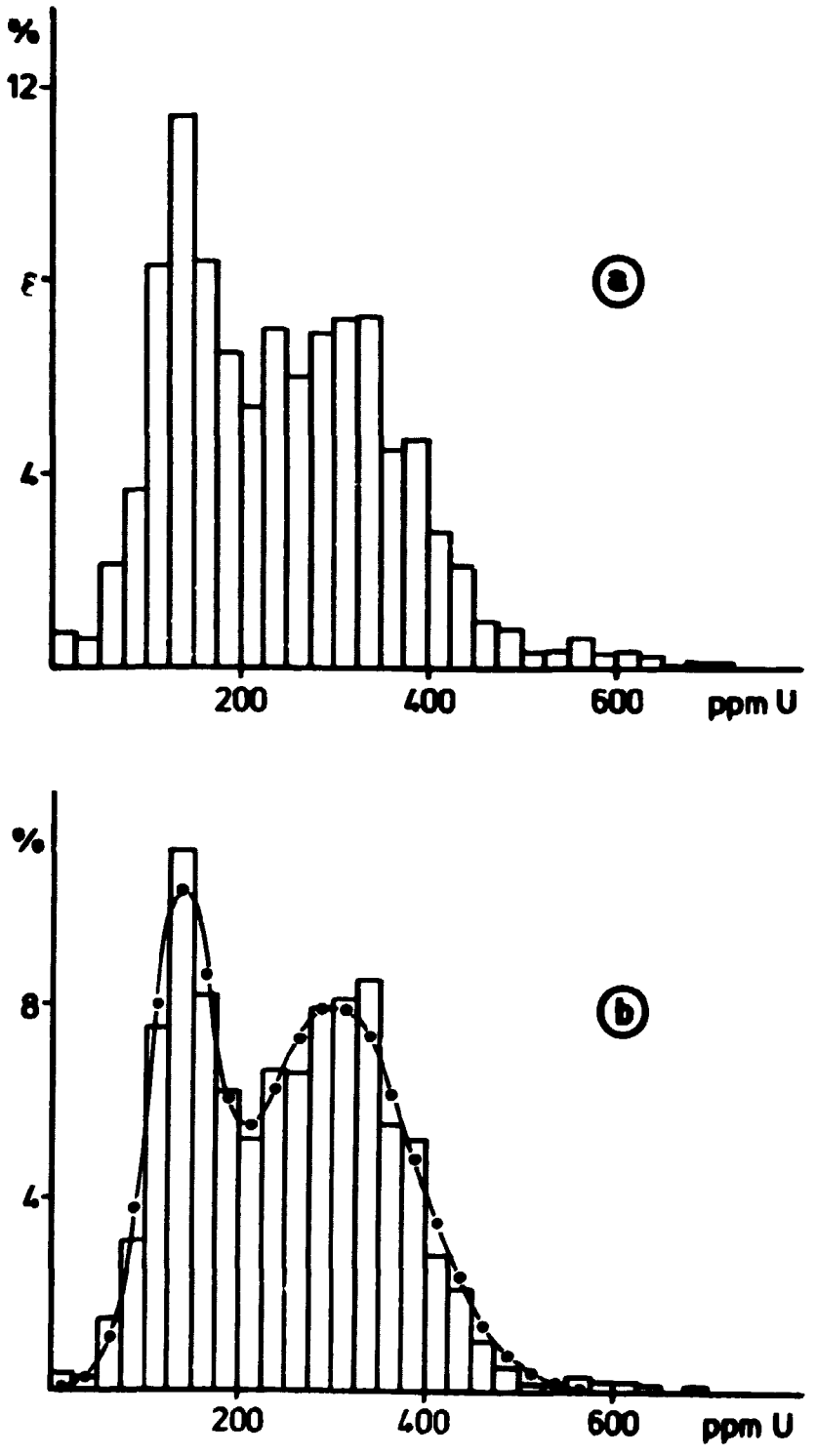

FIGURE 4-38: Histograms of uranium values in drill core samples from the Northern area. a) All fine-grained lujavrites including mixture samples (+) and b) all fine-grained lujavrites excluding mixture samples (+). A two-component normal distribution fitted to b) is shown.

TABLE 4-17: Final estimates of components from nonlinear least-squares fitting of distributions to different groups of data (Northern area). See table 4-2.

Type of data	N_s	N_i	N_{cp}	Type of distrib.	Mean	Std. dev.	%	RMS	χ^2	DF
Total sample set	2169	10	3	lognormal	74.6 153.1 325.0	170.3 44.0 77.1	34.9 28.8 36.4	$0.24 \cdot 10^{-2}$	30.6	16
Fine-grained lujavrites +	1478	6	2	normal	131.5 277.4	27.1 109.0	22.9 77.1	$0.56 \cdot 10^{-2}$	90.1	17
Fine-grained lujavrites :	1173	6	2	normal	134.6 300.2	32.8 86.9	30.1 69.9	$0.49 \cdot 10^{-2}$	31.5	13

nents. As was found in the Mine area, fine-grained lujavrites appear to be normally distributed. However, the fine-grained lujavrites in the Northern area differ considerably from those in the Mine area since they are composed of two populations. Removing samples of mixed geology does not account for the presence of the two modes, and it has, as yet, not been possible to relate the two modes by any geological explanation. However, Nyegaard (1979) states that the lower mode can be explained by the presence of low-grade samples in the uppermost parts of drill cores near the north-western contact (holes 64, 66, 67, 68 and 69, fig. 2-4).

The presence of a weak proportional effect in the Northern area can be seen from figure 4-39, in which local variances have been plotted against local means. Each pair of observations originates from one drill hole, representing about 50-100 samples altogether. Although the proportional effect is more pronounced than that found in the Mine area (fig. 4-4) it was not considered necessary to correct the data for this effect before the spatial variation was determined.

If the histograms from the two areas (figs. 4-1, 4-2, 4-37 and 4-38) and the scatter diagrams of local variance versus local mean (figs. 4-4 and 4-39) are compared, the following observations can be made:

(1) The uranium distribution in the Northern area represents both lower means and lower variances than those found in the Mine area. The reason for this is possibly the more homogeneous geology in the Northern area.

(2) The fine-grained lujavrites in the Northern area differ from the Mine area lujavrites in that two populations are present. It appears that the mean uranium value of the population representing the highest values is lower than the mean value for the corresponding Mine area population.

(3) The proportion of sample values higher than, say, 300 ppm is 44.5% in the Mine area and 24.0% in the Northern area. This implies a priori a lower uranium concentration in the Northern area. However, the samples taken in the Northern area represent a volume much larger than that covered by the Mine area samples.

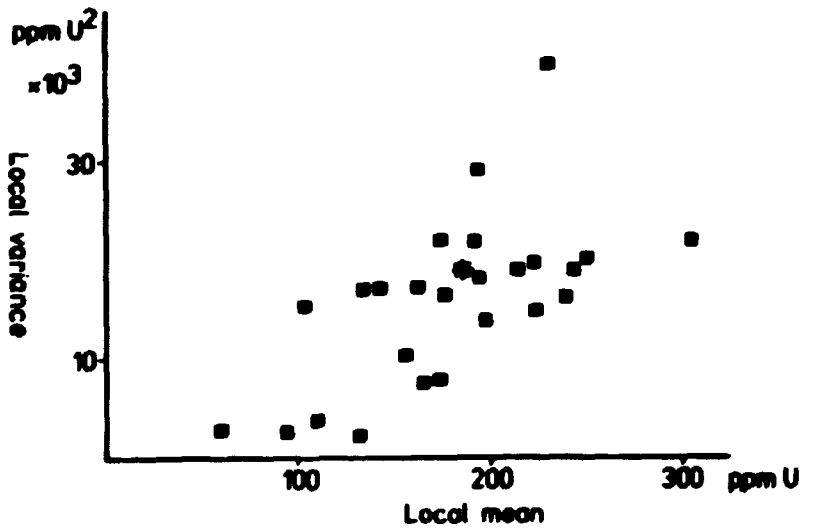

FIGURE 4-39: Testing for a proportional effect in the Northern area. Each value represents one drill hole. The overall mean and variance are indicated by the star.

4.3.2 Spatial structure.

Experimental semi-variograms were calculated down each drill hole using the program SEMI. These were averaged to give the overall vertical semi-variogram shown in figure 4-40. Again, attempts to calculate horizontal semi-variograms were frustrated by the large spacing between drill holes (approx. 140 metres). The spatial structure of the fine-grained lujavrites can also be seen from figure 4-40, as well as the overall semi-variogram from the Mine area which is shown for comparison.

The difference in the spatial structures of the uranium values within the two areas is obvious. Whereas the Mine area is characterized by a structure with a high nugget effect, a high sill value and a short range of influence, the Northern area semi-variograms display much lower sill values and, in at least one case, very long ranges of influence. This indicates a much more homogeneous distribution of uranium in this area which is due to the geology. The structure of uranium within the fine-grained lujavrites exhibits almost the same features as the structure from the total data set. Although the overall variance (the sill value) is considerably lower for these samples, the nugget effect and the range of influence appear to be almost unchanged. It may be noted that, because of the method of sampling of drill cores in this area (sec. 3.2.1), semi-variogram values can only be calculated at lags of even numbers of metres. However, two drill holes, 39 and 40 (fig. 2-4), which were drilled prior to 1977 were analyzed over every metre, allow the calculation of the semi-variogram at lags of odd metres. Since the numbers of pairs at these lags are substantially lower than at even-metre lags, the semi-variogram values differ from the overall structure, as can be seen in figure 4-40 (marked with open squares). Because of the scant information at these lags they were not considered when the model for the area was determined.

Trial and error, using programs FGAM2 and FGAM3 (appendix A), was used to fit the parameters of multi-component spherical

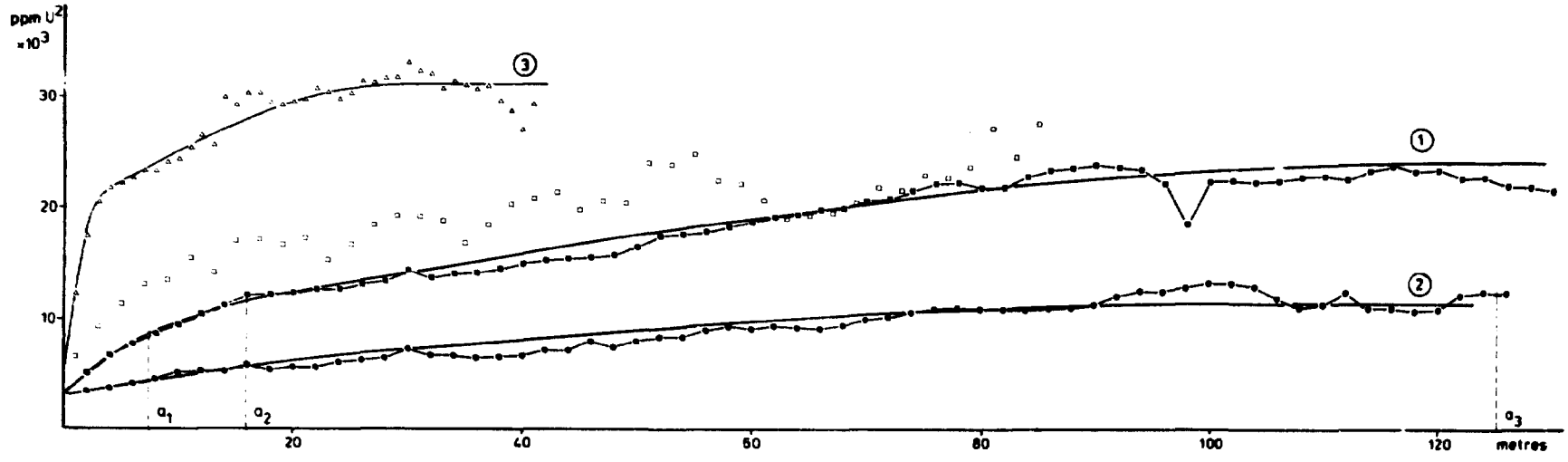

FIGURE 4-40: Experimental semi-variograms and core models from the Northern area, 1) total sample set (unfilled squares: contributions from holes 39 and 40) and 2) all fine-grained lujavrites. The experimental semi-variogram from the Mine area is also shown (3).

models with nugget effects (sec. 4.2.4) to the experimental semi-variograms of the total data set and to the fine-grained lujavrites. A first approximation for the overall model was given by the following:

$$C_o = 3300 \text{ ppm } U^2$$

$$a_{1\ell} = 7.5 \text{ metres}, \quad C_{1\ell} = 1600 \text{ ppm } U^2$$

$$a_{2\ell} = 16.0 \text{ metres}, \quad C_{2\ell} = 3800 \text{ ppm } U^2$$

$$a_{3\ell} = 125.0 \text{ metres}, \quad C_{3\ell} = 15700 \text{ ppm } U^2$$

That is, up to 16 metres the spatial structure of uranium values in drill core samples is dominated by a nugget effect and two small-scale spherical structures which contribute 35.7% of the total variance (the sill is 24400 ppm U^2). Beyond 16 metres the model consists of a nugget effect of 8700 ppm U^2 ($C_o+C_1+C_2$) and a large scale spherical component with a range of influence of 125 metres. The major difference between this model and the overall Mine area model is that the long range structure of the former contributes considerably to the total variation. In other words, the amount of random variation in the Northern area is much smaller than in the Mine area, implying that estimation in the Northern area can be performed with better precision.

The approximate core model was deregularised (sec. 4.2.7) to give the model:

$$C_o = 3300 \text{ ppm } U^2$$

$$a_1 = 6.5 \text{ metres}, \quad C_1 = 1733 \text{ ppm } U^2$$

$$a_2 = 15.0 \text{ metres}, \quad C_2 = 3931 \text{ ppm } U^2$$

$$a_3 = 124.0 \text{ metres}, \quad C_3 = 15764 \text{ ppm } U^2$$

By comparing the experimental semi-variogram of drill cores with the theoretical regularized curve for samples of length one metre given by the deregularised model (Clark, 1977) the fit was accepted (sec. 4.2.7).

The difference between the core model and the deregularised model is, apart from the ccrrections to the ranges of influence, equal to a difference of 328 ppm U^2 in the sill values (1.34%). This small value for the within-core variance is caused by the relatively large ranges of influence and by the small sill values of the short range components.

Similarly, a model was fitted to the experimental semi-variogram of the fine-grained lujavrites. The best fit was obtained using a two component spherical model with nugget effect, as defined by the parameters:

$$C_0 = 2800 \text{ ppm } U^2$$

$$a_1 = 20.0 \text{ metres}, \quad C_1 = 1200 \text{ ppm } U^2$$

$$a_2 = 105.0 \text{ metres}, \quad C_2 = 7500 \text{ ppm } U^2$$

This model mainly differs from the overall model by the absence of the spherical component representing the smallest range of influence. This indicates that the small scale structure is probably introduced by the inclusion samples. Apart from that, the model is in good accordance with the overall model although the variances of the individual components are less. Because of the relatively large ranges of influence found in the fine-grained lujavrites, deregularisation was considered unnecessary, and the model could therefore be used directly for kriging.

4.3.3 Block kriging.

Block kriging was done in the Northern area for the following purposes:

(1) To produce grade-tonnage curves based on kriging using the overall semi-variogram model. The effects of block size and bench height were investigated.

(2) To study how samples (bench composites) were weighted by kriging and how these weights were influenced by the block/bench size.

(3) To produce grade-tonnage curves based on selective kriging using the semi-variogram model for the fine-grained lujavrites. Input data and estimated blocks were sorted by their geology.

(4) To study the regression effect on the grade-tonnage curves.

The program TREREG was used throughout the study. Some difficulties arose when the drill core samples from the Northern area were read into the program, because of the bench compositing method (fig. 4-21). The program stops compositing whenever a gap is reached in the core. Consequently, the number of bench composites could be equal to the number of samples, and this would exeed the capacity of the program. It was therefore necessary to input data as if there were no gaps between samples, by specifying a (false) sample length of two metres. It is believed that estimation remained unaffected by this approximation, because sample values were averaged over the whole bench to form the bench composites.

4.3.3.1. Block pattern. As in the Mine area (sec. 4.2.10.1), a random stratified grid (RSG) was fitted to the drill hole pattern. An acceptable fit was obtained by a 140 by 140 metre grid as shown in figure 4-41. Most grid squares contained one drill hole, two contained no holes, two contained 2 holes and one contained 3 holes. This gave a total of 22 blocks to be estimated on each bench. The outline of the RSG almost coincided

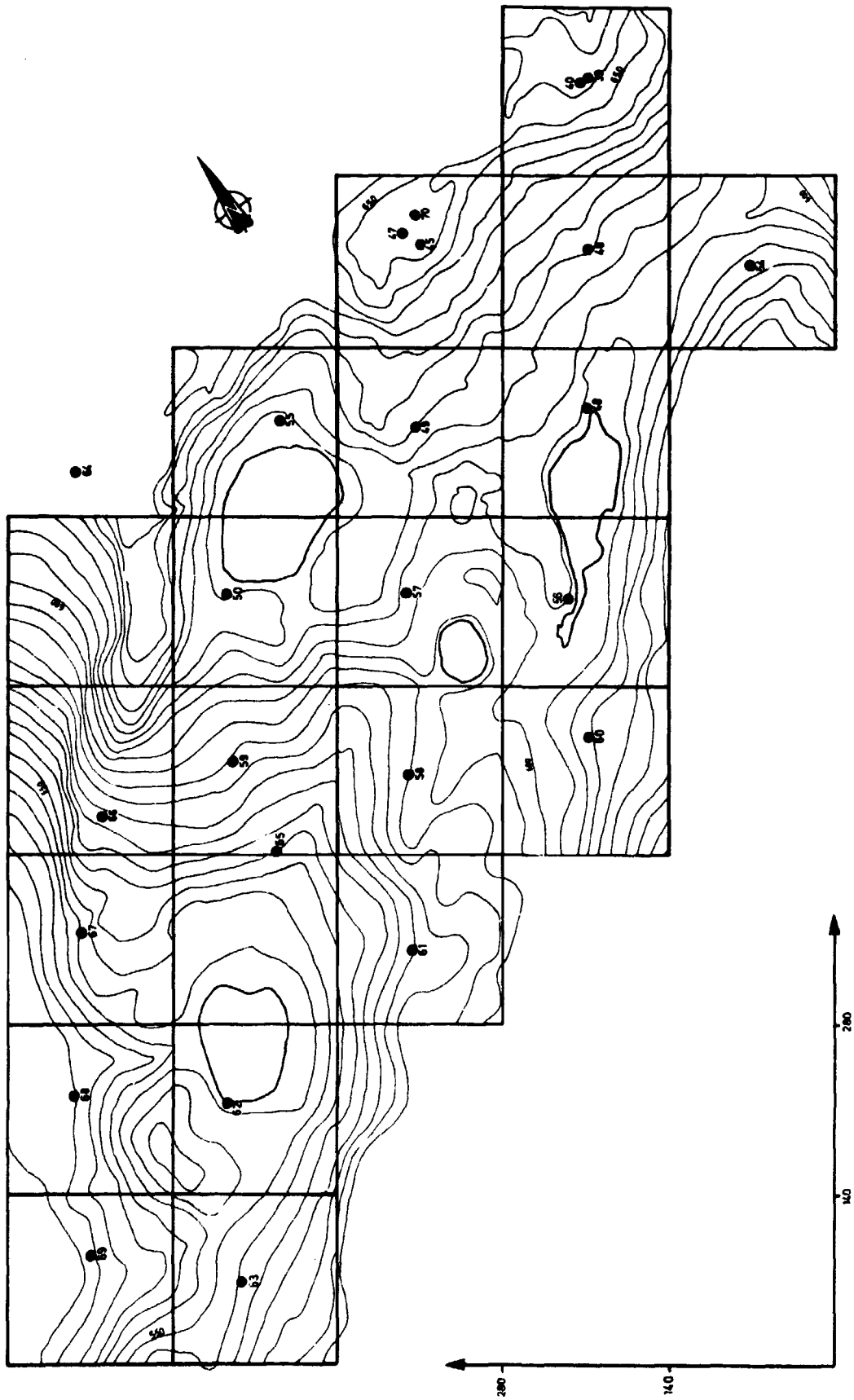

FIGURE 4-41: Random stratified grid fitted to the drill hole pattern in the Northern area (140x140 metres)

with the outline of the block pattern used in previous tonnage calculations (Nyegaard et al., 1977). A comparison of the two block patterns is given in plate I, and the location and orientation of the RSG is given in section 3.1 (CS_{north}).

4.3.3.2. Effect of block size/bench height. Global estimates. 3-dimensional block kriging was done within the outline of the RSG shown in figure 4-41. The overall (three-component) semi-variogram model was used for kriging and the following block sizes and bench heights were considered:

(a) Block size : 140 x 140 x H metres
Bench heights: 1, 10, 20, 50 and 100 metres.

(b) Block size : 70 x 70 x H metres,
Bench heights: 10, 20 and 50 metres.

It is obvious that a block size of 140 by 140 by one metre is unrealistic in a mining context. However, tonnage calculations published by Nyegaard et al. (1977) were based on accumulations of 'ore slices' of about that size. On the other hand, very large blocks of 140 by 140 by 100 metres will probably contain a mixture of several geological units, in which case only a poor distinction between ore and waste can be made.

The blocks estimated in the area were sorted geographically and with respect to the topography by the program SELNOR (appendix A). A summary of the results is listed in table 4-18, in which two estimates have been calculated for a block size of 140 by 140 by 20 metres by using different search volumes. In the first estimate samples within neighbouring blocks and in blocks above and below the bench were included (search area 112), whereas the second used only the samples within the estimated block and in blocks above and below the bench (search area 004). In the remaining cases search areas were established subjectively by considering the block size and the structure indicated by the semi-variogram model. Table 4-18 demonstrates that:

TABLE 4-18: Summary statistics from block kriging of uranium in the Northern area. The block volume is given in m^3, the block mean and the standard errors in ppm U.

Block size	No. of blocks	Block volume	Search area	Block mean	Block std.err.	$\bar{\sigma}_k$
140×140×1	2138	19600	004	160.9	105.5	107.5
140×140×10	584	196000	114	149.8	53.5	63.7
140×140×20	294	392000	112	150.2	49.4	63.2
140×140×20	279	392000	004	146.5	60.8	79.7
140×140×50	128	980000	112	151.8	41.6	59.0
140×140×100	60	1960000	111	164.3	35.3	53.4
70×70×10	2031	49000	113	152.9	72.1	96.5
70×70×20	1150	98000	222	150.5	53.8	92.2
70×70×50	512	245000	222	153.2	46.0	88.4

(1) The standard deviations of values from small blocks are higher than from large blocks, thus confirming the volume-variance relationship.

(2) The smallest blocks are estimated with the highest kriging errors.

(3) Disregarding the extreme block sizes of 140x140x1 and 140x140x100, kriging produces block estimates with a mean of 152 ppm uranium. In theory this value should lie close to the mean value of samples. However, the mean value of the samples is 186.8 ppm U (table 4-16), indicating that many low grade blocks have been estimated. Consulting the bench plans in the output from TREREG (appendix B), it was confirmed that blocks estimated at the 'bottom' of the deposit, and thus below the samples, were generally of low grade due to low grade samples at the bottom of several drill holes.

(4) The deviations of the mean value noted for the block size 140x140x1 are due to the low number of blocks which can be estimated outside the sampled volume (search area 004), and in the case of 140x140x100 metre blocks to a different global volume.

(5) Regarding the results from the 140x140x20 metre blocks it can be seen that search area 004 (max. 9 samples), compared with 112 (max. 45 samples), produced the highest block standard deviation. This implies that the inclusion of a large number of samples in the kriging system tends to smooth the block values considerably.

Grade and tonnage estimates for different cutoff values (150, 200 and 250 ppm U) are listed in table 4-19 and grade-tonnage curves are presented in figures 4-42 and 4-43. Due to the block variance the highest tonnage values are obtained from the smallest block sizes if cutoff > mean. If the cutoff value is close to the mean value of the blocks the differences in uranium tonnage naturally decrease, and the block size is of no importance. The most probable estimate of the uranium tonnage in the Northern area is consequently the tonnage obtained at a cutoff value close to 150 ppm U. This estimate is approx. 27.000 tons of uranium. At higher cutoff values the tonnage decreases sharply. This is probably explained by the exaggerated smoothing effect when such relatively large blocks are kriged.

The effects of the block size and bench height are illustrated in figure 4-44, where uranium tonnages are plotted against block volumes at cutoffs of 200 and 250 ppm. At cutoff 200 ppm a small decrease in the global uranium tonnage is produced when the block volume is increased. However, when the cutoff is raised the effect of the block volume becomes marked. Secondly, a distinction between 140x140 and 70x70 metre blocks is now possible. This indicates that the distribution of block estimates is not only effected by the sample volume, but also by its geometry. In terms of the kriging system this can be explained by the alterations in the $\bar{\gamma}$(sample,block) values.

TABLE 4-19: Grade-tonnage estimates at cutoff grades 150, 200 and 250 ppm uranium using different block sizes. Ore tonnage in millions of tons, uranium tonnage in tons, mean grade in ppm U.

Block size	Cutoff: 150 ppm U			Cutoff: 200 ppm U			Cutoff: 250 ppm U		
	Ore tonnage	Uranium tonnage	Mean grade	Ore tonnage	Uranium tonnage	Mean grade	Ore tonnage	Uranium tonnage	Mean grade
140×140×1	54.7	13799	252.4	39.8	11227	281.7	27.3	8406	307.9
140×140×10	132.8	26709	201.1	60.3	14256	236.3	19.1	5098	267.6
140×140×20	136.5	26804	196.3	59.3	13628	229.9	13.8	3639	264.5
140×140×20	123.3	25668	207.3	67.7	15867	234.3	15.9	4279	269.6
140×140×50	158.8	29691	187.0	47.6	10881	228.5	6.3	1343	253.7
140×140×100	190.5	35839	188.0	63.5	13588	214.0	-	-	-
70×70×10	121.7	26597	218.5	70.1	17607	251.1	30.7	8780	286.1
70×70×20	136.5	27221	199.4	59.5	13946	234.3	15.1	4097	271.6
70×70×50	158.8	30654	193.1	55.6	12784	230.1	8.6	2330	270.9

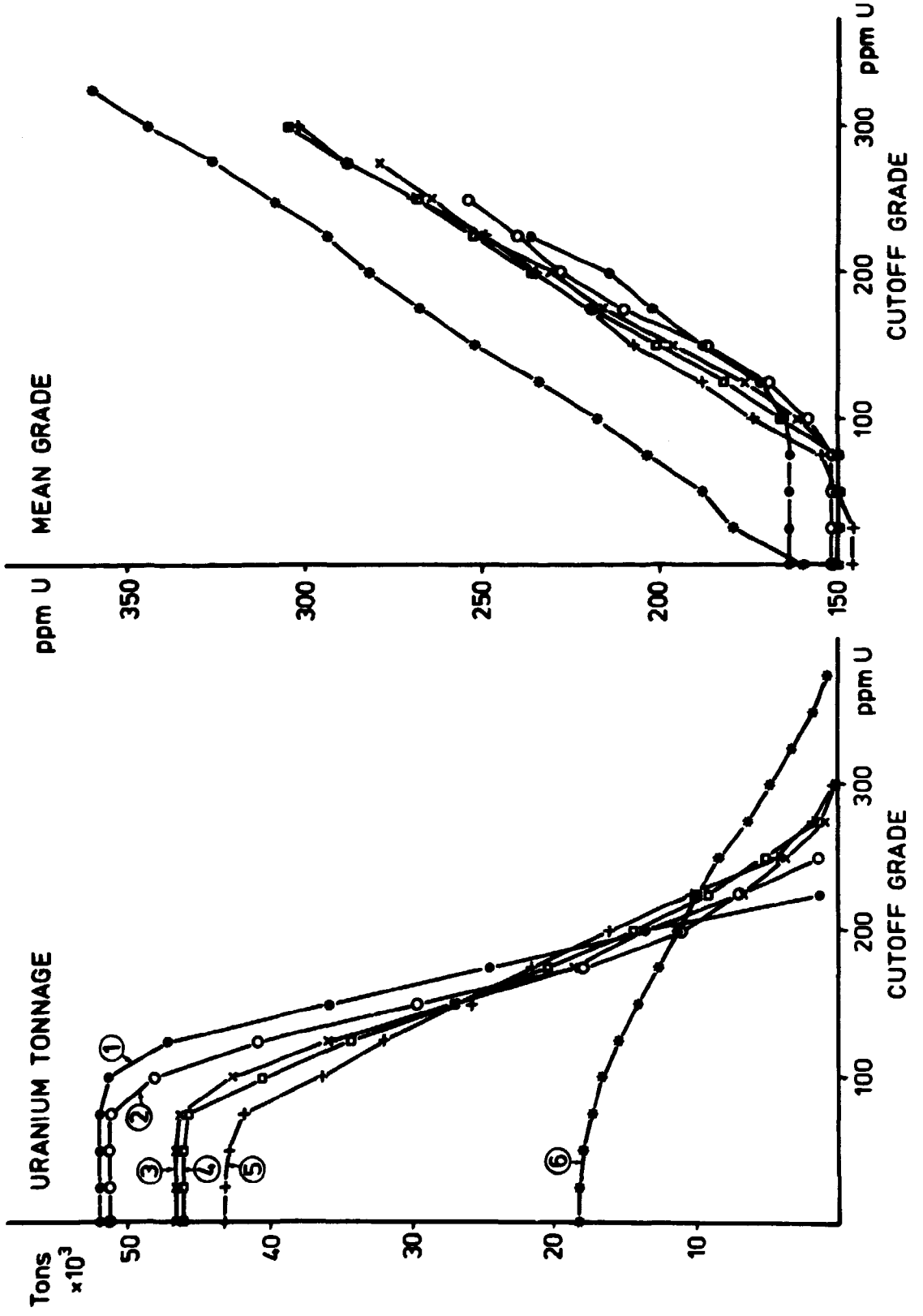

FIGURE 4-42: Estimated global reserves in the Northern area. Curves of uranium tonnage and average grade versus cutoff grade. Block size is 140x140 metres. Bench heights: 1) 100 m, 2) 50 m, 3) 20 m (search area 112), 4) 10 m, 5) 20 m (search area 004) and 6) 1 m.

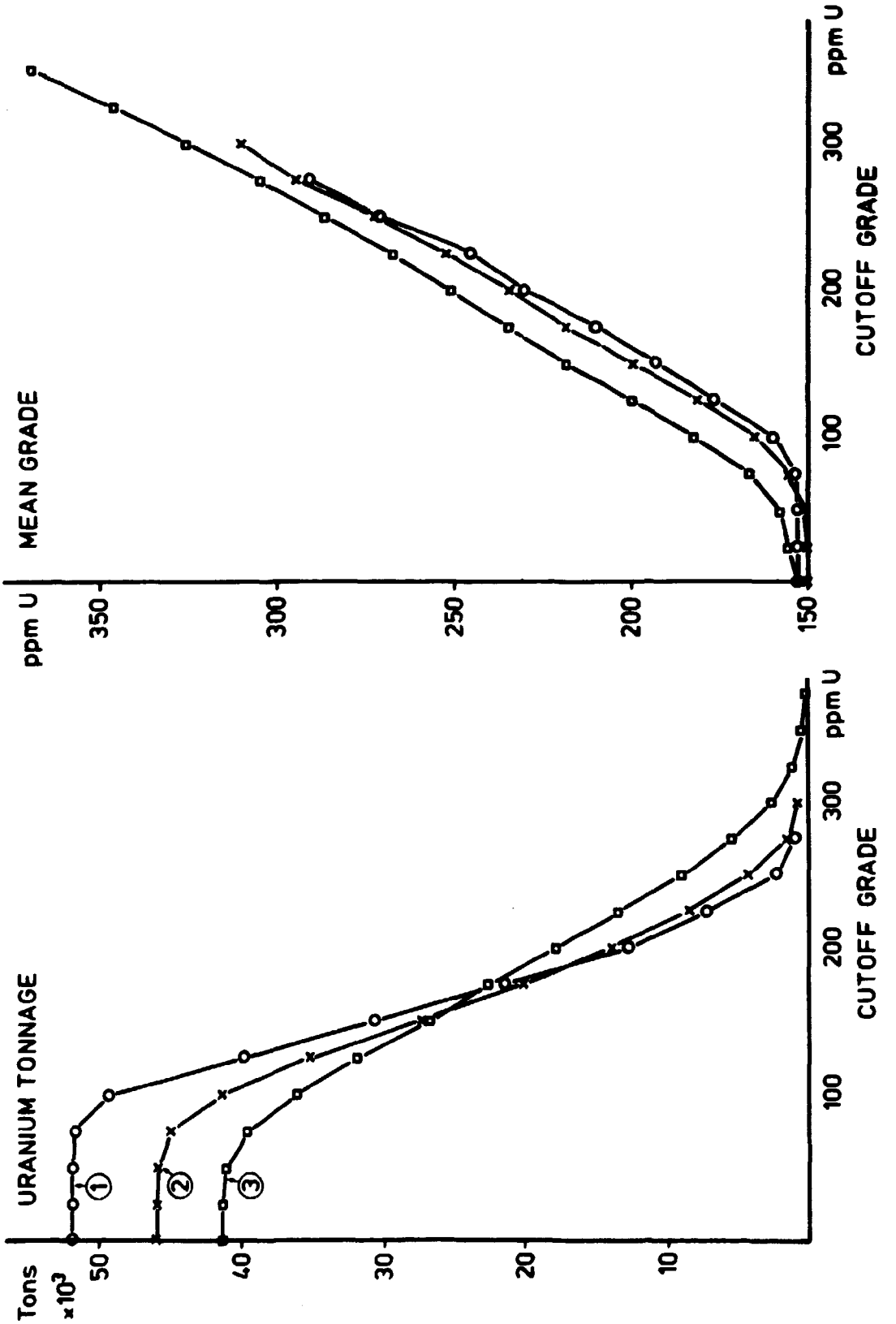

FIGURE 4-43: Estimated global reserves in the Northern area. Curves of uranium tonnage and average grade versus cutoff grade. Block size is 70x70 metres. Bench heights: 1) 50 m, 2) 20 m and 3) 10 m.

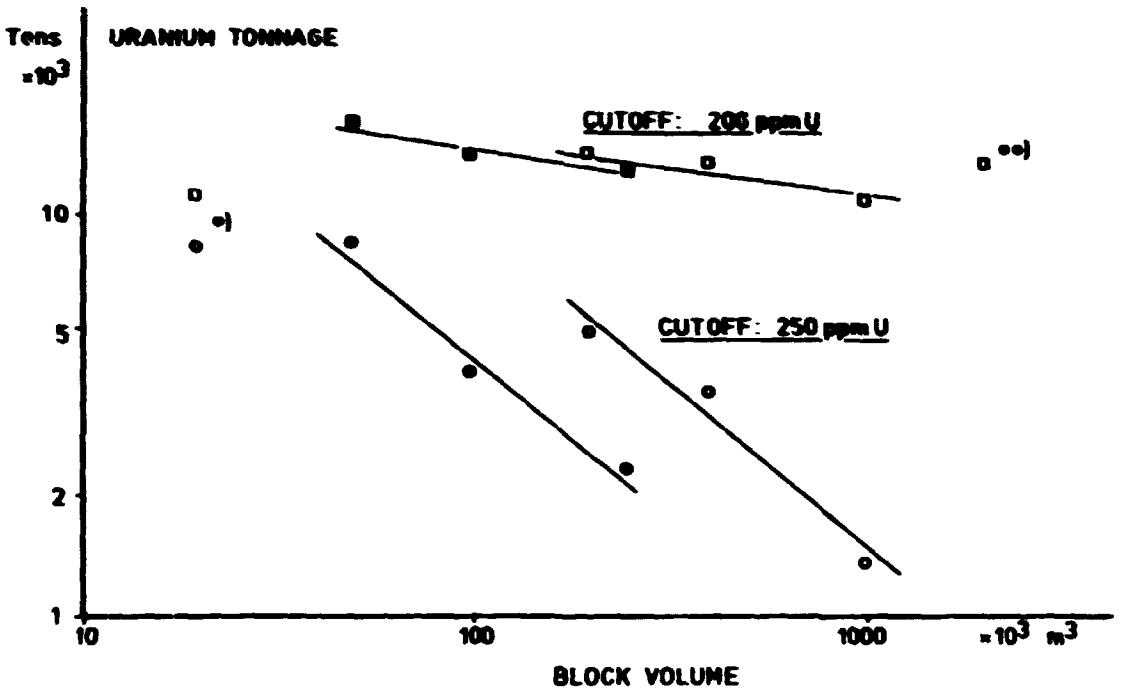

FIGURE 4-44: Illustration of the volume-variance relationship in the Northern area. Plots of estimated uranium tonnages above cutoffs 200 and 250 ppm U versus the block volume. Filled symbols: 70x70 metre blocks, unfilled symbols : 140x140 metres. Squares belong to a 200 ppm cutoff, circles to a 250 ppm cutoff. *) unreliable.

4.3.3.3 Block size and kriging weights. Figure 4-45 shows a typical bench plan for the estimation of the 140x140x10 metre block intersected by drill hole 58. The search area is 111 and the bench composites in the area are shown at their approximate locations. At each of the 24 samples is indicated the weight assigned by 3-dimensional kriging. The samples within, and immediately above and below the block estimated, contain less than half of the total information (46%) used to evaluate the block; the remaining 54% comes from the surrounding samples. On the other hand, the most remarkable feature is that samples in the benches above and below are assigned bigger weights (18%) than the samples located on the same bench as the blocks estimated (10%). Although this is intuitively hard to accept, it is a feature of the kriging system. Because of the combination of a semi-variogram with a large range of influence and a relatively thin block, kriging gives higher weights to external

samples as they contain more information, due to the large volume outside the block which they represent.

This weighting-pattern explains the smoothing effect demonstrated in the grade-tonnage curves. If, for example a high-grade lujavrite block is surrounded by samples intersecting low-grade inclusions, the block will be estimated as being medium or even low grade. The concentration of block values around the mean therefore seems to be due to an overweighting of waste material when 'ore' blocks are estimated. If small blocks could be estimated with acceptably small errors, i.e. if more samples were available, this impasse could probably be avoided.

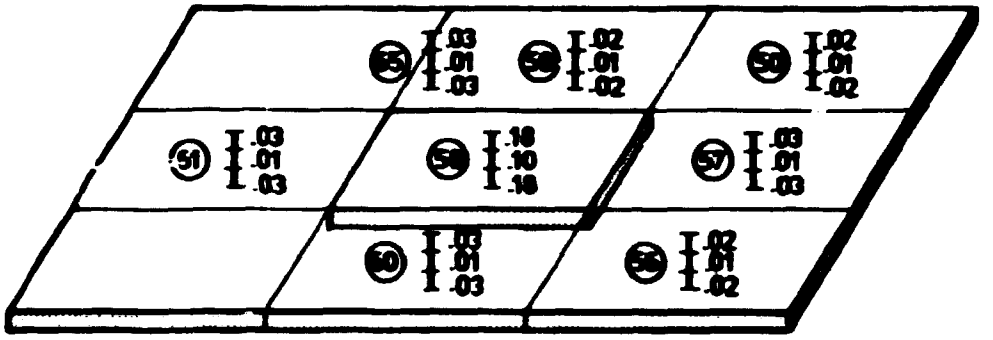

FIGURE 4-45: Typical bench plan from three-dimensional kriging. The central block intersected by drill hole 58 is estimated from the bench composites shown. The kriging weights are indicated.

The examples presented in figure 4-46a-c illustrate how the kriging weights are influenced by the block size and the bench height. If search area 002 or 004 is considered, that is, only the samples in the intersecting drill hole are used, it is again found that for a 140x140x10 metre block (fig. 4-46a) the largest weight is given to the sample farthest from the block. The importance of the internal sample is highest for the smallest search area. If the block size is decreased to 70x70 metres and the bench height increased to 20 metres (fig. 4-46b), the weights are changed significantly. The largest weights are now assigned to the internal samples and those

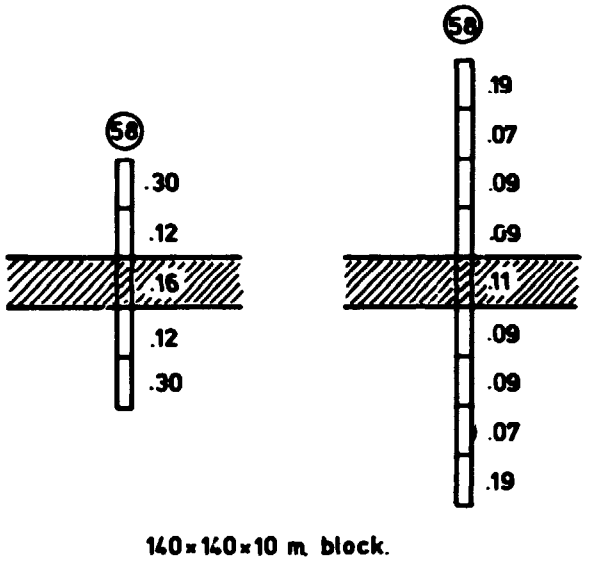

140×140×10 m. block.

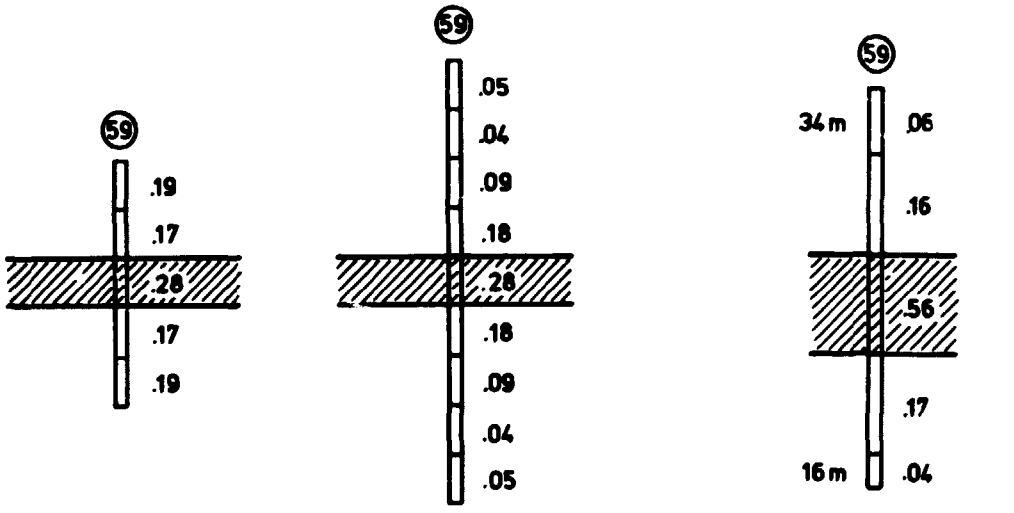

70×70×20 m. block

70×70×50 m. block

FIGURE 4-46: Effects on the kriging weights of the block size and the bench height. Northern area. Search areas used: 002 and 004.

close to the block. Slight increases in the weights can still be recognized going from the second most distant tc the most distant sample. Finally, if the bench height is further increased to 50 metres (fig.4-46c), the total information contained in the external samples becomes less than 50% and the most distant samples now get very small weights, as would be intuitively acceptable.

4.3.4 Selective kriging.

As a result of the marked smoothing effect of kriging demonstrated in the previous section, it was decided to krige selectively in order to avoid the effects of the inclusions. Selective kriging was done as follows. The volume considered was set equal to the volume used in ordinary block kriging (fig. 4-41) and block sizes 140x140x10 and 140x140x20 were used. The total volume was then estimated using the semi-variogram of the fine-grained lujavrites (sec. 4.3.2) and considering only those samples taken within the fine-grained lujavrite sections. In practice this was done by substituting assay values from non-fine-grained lujavrite samples by a 'missing value' in the input data file. In this way lujavrite blocks were evaluated using only lujavrite samples. However, blocks may be estimated in areas where non-lujavritic material is present (as indicated by drill core samples). Consequently, the estimated blocks were sorted taking both location and geology into account. The geology of an individual block was determined by comparing the lithological drill core logs (Nyegaard et al., 1977) with the bench plans. If at least 80% of the samples located within the block were of lujavrite, the block was considered as such. Otherwise, the block was removed from the data file. In cases where no drill holes intersected the block its geology was determined from the surrounding holes, still using the 80% criterion.

Grade-tonnage values from selective kriging are given in table 4-20 and the grade-tonnage curves appear in figure 4-47. 265 blocks out of 584 (table 4-18) were selected geologically when

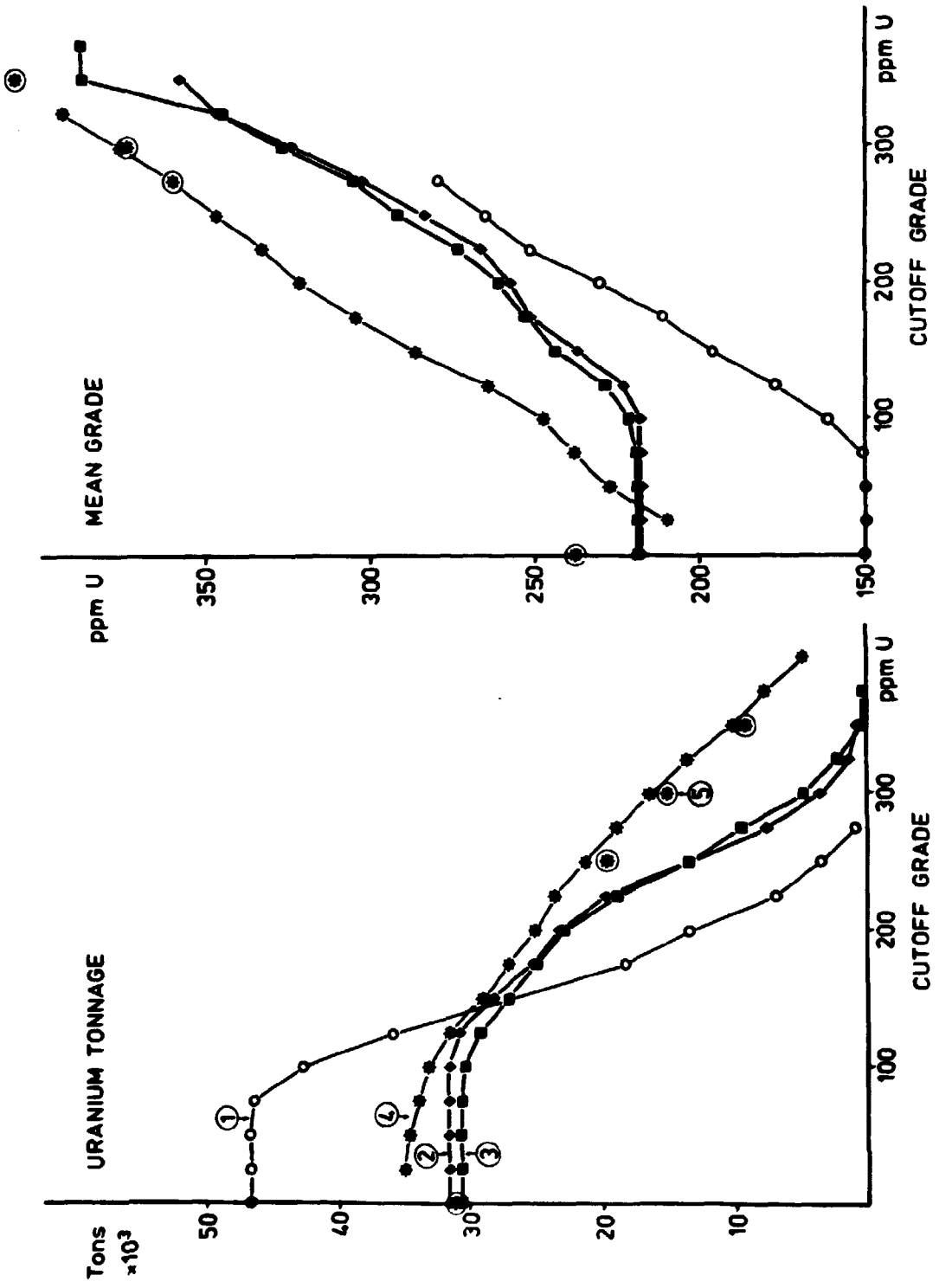

FIGURE 4-47: Comparison of global estimates of uranium tonnage and average grade in the Northern area. 1) Overall kriging (b.s. 140x 140x20, s.a. 112), 2) selective kriging (b.s. 140x140x20 m), 3) selective kriging (b.s. 140x140x10 m), 4) conventional methods (all rock types) and 5) conventional methods (fine-grained lujavrites). (4 and 5 from Nyegaard et al., 1977).

TABLE 4-20: Grade-tonnage estimates from selective kriging using two different block sizes. Units as in table 4-19.

Cutoff grade	No. of blocks	Ore tonnage	Uranium tonnage	Mean grade	Average stand.err.	Error on the global mean
Block size: 140x140x10 m						
0	265	140.2	30721	219.1	41.5	2.6
100	260	137.6	30469	221.6	41.1	2.6
200	267	88.4	23080	261.2	38.2	3.0
250	88	46.6	13561	291.2	37.5	4.0
300	28	14.8	4837	326.5	39.0	7.4
350	2	1.1	410	387.8	40.5	28.6
Block size: 140x140x20 m						
0	137	145.0	31678	218.5	39.3	3.5
100	137	145.0	31678	218.5	39.3	3.5
200	86	91.0	23407	257.2	36.4	4.0
250	45	47.6	13470	282.8	34.5	5.2
300	10	10.6	3431	324.2	37.6	12.0
350	2	2.1	756	357.2	36.8	26.0

the bench height was 10 metres. Using a 20 metre bench, 137 out of 294 blocks were selected. Figure 4-47 shows the grade-tonnage curves from the 'overall kriging' on 20 m. benches and from conventional estimation (Nyegaard et al., 1977). Good agreement between the three different estimation methods is found for the tonnage estimates near the mean value. However, the difference between overall kriging and selective kriging is pronounced as soon as higher cutoff values are considered. No significant differences in the uranium tonnage and the mean grade are observed when comparing the two bench heights, although the volume-variance relationship can still be recognized. Comparing selective kriging with the conventional methods shows clearly the strong effect of the volume-variance relationship.

The tonnage-value within fine-grained lujavrites at a cutoff value zero is estimated as approx. 30800 tons U by the conventional methods. This is confirmed by selective kriging (table 4-20). Furthermore, tonnage values of all rock types estimated by conventional methods are confirmed, to within less than 10%, by selective kriging at cutoff values in the interval from 100 to 225 ppm U; that is, between the mean value of the total data set and the mean value of the fine-grained lujavrites. However, estimates of the uranium tonnage become increasingly different between the two methods as higher (>200 ppm U) cutoff values are taken. For example, at a cutoff value of 300 ppm selective kriging gives some 10000 tons of uranium less than the conventional methods.

It is the author's opinion that the grade-tonnage curves produced by selective kriging represent the most reliable estimates of the resources in the Northern area. It can be seen in table 4-20 that on average blocks are estimated with a standard error of about 35-40 ppm U. Consequently, the 95% confidence interval for the individual block estimates is approx. +/- 75 ppm U.

Secondly, it is believed that the marked differences in grade-tonnage estimates found between selective kriging and conventional methods, of fine-grained lujavrite, are due simply to a volume-variance effect. The conventional estimation method was based on the accumulations of one-metre thick horizontal slices. The average grade of each slice was estimated as being the value of the sample of the core intersecting the slice, so the resulting distribution of block values was identical to the distribution of drill core samples. Thus, the grade-tonnage curves from the conventional methods are only true if the deposit is mined in units of one metre drill cores. This is of course a completely unrealistic approach. On the other hand, a 140x140x10 metre block is propably far too big for a mining unit, giving somewhat pessimistic estimates at high cutoff values. The most reliable estimate is found by using a block size equal to that of the actual mining unit. The kriging errors calculated in the present study (tables 4-18 and 4-20)

show, however, that this approach is impossible unless a much denser sampling pattern is available.

Recalling the results from the Mine area (table 4-15) good agreement wasfound between kriging estimates and the conventional methods. It is the author's opinion that the differences between the estimates from the two areas can be explained by two facts. Firstly, the spatial structure in the Mine area is characterized by a much smaller range of influence than that found in the Northern area. Therefore, from the study of the kriging weights it may be concluded that samples inside a block tend to be given higher weights in the Mine area. Hence, Mine area blocks are less affected by 'outside' samples than the Northern area blocks, and since conventional estimation in the Mine area was done using only the nearby samples, the agreement can be understood. Secondly, conventional estimation in the Mine area differs from the Northern area, in that 3 peripheral samples were averaged to form the block estimate instead of using only one internal sample. Using average values of the samples will automatically give the distribution of block values a lower variance than the corresponding sampling distribution. Hence, the estimates of such blocks are more like the kriged estimates, because kriging is itself a weighted average of sample values.

4.3.5 Georegression.

The 584 block estimates from overall kriging (140x140x10 m blocks, table 4-18) were corrected by the two georegression estimators described in sec. 4.2.14. Grade-tonnage estimates from least-squares (LS) and perpendicular distance (PD) georegression are presented in table 4-21, and their grade-tonnage curves are compared in fig. 4-48 with the corresponding curves when kriging is used alone. As demonstrated in the Mine area, PD georegression produces estimates which are more alike the kriged estimates than the LS georegression results. In fact, PD georegression hardly changes the estimates obtained by kriging, whereas LS georegression again tends to move block values

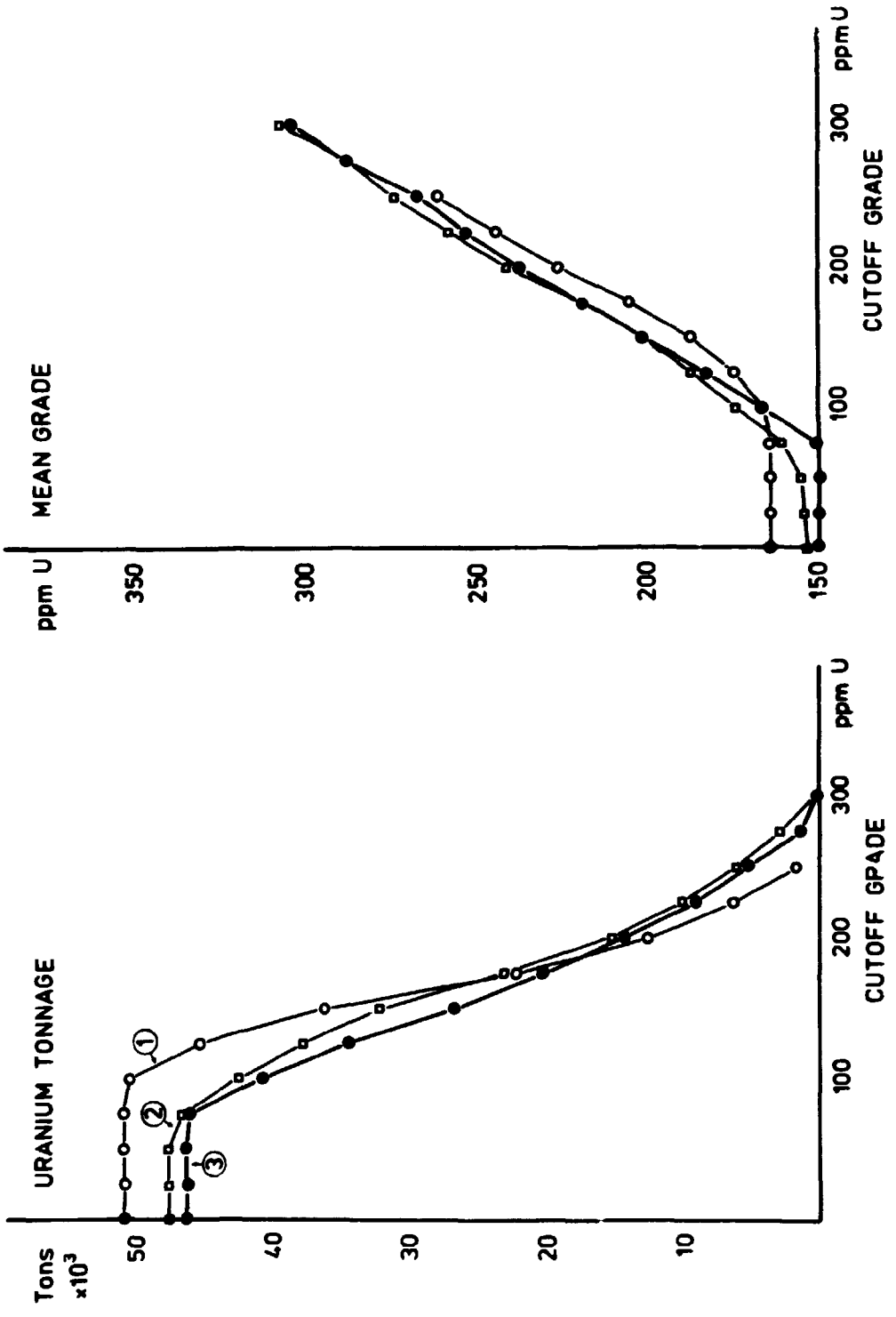

FIGURE 4-48: Estimated global reserves in the Northern area. Block size is 140x140x10 metres. 1) Least-squares georegression, 2) perpendicular distance georegression and 3) overall (uncorrected) kriged block values.

towards the mean value. Since PD georegression reduces errors both on the estimator and on the sample values, it will theoretically work better than LS georegression if 1) high analytical errors are present in the sample value 2) a high nugget effect is present and the locations of samples are uncertain. If the PD georegression estimator is considered to be the best correction method, because of highly erratic mineralization (Clark and Clausen, 1981), the results show that kriged global estimates of the Northern area give grade-tonnge curves which are almost unbiased. Hence, the results presented earlier, including the selective kriging estimates, do not need to be corrected for a regression effect.

It is believed that the different 'response' when georegression is applied to the kriged estimates from either the Mine area or the Northern area may arise from the differences in spatial structure. However, quantifying this difference is not, as yet, possible. Secondly, it should be recalled that the analytical errors of sample values are much higher in the Mine area than in the Northern area (sec. 3.2.2.1), and that the geographical locations of samples in the Mine area are much more uncertain than in the Northern area (table 3-1).

4.4 Uranium in the Northern area (logging data).

The uranium values obtained by gamma-spectrometric logging of drill holes were briefly investigated in order to:

(1) Compare the distribution of logging values with the distribution of assay values.

(2) Describe the spatial variation of the logging values and to use this for a geostatistical block estimation.

TABLE 4-21: Grade-tonnage estimates for uranium in the Northern area. Block estimates are corrected by georegression. The block size is 140x140x10 metres. Units as in table 4-19.

Cutoff grade	No. of blocks	Ore tonnage	Uranium tonnage	Mean grade	Average stand.err.	Error on the global mean
Least squares georegression						
0	584	309.1	50819	164.4	54.9	2.3
100	577	305.3	50454	165.2	54.9	2.3
200	106	56.1	12670	225.9	48.5	4.8
250	13	6.9	1792	260.5	47.9	13.3
300	-	-	-	-	-	-
Perpendicular distance georegression:						
0	584	309.1	47591	154.0	60.3	2.5
100	460	243.4	42371	174.1	59.4	2.8
200	119	63.0	15207	241.5	53.5	5.0
250	42	22.2	6095	274.2	52.1	8.1
300	4	2.1	649	306.9	57.6	28.9

4.4.1 Uranium distribution.

A histogram of 4268 logging values is shown in figure 4-49 and summary statistics are listed in table 4-22. The shape of the histogram is very much like the histogram of assay values (figure 4-37). However, the number of samples in the interval 0 to 25 ppm has increased, resulting in a slight decrease in the mean value and an increase in the standard deviation. The reason for this increase in the number of low grade samples is that all the inclusions (which are almost barren) have been logged whereas only a few of these had been sampled for assaying.

TABLE 4-22: Simple statistics for uranium (ppm) in logging data from the Northern area.

Type of data	N_s	Mean	Std. dev.	Coeff. of var.
Total sample set	4268	170.6	153.6	0.90

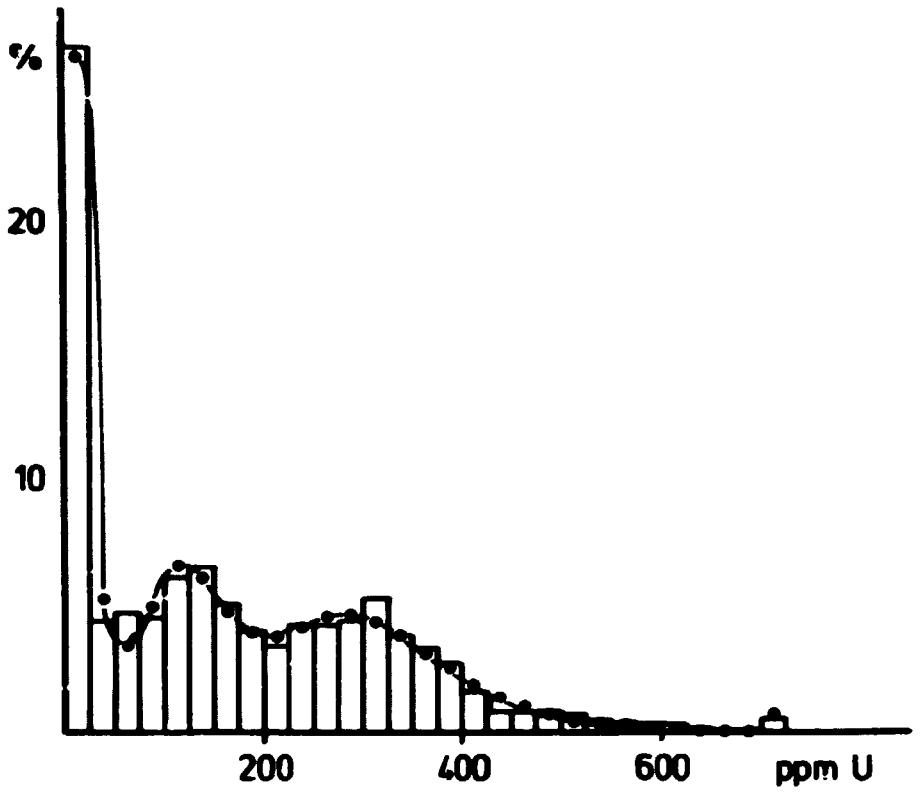

FIGURE 4-49: Histogram of uranium values in the logging data. A fit to a three-component log-normal distribution is shown. The number of samples is 4268.

Again, the best fit to the distribution was a mixture of three lognormal distributions with the parameters listed in table 4-23. Because of the additional low grade samples the fit deviates somewhat from the fit given to the assay histogram (table 4-17). The three components are comparable, however.

TABLE 4-?3: Final estimates of components from nonlinear LS fitting of distribution to uranium in logging data. See table 4-2.

Type of data	N_s	N_i	N_{cp}	Type of distrib.	Mean	Std. dev.	%	RMS		DF
Total sample set	4268	7	3	lognormal	67.8 142.4 325.0	362.2 48.5 88.8	41.2 24.6 34.2	$0.33\ 10^{-2}$	88.0	21

4.4.2 Spatial structure.

The overall vertical semi-variogram of the logging values is shown in figure 4-50. It is similar to the assay value semi-variogram (figure 4-40), but fewer fluctuations occur. The similarity is confirmed by the model which gave the best fit. The model, shown in 4-50, is composed of three spherical models and a nugget effect:

$$C_0 = 1000 \text{ ppm } U^2$$

$$a_1 = 5.0 \text{ metres}, \quad C_1 = 4200 \text{ ppm } U^2$$

$$a_2 = 20.0 \text{ metres}, \quad C_2 = 3500 \text{ ppm } U^2$$

$$a_3 = 105.0 \text{ metres}, \quad C_3 = 13700 \text{ ppm } U^2$$

It can be seen that the total sill of this model (22400 ppm U^2) is slightly lower than that of the assay values. Secondly, the nugget effect has decreased from 3300 to 1000 ppm U^2, whereas the sill value of the first spherical component has increased correspondingly. This, again, can be explained by the additional low grade samples.

It can be concluded that the spatial structures of uranium in the Northern area are equally well described by the assay data and the by logging data. This finding supports the conclusion that the semi-variogram model based on assay data is valid, although samples have been taken only at every second metre.

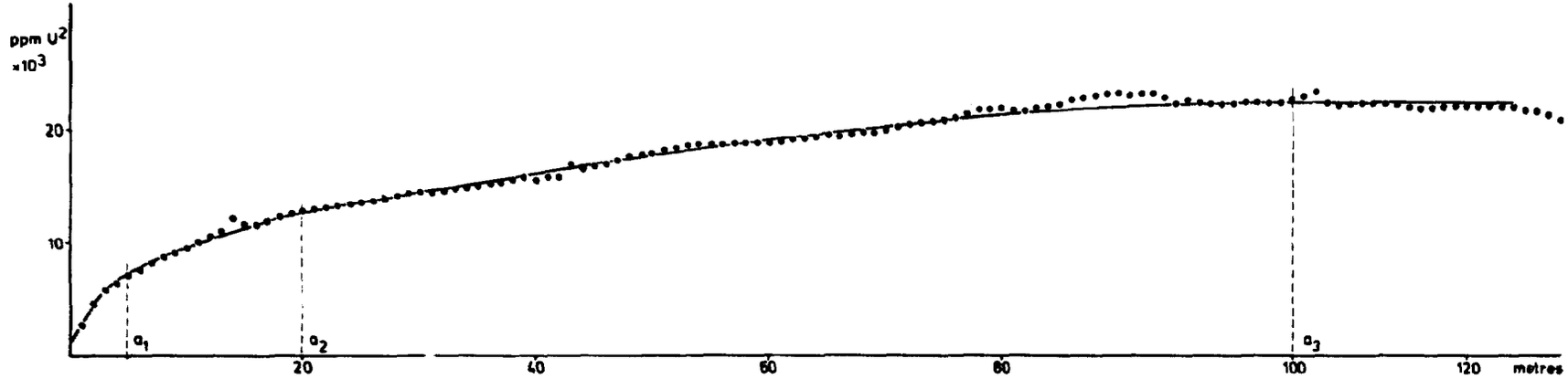

FIGURE 4-50: Experimental semi-variogram and model for uranium values in the logging data (Northern area).

4.4.3 Block kriging.

3-dimensional block kriging was done within the outline of the RSG used for kriging from the assay values. Estimates were made using two block sizes, 140x140x20 m. (S.A. 112) and 70x70x20 m. Grade-tonnage values for various cutoff grades are listed in table 4-24 and the following remarks can be made:

(1) The variance of the 'logging blocks' is much higher than the variance of 'assay blocks':

Block size:	140x140x20 m;	70x70x20 m;
Assay blocks:	2440	2894
Logging blocks:	5063	7102

This resulted in higher grades and tonnages at cutoff grades above the mean value. At the mean value grades and tonnages were comparable. Thus, the improvement in block selection made by taking more samples is clearly seen. Uranium tonnages estimated from the logging data by conventional methods (Løvborg et al., 1980) were higher than tonnages calculated from the assay values (Nyegaard et al., 1977).

(2) Kriging using logging data gave a slightly smaller average standard error than the assay data. This is explained by a) the lower value for the total sill and b) logging within areas which have not been sampled for assaying, i.e. more bench composites were available for kriging.

(3) The tonnage curves given by Løvborg et al. (1980) are indicated in figure 4-51, together with the grade-tonnage curves produced by kriging. As noted in the equivalent comparison of 'assay blocks', tonnages are comparable near the mean value of the samples, but differ at higher cutoff grades due to the volume-variance relationship. The conventional calculations using the logging data were, as with the assay values, based on accumulations of 1 metre thick ore slices.

TABLE 4-24: Grade-tonnage values from block kriging using the logging data. Units as in table 4-19.

Cutoff grade	No. of blocks	Ore tonnage	Uranium tonnage	Mean grade	Average stand.err.	Error on the global mean
Block size: 140×140×20						
0	289	305.9	48243	157.7	61.1	3.9
100	227	240.3	43384	180.6	59.3	4.3
200	75	79.4	19497	245.6	58.2	7.4
250	21	22.2	6901	310.5	77.8	19.3
300	7	7.4	3002	405.2	125.4	49.2
350	5	5.3	2315	437.5	144.3	64.7
Block size: 70×70×20						
0	1047	277.0	44625	161.1	94.4	3.0
100	785	207.7	40263	193.8	93.5	3.4
200	332	87.8	22923	260.9	92.3	5.2
250	159	42.1	12648	300.6	95.9	7.8
300	51	13.5	4793	355.1	104.6	15.2
350	24	6.4	2525	397.6	116.3	24.6

It is believed that the logging data, although subject to high analytical errors (sec. 3.2.3), produce more realistic estimates of the grade-tonnage curves in the Northern area. The additional samples obviously overcome some of the smoothing discovered when the assay values were used for estimation.

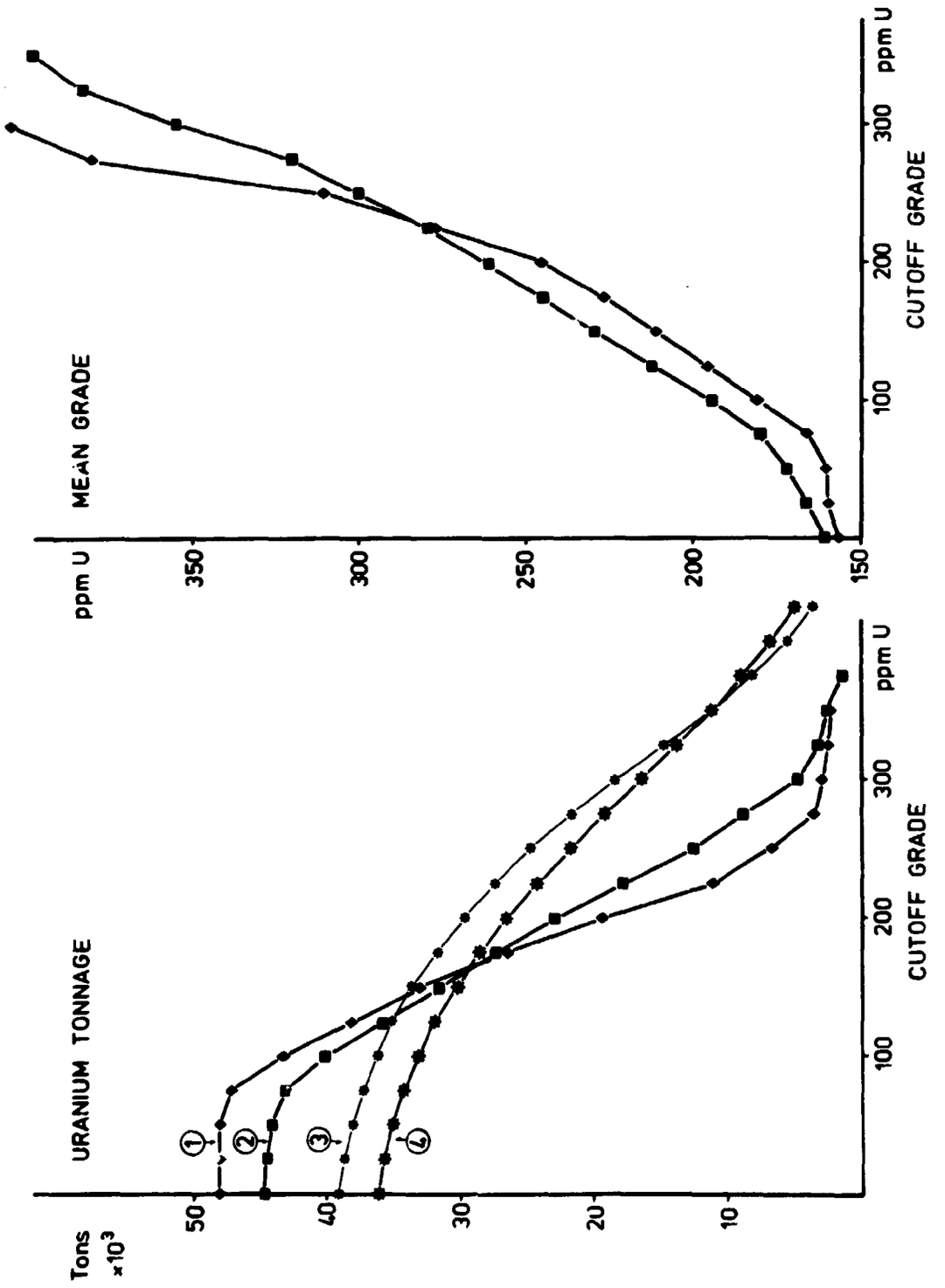

FIGURE 4-51: Estimation of the global reserves in the Norther area based on the logging data. 1) Block size 140x140x20 m, 2)block size 70x70x20 m. Estimation by conventional methods: 3) average value calibration, 4) individual hole calibration. (3 and 4 from Løvborg et al, 1980a).

5 URANIUM AND THORIUM IN THE KVANEFJELD TUNNEL

The data available from the Kvanefjeld tunnel (sec. 3.3.) were investigated in order to:

(1) Describe the distribution and the spatial variation of uranium and thorium values within the tunnel. The effect of the recognisable correlation between the two elements on the semi-variograms was examined.

(2) The analytical values from the batch samples obtained by on-site gamma-spectrometry, and the gamma-spectrometric values of the uranium concentration measured at 5 metre intervals within the tunnel, were valued by estimates based on the chip sample values.

(3) The uranium grade of the excavated material (the batch samples) was estimated from the chip samples using different conventional and geostatistical estimators. Results from the different estimators using different search areas, i.e. different numbers of samples, were compared.

It is important to note that the study of the data from the tunnel was performed 'locally', meaning that the data from this survey area were not used in integrated calculations of the global reserves. However, from the work presented here it is obvious that more attention must be paid to the ore volume discovered by the tunnel.

The planning of the sampling programme carried out in the Kvanefjeld tunnel is described in Clausen (1980b) and in Clausen et al. (in prep.). The chip sampling programme was designed in order to:

(1) Establish sufficient information about the uranium and thorium distributions, basically from a geostatistical point of view.

(2) Obtain enough information on which the determination of the horizontal structures of the uranium and thorium variation could be based. This could probably contribute new information about the structures already recognised from the vertical studies of drill holes.

(3) Obtain enough data to be able to estimate the batch samples sufficiently well.

In the Mine area the experimental semi-variogram is characterized by a high random component and a very short range of influence in the first spherical component. At distance zero metres the random component accounts for 29% of the total variation, whereas it is 56% when samples are 3.5 metres or more apart. In the Northern area the random variation is less pronounced although it is still present. The range of influence of the small scale spatial structure is 7.5 metres in this area. In view of these findings it was concluded that a denser sampling pattern should be used, and that the support of the samples should be significantly larger. Because of the high nugget effect approximately 2 metre vertical chip samples were selected. Furthermore, it was decided to sample each tunnel wall at two metre intervals. Only lujavrite sections and their contacts were sampled. In this way batch samples were more or less surrounded by information and, hence, geometrical bias neglected. Secondly, the mean variation across the tunnel could be compared to the variation along the tunnel, thus detecting any local spatial anisotropy.

5.1 Uranium and thorium distribution.

A histogram of the uranium values from the 674 chip samples is given in figure 5-1a. The histogram is characterized by, at least, two modes, representing a mixture of several populations such as were found in the drill hole data (figures 4-1, 4-37 and 4-49). The distribution comprising the lowest mode repre-

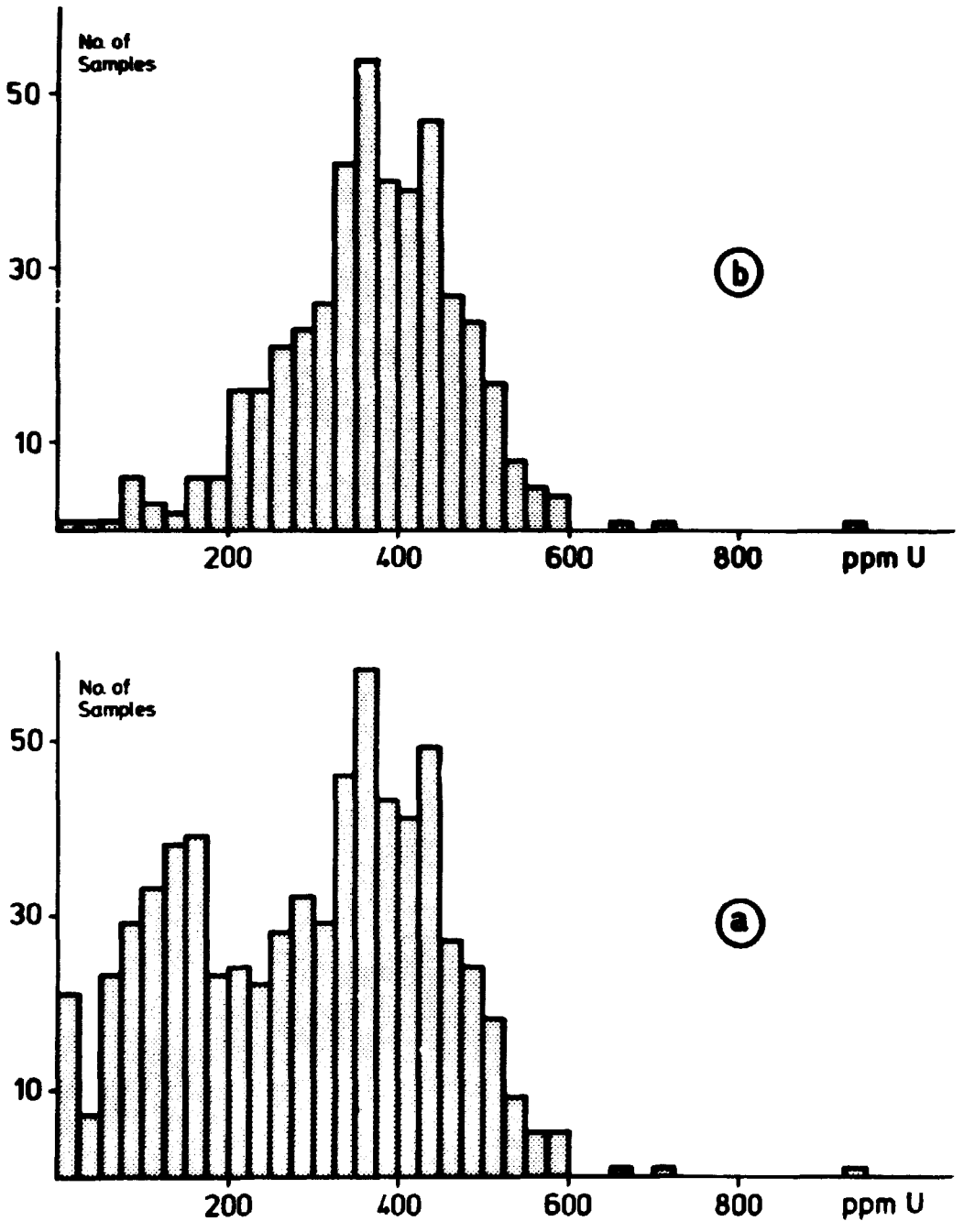

FIGURE 5-1: Histograms of uranium values in chip samples from the Kvanefjeld tunnel. a) Total sample set (674) and b) fine-grained lujavrites (438).

sents samples taken in m-c lujavrite and in xenoliths such as augite syenite, lamprophyric dykes and other unmineralised rocks. The distribution corresponding to the highest mode comprises the fine-grained naujakasite lujavrite samples. This is clearly seen in the histogram of the values from these samples (figure 5-1b). Although no attempt has been made to fit models to the distributions it appears that the distribution of uranium within the naujakasite lujavrite is of the normal type. This is in accordance with results from the drill core samples (sec. 4.2.1.).

Histograms of thorium values in the total sample set and in naujakasite lujavrite can be seen in figure 5-2a,b. Although the distribution in naujakasite lujavrite seems to be of the lognormal type the histograms have the same aspect as those of uranium, reflecting the correlation between the two elements (e.g. Nyegaard et al., 1977). When planning the position of the tunnel below the Kvanefjeld plateau the primary aim was to obtain as much uranium bearing material as possible from which it would be possible to select bulk samples with an average uranium content equal to or greater than the overall average of the mineralization (340 ppm U based on a cutoff grade of 250 ppm U, Per Nyegaard, pers. comm.); from the histogram in figure 5-1a this appears to have succeeded. However, the geostatistical estimates of grade and tonnage in the Northern area, which contains over three quarters of the total resources, show that the tunnel represents pronouncedly high grade 'ore'. On the other hand the histograms of uranium within naujakasite lujavrite samples from drill cores randomly scattered over the deposit have virtually the same shape and mode, as can be seen from table 5-1. It can therefore be concluded that the 'ore' from the Kvanefjeld tunnel is more typical of naujakasite lujavrite than of the whole deposit.

Parameters of the thorium distributions are listed in table 5-2.

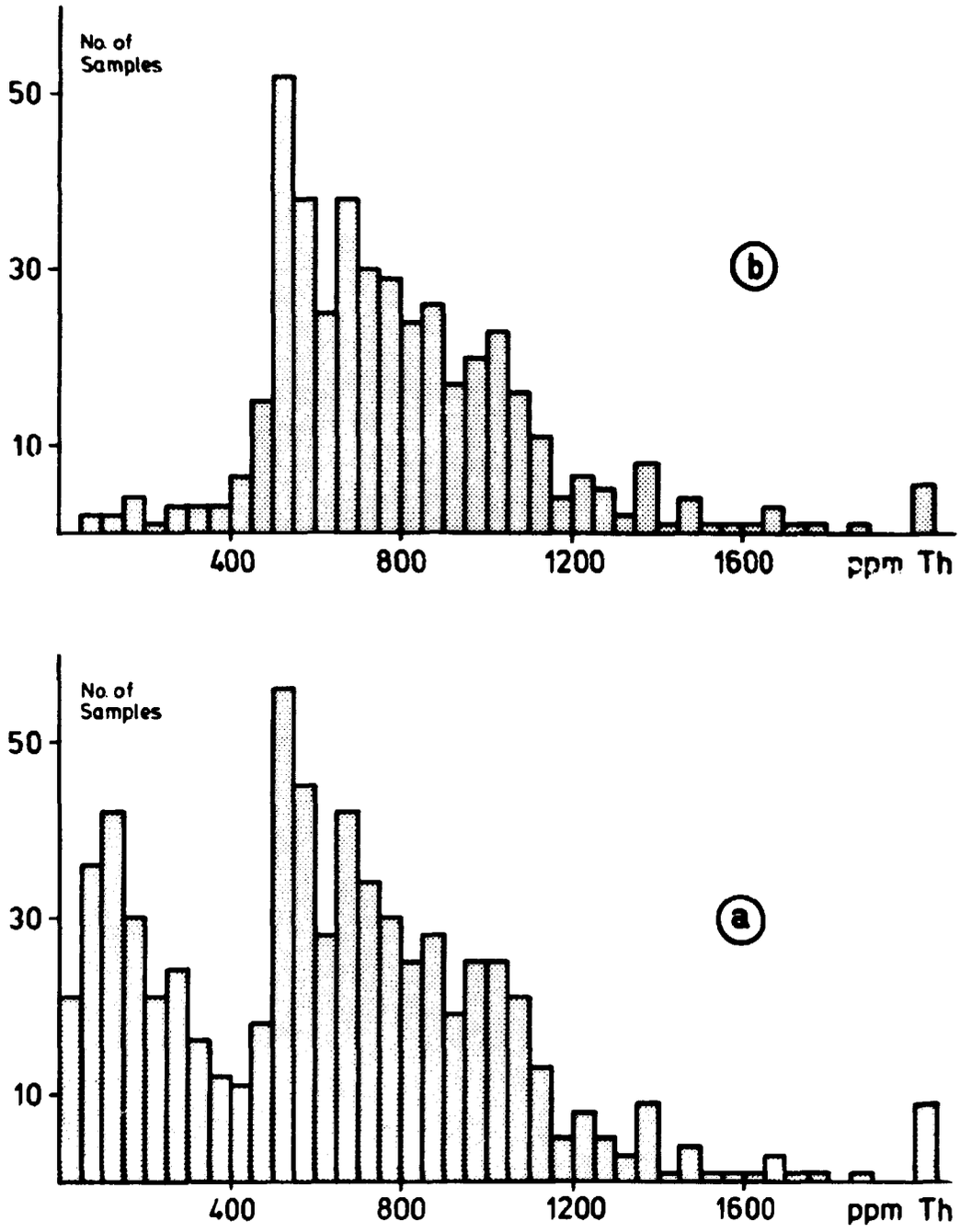

FIGURE 5-2: Histograms of thorium values in chip samples from the Kvanefjeld tunnel. a) Total sample set (674) and b) fine-grained lujavrites (438).

TABLE 5-1: Summary statistics for uranium (ppm) in chip samples from the Kvanefjeld tunnel compared with other sets of data.

Type of data	N_s	Mean	Std. Dev.	Coeff. of var.
Total sample set (chip samples)	674	293.3	147.9	0.50
Naujakasite lujavrite (chip samples)	438	369.2	108.1	0.29
Naujakasite lujavrite (drill cores - Mine area)	340	371.2	123.5	0.33
Naujakasite lujavrite (drill cores - Northern A.)	236	307.8	108.9	0.35

TABLE 5-2: Summary statistics for thorium (ppm) in chip samples.

Type of data	N_s	Mean	Std. dev.	Coeff. of var.
Total sample set	674	637.3	434.8	0.68
Naujakasite lujavrite	438	808.5	360.7	0.45

5.2 Spatial variation.

The spatial structure of uranium in the chip samples was investigated by experimental semi-variograms. The program MARVGM, developed at the University of Leeds, was used throughout the study. This program, which calculates the semi-variogram in specified directions, using tolerances on angle and distance between sample pairs (figure 5-3), is fully documented in Ahlefeldt-Laurvig (1981). For calculation convenience it was assumed that the tunnel was rectilinear and that the sample spacing was equal to two metres, although each sample had a

certain horizontal extension. Since samples were available only in the direction of the tunnel semi-variograms could only be calculated in this direction. However, one semi-variogram value could be calculated in the direction across the tunnel at a lag equal to the tunnel width.

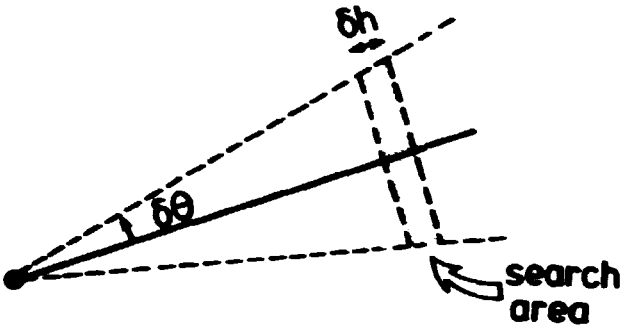

FIGURE 5-3: Search procedure for samples as used in the program MARVGM. Tolerances are allowed on the direction and the distance between sample pairs.

5.2.1 Experimental Semi-variograms and models.

Experimental semi-variograms were calculated for each tunnel wall, firstly ignoring rock type, and secondly using fine-grained lujavrite samples only. These were then averaged to form overall horizontal semi-variograms. Results from the uranium values are presented in figure 5-4, where curve A corresponds to the total data set and curve B the fine-grained lujavrites. The difference in 'height', i.e. variance, between the two curves expresses the difference in spatial homogeneity of the two sets of samples. Not surprisingly, samples comprising different geological units have the highest variance. Both curves exhibit a distinct discontinuity at the origin, indicating that about half of the total variation seems to be due to purely random behaviour. The parts of the curves between zero and approx. 24 metres increase continuously whereas beyond 24 metres sample values seem to be uncorrelated.

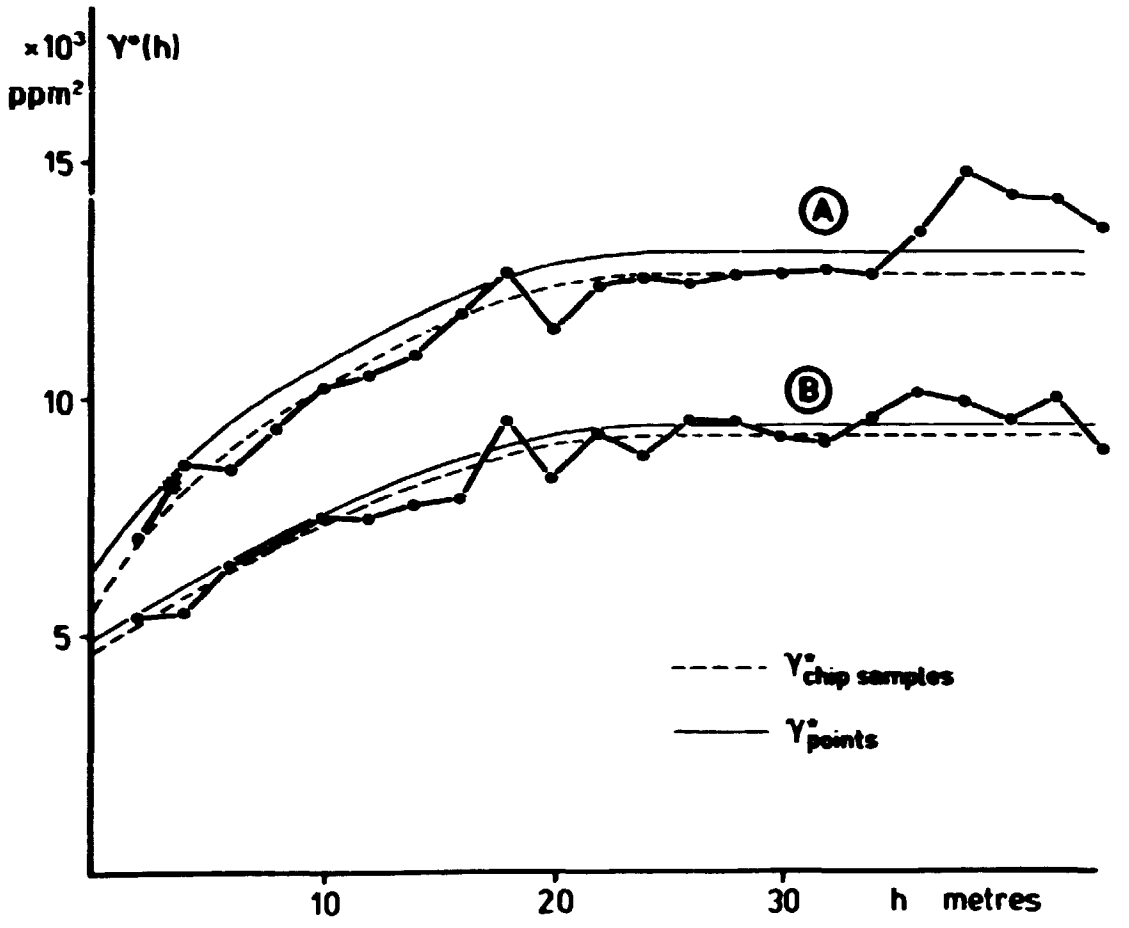

FIGURE 5-4: Experimental semi-variograms of uranium in chip samples. A) Total sample set, B) Fine-grained lujavrites. The de-regularised models are indicated by dashed curves, point models by solid curves. The star indicates the 'across-the-tunnel' semi-variogram value.

The two experimental curves could be modelled by a spherical scheme and a nugget effect (sec. 4.2.4.). For the fine-grained lujavrites the best fit (using trial-and-error) was given by a one-component spherical model plus nugget effect:

$$\gamma_L^*(h) = 4600 + 4600 \left[\frac{3h}{2 \cdot 24} - \frac{h^3}{2(24)^3} \right], \qquad 0 \leq h < 24 \text{ metres}$$

$$= 9200, \qquad h \geq 24 \text{ metres}$$

having a range of influence of 24 metres. The model can be seen in figure 5-4 and is indicated by the dashed line of curve B. Similarly, the curve for the total sample set could be modelled by a two-component spherical model plus nugget effect. The model, comprising ranges of influence at distances of 6 and 24 metres, is given by:

For distances less than 6.0 metres:

$$\gamma_L^*(h) = 5500 + 1300\left[\frac{3h}{12} - \frac{h^3}{2(6)^3}\right] + 5800\left[\frac{3h}{48} - \frac{h^3}{2(24)^3}\right]$$

For distances between 6 and 24 metres:

$$\gamma_L^*(h) = 6800 + 5800\left[\frac{3h}{48} - \frac{h^3}{2(24)^3}\right]$$

and for distances greater than 24 metres:

$$\gamma_L^*(h) = 12600$$

Hence the small scale structure, which was also detected in the drill core samples (sec. 4.2.4 and 4.3.2.), is due to a structure in the samples not taken in fine-grained lujavrite. It is interesting to note that 63% of these samples represent m-c lujavrite.

The subscript L has been used in both models to indicate that these represent the 'graded' semi-variogram (Journel and Huijbregts, 1978) over a constant thickness L (L=2 metres). The nugget effect of the total sample set (5500 ppm U^2) is almost equal to the nugget effect in the overall Mine area model (5600 ppm U^2). Since different types of sample have been considered in these models, the nugget effects need not be equal. This is because different sampling and assaying errors have been made.

Having detected equal nugget effects on different sample supports it may be concluded that the random variation is basically due to microstructures in the mineralisation.

The average 'across the tunnel' semi-variogram value is calculated at a distance equal the mean tunnel width of 3.39 metres, and is indicated on figure 5-4 by a star. It can be seen that at that particular scale isotropic spatial conditions exist because the value is equal to the value calculated along the tunnel. The value ($\simeq$8000 ppm U^2) indicates that across the tunnel the uranium grades differ by about 89.5 ppm on average.

Experimental semi-variograms for thorium are presented in figure 5-5. It can be seen that although variances are much higher than for uranium, the variogram type and shape does not differ significantly. This, again, reflects the high correlation between the two elements. On the other hand, the semi-variograms do not display stationarity at the sill, but are instead influenced by some kind of drift (Journel, 1969). Usually this means that simple kriging, as used in the present study, cannot be used for estimation. If, however, only that part of the semi-variogram which can be described by a stationary model (i.e. the spherical model) is used for estimation, the drift can be ignored. In the present case it means that samples at distances exceeding the range of influence should not be included in the kriging system. Because of the sampling pattern in the tunnel it was not necessary to consider such samples. The parameters for the model used to describe the spatial variation of the thorium are given by:

Total sample set:

$$C_0 = 87000 \text{ ppm } Th^2$$

$$a_1 = 6.0 \text{ metres}, \qquad C_1 = 15000 \text{ ppm } Th^2$$

$$a_2 = 24.0 \text{ metres}, \qquad C_2 = 43000 \text{ ppm } Th^2$$

Fine-grained lujavrites:

C_o = 45000 ppm Th^2

a = 24.0 metres, C = 50000 ppm Th^2

The models are indicated as dashed curves in figure 5-5.

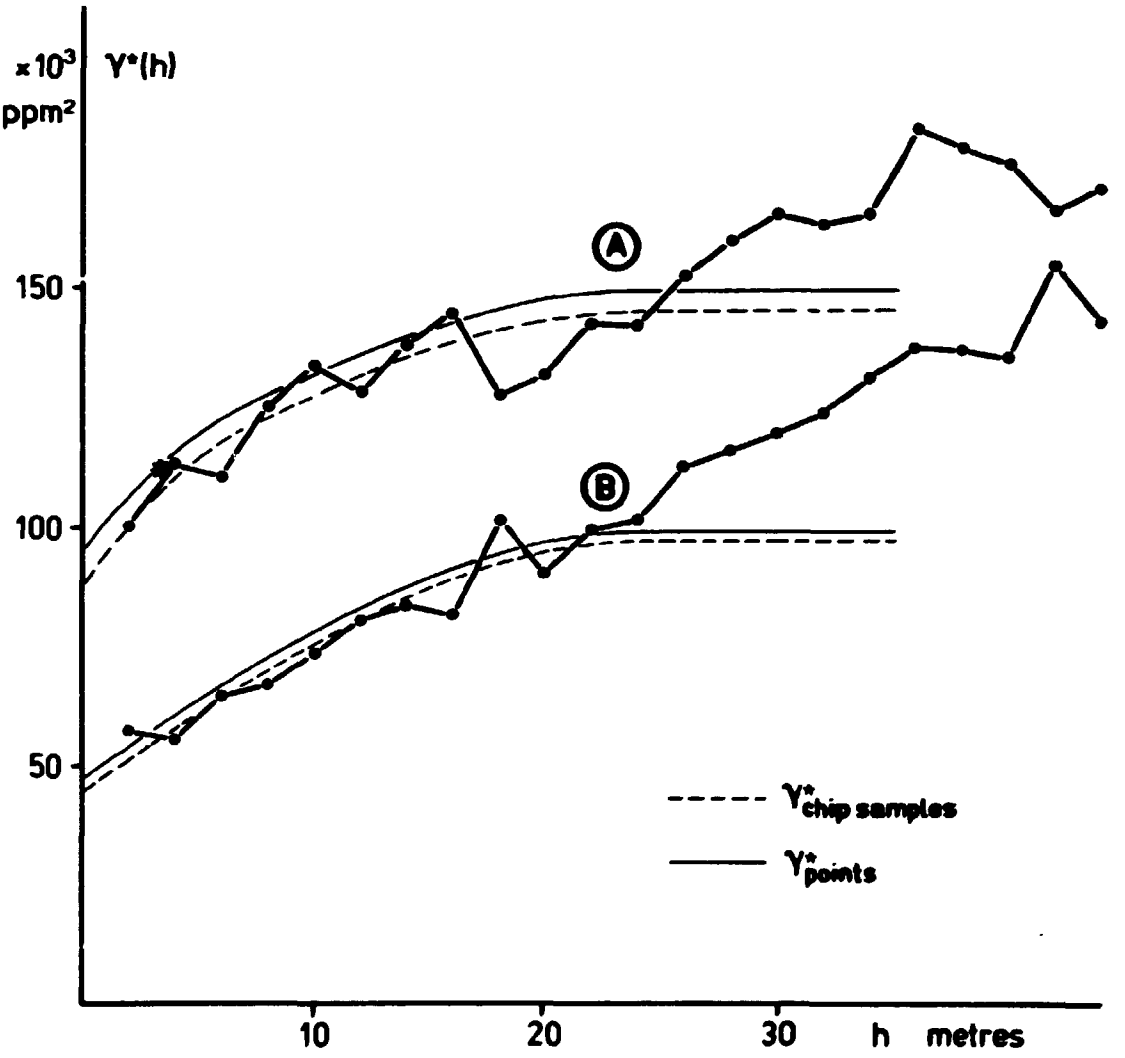

FIGURE 5-5: Experimental semi-variograms of thorium in chip samples. A) Total sample set, B) Fine grained lujavrites. The de-regularised models are indicated by dashed curves, point models by solid curves. The star indicates the 'across-the-tunnel' semi-variogram value.

The spatial structure in the first part of the tunnel (0-500 metres) was compared with the structure in the last part (500-900 metres) by the semi-variograms from these areas. The semi-variograms for the fine-grained lujavrite samples (figure 5-6a) indicate that, although some differences in variance exist at small distances, uranium values within these rock types display equal spatial behaviour in the two areas. This result implies that the same overall model can be used for estimation within fine-grained lujavrites in the two parts of the tunnel. If, on the contrary, the semi-variograms of the total sample set are examined (figure 5-6b), different behaviour is observed. Now, the samples from the first part of the tunnel exhibit much higher variances at all distances, indicating a higher degree of inhomogeneity. This is easily understood from the fact that more than 80% of the samples not taken in fine-grained lujavrites originate in this part of the tunnel.

5.2.2 Deregularisation

As mentioned in section 4.2.7 the regularised semi-variogram can be written as:

$$\gamma_L(h) = \bar{\gamma}(L,L+h) - \bar{\gamma}(L,L)$$

where $\bar{\gamma}(L,L+h)$ is the average value of $\gamma(n',n'')$ when n' takes all possible positions in a sample of length L and n'' all possible positions in a parallel sample of the same length at distance h. If the semi-variogram of points $\gamma(h)$ has a range a, then $\gamma_L(h)$ will have the same range if the regularisation takes place over constant thickness (Rendu, 1978). Thus, to deregularise the graded semi-variogram calculated by MARVGM to a semi-variogram for point samples, the value of $\bar{\gamma}(L,L)$ has to be added to the graded model. $\bar{\gamma}(L,L)$ represents the 'within-chip sample' variation and can be calculated by the auxiliary function F(L/a), (Clark, 1979a):

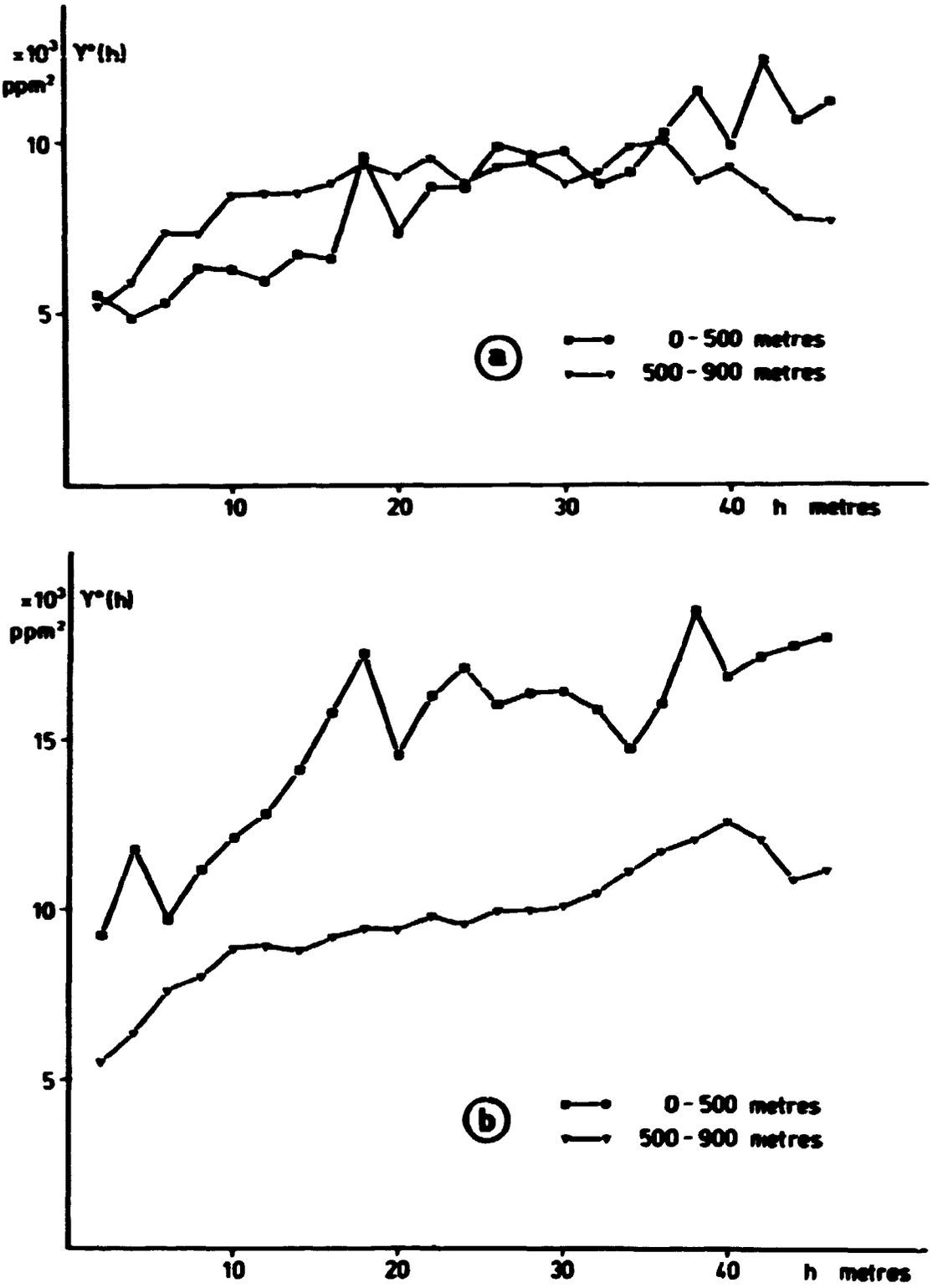

FIGURE 5-6: Experimental semi-variograms from the first and the last parts of the tunnel. Urarium values in a) fine-grained lujavrites and b) total sample set.

$$\bar{\gamma}(L,L) = F(L/a)$$

$$= \frac{1}{2}\frac{L}{a} - \frac{1}{20}\left(\frac{L}{a}\right)^3$$

where a is the range of influence and L the chip sample length. Deregularising the model for the total sample set (uranium) gives:

$$\gamma^*(h) = \gamma_L^*(h) + F(L/a_1) + F(L/a_2)$$

$$= \gamma_L^*(h) + C_1F(1/3) + C_2F(1/12)$$

$$= \gamma_L^*(h) + 1300 \cdot 0.165 + 5800 \cdot 0.041$$

$$= \gamma_L^*(h) + 453 \text{ ppm } U^2$$

and for the model of the fine-grained lujavrites:

$$\gamma^*(h) = \gamma_L^*(h) + F(L/a)$$

$$= \gamma_L^*(h) + 188 \text{ ppm } U^2$$

In other words, deregularisation of the graded model is done by adding the (constant) within-sample variance to the model. Effectively this results in an apparently higher nugget effect. However, the nugget effect itself is not deregularised since it is independent of the spatial variation. The deregularised models are indicated on figures 5-4 and 5-5 as solid curves.

5.3 Estimation of batch samples.

Several estimations of the mean grade of the individual batch samples were made by different conventional and geostatistical estimators. Input data were the uranium and thorium values in the chip samples. When geostatistics was used for estimation, the overall semi-variogram model based on the total data sample set was used in the kriging procedures. However, the effect of using this semi-variogram model instead of the fine-grained lujavrite model was studied.

5.3.1 Estimators.

The estimators used in all calculations were of the type

$$Z^*(A) = w_1 Z(x_1) + w_2 Z(x_2) + \ldots + w_n Z(x_n)$$

where $Z(x_i)$ is the value of the chip sample at location x_i and w_i the weight that particular sample is given. The weights were always calculated under the non-bias condition that their sum must be one. For each estimation method several 'search areas', defined in terms of the batch length, were used in order to investigate how many samples were necessary to estimate the batches with least errors (figure 5-7). The search areas are denoted 0, +1, +2 etc. as can be seen from figure 5-7. The estimators used are described in the following sections.

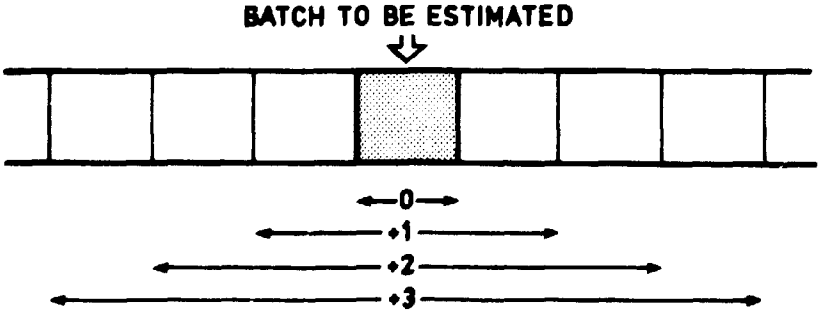

FIGURE 5-7: The search area is defined in terms of the block size. Geostatistical estimation of the batch samples of excavated material.

5.3.1.1. Arithmetric mean. The arithmetric mean estimator is a straight average of the samples:

$$Z^*(A) = 1/n \left[Z(x_1) + Z(x_2) + \ldots + Z(x_n) \right]$$

thus ignoring the relative locations of batch and samples. This was a priori regarded as a bad estimator since intuition tells that samples in the immediate vicinity of the batch contain more information than remote samples. Hence, the former should (intuitively) receive the highest weights. The Program MIDDEL used during the calculations is documented in Ahlefeldt-Laurvig, 1981.

5.3.1.2. Inverse distance weighting. Inverse distance weighting methods have been widely used in ore reserve estimation (Knudsen et al., 1978, Royle, 1980). The weight assigned the i'th sample is given by the formula:

$$w_i = \frac{1/d_i^k}{1/d_1^k + 1/d_2^k + \ldots + 1/d_n^k}$$

where d_i is the distance between the i'th sample and the centre of the batch. The exponent k took the values 1, 2 or 3 in this study. The method takes into consideration that samples far away from the batch ought to receive small weights. Furthermore, the choice of the exponent value allows a decision about the range of influence. That is, weights decrease more rapidly over small distances if high exponent values are selected. Calculations were performed by the program INVAF documented in Ahlefeldt-Laurvig (1981).

5.3.1.3. Kriging. The kriging estimator has been previously mentioned (sec. 4.2.5. and 4.2.10.2.) and needs no redefinition here. However, the main differences between the conventional estimators described above and the kriging estimators should be recalled. Firstly, kriging has been developed subject to the condition that errors of estimation are minimized. This is done

taking both the covariances between the samples, and between the samples and the unknown volume, into account. The error of estimation is called the kriging standard error (see below). Secondly, kriging takes not only the covariances between the samples into account, but considers also the actual shapes of these. As was demonstrated during volume-variance calculations, spatial behaviour depends on the volume of the samples and the block and hence on their covariances. The simplest kriging procedure is point kriging where both samples and the unknown value are on point support. In that case the covariances are obtained directly from the semi-variogram model. In ore reserve estimation it is more convenient to estimate mean values within definite shapes and 2-dimensional kriging (estimating a panel) and 3-dimensional kriging (estimating a 3-D block) have been developed. Covariances are calculated by auxiliary functions which give mean semi-variogram values.

In the present study batch samples were estimated by point kriging (1-D), 2-D and 3-D kriging. Point kriging was performed by a modified version of the program PTKR, called PTKTUN (sec. 4.2.5., for documention see Ahlefeldt-Laurvig, 1981). The program SPECKR developed at the University of Leeds (documented in Ahlefeldt-Laurvig, 1981) performed the 2-D kriging and TREREG the 3-D kriging (sec. 4.2.10.2.).

The points in the tunnel at which gamma-spectrometric measures of U and Th were available (5 metre intervals) were estimated from the chip samples using point kriging only. Another modified version of the program PTKR, PTKNET, was used during calculations (Ahlefeldt-Laurvig, 1981).

5.3.2 Estimation errors

The major advantage of geostatistics over the conventional methods is the estimation of the estimation error, which allows confidence intervals for the estimate to be calculated. The geostatistical estimation error is defined by the kriging variance:

$$\sigma_k^2 = \sum w_i \bar{\gamma}(g_i,A) + \lambda - \bar{\gamma}(A,A)$$

However, such an error can be calculated for any estimator providing the semi-variogram model is known. The general estimation variance is given by

$$\sigma_\epsilon^2 = 2\sum_{i=1}^{n} w_i \bar{\gamma}(g_i,A) - \sum_{i=1}^{n}\sum_{j=1}^{n} w_i w_j \bar{\gamma}(g_i,g_j) - \bar{\gamma}(A,A)$$

and it is this expression which is minimized by kriging.

5.4 Discussion of findings.

A full listing of the locations, ore tonnages and geology of the 58 individual batch samples is gives in appendix E. This listing also includes the gamma-spectrometric measures of the uranium and thorium grades as well as the 3-D kriging estimates and standard errors for the two elements. As shall be shown later, 3-D kriging using a +1 search area (figure 5-7) appears to be the most efficient estimation method (denoted $3D_1$). Figure 5-8 shows a histogram of the uranium values in the batch samples obtained by $3D_1$-kriging. Figures 5-9a,b compare the gamma-spectrometric values (stars) with those found by $3D_1$ kriging (dots). Chip sample values are also shown. Around each batch estimate an approx. 95%-confidence interval is indicated using $\pm$ two kriging standard deviations. It can be seen that the gamma-spectrometric measure of about one-third of the batches lies well within this interval. However, the kriging estimates have on average lower values than the corresponding gamma-spectrometer values. It is important to note that the uranium profile shown in figure 5-9a,b illustrates perfectly why the semi-variograms of the deposit are characterized by poor spatial structures and high nugget effects. Even in sections where the geology appears homogeneous at a macroscopic

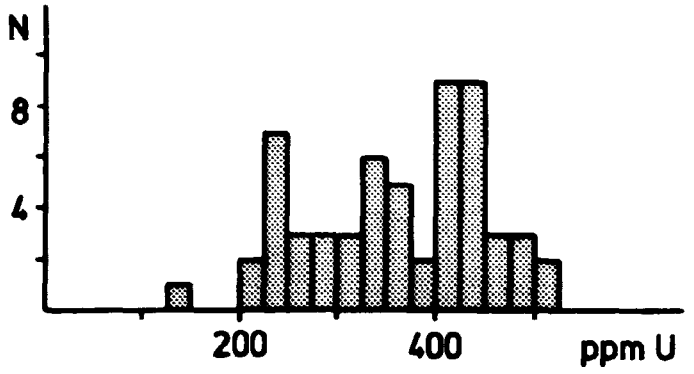

FIGURE 5-8: Histogram of 58 kriged batch sample values from the Kvanefjeld tunnel.

scale, e.g. the naujakasite lujavrite section at 250-350 metres, the uranium content changes rapidly over short distances. This is also reflected in the variation across the tunnel.

A comparison of the kriging estimates and the gamma-spectrometric measures for the 46 resulting batch samples is given by the scatter plot of figure 5-10 and by the parameters in table 5-3. The correlation coefficient of 0.78 is significant at the 99.99% level. The normal least squares regression line of the kriging estimates (Y) on the gamma-spectrometer values (X) is

$$Y = 0.85X + 28.4$$

with standard errors of the parameters of 0.10 and 40.8 respectively. The least squares regression line of X on Y is given by

TABLE 5-3: Comparison of statistics for uranium (ppm) in the resulting batch samples. ρ is the correlation coefficient.

Type of data	N_b	Mean	Std. dev.	Error of the mean	ρ
3-D_1 kriging estimates	46	357.33	88.47	13.04	0.78
Gamma-spectrometer values	46	387.15	81.08	11.95	

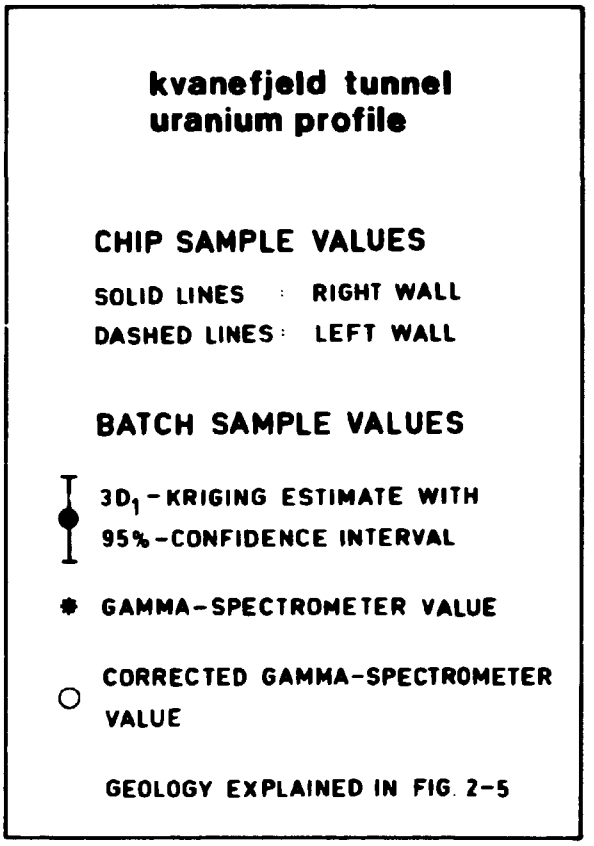

FIGURE 5-9: Uranium profile in the Kvanefjeld tunnel showing grades in chip samples and estimated and measured grades in batch samples. Location of samples and the geology are indicated.

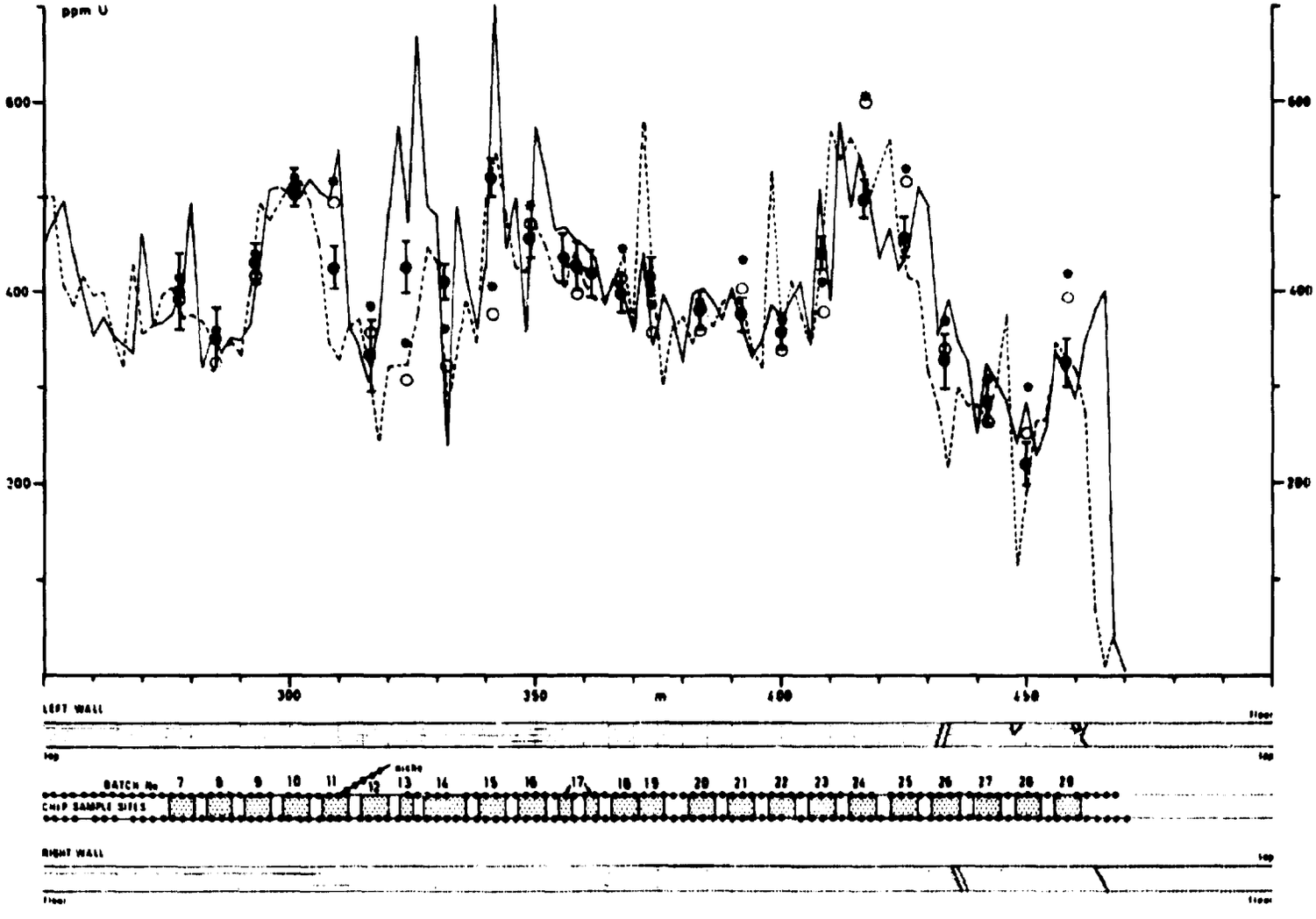
ppm U
600
400
200
300
350
m
400
450
LEFT WALL
Top
Floor
BATCH No
7
8
9
10
11
12
13
14
15
16
17
18
19
20
21
22
23
24
25
26
27
28
29
CHIP SAMPLE SITES
RIGHT WALL

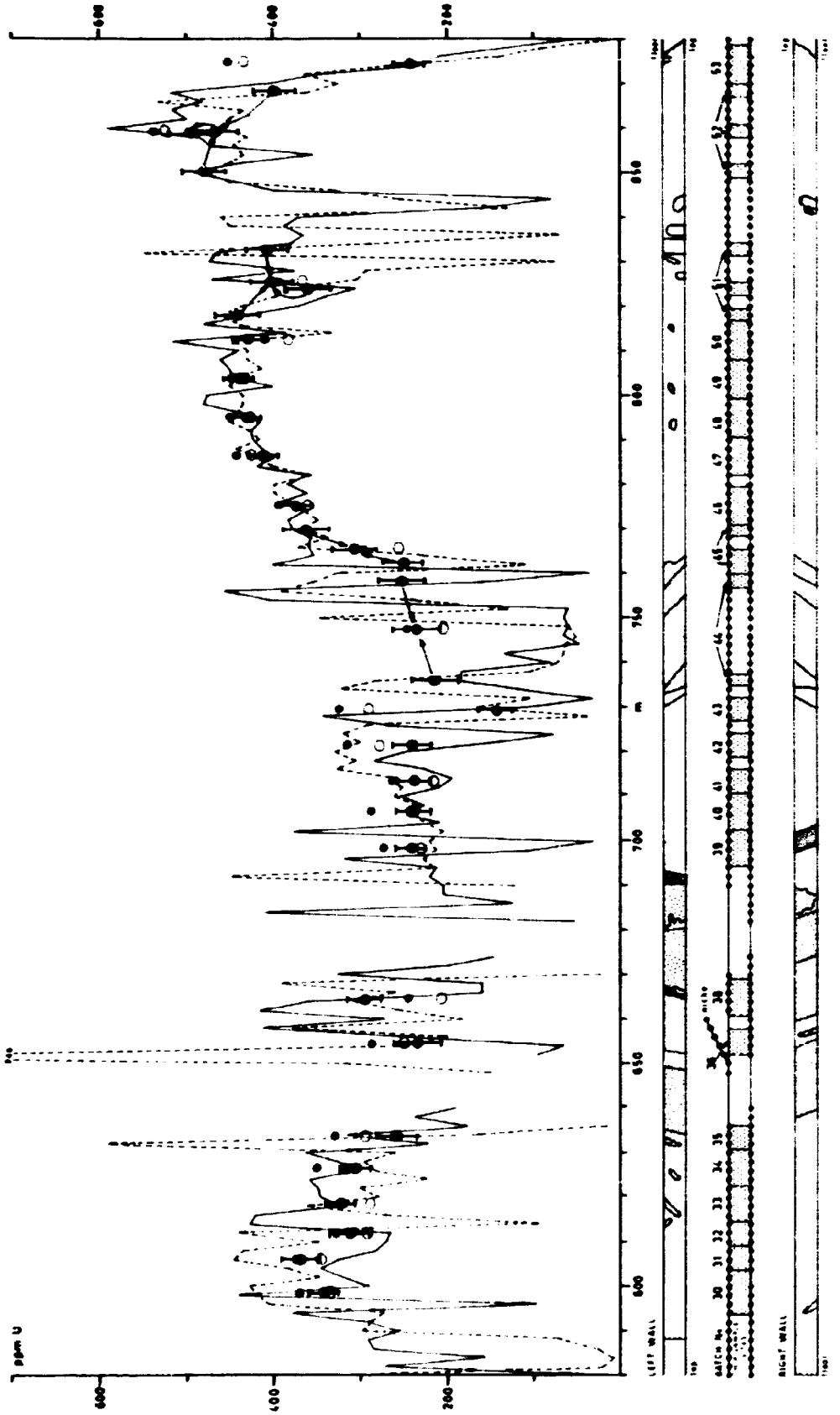

5-9

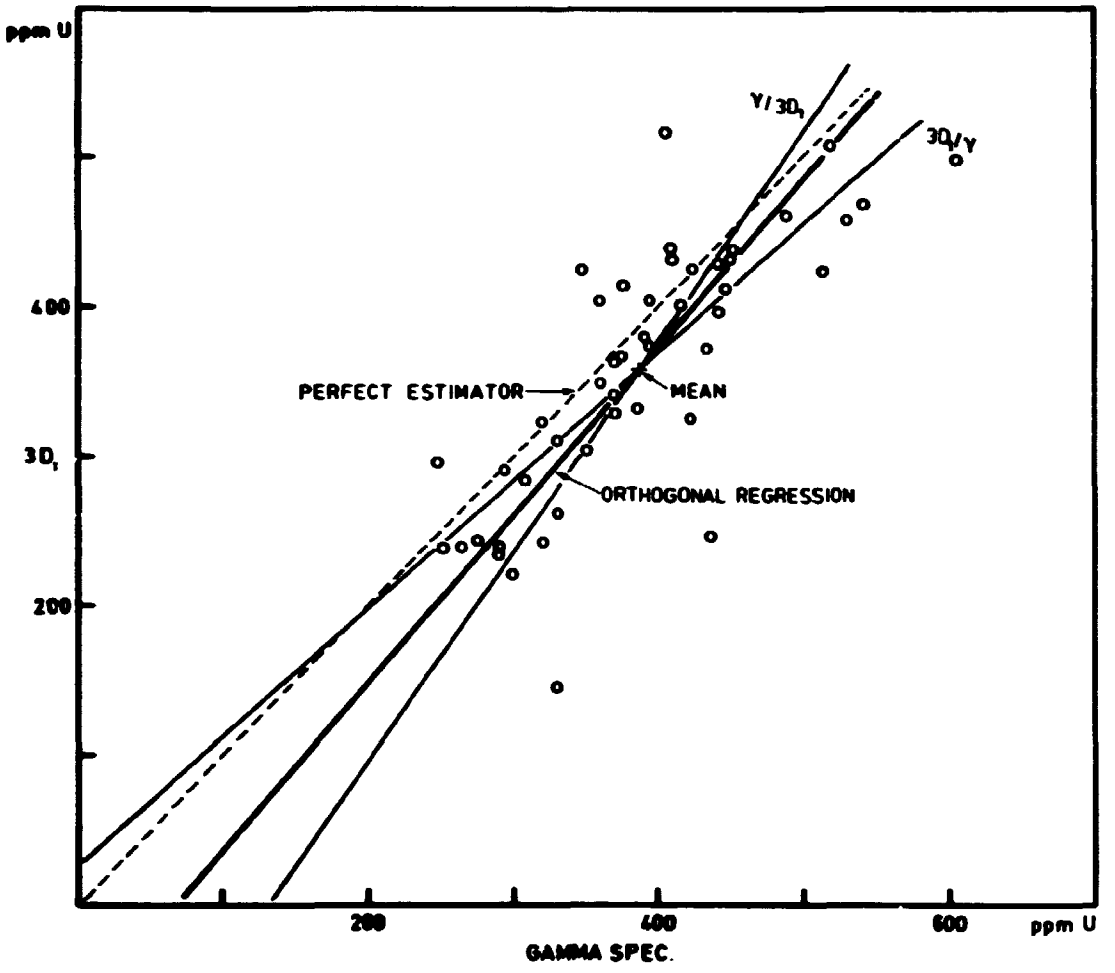

FIGURE 5-10: Scatter plot of $3D_1$-kriging estimates versus gamma-spectrometer values for batch samples. Least-squares and orthogonal regression lines are indicated.

$$X = 0.71Y + 132.2$$

with standard errors 0.08 and 31.9 respectively. However, it is believed that the best regression line is given by the orthogonal regression coefficient since both variables are subject to errors. The coefficient, which is based on a minimisation of the perpendicular distance to the regression line (figure 4-33), is calculated from:

$$b_o = \frac{S_y - S_x}{2S_{xy}} + \sqrt{1 + \left(\frac{S_y - S_x}{2S_{xy}}\right)^2}$$

where $S_x = \sum(x_i-\bar{x})^2$, $S_y = \sum(y_i-\bar{y})^2$ and $S_{xy} = \sum(x_i-\bar{x})(y_i-\bar{y})$. Using the parameters from table 5-3 gives

$$b_o = 1.12$$

and the regression line

$$Y = \bar{y} + b_o(X - \bar{x})$$

$$= 1.12X - 76.3$$

The three regression lines are shown in figure 5-10 together with the 'perfect' regression line Y = X. From the regression lines it appears that the gamma-spectrometer values most likely over-estimate the batches (assuming the kriging estimates to give a more valid grade value than the former). This can also be seen directly from the mean values of the two variables (table 5-3), giving a difference of 29.8 ppm U (the mean algebraic difference between the two variables). The standard error of this figure is, however, 56.8 ppm.

In order to check whether the orthogonal regression line can be used to obtain a better coincidence between corrected gamma-spectrometer values and the kriging estimates such values have been plotted on figure 5-9a,b as circles. It can be seen that 41% of the corrected gamma-spec. values now fall within the 95%-confidence interval of the estimates, hence giving an improvement.

The kriging estimates are subject to errors originating in the sampling and assaying of the chip samples and in the estimation process. They are, however, believed to give reliable estimates of the batch grades. It would be reasonable to conclude that the orthogonal regression line can be used to correct gamma-

spectrometer values towards a less biased grade value for the batch. The bias discovered during the study is believed to be due mainly to the calibration of the field spectrometer. It may be noted that although the bias probably can be explained by instrument calibration, the regression curve might also be influenced by a regression effect causing a slope different from unity. This effect indicates (disregarding the bias) that low values are underestimated whereas high values are overestimated. However, due to the limited number of points and the high variances this theory must be regarded with some suspicion.

In figure 5-11 the estimated batch values ($3D_1$) are compared with a forecast grade profile presented in Clausen (1979). The grade profile was estimated from average drill core values in adjacent holes using inverse distance weighting. As can be seen in figure 5-11 this estimation is completely unrealistic, often producing differences between 'actual' and estimated grades of more than 100 ppm. Hence, the difficulty of estimating local small blocks from remote observations is demonstrated.

Figure 6-12 gives a comparison of the gamma-spectrometric values from the survey carried out within the tunnel and the point-kriging estimates calculated at the measuring points. Because of the low accuracy of the gamma-spectrometric values

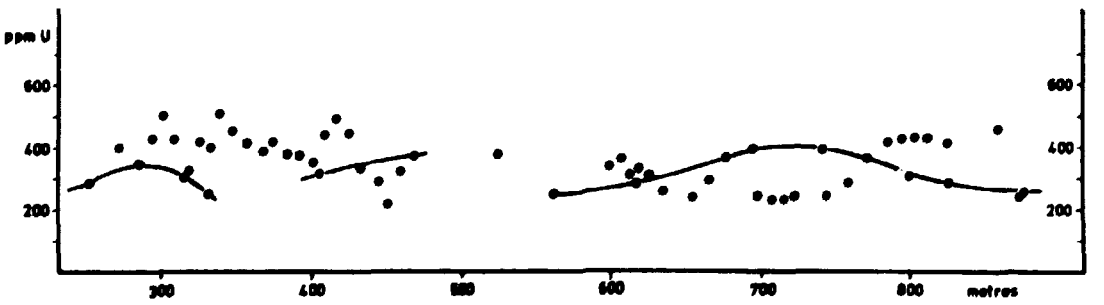

FIGURE 5-11: Comparison between forecast and 'actual' grade profiles in the Kvanefjeld tunnel. Stars indicate batch sample values. (Forecast profile from Clausen, 1979).

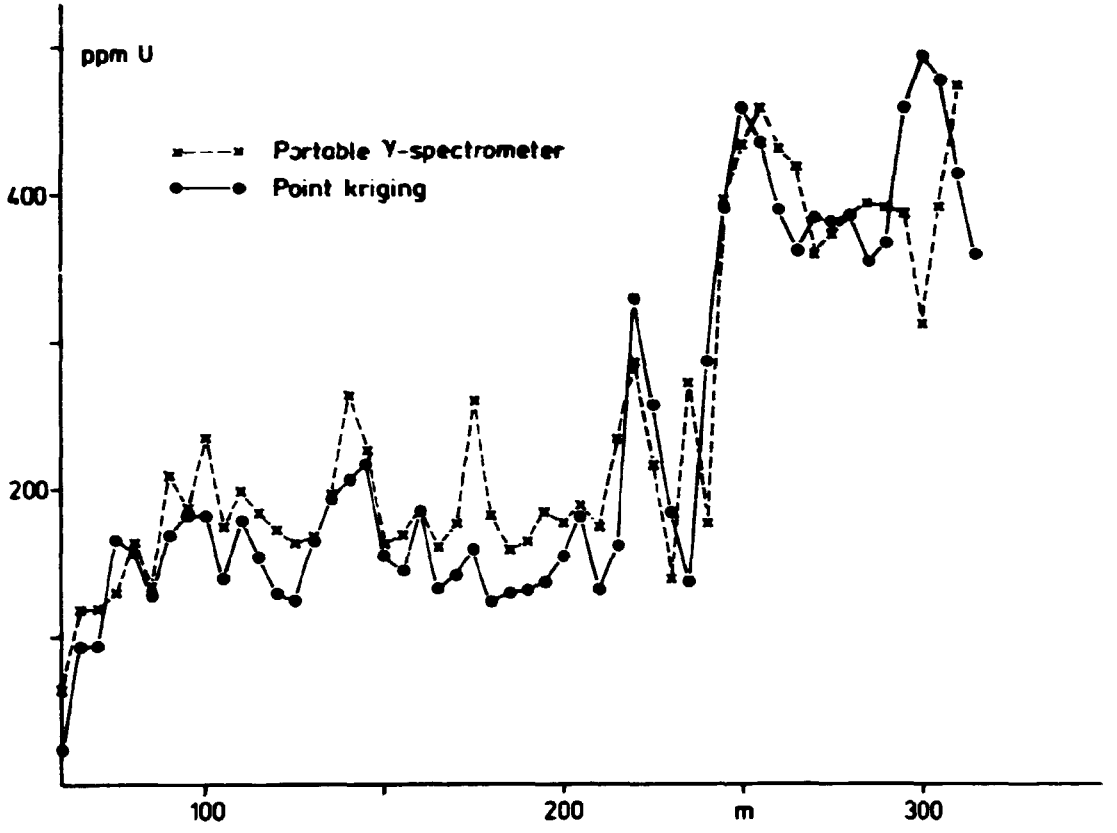

FIGURE 5-12: Comparison between point kriging estimates and in-situ gamma-spectrometer values in the first part of the Kvanefjeld tunnel.

it is surprising how well they describe the uranium profile of the tunnel. The coincidence between the two sets of values is even better than that observed for the batch samples, but a bias of the same magnitude as that earlier observed (approx. 30 ppm) can still be recognized.

It can be concluded that the portable gamma-spectrometer can be used easily to establish grade profiles within tunnels, as demonstrated here. The advantage of this method over other methods, e.g. chip sampling, is obvious and it can be recommended. However, the readings are subject to higher errors.

5.4.1 Comparison of estimation errors.

Results from the different estimates of the 58 batch samples are summarized in table 5-4, in terms of mean estimation or kriging variances. It appears that in all the methods, except the arithmetric mean, estimation variances decrease when the search area is increased from 0 to +1. When the search area is increased further no significant changes in the variances occur. This should be kept in mind because of the substantial increase in computing time, due to the increased number of samples. Not surprisingly, the arithmetric mean produces the highest variances whereas the lowest values are found from 2-D and 3-D kriging. This can be understood by recalling that it is much easier to estimate the mean value of a large volume (all variance within this volume is overlooked) than the value at a single point. This is also the reason why the $1/d^n$ methods and 1-D kriging produce similar results. The kriging variances from 1-D estimation are slightly bigger than the corresponding values for the conventional methods which, at first glance, should be impossible (sec. 4.2.5.). The deviation is, however, explained by rounding errors during matrix operations on the values of the Lagrangian multiplier, which are of the same magnitude as the σ_K^2's. The best choice of conventional method appears to be $1/d^2$ weighting using a +1 search area. The reduction in estimation variance when the search area is increased

TABLE 5-4: Estimation variances obtained when conventional and geostatistical methods are used to estimate the uranium content of batch samples.

Search area		Conventional			Kriging		
	$\bar{X}$	$1/d$	$1/d^2$	$1/d^3$	1D	2D	3D
0	8245	7928	7946	8022	8190	1638	159
+1	8306	7699	7551	7658	7661	884	128
+2	9039	7903	7553	7642	7650	862	124
+3	9768	8099	7563	7639	7648	860	123

from 0 to +1 is approximately 5%. The best geostatical method is 3-D kriging also with a +1 search area, giving an improvement in estimation variance between the $3\text{-}D_0$ and $3\text{-}D_1$ of 19.5%.

The overall choice of method is obviously 3-D kriging, which produces estimates with an average 95% confidence interval of about $\pm$ 23 ppm U ($2\sqrt{\sigma_K^2}$). When the +1 search area was selected kriging used approx. 25% more computing time than the conventional methods.

5.4.2 Comparison of estimates and gamma-spectrometer values.

The values obtained by the portable gamma-spectrometer have already been compared with the $3\text{-}D_1$ kriging estimates in section 5.4. A full comparison is given in table 5-5 where mean values of the algebraic (5-5a) and the squared (5-5b) differences between the gamma-spectrometer values and the corresponding estimates are listed. Three search areas 0, +1 and +2 were used. From table 5-5 it can be concluded that all estimation methods seem to be 'biased' compared with the gamma-spectrometric measure, in that all algebraic differences are positive. These differences, ranging between 23.7 and 30.2 ppm U, possibly reflect the bias caused by calibration of the portable spectrometer.

The comparison given in table 5-5 supports the overall choice of a +1 search area. On the other hand it is not possible to select the best estimation method by such a comparison since the gamma-spectrometer values are subject to errors themselves. If, for instance, the mean squared error for $3\text{-}D_1$ kriging is examined, it appears that the value ($\simeq$3900 ppm U^2) is very much bigger than the variance introduced during estimation ($\simeq$130 ppm U^2). A part from this, no method seems to produce estimates which, compared with the gamma-spectrometer values, deviate significantly from the other methods.

TABLE 5-5: Mean algebraic differences (table a) and mean squared differences (table b) between gamma-spectrometer values and estimates from 54 individual batch samples, using conventional and geostatistical methods.

Search area	$\bar{X}$	Conventional 1/d	$1/d^2$	$1/d^3$	Kriging 1D	2D	3D
Table a.							
0	24.0	24.3	24.5	24.6	23.7	23.5	24.5
+1	25.6	25.3	25.1	25.0	24.6	25.4	25.7
+2	30.2	27.5	27.1	25.4	26.5	25.8	25.6
Table b.							
0	4094	4038	4072	4153	4066	4000	3896
+1	3845	3717	3760	3881	4072	4030	3930
+2	4507	3893	3788	3902	4182	4047	3942

5.4.3 Comparison of estimates and 3-D kriging.

In order to evaluate the individual estimation methods against 3-D kriging, mean values of algebraic and squared differences are listed in table 5-6a,b. It can immediately be seen that no method appears to be biased compared with 3-D kriging (table 5-6a). For all methods except $1/d^3$ weighting, the squared differences increase when the search area is increased, indicating a different way of weighting samples when bigger search areas are used. This is discussed in the following section (5.4.4). Not surprisingly 1-D and 2-D kriging produce estimates which are most like the 3-D kriging estimates for a 0 search area. On the contrary, estimates made by the conventional methods of $1/d$ and $1/d^2$ are most like the 3-D kriging estimates when the search area is +1. This again indicates substantial differences in sample weighting made by different methods and search areas.

TABLE 5-6: Mean algebraic differences (table a) and mean squared differences (table b) between 3D-kriging estimates and other estimates from 54 individual batch samples.

Search area	$\bar{X}$	Conventional 1/d	$1/d^2$	$1/d^3$	Kriging 1D	2D
Table a.						
0	-0.44	-0.19	0.02	0.17	-0.74	-0.94
+1	-0.13	-0.43	-0.67	-0.78	-1.15	0.39
+2	5.35	2.57	0.65	-0.22	0.94	0.76
Table b.						
0	151	94	121	199	86	88
+1	980	420	196	171	362	298
+2	1723	695	267	181	405	324

5.4.4 Sample weights.

In the previous discussion it was shown that all the estimates are highly influenced by the size of the search area. This can be clearly illustrated if the individual sample weights are considered. Figure 5-13 displays the sample weights when batch 21 (at 391.7 metres) is estimated by either 1/d weighting or by one of the three kriging methods. The two search areas 0 (open symbols) and +1 (solid symbols) are used. The estimates and the estimation errors are listed in table 5-7.

It is noted that althougn the 'only' difference between the three kriging procedures is a consideration of the support of the object being estimated, very different sample weights are obtained. The most remarkable behaviour is seen in the $2D_o$ kriging weights. The central sample at 392 metres should, intuitively, receive the biggest weight. In practise, 2-D kriging gives more weight to the sample at 390 metres (17.6%) than

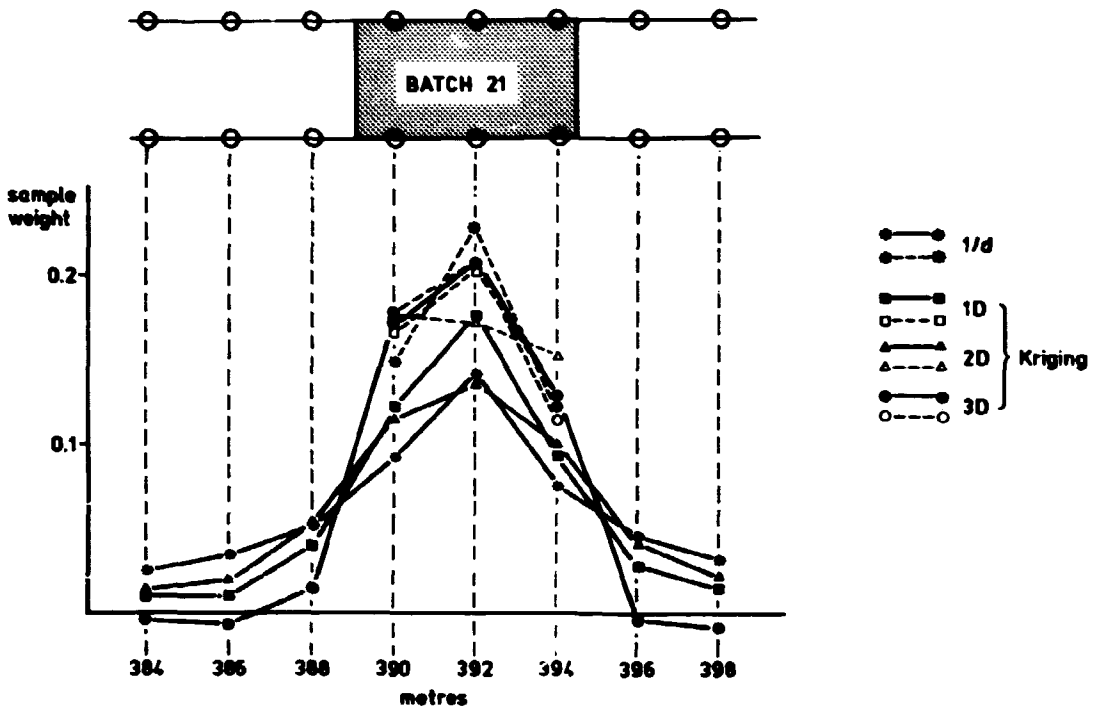

FIGURE 5-13: Sample weights obtained by different estimation methods. Inverse distance weighting, point -, panel - and block kriging are considered. Dashed lines: search area 0, solid lines: search area +1.

to the central sample (17.2%) with this particular block/sample pattern. When the search area is increased the weights change dramatically.

It can be seen that the kriging methods assign most weight to the internal samples whereas external samples are more or less screened off. 3-D kriging even gives negative weights to external samples. Furthermore, the internal weights of 3-D kriging seem unaffected by the size of search area.

This indicates that when 3-D kriging is used external samples will have only a slight effect on the estimates (table 5-7). However, the estimation error is reduced if some external samples are used (table 5-4).

It is believed that the 'screening off' of external samples to some extent can be explained by the short range of influence indicated by the semi-variogram (5.2.1).

From this example it can be concluded that conventional methods (here 1/d) and the individual kriging methods all produce significantly different sets of weights, which, in fact, do not always appear intuitively clear (see also sec. 4.3.3.3 and fig. 4-46).

TABLE 5-7: Comparison of estimates (Z^*) and kriging estimation errors (σ_k) of batch sample no. 21 using different estimation methods, search areas and semi-variogram models.

Estimation method	Search area 0				Search area +1			
	Overall model		Lujavrite model		Overall model		Lujavrite model	
	Z^*	σ_k	Z^*	σ_k	Z^*	σ_k	Z^*	σ_k
1/d	373.0	86.1	373.0	77.3	376.3	86.4	376.3	75.8
1D-kriging	373.0	87.2	371.0	77.6	374.7	86.4	374.6	75.0
2D-kriging	371.6	32.4	370.0	29.1	373.5	27.8	374.7	22.8
3D-kriging	374.9	9.1	375.0	5.4	373.0	8.9	373.3	5.3

5.4.5 Choice of semi-variogram model.

The semi-variogram model based on the total sample set (sec. 5.2.1) was used throughout this study in the kriging procedures, and all the data points were included during estimation. One could argue that a more reasonable approach would be to estimate 'lujavrite batches' from lujavrite samples only and using the lujavrite semi-variogram model (sec. 5.2.1) in the kriging procedures (selective kriging). In order to investigate the difference between two such procedures, estimation of the batches was also carried out selectively and the results, including the kriging weights, were compared with the overall estimation results. Tables 5-7 and 5-8 list the results from batch 21, which is a representative example. From table 5-7 it can be seen that the estimates are hardly affected by the change in semi-variogram model. On the other hand, kriging

TABLE 5-8: 3D-kriging weights of samples used in estimating batch no. 21. Two different semi-variogram models are considered. The sample position is given in metres from the tunnel entrance.

Sample position:		384	386	388	390	392	394	396	398
Search area 0	Overall	-	-	-	.178	.207	.115	-	-
	Lujavrite	-	-	-	.181	.205	.114	-	-
Search area +1	Overall	-.004	-.006	.015	.172	.206	.128	-.004	-.008
	Lujavrite	-.003	-.005	.018	.169	.203	.123	-.003	-.006

standard deviations are reduced 11-40% when selective kriging is performed, mainly due to the lower sill value of the semi-variogram. Confidence intervals presented in figure 5-9a,b might therefore be regarded as being somewhat pessimistic. If the individual sample weights are considered (table 5-8) the reason for obtaining equal estimates from the two types of estimator appears obvious. The use of either the lujavrite model or the total sample set model is not reflected in the weights.

Considering this result and the screening effect of external samples the estimates based on the total sample set become meaningful. Measures of the estimation error are, however, probably too high.

5.5 Estimating the total amount of ore in the bulk samples.

Four individual bulk samples were selected and shipped to RISØ. Three of these were composed of the tunnel batches (table 5-9), whereas the fourth comprised 'ore' from a side tunnel from which no chip sample data are available. The percent values given in brackets for the batches which were only partly-selected are approximate. No disposal during transportation was considered. The total (calculated) amount of ore is therefore

5.9% higher than the actual tonnage, estimated at 4701 tons (Jørgen Jensen, pers. comm.). The tonnage of the individual batches were obtained by multiplying the actual batch length by a mean tunnel cross-section of 9 m^2. A constant density of 2.7 was used. Table 5-9 gives mean grades based on gamma-spectrometer values and the $3D_1$ kriging results. If the former (431 ppm U) is corrected by the orthogonal regression relationship established in section 5.4 a value of 406.4 ppm U is obtained. This value lies close to the value estimated by $3D_1$ (408 ppm U). The average 95% confidence interval of the individual batch estimate is $\pm$ 22.6 ppm U if the semi-variogram model based on the total data set is used. The corresponding interval using the lujavrite model is $\pm$ 14.9.

TABLE 5-9: Summary table of mean grade (ppm U) and tonnages of bulk samples. The bulk samples are composed of the batch samples listed. Uranium tonnages based on $3D_1$-kriging results. *) Based on gamma-spectrometer value (GAM). No volume reduction during transportation is considered.

Bulk sample	Bulk composition	Mean grade GAM	Mean grade $3D_1$	Tons ore	Tons U
I	8(20%),9,10,11,16(60%),17,18,19,22,23, 24,25(80%),28(90%),29(90%)	424	412	1633	0.673
II	14(60%),15,16(40%),20,21,25(20%),26(20%)	410	420	623	0.262
III	46(80%),47,48,49,50,51(60%),52,53	448	401	1566	0.628
IV	Side tunnel	415	-	1157	0.480*

6 URANIUM IN SURFACE DATA

The uranium values from the gamma-spectrometric survey of the Kvanefjeld plateau were investigated for the following:

(1) The spatial variations of uranium in the total set of data and in lujavrite samples were examined.

(2) The spatial structure was modelled and used for point estimation of uranium values. Whether non-stationary geostatistics (universal kriging) reduced the estimation errors of simple kriging was examined.

(3) As a result of (2) the best estimation method was used to produce a denser grid (5 by 5 metres) of estimated point values. This grid was used as input data for an automatic contouring program which drew a contour map of the uranium values. The kriging standard errors of estimation were contoured as well to illustrate the reliability of the map.

The raw data values from the survey were used directly, and no attempt was made to correct for vegetation, snow, amount of outcrop etc. Neither were differences in elevation considered.

6.1 Uranium distribution and spatial structure.

The uranium distribution in the 2848 samples is shown in figure 6-1. The shaded part of the histogram shows the distribution within lujavrite samples. These were selected from the total data set by using the expression:

$$200 \leq \text{geology code} \leq 299$$

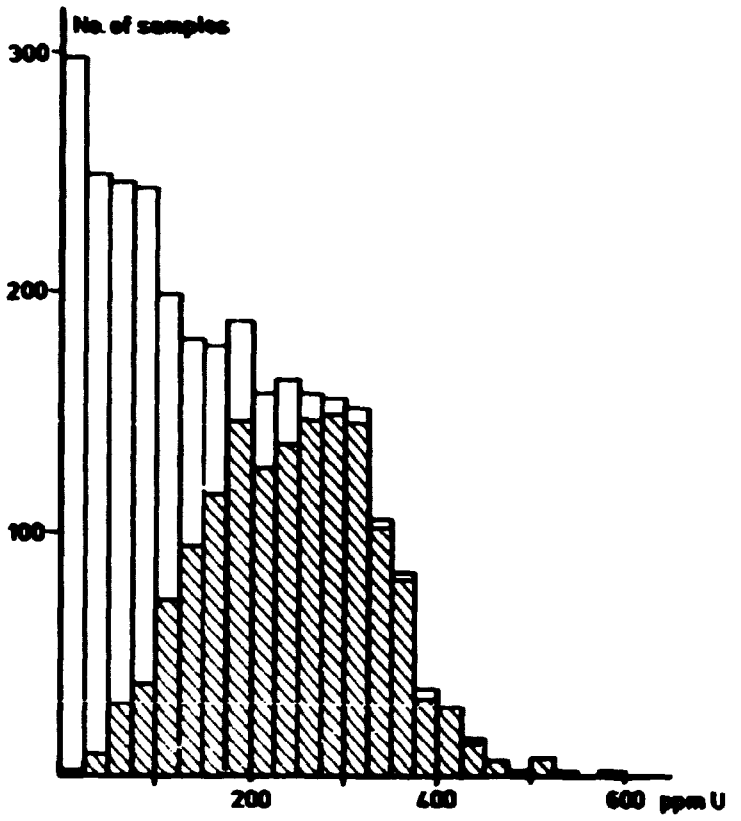

FIGURE 6-1: Histogram of uranium values in the surface data. The shaded area indicates the histogram of uranium at lujavrite sites. Total number of samples is 2848.

and hence comprise samples in which the lujavrite content amounts to more than 50%. The parameters of the distributions are listed in table 6-1.

The histograms in figure 6-1 show many similarities to the histograms of uranium values obtained from drill core assays and borehole logs (figs. 4-1,4-37 and 4-49). The distribution of the total set is highly skewed and multi-modal whereas, lujavrite samples display a nearly normal distribution.

The spatial structure of the data was investigated by semi-variograms. The program MARVGM (sec 5-2) was used throughout the study.

TABLE 6-1: Simple statistics of uranium (ppm) in the 'surface data'. Field gamma-spectrometric survey.

Type of data	N_s	Mean	Std. dev.	Coeff. of var.
Total data set	2848	165.3	113.6	0.69
Lujavrite sites	1480	242.4	89.2	0.37

Experimental semi-variograms were calculated in different directions in order to examine whether any anisotropic spatial structures exist. This could intuitively be the case because of the magmatic lamination in the lujavrites. The most convenient way of selecting directions was simply to use the directions of the grid. That is, parallel to the X- and the Y-axes and along the diagonals. Other directions may be used but they would give fewer sample pairs. The results from the total data set are presented in figure 6-2. Experimental semi-variograms are shown for the four main directions N-S, E-W, NW-SE and SW-NE. It should be mentioned that these designations are approximate since the coordinate system makes an angle of 12^{o} with the magnetic north. A fifth semi-variogram shows the overall horizontal structure where all directions are allowed. In practice this is calculated by MARVGM with the parameter $\partial\Theta$ (fig. 5-3) set to 90^{o}.

It can be clearly seen in figure 6-2 that at distances less than, say, 140 metres a distinct anisotropy is present. The semi-variogram in the E-W direction displays both a longer range of influence and a lower sill value than the N-S semi-variogram. This type of behaviour is called a zonal anisotropy (Journel and Huijbregts, 1978) and may arise from a number of causes, as discussed later. The semi-variograms along the diagonals and the overall horizontal semi-variogram lie between those from the E-W and the N-S, verifying the differences between them. Although it would be rather optimistic to suppose that the sample grid is orientated parallel to the directions of the structures, it is believed that the N-S and E-W direc-

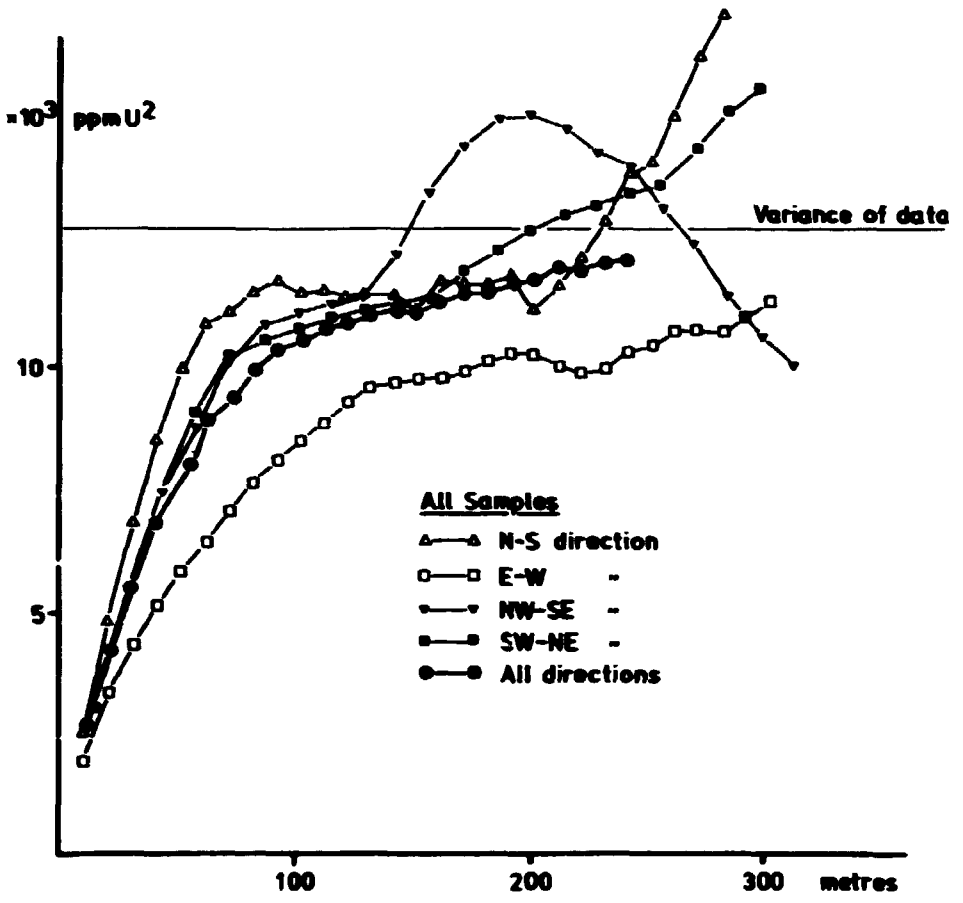

FIGURE 6-2: Experimental horizontal semi-variograms calculated from the surface data.

tions are fairly close to the main axes of the ellipse of anisotropy (Marechal and Shrivastava, 1977). No attempts are made to determine the true axes of the ellipse, mainly because of the unreliability of the data values and the character of the study.

It can be noted that all the semi-variograms in figure 6-2 display a very low nugget effect ($\simeq$600 ppm U^2) compared with the results from drill holes. This is probably due to the large sample volume. However, it is surprising that the high analytical errors have not produced high nugget effects.

The semi-variograms of fine-grained lujavrite samples (fig. 6-3) also display anisotropic conditions. Although their sills

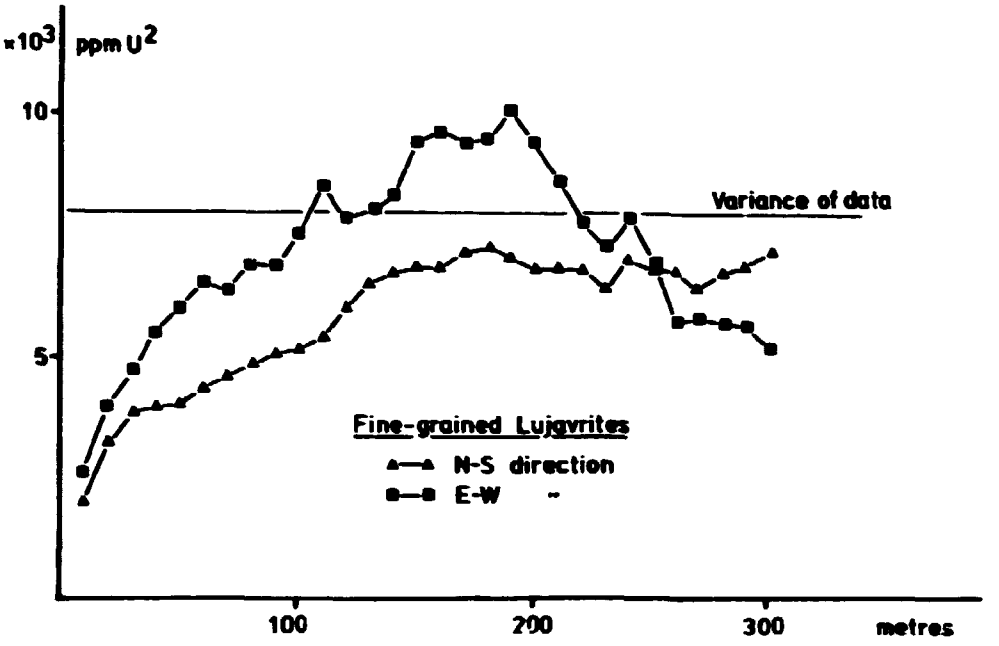

FIGURE 6-3: Experimental semivariograms for uranium values at fine-grained lujavrite sites.

are more difficult to determine it is still clear that the range of influence is greatest in the E-W direction. The sill values are naturally lower because of the more homogeneous nature of the material. However, the E-W direction now has the highest sill value, indicating that the samples removed produce very high spatial variances in the N-S direction when combined with the lujavrites.

6.2 Semi-variogram modelling.

As described in section 4.2.5. the most convenient way to check a model fitted to an experimental semi-variogram is by point kriging. The model which produces the smallest errors of estimation is selected as the best. It is also possible to test whether the intrinsic hypothesis is fulfilled. As earlier stated, stationary geostatistics is based on a second order stationarity of the difference D(x,h) between a regionalized

variable Z(x) and a variable Z(x+h) at locations x and x+h. If, however, the intrinsic hypothesis is not fulfilled, the first and second moments of D(x,h) will be dependent on the locations of the samples:

$$E\{D(x,h)\} = m(h)$$

$$E\{(D(x,h) - m(h))^2\} = 2\gamma(h)$$

If this is the case another kriging technique is used to estimate the RV. To do this the RV Z(x) is split into two components, a drift m(x) and a residual Y(x):

$$Z(x) = m(x) + Y(x)$$

The drift, which is conceptually similar to 'trend', is the expected value of Z at x (Journel, 1969). It may be defined as a systematic increase or decrease in the value of a non-stationary regionalized variable in a particular direction. The residual, equal to the difference between the RV and the drift at point x, is itself a RV and hence spatially correlated. If a semi-variogram of the residuals is used in conjunction with the drift function to estimate the RV, the estimation procedure is called universal kriging (UK).

The theoretical background of UK is described in Matheron (1969). An excellent introduction to the theory is given by Olea (1975) who also presents the application of UK for automatic contouring (Olea, 1974). The theory of UK and the UK program PTUK, which is used in the present study, is described by the author (Clausen, 1980). PTUK has been developed at the University of Leeds. A case study on practical UK and automatic contouring is partly carried through by the author (Royle et al., 1981).

Since the semi-variogram of residuals cannot be estimated if the drift function is unknown, and vice versa, UK is carried out using the following assumptions. The semi-variogram of

residuals is assumed to follow a linear scheme and the drift is either linear or quadratic. PTUK, which performs point UK, is run several times (trial-and-error) to obtain the optimum combination of drift type, the slope of the semi-variogram, and the size of the search area. The latter is important since it defines the scale at which the drift is described and the number of points which are used for estimation.

To summarize, the following comparisons were made:

(1) Several models were fitted to the overall horizontal semi-variogram and the E-W and N-S semi-variograms. The best model for estimation was found using program PTKR (simple kriging). Different search areas were tried.

(2) Program PTUK (universal kriging) was used to investigate whether the results found in (1) could be improved by taking the drift into account.

Three different models (Models 1-3) were fitted to the overall horizontal semi-variogram (fig. 6-4). From table 6-2 it is seen that these three models all comprise two spherical components and a nugget effect. The parameters for the models fitted to the E-W and N-S directions are also listed in table 6-2.

The results from the runs of PTKR and PTUK are listed in table 6-3. As usual the comparison is based on the statistics $E\{Z_i - Z_i^*\}$, $E\{|(Z_i - Z_i^*)|\}$ and $E\{(Z_i - Z_i^*)^2\}$. Two search areas, 12.5 by 12.5 metres and 25.0 by 25.0 metres, which included the nearest 8 grid points and 24 grid points respectively, were used. Larger search areas were believed to contain redundant information and the enlarged matrices waste computing time. Finally, PTKR was run subject to the condition that the spatial variation was anisotropic. This was done by multiplying all distances in the N-S direction by the ratio between the range of influences of the two main directions (Clark, 1979). In the present case the anisotropy factor is 150.0/65.0 = 2.31. It should be noted that this correction is not completely satisfactory (Journel and Huijbregts, 1978) since it does not correct for the zonal anisotropy. Secondly, it is not certain that the true main axes of

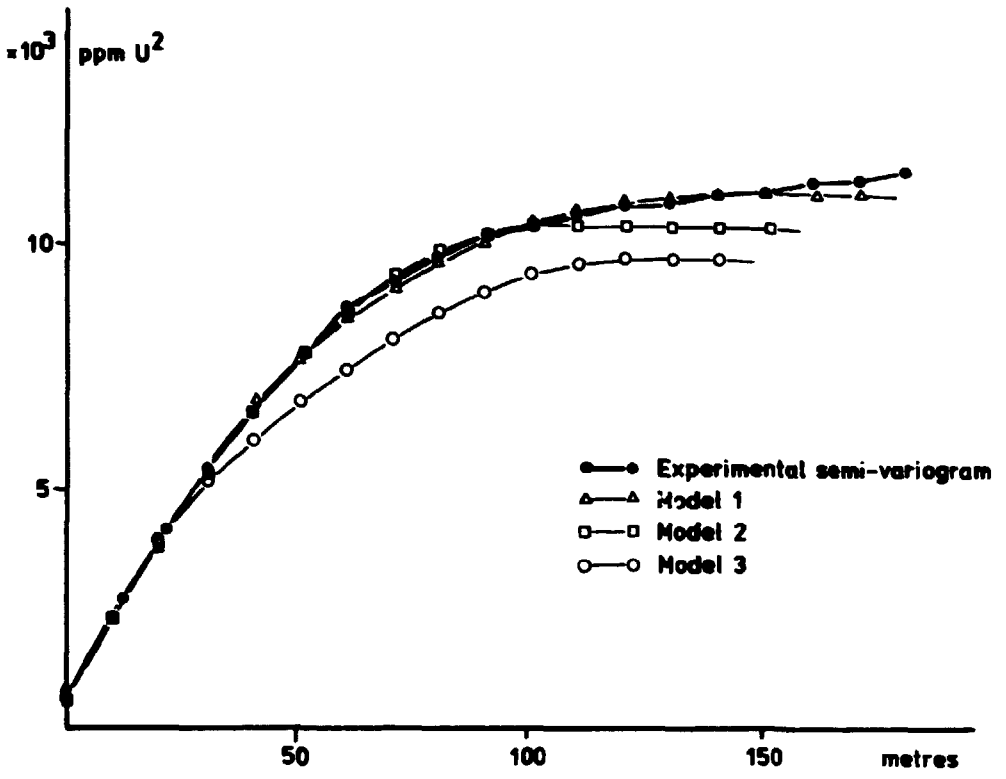

FIGURE 6-4: Different models fitted to the overall experimental semi-variogram of the surface data. The parameters of the models are listed in table 6-2.

TABLE 6-2: Parameters (range of influence and sill values) for spherical models fitted to the overall and the E-W and N-S experimental semi-variograms. a_1 and a_2 in metres, C_0, C_1 and C_2 in $(\text{ppm U})^2$.

Model	Nugget effect C_0	Spherical comp.1 a_1	C_1	Spherical comp.2 a_2	C_2
1	700	70	4300	140	6200
2	600	36	900	100	9000
3	600	30	180	120	7400
E-W	700	30	1400	150	7500
N-S	600	65	8000	120	2400

TABLE 6-3: Results from PTKR (point kriging) and PTUK (point universal kriging) of the surface data. Different semi-variogram models (PTKR) and drift types (PTUK) are used. N_s is the number of samples, F_a the anisotropy factor. The statistics S1, S2 and S3 are explained in the text. Units as in table 4-4.

Semi-var. model/ drift type	N_s	Search area	F_a	S1	S2	S3	σ^2_k
Simple kriging:							
1	2794	25.0	1.0	0.084	31.7	1947	2142
2	2794	25.0	1.0	0.052	31.5	1934	2141
3	2794	25.0	1.0	-0.028	31.3	1926	2246
E-W	1977	12.5	1.0	0.840	33.3	2113	2057
E-W	2794	25.0	1.0	-0.009	31.6	1940	2059
E-W	1977	12.5	2.31	0.551	31.9	1991	2457
E-W	2794	25.0	2.31	0.025	31.8	1996	2490
N-S	1977	12.5	1.0	0.810	33.1	2099	2483
N-S	2794	25.0	1.0	0.057	31.4	1927	2481
Universal kriging:							
Linear	1977	12.5	1.0	0.491	31.0	1824	-
Quadratic	1977	12.5	1.0	-0.014	36.7	2479	-
Linear	2794	25.0	1.0	0.062	31.1	1911	-
Quadratic	2794	25.0	1.0	-0.196	31.3	1939	-

anisotropy have been determined. If the results of simple kriging are examined, it can be seen that no significant differences in estimation errors are recorded between the different models. The mean algebraic errors of estimation ($E\{Z_i - Z_i^*\}$) are in all cases smallest with the larger search area, indicating that the estimator is more central. However, the mean absolute error and the mean squared error indicate that

estimation is only slightly improved by enlarging the search area. The best model found by simple kriging was the overall model 3, which surprisingly produces better estimates than the E-W model where a correction for anisotropy was made. The difference is, however, very small.

As for the universal kriging results, the best result is given by the smallest search area (12.5 by 12.5 metres) and a linear type of drift. The mean squared error of estimation using this choice of parameters, 1824 ppm U^2, is only 5.6% less than the value found by simple kriging and model 3 (1926 ppm U^2). It is therefore concluded that the spatial variation in the surface data is adequately described by a simple two component isotropic spherical semi-variogram model. It is not necessary to take account of the drift and the stationarity hypothesis is therefore believed to be fulfilled.

6.3 Point estimation and mapping.

Having accepted model 3 as the best possible description of the spatial variation, it was then used for point kriging on a regular grid. Input data were the actual values on a 10 by 10 metre grid. The surface described by estimated values is smoother than one based on raw data. This is because of the 'smoothing effect of kriging' which means that high values are underestimated and low ones are overestimated. It is clear that no estimate can be bigger that the highest data value because of the non-bias condition.

The selection of a suitable grid size is closely related to the contouring and the computer times, for which reason the user always has to compromise between the amount of detail on the map and its cost. There is, of course, an upper limit to the amount of detail since kriging cannot produce more information than that already contained in the data. On the other hand, estimating a denser grid has no effect on the estimation error.

A 5.0 by 5.0 metre grid was estimated by point kriging using semi-variogram model 3. The program used is a modified version of PTKR, called PTKNET, (Ahlefeldt-Laurvig, 1981). If a data value is present at the point to be estimated the value is recovered exactly since kriging is an exact interpolator. Naturally, the kriging standard errors at such points are zero. A search area of 25.0 by 25.0 metres was used and a minimum of 6 data points available for estimation was specified. If this condition was not fulfilled the program returned a 'dummy-estimate' of -10.0. The estimation of the grid (241 by 127 points) took 602 cpu seconds on the IBM 3033 computer at NEUCC. The estimated grid values, together with the kriging standard errors, were stored on magnetic tape ready for automatic contouring.

Contour maps of the uranium values and the kriging standard errors were produced using the programs SAM and DUEPLT. Both programs, which have been developed in the Department of Surveying and Photogrammetry, Technical University of Denmark, are documented in Spliid (1981). The principles of automatic contouring are found in Royle et al., (1981). SAM calculates the isolines with a contour interval specified by the user. Plotting is carried out by DUEPLT which draws the map on a Calcomp plotter. The version of DUEPLT used in the present study is an interactive program, which asks the user for details about the final map, such as type of pen, map scale, curve annotations etc.

The map of uranium values was calculated with a contour interval of 50 ppm U and the resulting map is presented in fig. 6-5. Positions of drill holes and lacuna and the shading of 'high grade' areas were added manually to the map. A hand-contoured map of the same values is found in Nyegaard et al., (1977). By comparing these two maps good accordance is seen but the map produced by automatic contouring contains, obviously, more detail. It can be seen from the map in fig. 6-5 that the high grade areas indicated by the surface data follow a border coincident with the northern contact. The highest values are found

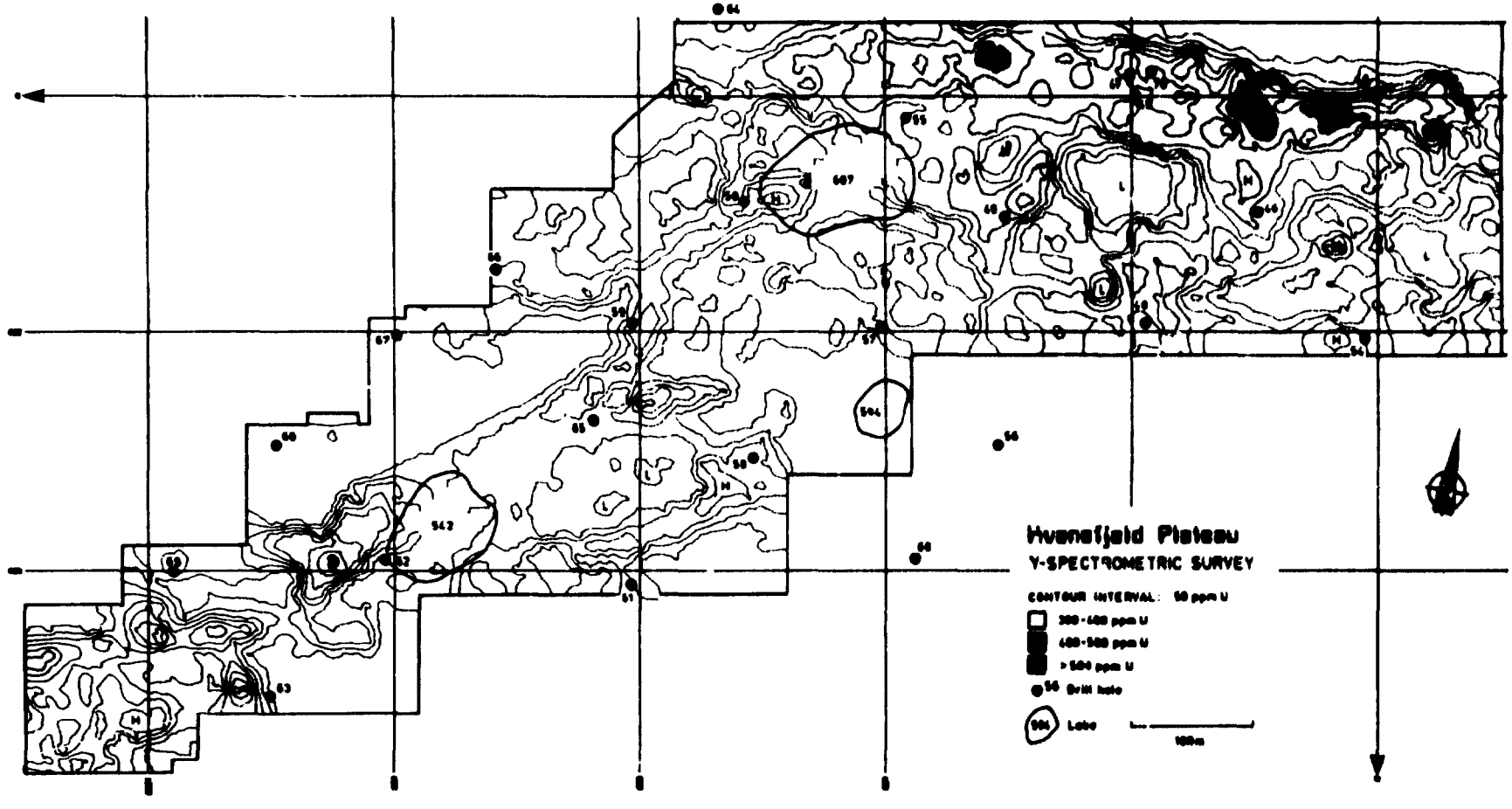

FIGURE 6-5: Iso-grade map of uranium values at the Kvanefjeld Plateau produced by point kriging and automatic contouring. L indicate low-grade areas, H indicate high-grade areas. Drill hole positions are indicated.

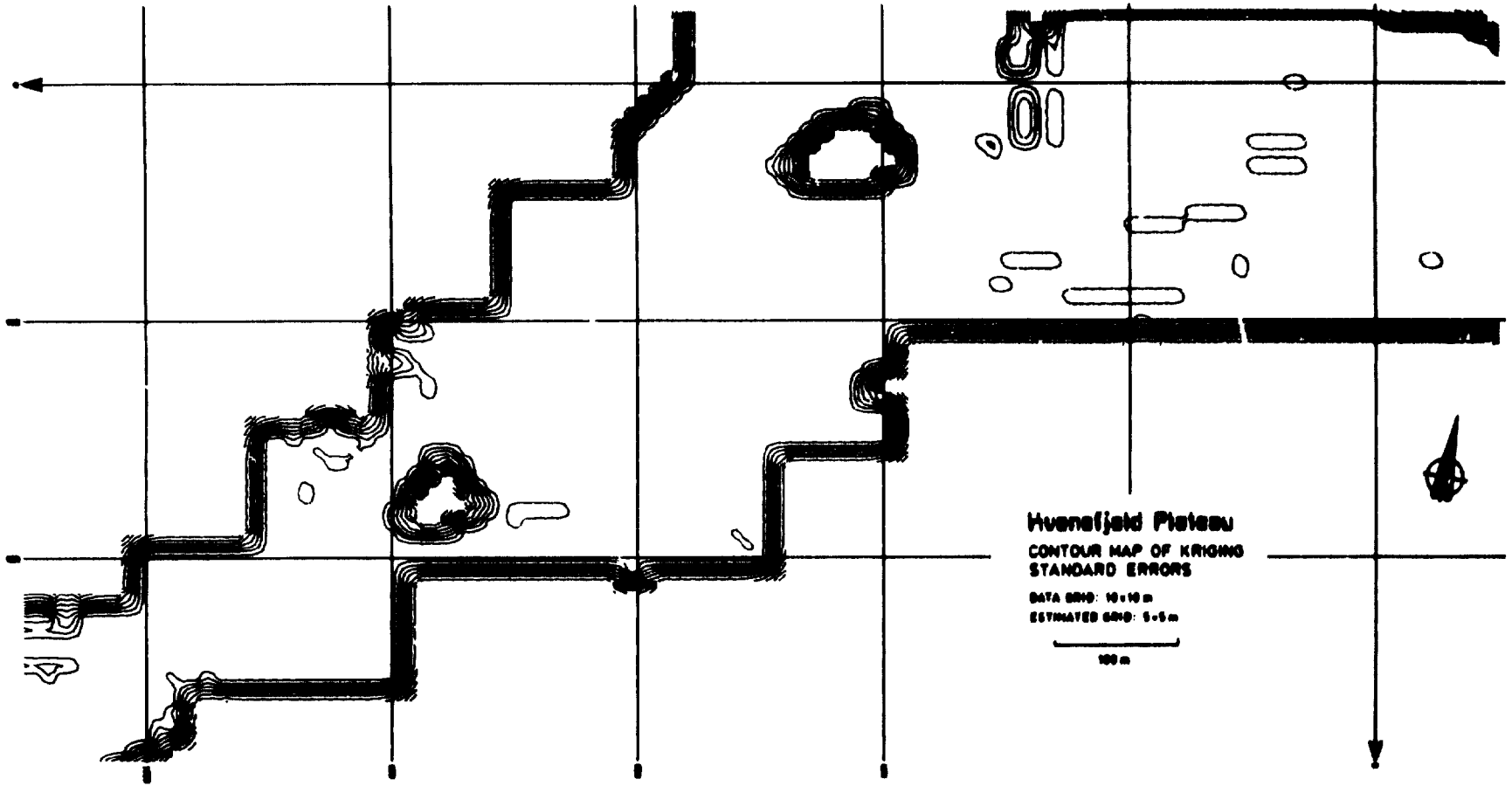

FIGURE 6-6: Contour map of kriging standard errors when a 5x5 metre grid is estimated from a 10x10 metre grid. Contour interval is 5 ppm U. The standard error at grid points in the middle of the test area is approx. 41-45 ppm U.

south and southwest of drill holes 39 and 40 in fine-grained lujavrite. North of this border the geology changes into a green ac-lujavrite and a naujaitic border pegmatite (Sørensen et al., 1974, Nyegaard et al., 1977). The rapid change in uranium content when this border is overstepped is clearly seen.

A validity map showing the dispersion distribution of the estimated surface is produced from the kriging standard errors (fig. 6-6). The value 41 ppm U was substituted for points where the kriging standard error was zero. This was done in order to smooth the central part of the map, and because only the estimated points are of interest. Not surprisingly, estimation is out of control where the boundary of data points is overstepped (e.g. at the lacuna). The contour interval on this map is 5 ppm U. Most of the contours in the central part of the area represent dispersions ranging from 41 to 45 ppm U while the estimation error increases strongly towards the edges.

6.4 Discussion of findings.

The most remarkable result obtained from the study of the spatial structure of the surface data is the pronounced zonal anisotropy. Although this anisotropy does not influence point kriging significantly, it suggests that there is a greater continuity in the E-W direction. In other words, sample values are less different in the E-W direction than in, for example the N-S direction. Although the true directions of anisotropy have not been determined a possible ellipse of ranges of influence may be drawn (fig. 6-7). This ellipse describes the behaviour of the correlation distances in the horizontal plan, but it does not take into account the fact that the variances also differ with direction (fig. 6-2). Since the experimental semivariograms are best described by two-component spherical models, the models of zonal anisotropy may be explained by a nested structure in which each component structure may have its own anisotropy.

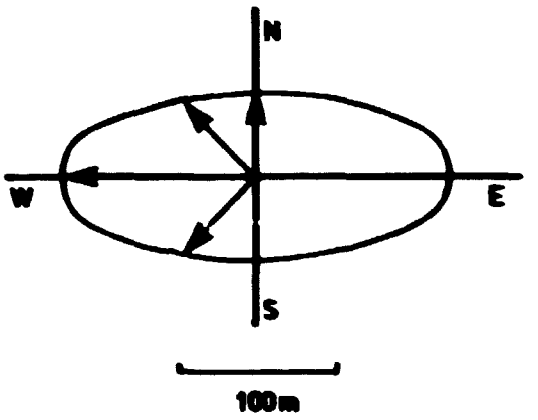

FIGURE 6-7: Ellipse of anisotropy expressed in terms of the range of influence in a given direction.

Spatial anisotropy corresponds to the existence of preferential directions at the time of the genesis of the studied phenomenon (Journel and Huijbregts, 1978). Examples of such directions are:

(I) The vertical direction in a deposit formed by deltaic deposition.

(II) The horizontal directions of the deposition currents in an alluvial deposit.

(III) The radial directions around a volcanic pipe in an intrusive deposit.

It is clear that none of these examples can be used to explain the phenomenon observed at Kvanefjeld since no direction of deposition is known. It is, however, possible to explain the anisotropic behaviour by the following observations (John Rose-Hansen, John Engell, pers. comm.):

a) The main direction of lujavrite propagation is close to the the E-W direction. This can be seen if the directions of foliation are examined (fig. 6-8).

b) The uranium seems to be concentrated in a border coincident with the contact (and thereby to some extent with the

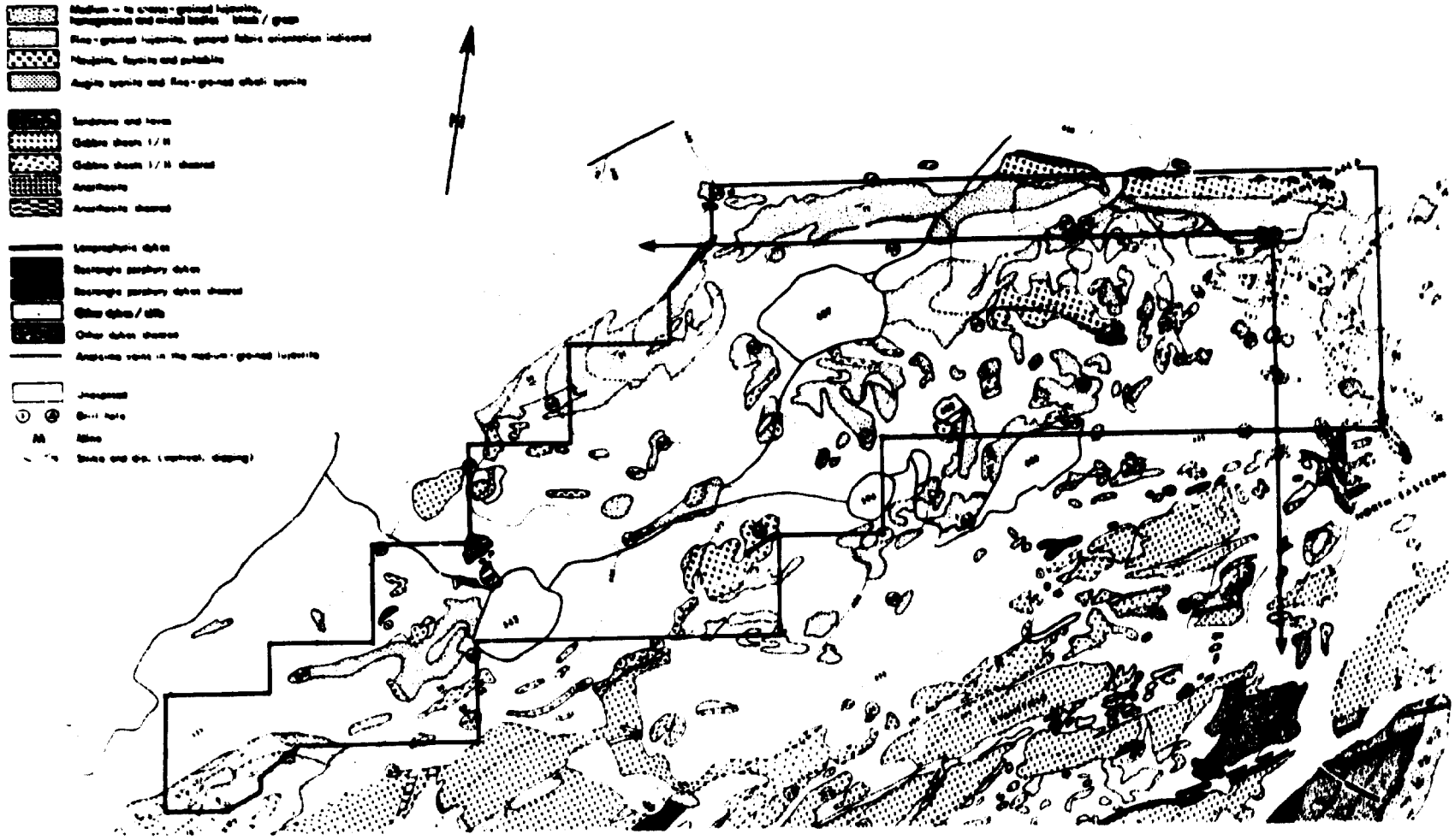

FIGURE 6-8: Geological map of the northern part of the Kvanefjeld area. The gamma-spectrometer survey area is indicated. (From Sørensen et al., 1974).

E-W direction). Hence the variability is greater across than along this border.

c) The determination of the gamma-radiation is to some extent influenced by the amount of vegetation, which in turn is dependent on the degree of porosity caused by weathering. The weathering is, in the area of investigation, most pronounced in rocks in contact with lujavrite. Since many of these weathered zones lie parallel to E-W direction, they may have contributed to the anisotropic conditions.

The anisotropy indicated by the surface data may exist at lower levels of the deposit, suggesting that the horizontal variation should be carefully studied in future exploration.

It is observed that the ratio of sill values in the two directions E-W and N-S is reversed on turning from the total sample set to lujavritic samples. This remarkable feature suggests that the material removed from the data set, i.e. xenolithic material, has a much higher variance in the N-S direction than in the E-W direction. This again indicates the rapid change in uranium content when the contact into non-lujavritic material is crossed.

The spatial variation is found to be best described by a two-component spherical structure with a small nugget effect. If the models fitted to the overall experimental semi-variograms are examined (fig. 6-4), models 1 or 2 would intuitively be selected due to their reasonably good fits over the first 100 metres. However, point kriging surprisingly suggests that model 3 should be used for estimation, probably because of a better fit over the first 20 metres, and it is exactly this part of the semi-variogram which is used for estimation. The advantage of using point kriging for model selection rather than a visual appraisal is therefore demonstrated.

7 MUTIVARIATE STATISTICAL ANALYSES.

The use of multivariate statistical methods in different branches of geology has been reported in numerous papers. Among these methods discriminant analysis and cluster analysis has found many successful applications (Davis, 1973). The case studies by Howarth (1971a), Hawkins and Rasmussen (1973), Park (1974), Conradsen et al. (1976) and Clausen and Harpøth (in press) should be mentioned. This chapter summarizes the results from a multivariate statistical study of 68 fine-grained lujavrite samples randomly selected from drill holes 44, 46, 48, 49, 51, 55 and 59 (figure 7-1). The study was presented in Conradsen and Clausen (1981) from which the following is extracted. The statistical analyses were carried out on untransformed data values; however, a more detailled study considering a larger number of samples and using both untransformed and log-transformed data is currently being undertaken (Conradsen, Clausen and Nyegaard, in prep.). A full listing of the 68 samples included in the study is given in appendix E.

The primary aim of the multivariate study was to investigate whether the chemical composition, or more precisely the trace element content of the individual sample, was specific for the geological units under consideration. A preliminary investigation of inhomogeneous material comprising more than 600 samples divided into at least 8 units showed that, due to the complexity of the material, multivariate analyses should be carried out on sub-sets for simple classification only. In the present study four different units were considered (table 7-1). Two different rock types, naujakasite lujavrite and arfvedsonite lujavrite, were represented and each of these was sub-divided into two groups by the criterion of presence or absence of the mineral villiaumite (NaF).

The statistical analyses were carried out in two simultaneous series using two different sets of variables (table 7-2a,b). The FULL data set contained the maximum number of possible elements (35). The REDUCED data set contained a number (20) of

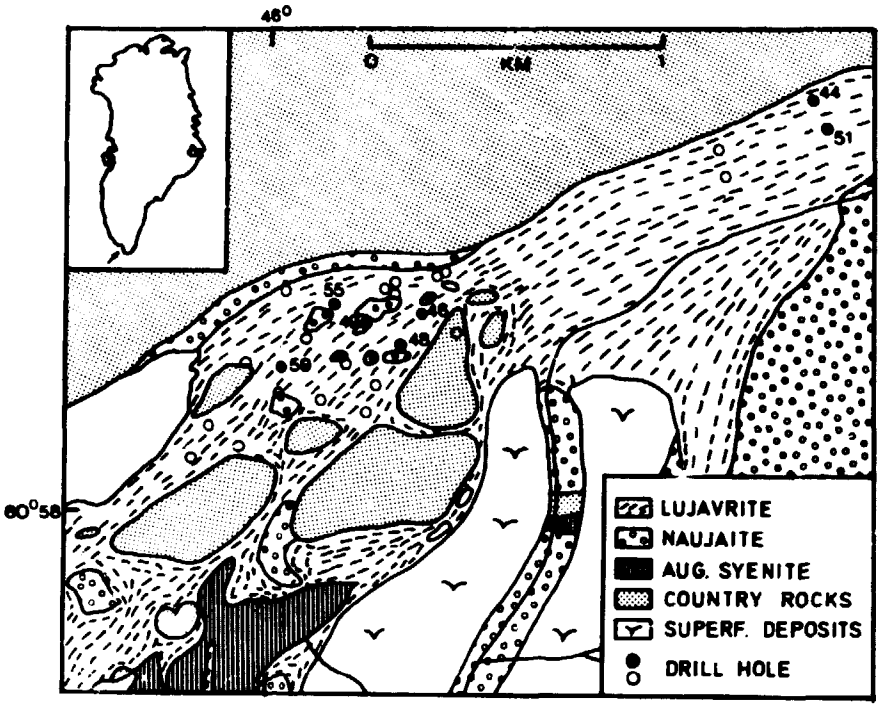

FIGURE 7-1: Simplified geological map of the Kvanefjeld mega-breccia with drill hole positions. Holes used in the multivariate study are indicated by filled circles. (After Ferguson, 1964).

TABLE 7-1: Number of samples in the four groups considered in the multivariate analyses.

Geological Unit	GGU code	N_s
Arfvedsonite lujavrite	299	15
Arfvedsonite lujavrite + villiaumite	296	19
Naujakasite lujavrite	295	19
Naujakasite lujavrite + villiaumite	297	15

TABLE 7-2: Variables used in the multivariate statistical analyses. The analytical methods and the method index are described in chapter 3. Note: two different data sets are used (FULL/REDUCED).

Analytical method	Index	Variables
Table a: FULL		
GAMSPEC	1	U,Th,K
XRF	2	Zr,Y,Sr,Rb,Th,Pb,Ga,Zn,Nb,Cs
ENAA	6	Na,Fe,La,Ce,Sm,Eu,Yb,Lu,Hf,Ta,Th
EDXPLU	7	K,Ti,Mn,Fe,Ni,Cu,Zn,Ga,Sr,Pb,Ca
Table b: REDUCED		
GAMSPEC	1	U,Th
XRF	2	Zr,Y,Nb
ENAA	6	Na,La,Ce
EDXPLU	7	-
Element ratios	-	Hf6/Ta6, Th1/U1, Mn7/Fe7, Zn7/Y2, Zn7/Pb7, Nb2/U1, Zn7/U1, Y2/Pb7, Y2/U1, Zr2/U1, Th1/Pb7, Fe7/Pb7

selected variables of which some were element ratios. These were a priori believed to be of major importance for the discrimination due to different within-group correlations (Nyegaard, 1979).

7.1 Cluster analysis

Cluster analysis divides hierarchically or non-hierarchically the observations into groups (clusters), but disregards the a priori grouping. In non-hierarchical cluster analysis the final

number of clusters must be pre-defined. Two commercial BMDP-cluster programs, BMDP2M and BMDPKM, were used (Dixon and Brown, 1979).

BMDP2M performs a hierarchical cluster analysis. Initially each case is considered to be in a cluster of its own. At each step the two clusters with the shortest distance between them are combined and treated as one cluster. This process of combining clusters continues until all cases are combined into one cluster. The distance measure is the Euclidian distance, i.e. the square root of the sum of squares of the differences between the values of the variables for two cases:

$$d_{j\ell} = \left[\sum_{i} (X_{ij} - X_{i\ell})^2 \right]^{\frac{1}{2}}$$

where X_{ij} is the value of the i'th variable in the j'th case. The data were standardised to z-scores.

The non-hierarchical clustering performed by BMDPkM is also based on an Euclidian distance measure, but here the distances between the cases and the centres of the clusters are considered. At the completion of the run each case belongs to the cluster whose centre is closest to the case and each cluster centre is the mean of cases belonging to that cluster. The program proceeds in a stepwise manner: the number of clusters is increased by one at each step by splitting one of the clusters into two. When the requested number of clusters is reached, cases are iteratively reallocated into the cluster whose centre is closest to them.

The distance d_{ij}^2 between case i and cluster j is:

$$d_{ij}^2 = \frac{1}{p}(\underline{X}_i - \underline{C}_j)M^{-1}(\underline{X}_i - \underline{C}_j)'$$

where $\underline{X}_i = (X_{i1}, X_{i2}, \ldots, X_{ip})$ designates case i and $\underline{C}_j = (C_{j1}, C_{j2}, \ldots, C_{jp})$ designates cluster j. M is a diagonal matrix with variances in the diagomonal.

7.1.1 Hierarchical analyses

Hierarchical analyses are more appropriate to cases where the underlying structure is expected to be a tree-structure. Although this, obviously, would not always be expected with geological data, some kind of tree-structure might be present in 68 selected lujavrite samples, as indicated in figure 7-2. Of the two possibilities tree A is the most satisfactory geologically, but which one is found (if any) depends on the variables indicated.

The analysis using the FULL data set gave no definite indications of the grouping structure. One 'group' comprising 296 and

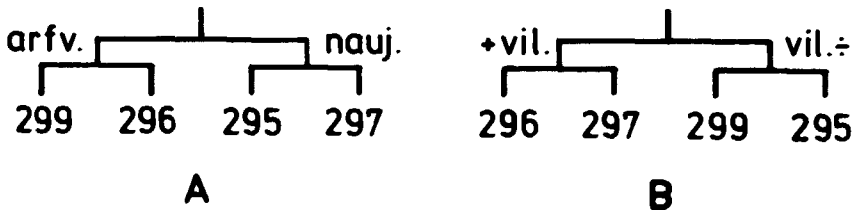

FIGURE 7-2: Possible tree-structure in the data.

299 was quite distinct. In this group samples from 299 were, generally speaking, merged together and so were the 266 samples, indicating a structure like the left hand side of tree A (figure 7-2). Another group was formed of samples from 295 and from 297 and 296. The latter were merged and the samples from 295 were merged. This somewhat strange behaviour is explained later in the sequel. Finally, one-third of the samples were joined to the groups described above or to new groups at very large distances, making interpretation difficult.

The tree-structure from the REDUCED data set was clearer. Four main groups seemed to be present. The first group mainly comprised 296 and 299 samples, the second the samples from 296 and 297 (the same as from the FULL data set), the third of 295 and 297 samples and fourth of samples from all four groups. Merging of samples often gave results which could be identified as following the A tree-structure.

It is clear from the previous paragraphs that tree-structures are not easy to recognize or interpret in the lujavrite samples. This might be due to the presence of too many 'nuisance' or 'noisy' elements in the analysis, which contribute to the distance d_{jl} in a random manner. If the number of nuisance elements is large compared to the number of discriminating elements, the systematic effect of the latter will easily be masked by random noise.

7.1.2 Non-hierarchical analyses

Non-hierarchical analyses are appropriate to cases where no tree-structure is expected, as in the present case, for instance. Analyses were carried out for 2, 3 and 4 clusters using both data sets.

The two-cluster analysis using the FULL data set returned with a group comprising twenty-six 295 and 297 samples and a group with all 299 and 296 samples plus eight samples from 297. That is, only eight samples were misclassified. Since these eight samples were successively entered into the group and all originate from the same core (48) the misclassification could not be explained as an outlier problem. However, re-logging the drill core discovered a possible continuous downwards transition from naujakasite lujavrite to arfvedsonite lujavrite at a depth of approx. 167 metres. The 8 misclassified samples could be re-labelled as 296 and hence, in the case of two groups and the FULL data set, no misclassifications were present.

Computations with 3 and 4 groups resulted in a splitting up of the groups established in the two-group case. However, the splitting did not reveal the four geological units but instead revealed two groups with 296 and 299 and two groups with 295 and 297 samples.

In the non-hierarchical analyses the results were much poorer with the REDUCED data set. For instance, only one of the mislabelled samples was put into the group with the samples from 296

and 299 in the computation with 2 groups. The results of using more groups were even less consistent with the geological units. It is therefore concluded that the analyses with the FULL data set gave the most successful results in the non-hierarchical clustering.

The most remarkable result of these clusters is firstly that some geological misclassifications were discovered, and secondly that no misclassifications from arfvedsonite lujavrite into naujakasite lujavrite or vice versa occur. These two units therefore seem to be consistently different. Within these groups it has not been possible to form groups consistent with the geology, indicating that some differences between, for example, the 296 samples might be bigger than the difference between samples from 296 and 299.

7.2 Discriminant analysis

In contradistinction to cluster analysis, discriminant analysis requires each observation to be classified a priori according to the predefined groups. For each group (t) a discriminant function is established as a linear combination of the variables:

$$D_t(\underline{X}) = c_{t1}X_1 + c_{t2}X_2 + \ldots + c_{tp}X_p + c_{to}$$

where the vector $(X_1, X_2, \ldots, X_p)$ comprises the variable measures; c_{ti} are the classification coefficients and c_{to} is a constant. The computation of the c_{ti}'s is given by Dixon and Brown (1979).

Firstly, a two-group step-wise analysis was carried out using the FULL data set (groups: 299+296 and 295+297) without correcting the mis-labelled samples (7.2.2). The order of entering the first 10 variables into the analysis is given in table 7-3. It is seen that the most significant variable is Zr2 followed

TABLE 7-3: The order of entering of the 10 most significant variables in the case of two groups and the FULL data set.

Step No.	1	2	3	4	5	6	7	8	9	10
Variable	Zr2	Eu6	Lu6	Th6	Pb2	Zn7	Ga2	Ti7	Cs2	Pb7
F-value	133.2	9.4	3.5	5.2	3.3	5.9	3.0	2.3	2.5	2.0

by Eu6 and Lu6. The classification functions produced a 100% correct classification. On the other hand, the jackknifed classification produced 84.8% and 85.3% correct classifications for the two groups, indicating an overfitting problem.

The 10 most significant variables in a four-group analysis are presented in table 7-4. Although differences are seen between table 7-3 and table 7-4, Zr2 and Eu6 still appear important in discrimination. Again, a 100% correct classification was obtained.

For the REDUCED data set similar classification results were obtained, again probably due to overfitting. In order to combat these overfitting problems a new set of analyses was performed with a limited number of steps. 7 steps (=7 variables) appeared to be a good choice and results from the two-group analysis (REDUCED data set) are presented in table 7-5. Again it was found that Zr2 was very important. There were four misclassified samples, that is, two from each group were classified into the other group. An interesting result is that the two samples from the 297+295 group were among the eight mis-labelled sam-

TABLE 7-4: The order of entering of the 10 most significant variables in the case of four groups and the FULL data set.

Step No.	1	2	3	4	5	6	7	8	9	10
Variable	Eu6	Zr2	K1	Ni7	U1	Pb7	Fe7	Ca7	Nb2	Hf6
F-value	50.3	17.2	6.3	7.5	4.8	5.6	3.9	4.5	4.6	3.6

ples. However, a remarkable feature was discovered when the a posteriori probabilities for the eight samples were inspected (table 7-6).

At increasing depths the probability for arfvedsonite lujavrite was increasing, reflecting a continuous transition.

TABLE 7-5: The order of entering of the 7 most significant variables in the case of two groups and the REDUCED data set.

Step no.	1	2	3	4	5	6	7
Variable	Zr2	Y2	Zr2/U1	Na6	Nb2/U1	Nb2	Mn7/Fe7
F-value	137.9	7.7	2.6	1.6	0.1	5.1	0.1

The same tendency was seen in the four-case analysis (table 7-7). On the other hand, it was noticed that 295 was significantly different from the other groups. A quantification of this difference is gived by the F-test statistic:

$$F_{m\ell} = \frac{(n-k-p+1)n_m n_\ell}{p(n-k)(n_m-n_\ell)} D^2_{m\ell}$$

which compares the group means of groups m and 1 having n_m and n_1 observations.

D^2_{m1} is the Mahalanobis distance, n the total number of observations, k the number of groups and p the number of variables. As can be seen from table 7-8, differences other than the presence or absence of NaF must be expected between 295 and 297. On the other hand the difference between 296 and 299 is hardly detectable. As the elements Eu6 and Zr2 appeared to be of major importance (tables 7-3 and 7-4) these were inspected with respect to their distributions. The standard deviation of Zr2 appeared clearly different between 295 and 297. Considering Eu6 a distribution-free test for equal means (Kruskal-Wallis test)

was clearly rejected by the comparison of 295 and 297, while the same test was accepted for 296 and 299.

TABLE 7-6: Posterior probabilities of the eight mislabelled samples from drill hole 48. (Two groups, REDUCED data set).

Sample no.	299+296	297+295
48168	0.074	0.926
48170	0.033	0.967
48176	0.035	0.965
48180	0.174	0.826
48182	0.323	0.677
48186	0.365	0.635
48190	0.880	0.120
48192	0.979	0.021

TABLE 7-7: Posterior probabilities of the eight mislabelled samples from drill hole 48. (Four groups, REDUCED data set).

Sample no.	299	296	297	295
48168	0.017	0.032	0.950	0.001
48170	0.008	0.014	0.977	0.001
48176	0.009	0.013	0.977	0.001
48180	0.048	0.079	0.871	0.002
48182	0.083	0.143	0.773	0.001
48186	0.106	0.162	0.731	0.001
48190	0.277	0.534	0.189	0.000
48192	0.549	0.420	0.031	0.000

TABLE 7-8: F-values for test for equality of group means. The degrees of freedom are (7,58). Seven variables are used (listed in table 7-5)

Group	299	296	297	295
299	0			
296	0.77	0		
297	9.00	10.18	0	
295	22.53	29.30	8.90	0

Discriminant analyses results using the FULL data set did not reveal any clear structures. This indicated that some of the ratios introduced act as new important discriminators. This was due to good correlations within some groups (e.g. Zr/U in 295 (and 297), Mn/Fe in 299 and 296).

A plot of the canonical variates and the coefficients of the variables in the computation of the canonical variables can be seen in figure 7-3. The following remarks can be made:

1) The larger difference between 297 and 295 than between 296 and 299 is easily recognized.

2) Arfvedsonite lujavrite (299+296) is characterized by a high value of Zr2.

3) Naujakasite lujavrite (295+297) is characterized by a high value of Zr2/U1.

4) Both 297 and 296 (villiaumite-containing) are characterized by a relatively high value of Na6.

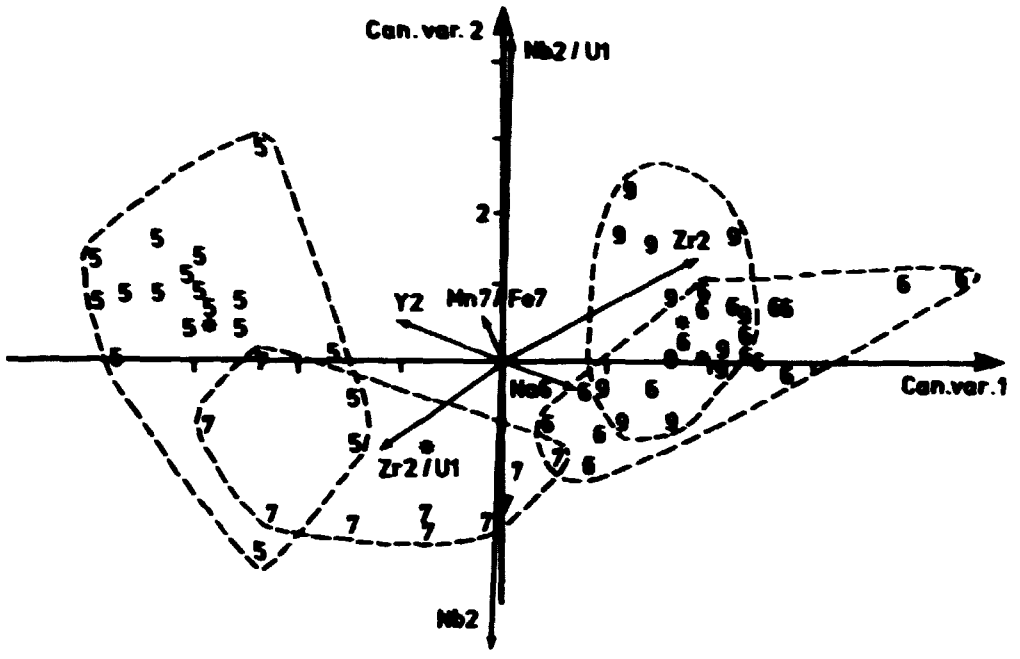

FIGURE 7-3: Plot of canonical variates and coefficients for each variable in the computation of each canonical variable. Group means are indicated by *, group members by the last digit in their geological code. The coefficient vectors are scaled with the standard deviation of the variable.

7.3 Summary remarks

The most important mineralogical differences between naujakasite lujavrite and arfvedsonite lujavrite are (sec. 2.3):

A) Naujakasite lujavrite contains naujakasite but never eudialyte (Zr-silicate) as a main constituent.

B) Eudialyte is often found in arfvedsonite lujavrite as a main constituent or as an accessory mineral. If eudialyte is the main constituent steenstrupine is generally not present (≃low uranium).

C) A greater number of accessory minerals is generally found in arfvedsonite lujavrite than in naujakasite lujavrite.

D) Within both types the presence or absence of villiaumite (NaF) is possible.

On the basis of these observations it had been expected that a multivariate analysis of the trace elements could reveal the geological structure to some extent. The analysis showed that a clear distinction can be made between the two lujavrite types both by cluster and discriminant analysis. In all cases the non-hierarchical (k-mean) cluster analysis was the most appropriate. Classification within the lujavrite types was unclear, but the group 295 appears to be consistently different from all other groups.

A number of mis-labelled samples from drill hole 48 were discovered during the cluster analysis. The a posteriori probabilities produced by the stepwise discriminant analysis showed that a continuous transition between the two lujavrite types might be present in the drill hole.

Both the F-test and the canonical plot indicate that there must be other differences between 295 and 297 than the presence or absence of NaF. The importance of Zr2 and Zr2/U in the discrimination reflect the above mentioned mineralogical differences.

8 CONCLUSION

Before summarising the work described in this thesis it may be as well to reiterate its aims. The purpose of the study was to collect and study different sets of spatially distributed data available from the Kvanefjeld uranium deposit in order to: a) establish a database containing all the information from drill holes, b) study the uranium and thorium values in the different types of sample by means of Regionalised Variable Theory and c) make global geostatistical estimates of the uranium reserves. To this end the mineralised area was divided into two parts, the Mine area and the Northern area, and two techniques were considered: a global approach to give overall estimates of grade and tonnage for the deposit and to determine the level of confidence for these figures, and a local approach in which different estimation methods were tested and discussed. Uranium values from drill core samples (assays and logs), chip samples taken in the Kvanefjeld tunnel and data from gamma-spectrometric surveys carried out on the surface exposures and in the tunnel were included in the study. The present chapter summarises the conclusions from each study and draws together the different threads.

In chapter 3 the data and the coordinate systems were described. It was noted that both the analytical values and the spatial location of samples were subject to errors. The contribution from these sources of error to the total error made when global ore reserve figures are established have been proven to be small compared with other factors. However, for local studies they are of major importance.

The uranium values from drill cores were studied in chapter 4. In producing classical summary statistics, including histograms and least-squares fits to the distributions, it was found that:

1) The histograms of the total sample sets originating from the Mine area and the Northern area reflected complex, multi-modal distributions which were difficult to inter-

pret. Artificial distributions, comprising two or three components, fitted to the histograms gave no clear explanation of the individual components of the histograms. As demonstrated, however, they can be used to make reliable global grade and tonnage estimates by considering the volume-variance relationship.

2) The distributions of uranium in the individual lujavrite types could be described by simple distributions. Both types of fine-grained lujavrites, naujakasite lujavrite and arfvedsonite lujavrite, appeared to be normally distributed about the same mean value. The standard deviations differed, indicating that arfvedsonite lujavrite should be a more inhomogeneous unit than naujakasite lujavrite. In chapter 7 both discriminant and cluster analyses showed that, although the mean grades of uranium were equal, a clear distinction between the two rock types could be made if other elements were considered in addition. The study also showed that naujakasite lujavrite is a more inhomogeneous unit than arfvedsonite lujavrite, which indicates that uranium itself is a poor discriminator between these two units. The histogram of the third lujavrite type, mc-lujavrite, was described by a log-normal distribution. Apart from this, it deviated from the fine-grained lujavrites by having a significantly higher coefficient of variation.

3) The histograms of the total sample sets from the two areas differed basically in the fact that the Mine area represented both a higher mean (35%) and a higher standard deviation (22%). The uranium in all the fine-grained lujavrites from the Mine area could be described by a uni-modal, probably normal, distribution whereas the Northern area displayed a distinctly bimodal distribution for these sample types. The lowest mode in this distribution can, according to the geologists, only be explained by the presence of low-grade samples in the uppermost part of drill cores near the north-western contact.

The spatial correlation was studied by experimental semi-variograms calculated along each of the (almost vertical) drill holes. These were later averaged to form overall semi-variograms. Usable semi-variograms could not be established horizontally, i.e. between-the-boreholes, since the drill hole spacing exceeded the range of influence. Neither could semi-variograms of the individual lujavrite types be calculated, probably because there were too few samples scattered over the whole deposit. The semi-variograms based on total data sets were, however, found to be stable even if more than 50% of the samples were randomly removed from the data set. It was therefore concluded that enough samples were available for the study of the spatial correlation.

A summary of the study of the spatial correlation is given in table 8-1. The table includes results from drill core samples as well as from tunnel chip samples and the surface data. The following conclusions may be drawn:

1) The spatial structure of the uranium values is complex, hence reflecting the geology. Three spherical structures can be recognized in the spatial behaviour of the uranium values. These can be characterised as a) a small scale structure (range of influence a = 2.5-6.5 metres), b) a medium scale structure (a = 20-40 metres) and c) a large scale structure (a = 105-150 metres). It was found that the small scale structure is probably due to micro-structures in mc-lujavrite. However, the xenoliths also contribute to this structure. The medium scale structure is an important feature primarily of the fine-grained lujavrites, whereas the long range structure seems to be a global phenomenon.

2) When 'small' samples are considered high nugget effects are always present, in some cases representing almost half of the total variation. The nugget effects discovered in the surface data and logging data were considerably lower than in the other types of sample because of the increased sample volume. The difference in total sill value between

TABLE 8-1: Summary of spatial correlation study. The table gives values of nugget effect and total sill in ppm U^2, and ranges of influence of the different spherical components in metres. Numbers in bracets give the percentage of the total sill for the particular variance component. †) Have been estimated by the eye.

AREA	DIRECTION	C_o	a_1	a_2	a_3	TOTAL SILL
Total sample set:						
Mine area	V	5600(16)	2.5(49)	29(35)	-	34530
Northern area	V	3300(13)	6.5(7)	15(16)	124(64)	24'30
Logging data	V	1000(5)	5.0(19)	20(15)	105(61)	22400
Chip samples, tunnel	'N-S'	5500(44)	6.0(10)	24(46)	-	13000
Surface data, overall	H	600(6)	-	30(19)	120(75)	9800
Surface data	E-W	700(7)	-	30(15)	150(78)	9600
Surface data	N-S	600(6)	-	65(72)	120(22)	11000
Fine-grained lujavrites:						
Northern area	V	2800(25)	-	20(10)	105(65)	11500
Chip samples, tunnel	'N-S'	4600(50)	-	24(50)	-	9400
Surface data †	E-W	1000(13)	-	-	150(87)	8000
Surface data †	N-S	800(11)	-	40(20)	150(69)	7000

the different sample sets reflect the degree of homogeneity of the mineralisation in a particular area. Because of its geology the Mine area displays a much more erratic uranium variation, with a higher sill value, than the Northern area. The chip samples in the tunnel display an even lower sill value, mainly because 80% of the samples were taken in naujakasite lujavrite.

3) Spatial anisotropy was detected in the surface data when the E-W and the N-S directions were compared. This can probably be explained by the direction of the lujavrite propagation, concentration of uranium along the northern contact and perhaps by a weathering phenomenon which affected the xenoliths.

4) No significant anisotropy was detected between the horizontal and the vertical directions. This gives credence to the 3-dimensional block-by-block estimations which were done using a vertical model.

5) The nugget effect mainly represents microstructures in the mineralisation rather than sampling or analytical errors. However, sampling and analytical errors contribute to its magnitude.

6) Although the geology at Kvanefjeld is different from other common uranium occurrences the uranium spatial variation shows many similarities to structures reported from other such deposits. Multi-component spherical schemes and high nugget effects appear to occur frequently in uranium mineralisations.

7) As a rule of thumb, an optimal sampling interval is given as 0.9 times the range of influence. Because of the composite models found it is difficult to define one optimal distance at Kvanefjeld. It is believed that most attention should be paid to the intermediate structure (table 8-1) because of its importance in the fine-grained lujavrites. Accepting this, a recommended sampling interval, i.e. drill hole spacing, in the Mine area is approx. 25 metres. In the Northern area a larger interval can be accepted, perhaps 50 metres. The drill hole spacing is at present approx. 50 and 140 metres respectively in the two areas.

Having examined the spatial correlations and established models for them by a trial-and-error procedure, these were then used in the geostatistical estimator named kriging. In chapter 6 comparisons between stationary (simple) kriging and non-sta-

tiona.y (universal) kriging showed that drift need not be considered, i.e. the second-order stationarity of simple kriging seemed to be fulfilled. Point kriging of drill core samples in the Mine area showed that an overall model could be used to obtain reliable local estimates. On the other hand, measures of the estimation error (the kriging standard error) tended to be too pessimistic if an overall, rather than a local, model was used. An equivalent result was obtained in chapter 5 when the batch samples of excavated material were estimated using either an overall or a 'fine-grained lujavrite' semi-variogram model.

Estimation of the global reserves was done by a 3-dimensional kriging procedure which included samples inside and outside the block. Random stratified grids were fitted to the individual drilling patterns with block sizes 50 by 50 m in the Mine area and 140 by 140 m in the Northern area. Different bench heights were tested. Studies of the effects of the block size and bench height on the grade-tonnage values showed that, if a cutoff value greater than the the mean value of the total volume was selected, small blocks produced high uranium tonnages estimated with high errors and vice versa. This fundamental result can be explained by the so-called volume-variance relationship. It is obvious that small volumes are more difficult to estimate than large volumes. Large blocks contain high internal variations whereas small blocks contain less variation. This was clearly demonstrated by the studies in the tunnel, where 1-dimensional (point), 2-dimensional (panel) and 3-dimensional (block) kriging were compared. Estimating many small blocks gave a histogram of block values with a higher variance than large blocks. If the histogram was truncated at a value higher than the mean value, this variance effect would influence the resulting metal tonnage. A possible cutoff value at Kvanefjeld is 250 ppm uranium. In the Mine area this value lies close to the average value within the area. The block size is therefore of minor importance, as differences in block variances are not detected. In practice, geostatistical estimation in the Mine area produced grade/tonnage figures which, probably due to the above considerations, were comparable with estimates obtained by conventional methods. Surprisingly, this result was obtained

even though quite different block sizes, ore volumes and estimation techniques were used. Disregarding the estimation error, block kriging gave a uranium tonnage of approx. 10025 tons with a mean grade of 304 ppm U (cutoff 250 ppm U). This corresponded to an 'ore' tonnage of 32.9 million tons. As blocks were not estimated independently, confidence intervals for the total uranium tonnage could not be established. However, the level of confidence can be expressed by the mean kriging standard error of the individual blocks - in the Mine area equal to 58.1 ppm U. An average 95% confidence interval for a single (50x50x10 m) block estimate is therefore $\pm$116.2 ppm U. Consequently very few blocks have grades above, say, a 250 ppm cutoff value if a high-level confidence criterion is applied. To narrow this interval a much denser sampling pattern is required. But as was demonstrated estimation in the Mine area will always be subject to high errors, even at very small scales. This can be explained by the poor spatial correlation in this area.

In the Northern area conventional estimates of grade and tonnage were not confirmed by geostatistics. Again it was found that the volume-variance relationship could be used to explain the deviations. The estimation of the uranium tonnage by conventional methods was done by adding slices of size approx. 140x140x1 metres. The grade value of the individual slice was assumed to be equal to the sample value in the intersecting drill core. Hence, the resulting histogram of block values on which cutoff selection was based was identical to the histogram of the drill core values. It is therefore emphasised that tonnage figures obtained from this histogram will be true only if selection is based on volumes of one-metre drill core samples. Of course, this is an unrealistic approach.

Overall kriging in the Northern area showed that block estimates tend to be smoothed out, resulting in grade values near to the mean value of the area. This was probably due to:

1) The extremely large blocks which had to be used in order a) to fit the sparse drilling pattern and b) to avoid increasing the errors of estimation.

2) Too many remote samples being included in kriging calculations. Some of these might comprise low-grade xenolithic material.

Estimation of smaller blocks by including samples above and below the bench did in fact improve the results slightly. However, because of the strong smoothing effect it was decided to do block estimation selectively. In this way blocks of lujavritic material were estimated by using only lujavrite samples in the kriging procedure and the spatial correlation between these samples. Using a block size of 140x140x10 metres produced an 'ore' tonnage of 46.6 mill. tons with a mean grade of 291 ppm U (cutoff 250 ppm U). This corresponded to a uranium tonnage of 13560 tons. An average 95% confidence interval for individual block estimates was $\pm$75 ppm U, i.e. significantly lower than in the Mine area. These figures are considerably lower than those produced by conventional methods. On the other hand, they are believed to represent the most accurate figures which, as yet, can be established from the information available.

The reserves estimated for the total deposit (cutoff 250 ppm U), excluding areas of possible additional reserves, was therefore 79.5 mill. tons of 'ore' with a mean grade of 297 ppm U corresponding to a uranium tonnage of 23600 tons. The figures for the global reserves lead to the following conclusions:

1) The <u>total</u> 'ore' reserves at Kvanefjeld were virtually confirmed by the geostatistical study, except that the reserves in the Mine area were estimated to be much larger than had previously been believed (lower cutoff value). This result, indicating the importance of this area, was confirmed by the uranium profile in that part of the tunnel which cuts the area.

2) The <u>total</u> uranium tonnage was estimated to be 13% lower than the tonnages indicated by the conventional methods.

3) The average grade above cutoff was estimated to be almost 50 ppm, i.e. 14%, lower than that forecast by conventional methods. In practice this would mean a daily 14% reduction in the rate at uranium which can be produced.

As stated earlier, it is recommended that the amount of sample information is increased considerably. Studies of the kriging weights from global estimates showed that for very large blocks estimated on thin benches some samples outside the block contain more information about the block than the sample(s) inside the block. If smaller blocks could be estimated from a dense sampling pattern, as was done in the tunnel, this problem could certainly be solved. The use of the logging data indicated that every metre of core should be analysed rather than every second metre. Because of the additional sample values in the log data, block values had a higher variance than the assay blocks and hence produced higher and probably truer uranium tonnages. It is believed that the additional cost of analysing every metre of core is small compared with drilling costs.

The use of georegression to correct for the regression effect on block values indicated that the grade-tonnage curves at Kvanefjeld, especially in the Mine area, will always be somewhat biased. This is due to the erratic mineralisation, i.e. to high nugget effects. The bias is important at high cutoffs but can be met by estimating small blocks from sample values affected by only small analytical errors.

In chapter 5 local estimation within the Kvanefjeld tunnel was described. Furthermore, it was demonstrated that sampling programmes can be improved by taking into account the spatial correlation when the sampling method and the sampling interval are determined. From the estimation studies of the batch samples of excavated material the following conclusions may be drawn:

1) Because of the dense sampling pattern batch samples were estimated with acceptably small errors, using 3-dimensional kriging. An average 95% confidence interval for batch estimates was $\pm$15-23 ppm U, depending on the semi-variogram model used.

2) A comparison of conventional and geostatistical methods showed that local estimates made by these methods hardly differ on average. However, the errors of estimation were

very much higher with the conventional methods than with kriging. Kriging is therefore preferable.

3) Based on the magnitudes of estimation errors the optimal search area was found to be one block on each side of the block being estimated. Samples outside the block received very small, or even negative, kriging weights. This is another example which clearly demonstrates how kriging handles a short range of influence and a large nugget effect.

4) Comparisons between geostatistical estimates and gamma-spectrometric measures of uranium grades in batch samples and at points along part of the tunnel showed a remarkable coincidence. It was emphasised that gamma-spectrometer measures were biased, producing values about 30 ppm too high. An orthogonal regression relationship was established to correct for this bias.

5) It was noted that kriging used approx. 25% more computing time than the conventional methods. This, compared with the reduction in estimation error, is regarded as a little but worth-while additional cost.

6) The uranium profile in the tunnel was estimated from the drill hole samples by using an inverse distance technique. This profile appeared to be far from reality when it was compared with the actual values in the batch samples. Estimating local grades from remote samples was obviously meaningless.

7) Based on the chip sample values the total amount of uranium in the bulk sample shipped to RISØ was estimated at 2043 kilogrammes.

Local estimation on 'points' was used in chapter 6 in order to investigate the effect of drift, if any, and to fit the best model to the experimental semi-variogram. It has been mentioned that no drift was detected. The testing of different models showed that the model which gave the poorest visual fit, actu-

ally produced the lowest mean squared errors. This was probably due to a good fit over the important part of the semi-variogram, i.e. the part near the origin. The advantage of using point kriging for model selection has therefore been demonstrated.

In chapter 7 different multi-variate techniques were used to classify a set of selected lujavrite samples. The analysis showed that a clear distinction can be made between naujakasite lujavrite and arfvedsonite lujavrite, based on their trace element content. Classification within the lujavrite types was difficult, but naujakasite lujavrite without villiaumite seemed to form a group consistently different from all other groups. Some of the variables discovered to be important classifiers could be related directly to known mineralogical differences. The a posterior probabilities of a number of mis-classified samples from drill hole 48 indicated that continuous transitions might exist between the two lujavrite types. This is, of course important in understanding the genesis of the deposit.

It is believed that the present study has contributed to a more realistic estimate of the global uranium reserves. Because of the spatial correlations determined it is possible to understand why ore reserve estimation at Kvanefjeld always will be subject to relatively high errors. However, geostatistics has been proved to work well on this deposit and many useful results have been obtained for the understanding of the mineralisation.

ACKNOWLEDGEMENT

Many people and institutions contributed to the preparation and completion of this work. I am much indebted to geologist Bjarne Leth Nielsen, formerly Head of the Section of Economic Geology at the Geological Survey of Greenland, who gave me the idea for and opportunity to carry out the study. I am also much indebted to engineer Leif Løvborg and his staff at the National Laboratory RISØ who spent much time producing and supplying most of the analytical data and who have shown such great interest in my work. I am grateful to my two instructors, Dr. Sven Karup-Møller of the Department of Mineral Industry and to lecturer Knut Conradsen of the Department of Mathematical Statistics and Operations Research, for their interest and helpful advice; to engineer Bjarne Lund Olesen who provided many valuable discussions and who critically went through the manuscript, and to my MSc student Christian Ahlefeldt-Laurvig for his patient and careful computational work.

Special thanks are due to geologist Per Nyegaard who followed the work with special interest and from whom I have learned much about the geology of the Kvanefjeld area. He also contributed to the planning of the tunnel sampling programme. Thanks are also due to engineer Poul Frederiksen and his staff at the Department of Surveying and Photogrammetry for their help with the contour mapping.

I am specially grateful to Dr. Isobel Clark of the Royal School of Mines, London and to lecturer A.G. Royle of the University of Leeds, who taught me all I know about geostatistics and who provided most of the geostatistical computer programs. They never showed when they were getting bored with my questions. Bon Royle did a tremendous job of plodding through the manuscript and made invaluable suggestions for improvements to both the text and the English language. Acknowledgements are due to the staff at the computing centre NEUCC who were always at hand to solve my computational problems. I am thankful to secretary Else Knudsen who typed most of the manuscript.

This research was financed by grants from the Technical University of Denmark. Funds to cover travel expenses and for buying computer programs were provided by the Danish Ministry for Commerce and by the Danish Technical Science Research Council. This financial support is gratefully acknowledged.

The author wishes to thank the Geological Survey of Greenland for their permission to use the data and to publish the results. Any shortcomings and inaccuracies in the text rest with me.

LIST OF REFERENCES

AGTERBERG, F.P. (1968): Application of trend analysis in the evaluation of the Whalesback mine, Newfoundland, In: Ore Reserve estimation and Grade Control, Can. Inst. Min. Metall. sp. vol.9, pp 77-88.

AHLEFELDT LAURVIG, C.W. (1981): En geostatistisk undersøgelse af uranværdier i nogle rumligt fordelte observationer i Kvanefjeldet, Sydgrønland, MSc thesis (unpubl.) Dept. Mineral Industry, Tech. Univ. Denmark, 108 pp + appendix.

ALLDREDGE, J.R. and ALLDREDGE, N.G. (1978): Geostatistics : a Bibliography. Int. Stat. Rev., 46, pp 77-88.

ASMUND, G. (1971): Chemistry and kinetics of the sulphating roasting of uranium-bearing silicates. RISØ Nat. Lab. Rep., 253, 125 pp.

BELL, G.D. and REEVES, M. (1979): Kriging and geostatics: A review of the literature available in English. Proc. Australas. Inst. Min. Metall. No 269, pp 17-27.

BLAIS, R.A. and CARLIER, P.A. (1968): Applications of geostatistics in ore evaluation. CIM spec. vol. 9, pp 41-68.

BLAXLAND, A.B., VAN BREEMEN, O. and STEENFELD, A. (1976): Age and origin of the major syenite centers in the Gardar province of South Greenland: Rb-Sr studies. Geol. Soc. Am. Bull. 89, pp 231- 244.

BOHSE, H., BROOKS, C.K. and KUNZENDORF, H. (1971): Field observations on the kakortokites of the Ilímaussaq intrusion, South Greenland. Rapp. Grønlands geol. Unders. 38, 43 pp.

CLARK, I. (1976): Some auxiliary functions for the spherical model of geostatistics. Comp. and Geosc., 1, pp. 255-263.

CLARK, I. (1977a): ROKE - a computer program for non-linear Least Squares decomposition of mixtures of distributions, Comp. and Geosc., 3, pp 245-256.

CLARK, I. (1977b): Regularization of a semi-variogram. Comp. and Geosci., 3, pp 341-346.

CLARK, I. (1977c): Practical kriging in three dimensions. Comp. and Geosci., 3 pp 173-180.

CLARK, I. (1978): Geostatistical reserve estimation in Cornish tin mining. PhD thesis, Dept. Mineral Resources Eng. Imperial College, London 260 pp + appendix.

CLARK, I. (1979a): Practical geostatistics. Applied Science Publ., London, 129 pp.

CLARK, I. (1979b): GSTOKOS - user documentation. Dept. Mineral Resources Eng. Imperial College, London, 17 pp.

CLARK, I. (1979c): GSTOKOS - technical documentation. The Geostokos partnership, London, 26pp.

CLARK, I. (1979d): Does geostatistics work? APCOM 79, 16th Int. Symp. on the application of computers and operations research in the Mineral Industries, Tucson, Arizona, American Inst. Min. Metall., pp 213-225.

CLARK, I. (1979e): The semi-variogram - Part 1. 'Geostatistics: Part 2 of a series'. Eng. Min. Jour., July, pp 90-94.

CLARK, I. (1979f): The semi-variogram - Part 2. 'Geostatistics: Part 3 of a series'. Eng. Min. Jour., August, pp 92-97.

CLARK, I. (1980: in press): Geostatistical interpolation - kriging without smoothing. Paper presented at Congres Geologique Internationale, 26e sess., sec. 12 (Mathematical Geology and Geological information scie.) Paris, France, July 7th-17th, 17 pp.

CLARK, I. and GARNETT, R.H.T. (1974): Identification of multiple mineralisation phases by statistical methods, Trans. Inst. Min. Metall., 83, no. 809, pp A43-A52.

CLARK, I. and CLAUSEN, F.L. (1981): Simple alternative to disjunctive kriging. Trans. Inst. Min. Metall. (Sec A: Min. industry), 90, pp A13-A24.

CLARK, M.W. (1976): Some methods for statistical analysis of multimodal distributions and their application to grain size data, Math. Geol., 8, pp 267-282.

CLAUSEN, F.L. (1979): Forslag til udtagning af prøvemalm fra minegang under Kvanefjeldet og Kvanefjeldsplateauet. Internal report. Dept. Mineral Industry. Tech. Univ. Denmark, 20 pp.

CLAUSEN, F.L. (1980a): KVANE - A Kvanefjeld Drill core database. RISØ Nat. Lab. Rep-M-2210, 18 pp.

CLAUSEN, F.L. (1980b): Forslag til prøvetagningsprogram i tunnel under Kvanefjeldet og Kvanefjeldsplateauet (revideret udkast). Internal report. Dept. Mineral Indust. Tech. Univ. Denmark, 8 pp.

CLAUSEN, F.L. (1980c): Using Universal kriging for automatic contouring. Descriptions of programs PTUK and CONTOUR. IMSOR. Dept. of Mathematical Statistics and Operations Research. Tech. Univ. Denmark, 29 pp.

CLAUSEN, F.L. (1981): Geostatistical ore reserve estimation at Kvanefjeld uranium deposit - South Greenland. Presented at 'Symp. on Applied Statistics' held at Tech. Univ. Denmark, January 21st to 23rd, 1981, Proceedings pp 283-313.

CLAUSEN, F.L. and HARPØTH, O (in press): On the use of discriminant analysis techniques for classifying chemical data from panned heavy-mineral concentrates - central East Greenland. Journ. Geoch. Expl.

CLAUSEN, F.L., NYEGAARD, P.L. and AHLEFELDT LAURVIG, C.W. (in prep.): The distribution of uranium and thorium in the Kvanefjeld tunnel - A geological and geostatistical approach.

CONRADSEN, K., KNUDSEN, J.G., LARSEN, M. and SCHØNWANDT, H.K. (1976): Multivariate statistical methods as a tool in the interpretation of heavy-mineral data. A case study on statistical pattern recognition of earth data. Presented at the 14th International Symposium on the Application of Computer Methods in the Mining Industries. The Pennsylvania State Univ. 13 pp.

CONRADSEN, K. and CLAUSEN, F.L. (1981): Classification and clustering of some drill core samples from Kvanefjeld - South Greenland. Presented at 'Symp. on Applied Statistics' held at Tech. Univ. Denmark, January 21st to 23rd, 1981, Proceedings pp 339-361.

CONRADSEN, K., CLAUSEN, F.L. and NYEGAARD, P. (in prep.): Classification and Clustering of lujavrite drill core samples from Kvanefjeld, the Ilimaussaq intrusion, South Greenland.

DAVID, M. (1976): The practice of kriging. In: M. Guarascio, M. David and C. Huijbregts, (Eds.), Advanced geostatistics in the mining industry; D. Reidel Publ. Co., Dordrecht, pp 31-48.

DAVID, M. (1977): Geostatistical ore reserve estimation, Elsevier, Amsterdam, 364 pp.

DAVID, M., DOWD, P.L. and KOROBOV,S. (1974): Forecasting departure from planning in open-pit design and grade control. APCOM 74, 12th Int. Symp. on the application of computers and operations research in the Mineral Industries, Colorado School of Mines, Golden, Co., vol 2, pp F131-149.

DAVIS, J.C. (1973): Statistics and data analysis in geology. John Wiley and Sons Inc., New York, 550 pp.

DELHOMME, I.P. and DELFINER, P. (1973): Application du krigeage á l'optimisation d'une campagne pluviométrique en zone aride. Symposium on the Design of Water Resources Projects with Inadequate Data, 1973, UNESCO-WHO-IAHS, Madrid, Spain, pp 191-210.

DIXON, W.J. and BROWN, M.B. (eds.) (1979): Biomedical Computer Programs, P-series. University of California Press, Berkeley, 88o pp.

EMELEUS, C.H. and UPTON, B.G.L. (1976): The Gardar Period in Southern Greenland. In: Escher A. and Watt W.S. (eds.), Geology of Greenland. Geological Survey of Greenland, Copenhagen, pp 153-81.

ENGELL, J. (1973): A closed system crystal-fractionation model for the agpaitic Ilímaussaq intrusion, South Greenland with special reference to the lujavrites. Bull. Geol. Soc. Denmark, 22, pp 334-362.

FERGUSON, J. (1964): Geology of the Ilímaussaq alkaline intrusion, South Greenland. Bull. Grønlands geol. Unders. 39, (also Meddr. Grønland 172, 4) 82 pp.

FERGUSON, J. (1970a): The differentiation of agpaitic magmas: The Ilímaussaq intrusion, South Greenland, Can. Miner. 10, pp 335-349.

FERGUSON, J. (1970b): The significance of the kakortokite in the evolution of the Ilímaussaq intrusion, South Greenland. Bull. Grønlands geol. Unders. 89 (also Meddr. Grønland 190,1) 193 pp.

GAMBORG-HANSEN, J.K. (1977): Sulphatising roasting of a Greenlandic uranium ore, reactivity of minerals and recovery. RISØ Nat. Lab. Rep. 355.

GUARASCIO, M. (1976): Improving the uranium deposits estimations (the Novazza case). In: M. Guarascio, M. David and C. Huijbregts,(Eds.), Advanced geostatistics in the mining industry: D. Reidel Publ. Co., Dordrecht, pp. 351-376.

HAMILTON, E.I. (1964): The geochemistry of the northern part of the Ilímaussaq intrusion, S.W. Greenland. Bull. Grønlands geol. Unders. 42 (also Meddr. Grønland 162,10), 104 pp.

HAWKINS, D.M. and RASMUSSEN, S.E. (1973): Use of discriminant analyses for classification of strata in sedimentary successions. Jour. Math. Geology, 5, pp 163-177.

HELWIG, J.T. and COUNCIL, K.A. (eds.) (1979): SAS users guide, 1979 edition. SAS Inst. Inc. Raleigh, North Carolina. 494 pp.

HOWARTH, R.J. (1971): Empirical discriminant classification of regional stream-sediment geochemistry in Devon and East Cornwall. Trans. Inst. Min. Metall. London, 80,pp B142-149.

JOURNEL, A. (1969): Rapport d'études sur l'estimation d'une variable regionalisée. Application à la cartographie automatique. Ecole des Mines de Paris. Dept. Geostatistique, Centre de Morphol. Math., Fontainebleau, 87 pp.

JOURNEL, A.G. (1973) Geostatistics and sequential exploration. Min. Eng., 25, pp 44-48.

JOURNEL, A.G. and HUIJBREGTS, C.J. (1978): Mining Geostatistics. Academic Press, London, New York, San Fransisco, 600 pp.

JØRGART, T. (1977): Neutronaktiveringsanalyse af geologisk materiale. Dansk geol. Foren., Årsskrift for 1976, København, pp 23-27.

KENNEDY, J.B. and NEVILLE, A.M. (1976): Basic statistical methods for engineers and scientists, 2nd ed. Harper and Row, New York, 353 pp.

KIM, Y.C. and KNUDSEN, H.P. (1977): Geostatistical ore reserve estimation for a roll-front type uranium deposit (Practitioners' guide). U.S. energy research and development adm Grand Junction, Colorado 81501, U.S.A. 61 pp + appendix.

KNUDSEN, H.P. and KIM, Y.C. (1978): A short course on geostatistical ore reserve estimation. Dept. Mining and Geological Eng., College of Mines, Univ. Arizona, 224 pp + appendix.

KNUDSEN, H.P., KIM, Y.C. and MUELLER,C. (1978): Comparative study of the geostatistical ore reserve estimation method over the conventional methods. Min. Eng., January, pp 54-58.

KRIGE, D.G. (1951): A statistical approach to some basic mine valuation problems on the Witwatersrand. J. chem. metall. *Soc. S. Afr. 52, pp 119-139.*

KRIGE, D.G. (1959): A study of the relationship between development values and recovery grades on the South African goldfields. J. S. Afr. Inst. Min. Metall., 59, pp 317-331.

KRIGE, D.G. (1966): Ore value trend surfaces for the South African gold mines, based on a weighted moving average. APCOM 66, 6th. Int. Symp. on the application of computers and operations research in the Mineral Industries, Pennsylvania State Univ., Univ. Park, Pa., Vol 1, pp G1-29

KUNZENDORF, H., NYEGAARD, P.L. and NIELSEN, B.L. (in prep.): The distribution of characteristic elements in the radioactive rocks of the northern part of Kvanefjeld, South Greenland.

LØVBORG, L. (1972): Assessment of uranium by gamma-ray spectrometry. In: Bowie, S.H.U., Davis, M and Ostle, D. (eds). Uranium prospecting handbook, London, Inst. Min. Metall, pp 157-173.

LØVBORG, L., KUNZENDORF, H. and HANSEN, J. (1968): Use of field gamma-spectrometry in the exploration of uranium and thorium deposits in South Greenland. Nuclear Techniques and Mineral Resources IAEA, Vienna, pp 197-211.

LØVBORG, L., WOLLENBERG, H., SØRENSEN, P. and HANSEN, J. (1971): Field determination of uranium and thorium by gamma-ray spectrometry exemplified by measurements in the Ilímaussaq alkaline intrusion, South Greenland. Econ. Geol. 66, pp 368-384.

LØVBORG, L., WOLLENBERG, H., ROSE-HANSEN, J and NIELSEN, B.L. (1972): Drill core scanning for radioelements by gamma-ray spectrometry. Geophysics, vol. 37, No. 4, pp 675-693.

LØVBORG, L., BØTTER-JENSEN, L. and KIRKEGAARD, P. (1978): Experiences with concrete calibration sources for radiometric field instruments: Geophysics, vol. 43, pp 543-549.

LØVBORG, L., BØTTER-JENSEN, L., KIRKEGAARD, P. and CHRISTIANSEN, E.M. (1979): Monitoring of natural soil radioactivity with portable gamma-ray spectrometers: Nucl. Instr. and Meth. 167, pp 341-348.

LØVBORG, L., NYEGAARD, P., CHRISTIANSEN, E.M. and NIELSEN, B.L. (1980a): Borehole logging for uranium by gamma-ray spectrometry. Geophysics, vol. 45, No.6, pp 1077-1090.

LØVBORG, L., BØTTER-JENSEN, L., CHRISTIANSEN, E.M. and NIELSEN, B.L. (1980b): Gamma-ray measurements in an area of high natural radioactivity: The National Radiation Environment III (DOE, Springfield, Va.) (CONF-780422), vol.2, pp 912-926.

MAKOVICKY, M., MAKOVICKY, E., NIELSEN, B.L., KARUP-MØLLER, S. and SØRENSEN, E. (1980): Mineralogical, radiographic and uranium leaching studies on the uranium ore from Kvanefjeld, Ilímaussaq complex, South Greenland. RISØ Nat. Lab. Rep-R-416, 186 pp.

MAKOVICKY, M. and KARUP-MØLLER, S. (1981): Crystalline steenstrupine from Tunugdliarfik in the Ilímaussaq alkaline intrusion, South Greenland. N. Jb. Miner. Abh., 140, 3, pp 300-330.

MARECHAL, A. (1976): Selecting minable blocks; experimental results observed on a simulated ore body. In: M. Guarascio, M. David and C. Huijbregts (Eds.), Advanced geostatistics in the mining industry, D. Reidel Publ. Co., Dordrecht, pp 137-161.

MARECHAL, A. and SHRIVASTAVA, P. (1977): Geostatistical study of a Lower Proterozoic iron orebody in the Pilbara region of Western Australia. APCOM 77. 15th Int. Symp. on the application of computers and operations research in the Mineral Industry, Brisbane, Australia, pp 221-230.

MATHERON, G. (1963): Principles of geostatistics. Econ. Geol. vol. 58, pp 1246-1266.

MATHERON, G. (1969): Le krigeage Universel. Cah. Centre de Morphologie Mathematique de Fontainebleau, No. 1, 83 pp.

MATHERON, G. (1971): The theory of regionalized variables and its applications, Cahier E, Centre de Morphologie Mathematique de Fontainebleau, No. 5, 211 pp.

MATHERON, G. (1976): A simple substitute for conditional expectation: disjunctive kriging. In: M. Guarascio, M. David and C. Huijbregts (Eds.), D. Reidel Publ. Co., Dordrecht, pp 221-236.

NIELSEN, B.L. (1977): Uran i Kvanefjeld. Varv, 4, pp 122-125.

NIELSEN, B.L. (1980): The exploration history of the Kvanefjeld uranium deposit, the Ilímaussaq intrusion, South Greenland. Presented at: 'Case histories of uranium exploration', A NEA/IAEA Advisory Group Meeting, Vienna, Nov. 26th to 30th, 1979.

NIELSEN, B.L. and STEENFELT, A. (1978): Intrusive events at Kvanefjeld in the Ilímaussaq igneous complex. Bull. Geol. Soc. Denmark, vol. 27, pp 143-155.

NYEGAARD, P.L. (1979): Evaluation of uranium deposit at Kvanefjeld. Internal Report. Geol. Surv. Greenland. Manuscript, 39 pp + appendix.

NYEGAARD, P.L. (1980a): Uranudvindingsprojektet. Geologisk arbejde i Kvanefjeld tunnelen 1979/80. Internal Report. Geol. Surv. Greenland. Manuscript 19 pp + figures and tables.

NYEGAARD, P.L. (1980b): Geologisk kort over Kvanefjeld tunnelen, 1:100. Internal Report. Geol. Surv. Greenland.

NYEGAARD, P.L., NIELSEN, B.L., LØVBORG, L. and SØRENSEN, P. (1977): Kvanefjeld uranium project drilling programme 1977. Internal Report. Geol. Surv. Greenland. Manuscript, 46 pp + tables and figures.

ROYLE, A.G. (1980): Estimating global ore reserves in a single deposit. Min. Sci. Eng., Vol. 12, No. 1, pp 37-50.

ROYLE, A.G. and NEWTON, M.J. (1972): Mathematical models, sample sets and ore-reserve estimation. Trans. Inst. Min. Metall. (Sect. A: Min. industry), 81 pp A121-A128.

ROYLE, A.G., CLAUSEN, F.L. and FREDERIKSEN, P. (1981): Practical Universal kriging and automatic contouring. Geo-Proc., 1, pp 377-394.

SANDEFUR, R.L. and GRANT, D.C. (1980): Applying geostatistics to roll front uranium in Wyoming. 'Geostatistics: Part 8 of a series.' Eng. Min. Jour., February, pp 90-96.

SICHEL, H.S. (1966): The estimation of means and associated confidence limits for small samples from lognormal populations, Symp. on mathematical statistics & computer applications in ore valuation, S. Afr. Inst. Min. Metall, pp 106-123.

SINCLAIR, A.J. and DERAISME, J. (1974): A geostatistical study of the Eagle copper vein, northern British Columbia. Bull. Can. Inst. Min. Metall., 67, No 746, pp 131-142.

SINGH, T.R.P. (1976): Point-block covariance: a general solution for the two-dimensional random functions, Math. Geol., 8, pp 627-634.

SPLIID, A.M. (1981): Beskrivelse af programpakken DMT, Dept. of Surveying and Photogrammetry. Tech. Univ. Denmark. 46 pp.

STANLEY, B.T. (1976): From drill hole to total estimate, a workable geostatistical case study. APCOM 76, 14th Int. Symp. on the application of computers and operations research in the Mineral Industry. Pennsylvania State Univ. USA.

SØRENSEN, H. (1958): The Ilímaussaq batholith, a review and discussion. Bull. Grønlands geol. Unders., 19 (also Meddr. Grønland 162,3), 48 pp.

SØRENSEN, H. (1962): On the occurrence of steenstrupine in the Ilímaussaq massif, Southwest Greenland. Bull. Grønlands geol. Unders. 32 (also Meddr. Grønland, 167,1) 251 pp.

SØRENSEN, H. (1966): Gardar rift-systemet II: På spor af sjældne metaller; Sydgrønland. Grønland, pp 163-176.

SØRENSEN, H. (1970): Internal structures and geological setting of the three agpaitic intrusions - Khibina and Lovozero of the Kola Peninsula and Ilímaussaq, South Greenland. Can. Miner. 10, pp 299-334.

SØRENSEN, H. (1978): The position of the augite syenite and pulaskite in the Ilímaussaq intrusion, South Greenland. Bull. Geol. Soc. Denmark. 27, special issue pp 15-23.

SØRENSEN, H., HANSEN, I. and BONDESEN, E. (1969): Preliminary account of the geology of the Kvanefjeld area of the Ilímaussaq intrusion, South Greenland. Rapp. Grønlands geol. Unders. 18, 40 pp.

SØRENSEN, H., ROSE-HANSEN, J. and NIELSEN, B.L. (1971): Geologisk beskrivelse af uranforekomsterne på Kvanefjelds-plateauet, Sydgrønland. Internal report. Geol. Surv. Greenland. 105 pp.

SØRENSEN, H., ROSE-HANSEN, J., NIELSEN, B.L., LØVBORG, L., SØRENSEN, E. and LUNDGAARD, T. (1974): The uranium deposit at Kvanefjeld, the Ilímaussaq intrusion, South Greenland. Rapp. Grønlands geol. Unders. 60, 54 pp.

SØRENSEN, P. (1979): Konstruktion af gamma-spektrometrisk opstilling til måling af malmprøver fra prøvebeningstunnelen på Kvanefjeld. Elektronikafdelingens notater. Internal report RISØ Nat. Lab., 15 pp.

USSING, H.V. (1912): Geology of the country around Julianehaab, Greenland. Meddr. Grønland 38, 376 pp.

WATT, W.S. (1966): Chemical analyses from the Gardar Igneous Province, South Greenland. Rapp. Grønlands geol. Unders. 6, 92 pp.

deWIJS, H.J. (1972): Method of successive differences applied to mine sampling, Trans. Inst. Min. Metall., vol. 81, No 788, pp A129-A132.

APPENDICES

APPENDIX A1

List of programs not written by the author.

PROGRAM	SOURCE	DESCRIPTION (documentation)
Semi-variogram programs:		
MARVGM	A.G. Royle	Calculates experimental semi-variograms from scattered data points in given directions. (Ahlefeldt-Laurvig, 1981)
SEMI	I. Clark	Calculates down-the-hole semi-variograms and average vertical, N-S and E-W s-v's. (Clark, 1979b).
Estimation programs:		
INVAF	C.W.A-Laurvig	Estimation of batch samples by inverse distance weighting (Ahlefeldt-Laurvig, 1981)
MIDDEL	C.W.A-Laurvig	Estimation of batch samples by arithmetric mean (Ahlefeldt-Laurvig, 1981).
PTKR	A.G. Royle	Performs point kriging of samples (Ahlefeldt-Laurvig, 1981).
PTUK	A.G. Royle	Performs point universal kriging of samples (Clausen, 1980c).
PTKTUN	C.W.A-Laurvig	Modified version of SPECKR used for two-dimensional estimation of batch samples.
PTKNET	C.W.A-Laurvig	Performs point kriging on a regular grid (Ahlefeldt-Lauvig, 1981).
SPECKR	A.G. Royle	Performs two-dimensional panel kriging.
TREREG	I. Clark	Performs three-dimensional block kriging with georegression. (Clark, 1979b,c)

Other programs:

SAM	Surveying & photogrammetry	Calculates contours from regionalised variables located on a regular grid (Spliid, 1981)
DUEPLT	Surveying & photogrammetry	Plots contours on a drum plotter (Spliid, 1981)
ROKE	I.Clark	Least-squares fitting of multi-component distributions to histograms (Clark, 1977a)

APPENDIX A2

Listing of selected programs written by the author

CRKVAN	Program used to create the drill core database KVANE. (Statistical Analysis System).
GRATON	Program to calculate grade-tonnage values at various cutoff values or according to the estimation error. (FORTRAN)
BLSELOLD	Program to select blocks estimated by TREREG in the Mine area. (SAS).
BLSELNEW	Program to select blocks estimated by TREREG in the Northern area. (SAS)
FGAM	Calculates gamma-values of a one-component spherical scheme. (FORTRAN)
FGAM2	Calculates gamma-values of a Two-component spherical scheme. (FORTRAN)
FGAM3	Calculates gamme-values of a three-component spherical scheme. (FORTRAN)
FRESP2	Calculates the regularised semi-variogram of a two-com ponent spherical scheme. The routine REGSPH is used (Clark, 1977b). (FORTRAN)
BMDP7M	Example of setup for step-wise discriminant analysis (SAS/BMDP).
BMDPKM	Example of setup for K-mean clustering (SAS/BMDP).

Program: CRKVAN

```
00010 //A179002F JOB (***,NEU,60,45,,,1),'F MASTERFIL  ',REGION=450K,
00020 // RATE=SLOW,IO=10000
00030 /*ROUTE  PRINT LOCAL
00040 // EXEC SAS
00050 //A DD DSN=NEU.A179002.KUTDATA2,DISP=OLD
00060 //B DD DSN=NEU.A179002.XYZSTART,DISP=OLD
00070 //C DD DSN=NEU.A179002.KVDATA,DISP=OLD
00080 //P DD DSN=NEU.A179002.KVDATA(FLOUR),DISP=OLD
00090 //  DD DSN=NEU.A179002.KVDATA(FLOUR2),DISP=OLD
00100 //  DD DSN=NEU.A179002.KVDATA(FLOUR3),DISP=OLD
00110 //D DD DSN=NEU.A179002.XRFRISO(KUNZ),DISP=OLD
00120 //  DD DSN=NEU.A179002.XRFRISO(SUPPL),DISP=OLD
00130 //E DD DSN=NEU.A179002.GWOZDZ(CORE44A),DISP=OLD
00140 //  DD DSN=NEU.A179002.GWOZDZ(CORE44B),DISP=OLD
00150 //  DD DSN=NEU.A179002.GWOZDZ(CORE46),DISP=OLD
00160 //  DD DSN=NEU.A179002.GWOZDZ(CORE48),DISP=OLD
00170 //  DD DSN=NEU.A179002.GWOZDZ(CORE49A),DISP=OLD
00180 //  DD DSN=NEU.A179002.GWOZDZ(CORE49B),DISP=OLD
00190 //  DD DSN=NEU.A179002.GWOZDZ(CORE51),DISP=OLD
00200 //  DD DSN=NEU.A179002.GWOZDZ(CORE55B),DISP=OLD
00210 //  DD DSN=NEU.A179002.GWOZDZ2(CORE55A),DISP=OLD
00220 //  DD DSN=NEU.A179002.GWOZDZ2(CORE52),DISP=OLD
00230 //  DD DSN=NEU.A179002.GWOZDZ2(CORE53),DISP=OLD
00240 //  DD DSN=NEU.A179002.GWOZDZ2(CORE50),DISP=OLD
00250 //  DD DSN=NEU.A179002.GWOZDZ2(CORE45),DISP=OLD
00260 //  DD DSN=NEU.A179002.GWOZDZ2(CORE56),DISP=OLD
00270 //  DD DSN=NEU.A179002.GWOZDZ2(CORE57A),DISP=OLD
00280 //  DD DSN=NEU.A179002.GWOZDZ2(CORE57B),DISP=OLD
00290 //  DD DSN=NEU.A179002.GWOZDZ2(CORE59A),DISP=OLD
00300 //  DD DSN=NEU.A179002.GWOZDZ2(CORE59B),DISP=OLD
00310 //Q DD DSN=NEU.A179002.EDXPLU(CORE44),DISP=OLD
00320 //  DD DSN=NEU.A179002.EDXPLU(CORE46),DISP=OLD
00330 //  DD DSN=NEU.A179002.EDXPLU(CORE48),DISP=OLD
00340 //  DD DSN=NEU.A179002.EDXPLU(CORE49),DISP=OLD
00350 //  DD DSN=NEU.A179002.EDXPLU(CORE51),DISP=OLD
00360 //  DD DSN=NEU.A179002.EDXPLU(CORE55),DISP=OLD
00370 //  DD DSN=NEU.A179002.EDXPLU(CORE59),DISP=OLD
00380 //F DD DSN=NEU.A179002.MFIL,DISP=OLD
00390 //SYSIN DD *
00400 ****************SAS-PROGRAM PGM1*********************************;
00410 *;
00420 * THE FOLLOWING IS READ IN FROM FILE * ;
00430 *;
00440 *   1) DRILL HOLE;
00450 *   2) DEPTH TO SAMPLE;
00460 *   3) GEOLOGY CODE;
00470 *   4) U, TH, AND K ANALYSES AND STANDARD DEVIATIONS;
00480 *;
00490 *;
00500    DATA START1;
00510    INFILE A;
00520    LENGTH DEFAULT=4;
00530    INPUT BH DYBDE1 DYBDE2 GEOLOGI K_PCT1 KSTDV U_PPM1 USTDV
00540          TH_PPM1 THSTDV;
```

```
00550 OUTPUT;
00560 PROC SORT; BY BH;
00570 *;
00580 *  START COORDINATES FOR DRILL HOLES ARE READ IN;
00590 *;
00600    DATA XYZ;
00610    INFILE B;
00620    LENGTH DEFAULT=4;
00630    INPUT BH XSTART YSTART ZSTART AZIMUTH DIP;
00640 OUTPUT;
00650 PROC SORT; BY BH;
00660 *;
00670 * MERGING OF K-U-TH DATA WITH SPATIAL COORDINATES;
00680 *;
00690    DATA MIX;
00700    MERGE START1 XYZ;
00710    BY BH;
00720 *;
00730 *  SORTING BETWEEN INCLINED AND VERTICAL HOLES;
00740 *  CALCULATION OF SAMPLE COORDINATES;
00750 *;
00760    DATA FLEM; SET MIX;
00770       PR_NR=(BH*1000)+DYBDE1;
00780       AC=DYBDE1;
00790       AZI=AZIMUTH+12;
00800       AZIRAD=(AZI*3.141592)/180;
00810       DIPRAD=(DIP*3.141592)/180;
00820   IF DIP=. THEN GO TO VERT;
00830       X=XSTART-((SIN(AZIRAD))*(AC*(COS(DIPRAD))));
00840       Y=YSTART+((COS(AZIRAD))*(AC*(COS(DIPRAD))));
00850       Z=ZSTART-(AC*(SIN(DIPRAD)));
00860 RETURN;
00870 VERT:
00880       X=XSTART;
00890       Y=YSTART;
00900       Z=ZSTART-AC;
00910 DATA KUTH; SET FLEM;
00920      XTR=1100-X;
00930      YTR=Y+1100;
00940      ZTR=Z;
00950      KEEP BH PR_NR GEOLOGI X Y Z XTR YTR ZTR DYBDE1 DYBDE2
00960           AZIMUTH DIP U_PPM1 TH_PPM1 K_PCT1;
00970 PROC SORT; BY BH PR_NR;
00980 *
00990 ********************SASPROGRAM PGM2*******************************
01000 *
01010 *   XRF-ANALYSES ARE READ IN
01020 *;
01030   DATA START2;
01040   INFILE C(XRFGEO);
01050   LENGTH DEFAULT=4;
01060     INPUT BH 1-2 @3 METER GEOLOGI2 X ZR_PPM2 Y_PPM2 SR_PPM2
01070           RB_PPM2 TH_PPM2 PB_PPM2 GA_PPM2 ZN_PPM2 NB_PPM2;
01080   OUTPUT;
01090   DATA XRFGEO; SET START2;
01100   PR_NR=(BH*1000)+METER;
01110   DROP X METER;
```

```
01120   PROC SORT; BY BH PR_NR;
01130 ************************SASPROGRAM PGM3*****************************;
01140 *;
01150 *  EDX-CD ANALYSES ARE READ IN;
01160 *  EACH OBSERVATION CONSISTS OF 10 CARDS;
01170 *;
01180  DATA START3;
01190  INFILE D;
01200  LENGTH DEFAULT=4;
01210   INPUT @5 BH 2. @7 METER 3. @33 A $ 2. @62 PE_PCT3 6. £2 @33 B $ 2.
01220         RB_PPM3 62-66 £3 @33 C $ 2. SR_PPM3 62-66 £4 @33 D $ 2.
01230         Y_PPM3 62-66 £5 @33 E $ 2. ZR_PPM3 62-66 £6 @33 F $ 2.
01240         NB_PPM3 62-66 £7 @33 G $ 2. MO_PPM3 62-66 £8 @33 H $ 2.
01250         PB_PPM3 62-66 £9 @33 I $ 2. TH_PPM3 62-66 £10 @33 J $ 2.
01260         U_PPM3 62-66;
01270   OUTPUT;
01280   DATA XRFRISO; SET START3;
01290   PR_NR=(BH*1000)+METER;
01300   DROP A B C D E F G H I J METER;
01310 *;
01320   PROC SORT; BY BH PR_NR;
01330 ************************SASPROGRAM PGM4*****************************
01340 *
01350 *  FLOUR-ANALYSES ARE READ IN;
01360 *;
01370   DATA START4;
01380   INFILE P;
01390   LENGTH DEFAULT=4;
01400     INPUT BH 1-2 @3 METER GEOLOGI4 X FLOURP DETEK;
01410   OUTPUT;
01420   DATA FLOUR; SET START4;
01430   PR_NR=(BH*1000)+METER;
01440    F_PCT4=.;
01450    IF DETEK=0 THEN F_PCT4=-99.;
01460    IF DETEK=. THEN F_PCT4=FLOURP;
01470    DROP X METER DETEK FLOURP;
01480 *;
01490   PROC SORT; BY BH PR_NR;
01500 ************************SASPROGRAM PGM5*****************************
01510 *
01520 *  OPSPEC-DATA ARE READ IN;
01530 *;
01540   DATA START5;
01550   INFILE C(LIOGBE);
01560   LENGTH DEFAULT=4;
01570     INPUT BH 1-2 @3 METER GEOLOGI5 X BE_PPM5 LI_PPM5;
01580   OUTPUT;
01590   DATA LIOGBE; SET START5;
01600   PR_NR=(BH*1000)+METER;
01610   DROP X METER;
01620 *;
01630   PROC SORT; BY BH PR_NR;
01640 ************************SASPROGRAM PGM6*****************************
01650 *
01660 *   NEAA-ANALYSES ARE READ IN
01670 *   EACH OBSERVATION CONSISTS OF 16 CARDS
01680 *   THE PROGRAM HAS AN ERROR CHECKING BUILD IN
```

```
01690 *;
01700   DATA START;
01710   INFILE E;
01720   LENGTH DEFAULT=4;
01730   INPUT BH 1-2 @4 METER 3. £2
01740    @29 A 2. NA 32-35 NATEGN $ 36 NAEXP 37-38
01750    @54 B 2. K 57-60 KTEGN $ 61 KEXP 62-63 LIM 70-73 £3
01760    @29 C 2. SC 32-35 SCTEGN $ 36 SCEXP 37-38
01770    @54 D 2. CR 57-60 CRTEGN $ 61 CREXP 62-63 £4
01780    @4 E 2. MN 7-10 MNTEGN $ 11 MNEXP 12-13
01790    @29 F 2. FE 32-35 FETEGN $ 36 FEEXP 37-38
01800    @54 G 2. CO 57-60 COTEGN $ 61 COEXP 62-63 £5
  810    @4 H 2. ZN 7-10 ZNTEGN $ 11 ZNEXP 12-13 £6
01820    @54 I 2. RB 57-60 RBTEGN $ 61 RBEXP 62-63 £7
01830    @29 J 2. ZR 32-35 ZRTEGN $ 36 ZREXP 37-38 £9
01840    @4 K1 2. SN 7-10 SNTEGN $ 11 SNEXP 12-13
01850    @29 L 2. SB 32-35 SBTEGN $ 36 SBEXP 37-38
01860   @54 M 2. M1 57-60 MTEGN $ 61 MEXP 62-63 £10
01870   @4  N 2. N1  7-10 NTEGN $ 11 NEXP 12-13
01880   @29 O 2. O1 32-35 OTEGN $ 36 OEXP 37-38
01890   @54 P 2. P1 57-60 PTEGN $ 61 PEXP 62-63 £11
01900   @4  Q 2. Q1  7-10 QTEGN $ 11 QEXP 12-13
01910   @29 R 2. R1 32-35 RTEGN $ 36 REXP 37-38
01920   @54 S 2. S1 57-60 STEGN $ 61 SEXP 62-63 £12
01930   @4  T 2. T1  7-10 TTEGN $ 11 TEXP 12-13
01940   @29 U 2. U1 32-35 UTEGN $ 36 UEXP 37-38
01950   @54 V 2. V1 57-60 VTEGN $ 61 VEXP 62-63 £13
01960   @4  X 2. X1  7-10 XTEGN $ 11 XEXP 12-13
01970   @54 Y 2. Y1 57-60 YTEGN $ 61 YEXP 62-63 £14
01980   @4  Z 2. Z1  7-10 ZTEGN $ 11 ZEXP 12-13
01990   @29 XZ 2. XZ1 32-35 XZTEGN $ 36 XZEXP 37-38
02000   @54 XY 2. XY1 57-60 XYTEGN $ 61 XYEXP 62-63 £15
02010   @4  XX 2. XX1  7-10 XXTEGN $ 11 XXEXP 12-13 £16
02020   @4  XV 2. XV1  7-10 XVTEGN $ 11 XVEXP 12-13
02030   @29 XU 2. XU1 32-35 XUTEGN $ 36 XUEXP 37-38;
02040   NB=' ** ';
02050   IF A ~=11 OR B ~=19 OR C ~=21 OR D ~=24 OR E ~=25 OR F ~=26
02060   OR G ~=27 OR H ~=30 OR I ~=37 OR J ~=40 OR K1 ~=50 OR L ~=51
02070  OR M ~=53 AND M ~=55 OR N ~=55 AND N ~=56
02080  OR O ~=56 AND O ~=57 OR P ~=57 AND P ~=58
02090  OR Q ~=58 AND Q ~=59 OR R ~=59 AND R ~=60
02100  OR S ~=60 AND S ~=62 OR T ~=62 AND T ~=63
02110  OR U ~=63 AND U ~=64 OR V ~=64 AND V ~=65
02120  OR X ~=65 AND X ~=66 OR Y ~=67 AND Y ~=70
02130  OR Z ~=70 AND Z ~=71 OR XZ ~=71 AND XZ ~=72
02140  OR XY ~=72 AND XY ~=73 OR XX ~=73 AND XX ~=74
02150  OR XV ~=80 AND XV ~=90 OR XU ~=90 AND XU ~=92
02160  THEN NB='FEJL';
02170     DATA NY; SET START;
02180     PR_NR=(BH*1000)+METER;
02190     DROP METER;
02200   IF NATEGN='+' THEN NA_PPM6=NA*(10**NAEXP);
02210   IF NATEGN='-' THEN NA_PPM6=NA*(10**(-NAEXP));
02220   DROP NA NATEGN NAEXP;
02230   IF KTEGN='+' THEN K_PPM6=K*(10**KEXP);
02240   IF KTEGN='-' THEN K_PPM6=K*(10**(-KEXP));
02250   IF LIM=0.0 THEN K_PPM6=.;
```

```
02260   DROP K KTEGN KEXP LIM;
02270   IF SCTEGN='+' THEN SC_PPM6=SC*(10**SCEXP);
02280   IF SCTEGN='-' THEN SC_PPM6=SC*(10**(-SCEXP));
02290   DROP SC SCTEGN SCEXP;
02300   IF CRTEGN='+' THEN CR_PPM6=CR*(10**CREXP);
02310   IF CRTEGN='-' THEN CR_PPM6=CR*(10**(-CREXP));
02320   DROP CR CRTEGN CREXP;
02330   IF MNTEGN='+' THEN MN_PPM6=MN*(10**MNEXP);
02340   IF MNTEGN='-' THEN MN_PPM6=MN*(10**(-MNEXP));
02350   DROP MN MNTEGN MNEXP;
02360   IF FETEGN='+' THEN FE_PPM6=FE*(10**FEEXP);
02370   IF FETEGN='-' THEN FE_PPM6=FE*(10**(-FEEXP));
02380   DROP FE FETEGN FEEXP;
02390   IF COTEGN='+' THEN CO_PPM6=CO*(10**COEXP);
02400   IF COTEGN='-' THEN CO_PPM6=CO*(10**(-COEXP));
   .0   DROP CO COTEGN COEXP;
02420   IF ZNTEGN='+' THEN ZN_PPM6=ZN*(10**ZNEXP);
02430   IF ZNTEGN='-' THEN ZN_PPM6=ZN*(10**(-ZNEXP));
02440   DROP ZN ZNTEGN ZNEXP;
02450   IF RBTEGN='+' THEN RB_PPM6=RB*(10**RBEXP);
02460   IF RBTEGN='-' THEN RB_PPM6=RB*(10**(-RBEXP));
02470   DROP RB RBEXP RBTEGN;
02480   IF ZRTEGN='+' THEN ZR_PPM6=ZR*(10**ZREXP);
02490   IF ZRTEGN='-' THEN ZR_PPM6=ZR*(10**(-ZREXP));
02500   DROP ZR ZRTEGN ZREXP;
02510   IF SNTEGN='+' THEN SN_PPM6=SN*(10**SNEXP);
02520   IF SNTEGN='-' THEN SN_PPM6=SN*(10**(-SNEXP));
02530   DROP SN SNTEGN SNEXP;
02540   IF SBTEGN='+' THEN SB_PPM6=SB*(10**SBEXP);
02550   IF SBTEGN='-' THEN SB_PPM6=SB*(10**(-SBEXP));
02560   DROP SB SBTEGN SBEXP;
02570 IF XV=80 THEN GO TO NYAN;
02580   IF MTEGN='+' THEN CS_PPM6=M1*(10**MEXP);
02590   IF MTEGN='-' THEN CS_PPM6=M1*(10**(-MEXP));
02600   IF NTEGN='+' THEN BA_PPM6=N1*(10**NEXP);
02610   IF NTEGN='-' THEN BA_PPM6=N1*(10**(-NEXP));
02620   IF OTEGN='+' THEN LA_PPM6=O1*(10**OEXP);
02630   IF OTEGN='-' THEN LA_PPM6=O1*(10**(-OEXP));
02640   IF PTEGN='+' THEN CE_PPM6=P1*(10**PEXP);
02650   IF PTEGN='-' THEN CE_PPM6=P1*(10**(-PEXP));
02660   IF RTEGN='+' THEN ND_PPM6=R1*(10**REXP);
02670   IF RTEGN='-' THEN ND_PPM6=R1*(10**(-REXP));
02680   IF STEGN='+' THEN SM_PPM6=S1*(10**SEXP);
02690   IF STEGN='-' THEN SM_PPM6=S1*(10**(-SEXP));
02700   IF TTEGN='+' THEN EU_PPM6=T1*(10**TEXP);
02710   IF TTEGN='-' THEN EU_PPM6=T1*(10**(-TEXP));
02720   IF UTEGN='+' THEN GD_PPM6=U1*(10**UEXP);
02730   IF UTEGN='-' THEN GD_PPM6=U1*(10**(-UEXP));
02740   IF VTEGN='+' THEN TB_PPM6=V1*(10**VEXP);
02750   IF VTEGN='-' THEN TB_PPM6=V1*(10**(-VEXP));
02760   IF YTEGN='+' THEN YB_PPM6=Y1*(10**YEXP);
02770   IF YTEGN='-' THEN YB_PPM6=Y1*(10**(-YEXP));
02780   IF ZTEGN='+' THEN LU_PPM6=Z1*(10**ZEXP);
02790   IF ZTEGN='-' THEN LU_PPM6=Z1*(10**(-ZEXP));
02800   IF XZTEGN='+' THEN HF_PPM6=XZ1*(10**XZEXP);
02810   IF XZTEGN='-' THEN HF_PPM6=XZ1*(10**(-XZEXP));
02820   IF XYTEGN='+' THEN TA_PPM6=XY1*(10**XYEXP);
```

```
02830   IF XYTEGN='-' THEN TA_PPM6=XY1*(10**(-XYEXP));
02840   IF XVTEGN='+' THEN TH_PPM6=XV1*(10**XVEXP);
02850   IF XVTEGN='-' THEN TH_PPM6=XV1*(10**(-XVEXP));
02860 GO TO STOPS;
02870 NYAN:
02880   IF NTEGN='+' THEN CS_PPM6=N1*(10**NEXP);
02890   IF NTEGN='-' THEN CS_PPM6=N1*(10**(-NEXP));
02900   IF OTEGN='+' THEN BA_PPM6=O1*(10**OEXP);
02910   IF OTEGN='-' THEN BA_PPM6=O1*(10**(-OEXP));
02920   IF PTEGN='+' THEN LA_PPM6=P1*(10**PEXP);
02930   IF PTEGN='-' THEN LA_PPM6=P1*(10**(-PEXP));
02940   IF QTEGN='+' THEN CE_PPM6=Q1*(10**QEXP);
02950   IF QTEGN='-' THEN CE_PPM6=Q1*(10**(-QEXP));
02960   IF STEGN='+' THEN ND_PPM6=S1*(10**SEXP);
02970   IF STEGN='-' THEN ND_PPM6=S1*(10**(-SEXP));
02980   IF TTEGN='+' THEN SM_PPM6=T1*(10**TEXP);
02990   IF TTEGN='-' THEN SM_PPM6=T1*(10**(-TEXP));
03000   IF UTEGN='+' THEN EU_PPM6=U1*(10**UEXP);
    0   IF UTEGN='-' THEN EU_PPM6=U1*(10**(-UEXP));
03020   IF VTEGN='+' THEN GD_PPM6=V1*(10**VEXP);
03030   IF VTEGN='-' THEN GD_PPM6=V1*(10**(-VEXP));
03040   IF XTEGN='+' THEN TB_PPM6=X1*(10**XEXP);
03050   IF XTEGN='-' THEN TB_PPM6=X1*(10**(-XEXP));
03060   IF ZTEGN='+' THEN YB_PPM6=Z1*(10**ZEXP);
03070   IF ZTEGN='-' THEN YB_PPM6=Z1*(10**(-ZEXP));
03080   IF XZTEGN='+' THEN LU_PPM6=XZ1*(10**XZEXP);
03090   IF XZTEGN='-' THEN LU_PPM6=XZ1*(10**(-XZEXP));
03100   IF XYTEGN='+' THEN HF_PPM6=XY1*(10**XYEXP);
03110   IF XYTEGN='-' THEN HF_PPM6=XY1*(10**(-XYEXP));
03120   IF XXTEGN='+' THEN TA_PPM6=XX1*(10**XXEXP);
03130   IF XXTEGN='-' THEN TA_PPM6=XX1*(10**(-XXEXP));
03140   IF XUTEGN='+' THEN TH_PPM6=XU1*(10**XUEXP);
03150   IF XUTEGN='-' THEN TH_PPM6=XU1*(10**(-XUEXP));
03160 STOPS:
03170  DROP A B C D E F G H I J K1 L M N O P Q R S T U V X Y Z XZ XY XX
03180  XV XU MEXP M1 MTEGN NEXP N1 NTEGN O1 OEXP OTEGN P1 PTEGN PEXP
03190  Q1 QTEGN QEXP R1 REXP RTEGN S1 STEGN SEXP T1 TEXP TTEGN U1 UTEGN
03200  UEXP V1 VTEGN VEXP X1 XTEGN XEXP Y1 YTEGN YEXP Z1 ZTEGN ZEXP XZ1
03210  XZTEGN XZEXP XY1 XYTEGN XYEXP XX1 XXTEGN XXEXP XV1 XVTEGN XVEXP
03220  XU1 XUTEGN XUEXP;
03230 DATA GWOZDZ; SET NY;
03240 PROC SORT; BY BH PR_NR;
03250 *
03260 **************************SAS-PROGRAM PGM7************************
03270 *
03280 *  EDX-PLU ANALYSES ARE READ IN
03290 *;
03300   DATA RISPLU;
03310   INFILE Q;
03320   LENGTH DEFAULT=4;
03330    INPUT @4 BH : 2. MET : 3. @22 GEOLOGI7 3. @33 A $ 2. K_PCT7 62-67
03340     £2 @33 B $ 2. CA_PCT7 62-67
03350     £3 @33 C $ 2. TI_PCT7 62-67
03360     £6 @33 D $ 2. MN_PPM7 62-67
03370     £7 @33 E $ 2. FE_PCT7 62-67
03380     £8 @33 F $ 2. NI_PPM7 62-67
03390     £9 @33 G $ 2. CU_PPM7 62-67
```

```
03400    £10 @33 H $ 2. ZN_PPM7 62-67
03410    £11 @33 I $ 2. GA_PPM7 62-67
03420    £12 @33 J $ 2. SR_PPM7 62-67
03430    £13 @33 K $ 2. PB_PPM7 62-67;
03440  PR_NR=(BH*1000)+MET;
03450  CHECK=' ** ';
03460 *
03470 *;
03480   IF B ~= '20' THEN CHECK='FEJL';
03490   IF C ~= '22' THEN CHECK='FEJL';
03500   IF D ~= '25' THEN CHECK='FEJL';
03510   IF E ~= '26' THEN CHECK='FEJL';
03520   IF F ~= '28' THEN CHECK='FEJL';
03530   IF G ~= '29' THEN CHECK='FEJL';
03540   IF H ~= '30' THEN CHECK='FEJL';
03550   IF I ~= '31' THEN CHECK='FEJL';
03560   IF J ~= '38' THEN CHECK='FEJL';
03570   IF K ~= '82' THEN CHECK='FEJL';
03580  DROP MET A B C D E F G H I J K CHECK;
03590  PROC SORT; BY BH PR_NR;
03600 *
03600 *
03610 *
03620 ********************  MASTERFILE KVANE IS FORMED  ****************
03630 *
03640 *;
03650   DATA KVANE;
03660   MERGE KUTH XRFGEO XRFRISO FLOUR LIOGBE GWOZDZ RISPLU;
03670   BY BH PR_NR;
03680 PROC PRINT; BY BH;
```

Program: GRATON

```
00010 //A179002F JOB (***,NEU,2,3),'F GRADE/TONNAGE',RATE=NORM
00020 /*ROUTE  PRINT LOCAL
00030 // EXEC FORTG
00040 //FT09F001 DD DSN=NEU.A179002.NEWBLKS2(PERPDIS),DISP=SHR,LABEL=(,,,IN)
00050 //CSYSIN DD *
00060 C     *************** PROGRAM GRATON **************
00070 C
00080 C     THIS PROGRAM CALCULATES GRADE/TONNAGE CURVES FOR BLOCK ESTIMATES
00090 C
00100 C     SUBROUTINE FUP  DO IT ACCORDING TO CERTAIN CUT-OFF GRADES
00110 C     SUBROUTINE FDOWN DO IT ACCORDING TO THE ESTIMATION ERROR.
00120 C
00130       DIMENSION ITL(20),NAME(2),FMT(10),DIV(1),TAB(52)
00140       DIMENSION X(1000),Y(1000),Z(1000)
00150       DIMENSION VALUE(1000),SDK(1000),VARK(1000)
00160 C
00170       READ(5,94) (ITL(I),I=1,20)
00180  94   FORMAT(20A4)
00190       READ(5,4)  TFAC,HBENCH
00200  4    FORMAT(F12.2,F5.1)
00210       READ(5,10) COGVAL,STPVAL,COGERR,STPERR
00220       READ(5,14) CS1
00230       READ(5,700) BL,BU,NCLASS
00240  700  FORMAT(2F10.2,I3)
00250  10   FORMAT(4F10.2)
00260  14   FORMAT(F10.2)
00270       READ(5,3) (NAME(I),I=1,2)
00280  3    FORMAT(2A4)
00290       READ(5,27) FMT
00300  27   FORMAT(10A4)
00310 C
00320       L=0
00330  1    READ (9,FMT,END=2) XA,YA,ZA,VAL,ERR
00340       IF(VAL.LT.COGVAL) GO TO 17
00350       IF(ERR.GT.CS1) GO TO 17
00360       L=L+1
00370       X(L)=XA
00380       Y(L)=YA
00390       Z(L)=ZA
00400       VALUE(L)=VAL
00410       SDK(L)=ERR
00420        VARK(L)=ERR*ERR
00430  17   GO TO 1
00440  2    CONTINUE
00450       NBLOC=L
00460       DO 645 JJ=1,52
00470       TAB(JJ)=0.0
00480   645 CONTINUE
00490       K=(-1)*NCLASS
00500       CALL BDCOU1(VALUE,NBLOC,K,DIV,BU,BL,TAB,IER)
00510       WRITE(6,116) (ITL(J),J=1,20)
00520  116  FORMAT(1H1,2X,20A4)
00530       WRITE(6,120)
00540  120  FORMAT(1H ,2X,80('-'))
```

```
00550       WRITE(6,117)
00560  117  FORMAT(1H0,3X,'BLOCK',3X,'X-COORD.',4X,'Y-COORD.',4X,
00570      2'Z-COORD.',4X,'  PPM  ',4X,'KR.STD.')
00580       WRITE(6,118) (NAME(I),I=1,2),(NAME(I),I=1,2)
00590  118  FORMAT(1H ,4X,'NO.',4X,'LOW.LEFT',4X,'LOW.LEFT',4X,'LOW.LEFT',
00600      24X,2A4,3X,2A4//)
00610       DO 122 J=1,NBLOC
00620       WRITE(6,119) J,X(J),Y(J),Z(J),VALUE(J),SDK(J)
00630  122  CONTINUE
00640  119  FORMAT(1H ,3X,I3,3F12.2,F11.2,F10.2)
00650       WRITE(6,116) (ITL(J),J=1,20)
00660       WRITE(6,120)
00670       SBAR=FM(SDK,NBLOC)
00680       VBAR=FM(VARK,NBLOC)
00690       VALBAR=FM(VALUE,NBLOC)
00700       VALVAR=FVAR(VALUE,NBLOC,VALBAR)
00710       SSBAR=FVAR(SDK,NBLOC,SBAR)
00720       WRITE(6,121)
00730       WRITE(6,121)
00740  121  FORMAT(1H0)
00750       WRITE(6,130) (NAME(J),J=1,2)
00760       WRITE(6,311)
00770       WRITE(6,131) HBENCH,TFAC
00780       WRITE(6,124) NBLOC
00790       WRITE(6,125) VALBAR,VALVAR
00800       WRITE(6,126) SBAR,SSBAR
00810       WRITE(6,127) VBAR
00820       WRITE(6,121)
00830       WRITE(6,121)
00840       WRITE(6,401)
00850   401 FORMAT(1H ,18X,'HISTOGRAM OF BLOCK VALUES:')
00860       WRITE(6,402)
00870   402 FORMAT(1H ,18X,26('-'))
00880       WRITE(6,121)
00890       WRITE(6,403)
00900   403 FORMAT(1H0,6X,'LOWER',6X,'UPPER',6X,'NUMBER OF')
00910       WRITE(6,404)
00920   404 FORMAT(1H ,6X,'LIMIT',6X,'LIMIT',6X,'  BLOCKS '/)
00930       CLASS=(BU-BL)/FLOAT(NCLASS)
00940       DO 1001 J=1,NCLASS
00950       ALOW=BL+(J-1)*CLASS
00960       AHIG=BL+J*CLASS
00970       NUM=IFIX(TAB(J+1))
00980       WRITE(6,406) ALOW,AHIG,NUM
00990  1001 CONTINUE
01000   406 FORMAT(1H ,5X,F6.1,5X,F6.1,9X,I4)
01010  124  FORMAT(1H0,6X,'THE NUMBER OF ESTIMATED BLOCKS CONSIDERED HERE',
01020      2' IS: ',I4)
01030  125  FORMAT(1H0,6X,'THE AVERAGE VALUE OF THE BLOCKS IS: ',F10.2/
01040      26X,' AND THE VARIANCE OF THESE ESTIMATES IS: ',F10.2)
01050  126  FORMAT(1H0,6X,'THE AVERAGE KRIGING STANDARD DEVIATION IS: ',
01060      2F10.2/6X,' AND THESE HAVE A VARIANCE OF: ',F10.2)
01070  127  FORMAT(1H0,6X,'THE AVERAGE KRIGING VARIANCE IS PROBABLY: ',
01080      2F10.2)
01090  130  FORMAT(1H ,18X,'MAJOR STATISTICS FOR ESTIMATED BLOCKS OF ',2A4)
01100  311  FORMAT(1H ,59X,8('-'))
01110  131  FORMAT(1H-,6X,'THE BENCH HEIGHT IS: ',F5.1,' AND THE'
```

```
01120      2,' TONNAGE FACTOR (A*B*RHO) IS: ',F12.2)
01130 C
01140       CALL FUP(NBLOC,VALUE,SDK,COGVAL,STPVAL,ITL,NAME,TFAC,HBENCH)
01150       CALL FDOWN(NBLOC,VALUE,SDK,COGERR,STPERR,ITL,NAME,TFAC,HBENCH)
01160       STOP
01170       END
01180 C
01190 C
01200       FUNCTION FM(Z,N)
01210       DIMENSION Z(N)
01220       FM=0.0
01230       FN=1.0/FLOAT(N)
01240       DO 11 I=1,N
01250    11 FM=FM+Z(I)
01260       FM=FM*FN
01270       RETURN
01280       END
01290 C
01300       FUNCTION FVAR(Z,N,A)
01310       DIMENSION Z(N)
01320       FVAR=0.0
01330       FN=1.0/FLOAT(N-1)
01340       DO 12 I=1,N
01350    12 FVAR=FVAR+(Z(I)-A)*(Z(I)-A)
01360       FVAR=FVAR*FN
01370       RETURN
01380       END
01390 C
01400       SUBROUTINE FUP(NBLK,VAL,SDK,COG,STEP,ITL,NAME,TFAC,HBENCH)
01410       DIMENSION VAL(1000),SDK(1000),ITL(20),NAME(2)
01420       WRITE(6,92) (ITL(I),I=1,20)
01430    92 FORMAT(1H1,4X,20A4,20X,'TABLE')
01440       WRITE(6,93)
01450    93 FORMAT(1H ,4X,80('-'),20X,12('-'))
01460       WRITE(6,15) (NAME(I),I=1,2)
01470    15 FORMAT(1HO,4X,'GRADE/TONNAGE CURVE FOR ',2A4,' CONSIDERING ',
01480      2'DIFFERENT CUT-OFF GRADES.')
01490       WRITE(6,18)
01500    18 FORMAT(1H ,4X,24(1H-),8(1H*),38(1H-))
01510       WRITE(6,611)
01520   611 FORMAT(1HO,4X,'CUT-OFF',6X,'NUMBER OF',
01530      28X,'CUMULATED',8X,'  TONS    ',3X,'MEAN GRADE',3X,'POSSIBLE',
01540      38X,'AVERAGE')
01550       WRITE(6,612) (NAME(I),I=1,2),(NAME(I),I=1,2)
01560   612 FORMAT(1H ,5X,'GRADE',8X,'BLOCKS',10X,
01570      2'RESERVES',9X,2A4,6X,2A4,5X,'STAND.ERROR',4X,'STAND.ERROR')
01580 C
01590       AVEVAL=0.0
01600       DO 12 I=1,50
01610       SUMVAL=0.0
01620       SDAVE=0.0
01630       SDKAVE=0.0
01640       AVESDK=0.0
01650       AVEKSD=0.0
01660       TONGRP=0.0
01670       TONELE=0.0
01680       NBGR=0
```

```
01690       CUTOFF=(50-I)*STEP+COG
01700       DO 11 J=1,NBLK
01710       IF(VAL(J).LT.CUTOFF) GO TO 11
01720       SUMVAL=SUMVAL+VAL(J)
01730       SDAVE=SDAVE+SDK(J)*SDK(J)
01740       SDKAVE=SDKAVE+SDK(J)
01750       NBGR=NBGR+1
01760       TONGRP=NBGR*TFAC*HBENCH
01770       TONELE=TONELE+((TFAC*HBENCH*VAL(J))/1000000.0)
01780    11 CONTINUE
01790       IF(NBGR.NE.0) GO TO 13
01800       GO TO 14
01810    13 FN=1.0/FLOAT(NBGR)
01820       AVEVAL=SUMVAL*FN
01830       AVESDK=SQRT(SDAVE)*FN
01840       AVEKSD=SDKAVE*FN
01850       ELECUM=ELECUM+TONELE
01860    14 WRITE(6,111) CUTOFF,NBGR,TONGRP,TONELE,AVEVAL,
01870      2AVESDK,AVEKSD
01880    12 CONTINUE
01890   111 FORMAT(1H ,4X,F7.2,9X,I3,8X,F12.1,6X,F9.1,6X,F6.2,6X,F6.2,
01900      29X,F6.2)
01910       RETURN
01920       END
01930 C
01940       SUBROUTINE FDOWN(NBLK,VAL,SDK,COG,STEP,ITL,NAME,TFAC,HBENCH)
01950       DIMENSION VAL(1000),SDK(1000),ITL(20),NAME(2)
01960       WRITE(6,192) (ITL(I),I=1,20)
01970    192 FORMAT(1H1,4X,20A4,20X,'TABLE')
01980       WRITE(6,193)
01990    193 FORMAT(1H ,4X,80('-'),20X,12('-'))
02000       WRITE(6,115) (NAME(I),I=1,2)
02010    115 FORMAT(1HO,4X,'GRADE/TONNAGE CURVE FOR ',2A4,' CONSIDERING ',
02020      2'THE KRIGING STANDARD ERROR OF BLOCKS.')
02030       WRITE(6,118)
02040    118 FORMAT(1H ,4X,24(1H-),8(1H*),48(1H-))
02050       WRITE(6,111)
02060    111 FORMAT(1HO,4X,'CUT-OFF',6X,'NUMBER OF',
02070      26X,'CUMULATED',9X,'   TONS  ',3X,'MEAN GRADE',4X,'POSSIBLE',
02080      37X,'AVERAGE')
02090       WRITE(6,112) (NAME(I),I=1,2),(NAME(I),I=1,2)
02100    112 FORMAT(1H ,2X,'KR.ST.DEV',7X,'BLOCKS',8X.
02110      2'RESERVES',11X,2A4,4X,2A4,4X,'STAND.ERROR',4X,'STAND.ERROR')
02120 C
02130       AVEVAL=0.0
02140       DO 312 I=1,50
02150       SUMVAL=0.0
02160       SDAVE=0.0
02170       SDKAVE=0.0
02180       AVESDK=0.0
02190       AVEKSD=0.0
02200       TONGRP=0.0
02210       TONELE=0.0
02220       NBGR=0
02230       CUTOFF=(I-50)*STEP+COG
02240       DO 311 J=1,NBLK
02250       IF(SDK(J).GT.CUTOFF) GO TO 311
```

```
02260        SUMVAL=SUMVAL+VAL(J)
02270        SDAVE=SDAVE+SDK(J)*SDK(J)
02280        SDKAVE=SDKAVE+SDK(J)
02290        NBGR=NBGR+1
02300        TONGRP=NBGR*TFAC*HBENCH
02310        TONELE=TONELE+((TFAC*HBENCH*VAL(J))/1000000.0)
02320    311  CONTINUE
02330        IF(NBGR.NE.0) GO TO 31
02340        GO TO 41
02350    31  FN=1.0/FLOAT(NBGR)
02360        AVEVAL=SUMVAL*FN
02370        AVESDK=SQRT(SDAVE)*FN
02380        AVEKSD=SDKAVE*FN
02390    41  WRITE(6,711) CUTOFF,NBGR,TONGRP,TONELE,AVEVAL,
02400       2AVESDK,AVEKSD
02410    312  CONTINUE
02420    711  FORMAT(1H ,4X,F7.2,9X,I3,8X,F12.1,6X,F9.1,6X,F6.2,6X,F6.2,
02430       29X,F6.2)
02440        RETURN
02450        END
02460 //GSYSIN DD *
02470 KRIGING ESTIMATED BLOCKS IN KVANEFJELD NORTH AREA (140X140X10 METRES)
02480     52920.0 10.0
02490       0.00     25.00    150.00      5.00
02500     200.00
02510       0.0     600.0  24
02520 URANIUM
02530 (5F10.2)
```

Program: BLSELOLD

```
00010 DATA START; INFILE A;
00020 INPUT X Y Z EST STDV;
00030 DATA ET; SET START;
00040  IF X=250. AND Y=400. AND Z<=530. OR
00050     X=0.   AND Y=350. AND Z<=550. OR
00060     X=150. AND Y=350. AND Z<=570. OR
00070     X=200. AND Y=350. AND Z<=530. OR
00080     X=150. AND Y=250. AND Z<=580. OR
00090     X=200. AND Y=250. AND Z<=580. OR
00100     X=300. AND Y=250. AND Z<=590. OR
00110     X=500. AND Y=250. AND Z<=610. OR
00120     X=150. AND Y=200. AND Z<=590. OR
00130     X=200. AND Y=200. AND Z<=590. OR
00140     X=250. AND Y=200. AND Z<=590. OR
00150     X=300. AND Y=200. AND Z<=600. OR
00160     X=400. AND Y=200. AND Z<=570. OR
00170     X=500. AND Y=200. AND Z<=630. OR
00180     X=550. AND Y=200. AND Z<=590. OR
00190     X=100. AND Y=150. AND Z<=580. OR
00200     X=150. AND Y=150. AND Z<=580. OR
00210     X=200. AND Y=150. AND Z<=600. ;
00220 PROC SORT; BY Z X Y;
00230 DATA TO; SET START;
00240 IF  X=250. AND Y=150. AND Z<=610. OR
00250     X=300. AND Y=150. AND Z<=600. OR
00260     X=350. AND Y=150. AND Z<=600. OR
00270     X=400. AND Y=150. AND Z<=590. OR
00280     X=450. AND Y=150. AND Z<=590. OR
00290     X=500. AND Y=150. AND Z<=570. OR
00300     X=550. AND Y=150. AND Z<=550. OR
00310     X=250. AND Y=100. AND Z<=600. OR
00320     X=300. AND Y=100. AND Z<=590. OR
00330     X=350. AND Y=100. AND Z<=590. OR
00340     X=400. AND Y=100. AND Z<=600. OR
00350     X=450. AND Y=100. AND Z<=600. OR
00360     X=500. AND Y=100. AND Z<=560. OR
00370     X=300. AND Y=50.  AND Z<=600. OR
00380     X=350. AND Y=50.  AND Z<=590. OR
00390     X=400. AND Y=50.  AND Z<=600. OR
00400     X=450. AND Y=50.  AND Z<=570. OR
00410     X=500. AND Y=50.  AND Z<=620. OR
00420     X=300. AND Y=0.   AND Z<=580. OR
00430     X=350. AND Y=0.   AND Z<=590. OR
00440     X=400. AND Y=0.   AND Z<=590. ;
00450 PROC SORT; BY Z X Y;
00460 DATA MIX; UPDATE ET TO; BY Z X Y;
00470 FILE B;
00480 PUT (X Y Z EST STDV)(5*10.2);
```

Program: BLSELNEW

```
00010 DATA START; INFILE A1 FIRSTOBS=2;
00020 INPUT X Y Z1 EST STDV;
00030 Z=Z1+20.0;
00040 DATA ET; SET START;
00050  IF (X=0.0 OR X=70.0)  AND (Y=560. OR Y=630.) AND Z<=530. OR
00060     (X=140. OR X=210.) AND (Y=560. OR Y=630.) AND Z<=530. OR
00070     (X=280. OR X=350.) AND (Y=560. OR Y=630.) AND Z<=540. OR
00080     (X=420. OR X=490.) AND (Y=560. OR Y=630.) AND Z<=580. OR
00090     (X=560. OR X=630.) AND (Y=560. OR Y=630.) AND Z<=610. OR
00100     (X=0.0 OR X=70.)  AND (Y=420. OR Y=490.) AND Z<=560. OR
00110     (X=140. OR X=210.) AND (Y=420. OR Y=490.) AND Z<=540. OR
00120     (X=280. OR X=350.) AND (Y=420. OR Y=490.) AND Z<=550. OR
00130     (X=420. OR X=490.) AND (Y=420. OR Y=490.) AND Z<=570. OR
00140     (X=560. OR X=630.) AND (Y=420. OR Y=490.) AND Z<=600. OR
00150     (X=700. OR X=770.) AND (Y=420. OR Y=490.) AND Z<=610. OR
00160     (X=280. OR X=350.) AND (Y=280. OR Y=350.) AND Z<=570. OR
00170     (X=420. OR X=490.) AND (Y=280. OR Y=350.) AND Z<=580. OR
00180     (X=560. OR X=630.) AND (Y=280. OR Y=350.) AND Z<=600. OR
00190     (X=700. OR X=770.) AND (Y=280. OR Y=350.) AND Z<=610. OR
00200     (X=840. OR X=910.) AND (Y=280. OR Y=350.) AND Z<=640. OR
00210     (X=420. OR X=490.) AND (Y=140. OR Y=210.) AND Z<=600. OR
00220     (X=560. OR X=630.) AND (Y=140. OR Y=210.) AND Z<=590. OR
00230     (X=700. OR X=770.) AND (Y=140. OR Y=210.) AND Z<=600. OR
00240     (X=840. OR X=910.) AND (Y=140. OR Y=210.) AND Z<=620. OR
00250     (X=980. OR X=1050.) AND (Y=140. OR Y=210.) AND Z<=650. OR
00260     (X=840. OR X=910.) AND (Y=0.0 OR Y=70.)  AND Z<=610. ;
00270 FILE B1;
00280 PUT (X Y Z EST STDV)(5*10.2);
```

Program: FGAM

```
00050 C     PROGRAM **FGAM** VERSION 1
00060 C
00070 C     THIS PROGRAMME COMPUTES THE GAMMA-VALUE FOR DIFFERENT VALUES
00080 C     OF H OF A ONE-COMPONENT SPHERICAL SCHEME.
00100 C
00110       DIMENSION GAM(50)
00120       A1=2.5
00140       C1=28.932E+3
00160       C0=5.6E+3
00170 C
00180       WRITE(6,12) C0,C1,A1
00190    12 FORMAT(1X,'GAMMA-VALUES OF A ONE-COMPONENT SPHERICAL SCHEME WITH F
00200      1OLLOWING PARAMETERS'//2X,'C0= ',F9.2,4X,'C1= ',F9.2,4X,'A1= ',F6.1
00210      2,1X,'METERS',///)
00220       WRITE(6,13)
00230    13 FORMAT(10X,'DISTANCE H',5X,'GAMMA(H)'//)
00240 C
00241        IANT=IFIX(A1)+5
00250       DO 10 I=1,IANT
00260       IF(I.LT.IFIX(A1)) GO TO 4
00280       GAM(I)=C0+C1
00290       GO TO 16
00300     4 GAM(I)=C0+C1*((1.5*(I/A1))-(0.5*((I/A1)**3)))
00340    16 WRITE(6,14) I,GAM(I)
00350    14 FORMAT(14X,I2,8X,F9.2)
00360    10 CONTINUE
00370       STOP
00380       END
```

Program: FGAM2

```
00010 C      PROGRAM **FGAM2** VERSION 2
00020 C
00030 C
00040 C      THIS PROGRAM COMPUTES THE GAMMA-VALUES FOR DIFFERENT VALUES
00050 C      OF H OF A 2-COMPONENT SEMIVARIOGRAM. EACH COMPONENT FOLLOWS
00060 C      A SPHERICAL SCHEME.
00070 C
00080        DIMENSION GAM(150)
00090        A1=20.0
00100        A2=105.0
00110        C1=1.2E+3
00120        C2=7.5E+3
00130        C0=2.8E+3
00140 C
00150        WRITE(6,12) C0,C1,A1,C2,A2
00160    12  FORMAT(1X,'GAMMA-VALUES OF A TWO-COMPONENT SPHERICAL SCHEME WITH
00170       1FOLLOWING PARAMETERS'//2X,'C0= ',F9.2,4X,'C1= ',F9.2,4X,'A1= ',
00180       2F6.1,1X,'METERS'//19X,'C2= ',F9.2,4X,'A2= ',F6.1,' METERS'///)
00190        WRITE(6,13)
00200    13  FORMAT(10X,'DISTANCE H',5X,'GAMMA(H)'//)
00210 C
00220        IANT=IFIX(A2)+5
00230        DO 10 I=1,IANT,2
00240        IF (I.LE.IFIX(A1)) GO TO 5
00250        IF (I.GT.IFIX(A1).AND.I.LT.IFIX(A2)) GO TO 4
00260        GAM(I)=C0+C1+C2
00270        GO TO 16
00280     4  GAM(I)=C0+C1+C2*((1.5*(I/A2))-(0.5*((I/A2)**3)))
00290        GO TO 16
00300     5  GAM(I)=C0+C1*((1.5*(I/A1))-(0.5*((I/A1)**3)))+C2*((1.5*(I/A2))-
00310       2(0.5*((I/A2)**3)))
00320    16  WRITE(6,14) I,GAM(I)
00330    14  FORMAT(14X,I2,8X,F9.2)
00340    10  CONTINUE
00350        STOP
00360        END
```

Program: FGAM3

```
C     PROGRAM **FGAM3** VERSION 1
C
C     THIS PROGRAMME COMPUTES THE GAMMA-VALUE FOR DIFFERENT VALUES
C     OF H OF A 3-COMPONENT SEMIVARIOGRAM. EACH COMPONENT FOLLOWS
C     A SPHERICAL SCHEME AND A FOURTH COMP. (THE NUGGET EFFECT) IS
C     ALSO ENCOUNTERED.
C
      DIMENSION GAM(120)
      A1=5.0
      A2=20.0
      A3=105.0
      C1=4.2E+3
      C2=3.5E+3
      C3=13.7E+3
      C0=1.0E+3
C
      WRITE(6,12) C0,C1,A1,C2,A2,C3,A3
   12 FORMAT(1X,'GAMMA-VALUES OF A   3-COMPONENT SPHERICAL SCHEME WITH F
     1OLLOWING PARAMETERS'//2X,'C0= ',F9.2,4X,'C1= ',F9.2,4X,'A1= ',F6.1
     2,1X,'METERS',/19X,'C2= ',F9.2,4X,'A2= ',F6.1,1X,'METERS',
     3/,19X,'C3= ',F9.2,4X,'A3= ',F6.1,' METRES.',///)
      WRITE(6,13)
   13 FORMAT(10X,'DISTANCE H',5X,'GAMMA(H)'//)
C
      DO 10 I=1,130
      IF(I.LT.IFIX(A1)) GO TO 5
      IF(I.GE.IFIX(A1).AND.I.LT.IFIX(A2)) GO TO 4
      IF(I.GE.IFIX(A2).AND.I.LT.IFIX(A3)) GO TO 3
      GAM(I)=C0+C1+C2+C3
      GO TO 16
    3 GAM(I)=C0+C1+C2+C3*((1.5*(I/A3))-(0.5*((I/A3)**3)))
      GO TO 16
    4 GAM(I)=C0+C2*((1.5*(I/A2))-(0.5*((I/A2)**3)))+C3*((1.5*(I/A3))-(0.
     15*((I/A3)**3)))+C1
      GO TO 16
    5 GAM(I)=C0+C1*((1.5*(I/A1))-(0.5*((I/A1)**3)))+C2*((1.5*(I/A2))-(0.
     15*((I/A2)**3)))+C3*((1.5*(I/A3))-(0.5*((I/A3)**3)))
   16 WRITE(6,14) I,GAM(I)
   14 FORMAT(14X,I3,8X,F9.2)
   10 CONTINUE
      STOP
      END
```

Program: FRESP2

```
01000 //A179002F JOB (***,NEU,2,1),'F SEMI REGULARI',REGION=200K,RATE=NORM
02000 /*ROUTE  PRINT INTERNAL
03000 // EXEC FORTG,CPRINT=DUMMY,LPRINT=DUMMY
04000 //CSYSIN DD *
10000 C     PROGRAM ***FRESP2*** WHICH CALCULATES THE REGULARIZED SEMIVARIGRAM
20000 C     OF A TWO COMPONENT SPHERICAL MODEL, BY USE OF ROUTINE REGSPH.
30000 C
40000       DIMENSION GL(35),GL1(35),GL2(35),H(35)
50000       C0=5.6E+03
60000       A1=2.5
70000       A2=29.0
80000       C1=16.932E+03
90000       C2=12.0E+03
100000 C     NUMBER OF POINTS TO BE ESTIMATED
110000       NH=35
120000       DO 10 I=1,NH
130000       H(I)=FLOAT(I)
140000    10 CONTINUE
150000       CALL REGSPH(GL1,H,NH,A1,C1,1.0)
160000       CALL REGSPH(GL2,H,NH,A2,C2,1.0)
170000       WRITE(6,101) C0,A1,C1,A2,C2
180000   101 FORMAT(2X,'REGULARIZED SEMIVARIOGRAM FOR A TWO COMPONENT'/
190000      12X,'SPHERICAL MODEL (POINT), WITH FOLLOWING PARA-'/
200000      22X,'METERS:'//1X,'C0= ',F7.1,', A1= ',F4.1,' METERS,  C1= ',
210000      3F8.1,', A2= ',F4.1,' METERS,  C2= ',F8.1,'.',/)
220000       WRITE(6,102)
230000       WRITE(6,103)
240000       WRITE(6,104)
250000   102 FORMAT(2X,'THE CALCULATIONS ARE CARRIED OUT BY ROUTINE'/
260000      12X,'REGSPH (COMP & GEOSC. VOL 3 PP. 341-346)'/)
270000   103 FORMAT(2X,'GAMMAL = C0 + GAMM1 + GAMM2'//)
280000   104 FORMAT(1X,'DISTANCE',4X,'GAMM1',7X,'GAMM2',7X,'GAMMAL'/)
290000       DO 20 I=1,NH
300000       GL(I)=GL1(I)+GL2(I)+C0
310000       WRITE(6,100) H(I),GL1(I),GL2(I),GL(I)
320000   100 FORMAT(2X,F5.1,3X,F9.1,3X,F9.1,3X,F9.1)
330000    20 CONTINUE
340000       STOP
350000       END
```

Program: BMDP7M

```
00010 //A179002F JOB (***,NEU,04,04),'F BMDP7M-LUJA SUB',REGION=300K,
00020 // RATE=NORMAL,NOTIFY=A179002
00030 /*ROUTE  PRINT INTERNAL
00040 // EXEC SASBMDP
00050 //SUB DD DSN=NEU.A179002.KVANESUB,DISP=OLD
00060 //SYSIN DD *
00070 DATA START; SET SUB.LUJA;
00080 IF GEO='499' OR GEO='239' THEN DELETE;
00090 IF NUMBER='55016' OR NUMBER='55018' OR NUMBER='55030' OR NUMBER='55040'
00100 THEN DELETE;
00110 IF NUMBER='59120' THEN DELETE;
00120  IF NUMBER='48168' THEN GEO='296';
00130  IF NUMBER='48170' THEN GEO='296';
00140  IF NUMBER='48176' THEN GEO='296';
00150  IF NUMBER='48180' THEN GEO='296';
00160  IF NUMBER='48182' THEN GEO='296';
00170  IF NUMBER='48186' THEN GEO='296';
00180  IF NUMBER='48190' THEN GEO='296';
00190  IF NUMBER='48192' THEN GEO='296';
00200 GEO1=0;
00210 IF GEO='299' THEN GEO1=1;
00220 IF GEO='296' THEN GEO1=2;
00230 IF GEO='297' THEN GEO1=2;
00240 IF GEO='295' THEN GEO1=1;
00250 PROC SORT; BY NUMBER;
00260 PROC PRINT;
00270 DATA CC; SET START;
00280 DROP NUMBER GEO;
00290 PROC BMDP PROG=BMDP7M;
00300 VAR GEO1  NA6 ZR2 NB2 U1 TH1 Y2 CE6 LA6 HF6TA6 TH1U1 MN7FE7
00310     ZN7Y2 ZN7PB7 NB2U1 ZN7U1 Y2PB7 Y2U1 ZR2U1 TH1PB7 FE7PB7;
00320 PARMCARDS;
00330 /PROB TITLE IS 'DATA WITH GAM-SPEC, EDXPLU, ENAA AND XRF'.
00340 /INPUT UNIT=3. CODE='CC'. VARIABLES ARE 22.
00350 /VARIAB GROUP=GEO1.
00360 /GROUP CODE= 1 TO 2.
00370        NAMES ARE ARFV,NAUJ.
00380 /DISC ENTER=.01 .
00390       REMOVE=0.0 .
00400 /END
```

Program: BMDPKM

```
00010 //A179002F JOB (***,NEU,04,02),'F BMDPKM',NOTIFY=A179002,RATE=FAST,
00020 // REGION=500K,IO=2000
00030 /*ROUTE  PRINT INTERNAL
00040 // EXEC BMDP,PROG=BMDPKM
00050 //FT11F001 DD DSN=NEU.A179002.SUBKVA,DISP=OLD
00060 //SYSIN DD *
00070 /PROB TITLE IS 'DATA WITH GAM-SPEC, EDXPLU, ENAA AND XRF'.
00080 /INPUT UNIT=11. VARIABLES ARE 37.
00090        FORMAT IS '(A3,A4,1X,2F6.0,33F9.3)'.
00100 /VARIAB NAMES ARE GEO,NUMBER,NA6,FE6,K1,U1,TH1,ZR2,Y2,SR2,RB2,TH2,
00110                   PB2,GA2,ZN2,NB2,CS2,LA6,CE6,SM6,EU6,YB6,LU6,
00120                   HF6,TA6,TH6,K7,CA7,TI7,MN7,FE7,NI7,CU7,ZN7,
00130                   GA7,SR7,PB7.
00140         LABELS ARE GEO,NUMBER.
00150 /CLUSTER NUMBER IS 8.
00160          STANDARD=VAR.
00170 /END
```

APPENDIX B1

A simple kriging example in two dimensions.

The example given below explains how two dimensional kriging is carried out in practice. Because of of the simple block-sample pattern chosen, the calculations can be performed by hand. The problem is shown in the following diagram:

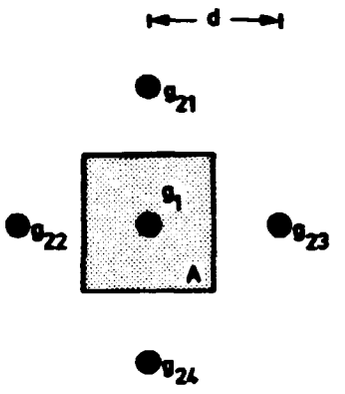

in which block A is to be estimated from the samples g_{ij}. The internal sample is denoted by 1 and the external samples by 2. In this example the distance d is 50 metres; that is, the block to be estimated has the size 50 x 50 metres. The semi-variogram model is the point model found in the Mine area, and is given by:

	C_0 = 5600 ppm U^2
a_1 = 2.5 metres,	C_1 = 16932 ppm U^2
a_2 = 29.0 metres,	C_2 = 12000 ppm U^2
Total sill:	3453? ppm U^2

The <u>effective</u> nugget effect constitutes:

At distance h = 0:	16.2%	(C_0 = 5,600)
At distance h = 2.5:	65.3%	($C_0' = C_0+C_1$)

of the total variation. The kriging estimator has the form:

$$Z^*(A) = w_1 Z(g_1) + w_2 Z(g_2)$$

where, because of symmetry:

$$Z(g_2) = 0.25(Z(g_{21}) + Z(g_{22}) + Z(g_{23}) + Z(g_{24}))$$

Now, since there are only two coefficients to be estimated, w_1 and w_2, it follows from the non-bias condition that

$$w_1 = 1 - w_2$$

so that the kriging systems of equations can be written:

$$\begin{cases} w_1\bar{\gamma}(g_1,g_1) + (1-w_1)\bar{\gamma}(g_1,g_2) + \lambda = \bar{\gamma}(g_1,A) \\ w_1\bar{\gamma}(g_2,g_1) + (1-w_1)\bar{\gamma}(g_2,g_2) + \lambda = \bar{\gamma}(g_2,A) \end{cases}$$

Subtraction of the first of these from the second eliminates λ and gives:

$$w_1 = \frac{\bar{\gamma}(g_2,A) - \bar{\gamma}(g_1,A) + \bar{\gamma}(g_1,g_2) - \bar{\gamma}(g_2,g_2)}{2\bar{\gamma}(g_1,g_2) - \bar{\gamma}(g_1,g_1) - \bar{\gamma}(g_2,g_2)}$$

Thus, all that remains is to evaluate the $\bar{\gamma}$-terms. The between-sample terms are calculated directly from the model formula:

Between-sample terms:

a) $\bar{\gamma}(g_1,g_1) = 0$ (point samples)

b) $\bar{\gamma}(g_1,g_2) = \bar{\gamma}(g_2,g_1)$

$= \gamma(50) = C_o + C_1 + C_2 = 34532$ ppm U^2

c) $\bar{\gamma}(g_2,g_2) = 1/4\left[\bar{\gamma}(g_{21},g_{21}) + \bar{\gamma}(g_{21},g_{22}) + \bar{\gamma}(g_{21},g_{23}) + \bar{\gamma}(g_{21},g_{24})\right]$

$= 1/4\left[\gamma(0) + 2\gamma(50\sqrt{2}) + \gamma(100)\right]$

$= 3/4\left[C_o + C_1 + C_2\right]$

$= 25899$ ppm U^2

The sample-block terms are calculated using the auxiliary function $H(\ell,b)$ which gives the mean semi-variogram value between a point and a panel. Using the symmetrical pattern:

Sample-block terms:

$$\text{a) } \bar{\gamma}(g_1,A) = \left[4 \cdot 25.0^2 \cdot H(25.0,25.0)\right] / \ 50.0^2$$

$$= H(25.0,25.0)$$

$$= C_0 + C_1 H_1(25.0/2.5,25.0/2.5) + C_2 H_2(25.0/29.0,25.0/29.0)$$

$$= 5600 + 16932(\simeq 1) + 12000 \cdot 0.788$$

$$= 31988 \text{ ppm } U^2$$

$$\text{b) } \bar{\gamma}(g_2,A) = \left[2 \cdot 75.0 \cdot 25.0 \cdot H(25.0,75.0) - 2 \cdot 25.0^2 \cdot H(25.0,25.0)\right] / \ 50.0^2$$

$$= 1.5 \cdot H(25.0,75.0) - 0.5 \cdot H(25.0,25.0)$$

$$= 1.5\left[C_0 + C_1 \cdot H_1(25.0/2.5,75.0/2.5) + C_2 \cdot H_2(25.0/29,75.0/29)\right]$$
$$-0.5\left[C_0 + C_1 \cdot H_1(25.0/2.5,25.0/2.5) + C_2 \cdot H_2(25.0/29,25.0/29)\right]$$

$$= 1.5\left[C_0 + C_1(\simeq 1) + C_2 \cdot 0.926\right] - 0.5\left[C_0 + C_1(\simeq 1) + C_2 \cdot 0.788\right]$$

$$= 34472 \text{ ppm } U^2$$

The within-block variance is finally calculated to be used in the calculation of the kriging variance:

Within-block variance:

$$\bar{\gamma}(A,A) = F(50.0,50.50)$$

$$= C_0 + C_1 F_1(20.0,20.0) + C_2 F_2(1.72,1.72)$$

$$= 5600 + 16932(\simeq 1) + 12000 \cdot 0.844$$

$$= 32660 \text{ ppm } U^2$$

The kriging weights can now be calculated:

$$w_1 = \frac{34472 - 31988 + 34532 - 25899}{2 \cdot 34532 - 0 - 25899}$$

$$= 0.258$$

$$w_2 = 1 - w_1 = 0.742 \qquad (1/4 \cdot w_2 = 0.186)$$

The Lagrangian Multiplier is found from the kriging system of equations:

$$(1-w_1)\bar{\gamma}(g_1,g_2) + \lambda = \bar{\gamma}(g_1,A)$$

$$0.742 \cdot 34532 + \lambda = 31988 \Rightarrow \lambda = 6365.2$$

Finally, the kriging variance (or the kriging standard error) is calculated:

$$\sigma_k^2 = \sum w_i \bar{\gamma}(g_i,A) + \lambda - \bar{\gamma}(A,A)$$

$$= 0.258 \cdot 31988 + 0.742 \cdot 34472 + 6365.2 - 32660$$

$$= 7536 \text{ ppm } U^2$$

$$\sigma_k = 86.8 \text{ ppm U}$$

The values for the auxiliary functions H and F have been obtained from standardised tables, e.g. Royle (1977).

On the following page six sample-block patterns have been evaluated by simple kriging. In each case the sample weights have been calculated and the error of estimation determined. The block size is in all cases 10 x 10 metres. As in the previous example, the point semi-variogram model from the Mine area has been used in the kriging procedure.

Practical kriging examples.

$w_1 = 1$

$\sigma_k^2 = 18532$
$\sigma_k = 136.1$

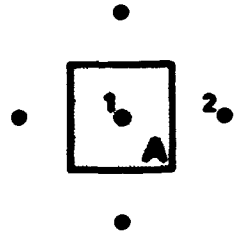

$w_1 = 0.277$
$w_2 = 0.181$

$\sigma_k^2 = 5650$
$\sigma_k = 75.2$

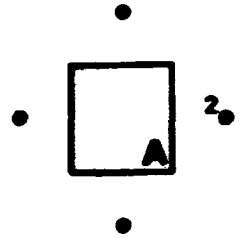

$w_2 = 0.250$

$\sigma_k^2 = 8467$
$\sigma_k = 92.0$

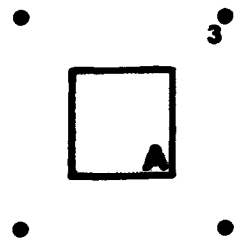

$w_3 = 0.250$

$\sigma_k^2 = 10883$
$\sigma_k = 104.3$

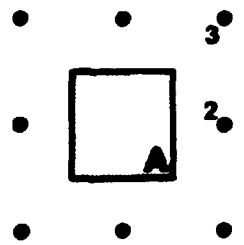

$w_2 = 0.148$
$w_3 = 0.102$

$\sigma_k^2 = 6267$
$\sigma_k = 79.2$

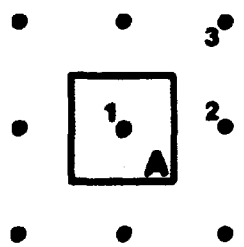

$w_1 = 0.225$
$w_2 = 0.114$
$w_3 = 0.080$

$\sigma_k^2 = 4701$
$\sigma_k = 68.6$

APPENDIX B2

Example of output from TREREG (block kriging). Estimation in the Northern area.

THE BOREHOLE DATA READ IN IS AS FOLLOWS:

NUMBER	IDENTIFIER		POSITION	
1	39	1060.73	204.18	664.46
2	40	1056.54	212.43	659.36
3	45	924.78	345.88	651.00
4	46	922.65	205.96	621.00
5	47	932.90	361.23	651.00
6	48	790.54	205.36	601.00
7	49	775.79	351.31	619.00
8	50	635.13	511.65	607.00
9	54	906.22	69.84	617.00
10	55	781.35	467.20	607.00
11	56	613.81	221.95	601.00
12	57	635.23	359.14	603.00
13	58	499.89	356.44	589.00
14	59	501.57	507.30	583.00
15	60	520.47	204.14	603.00
16	61	334.68	355.15	571.00
17	62	219.52	513.06	543.00
18	63	71.74	500.23	517.00
19	64	739.76	640.84	625.00
20	65	421.03	471.65	557.00
21	66	456.12	617.71	573.00
22	67	361.05	637.12	473.00
23	68	226.31	644.21	463.00
24	69	54.22	628.84	521.00
25	70	548.75	343.95	651.00

THE FINAL NUMBER OF BENCH COMPOSITES FORMED IS 249

ESTIMATED MEAN OF COMPLETE VOLUME IS 177.25 AND

ITS STANDARD ERROR IS 15.92

```
   TITLE FOR THIS RUN IS BLOCK-KRIGING  IN NORTHERN AREA OF KVANEFJELD  (KRIGING ONLY) S: 140X140X20

YOU HAVE REQUESTED KRIGING WITHOUT (?) GEOREGRESSION
YOUR MODEL FOR THE SEMI-VARIOGRAM CONTAINS 3 SPHERICAL COMPONENTS
     AND A NUGGET EFFECT OF    3300.00
    THE PROGRAM WILL USE ANISOTROPY FACTORS OF
                1.00 FOR THE EASTINGS
                1.00 FOR THE NORTHINGS, AND
                1.00 FOR THE ELEVATIONS

THE PARAMETERS FOR YOUR MODEL ARE

     RANGE OF INFLUENCE           SILL
              6.5               1731.00
             15.0               3931.00
            124.0              15764.00


THE KRIGING PROCEDURE WILL SEARCH 0 BLOCKS EAST AND WEST,
     0 BLOCKS NORTH AND SOUTH, AND 4 BLOCKS ABOVE AND BELOW THE BENCH.

THE BOREHOLE DATA IS EXPECTED TO BE ON CHANNEL 9

THE DATA IS EXPECTED TO BE IN THE FORM
     IDENTIFIER, VALUE, EASTING, NORTHING, ELEVATION - AND YOU HAVE SPECIFIED THE FOLLOWING FORMAT
      (A4,13X,F8.2,3F9.2)

STIMATED BLOCKS WILL BE OUTPUT (IN 5F10.2) TO CHANNEL 8      (SEE DOCUMENTATION)

BLOCK SIZE REQUIRED IS 140.0 (EAST), BY 140.0 (NORTH),
 BENCH HEIGHT IS   20.0

THE VOLUME TO BE CONSIDERED IS
        0.0 TO  1120.0 EAST,        0.0 TO   700.0 NORTH AND   270.0 TO   670.0 IN ELEVATION
```

BLOCK-KRIGING IN NORTHERN AREA OF KVANEFJELD (KRIGING ONLY) S: 140X140X20

BENCH NUMBER 10 ELEVATION 470.0 TO 490.0 PAGE NUMBER 1

THIS PAGE COVERS 0.0 TO 1120.0 EAST
AND 0.0 TO 700.0 NORTH.

167.05 69.59	97.34 93.44	74.66 92.94	63.00 69.28	-10.00 -10.00	123.01 69.51	-10.00 -10.00	-10.00 -10.00	
122.55 65.05	236.71 65.88	-10.00 -10.00	174.32 45.06	161.38 64.90	148.90 65.65	-10.00 -10.00	-10.00 -10.00	
-10.00 -10.00	-10.00 -10.00	224.06 60.46	255.43 61.95	240.93 61.74	238.85 61.49	240.85 76.70	-10.00 -10.00	
110.59 102.62	125.97 99.91	140.13 104.83	258.74 54.46	127.59 52.74	156.14 53.62	178.11 60.72	144.91 75.74	
146.25 92.57	125.90 93.73	152.00 96.26	160.20 76.87	159.18 82.92	162.72 79.55	94.10 54.13	181.91 113.77	

TITLE FOR THIS RUN IS BLOCK-KRIGING IN NORTHERN AREA OF KVANEFJELD (KRIGING ONLY) S: 140X140X20

SUMMARY STATISTICS FOR THIS RUN OF TREREG
KRIGING WITH GEOREGRESSION

THE NUMBER OF BLOCKS ESTIMATED IN THIS RUN IS 515

THE AVERAGE VALUE OF THE BLOCKS IS 140.5539
AND THE STANDARD DEVIATION OF THESE VALUES IS 62.4061

THE AVERAGE KRIGING STANDARD DEVIATION IS 85.1403
AND THESE HAVE A STANDARD DEVIATION OF 26.5814

THE AVERAGE KRIGING VARIANCE IS PROBABLY 8673.9883

THE BLOCK VALUES GIVE THE FOLLOWING HISTOGRAM

ENDPOINT	FREQ.	
16.814	8	I**********
33.627	3	I***
50.441	23	I**************************
67.255	8	I**********
84.068	35	I**
100.882	57	I**
117.696	41	I**
134.510	46	I**
151.323	60	I**
168.137	54	I**
184.951	51	I***
201.764	31	I**
218.578	31	I**
235.392	21	I****************************
252.205	20	I**************************
269.019	8	I**********
285.833	8	I**********
302.646	6	I*******
319.460	1	I*
336.273	2	I**
353.087	0	I
369.901	1	I*
386.715	0	I
403.528	0	I
420.342	0	I

APPENDIX C1

Examples of input data formats.

Examples of input format of the data considered in this study are given below. Description of the individual input records is given by the computer program CRKVAN listed in appendix A.

Example 1: Fluorine analyses (FLUOR)

```
5896,296,15,0.72
58100,296,15,1.52
58104,296,15,1.01
58110,296,15,1.42
58114,296,15,0.90
58118,296,15,1.01
58122,296,15,1.10
58126,296,15,1.11
58130,296,15,0.48
58134,296,15,0.47
58138,296,15,0.51
58142,296,15,0.72
58146,296,15,0.73
58150,296,15,1.01
58154,296,15,1.40
58158,296,15,1.45
58162,296,15,1.19
58166,296,15,1.40
```

Example 2: Lithium and beryllium analyses (OPSPEC)

```
4660,295,14,65,1950
4670,295,14,44,1500
46150,296,14,74,2850
4860,295,14,74,1850
48150,297,14,46,2500
48160,297,14,80,2600
48170,297,14,78,2350
48180,297,14,62,2050
48190,297,14,46,2350
4930,295,14,58,1550
49120,296,14,55,2350
49130,296,14,60,2350
49140,296,14,88,2050
49150,296,14,46,2850
49160,296,14,44,3300
5000,295,14,84
5010,299,14,60
5020,299,14,53
```

Example 3: Energy dispersive X-ray fluorscence (EDX-CD).

One observation is composed of 10 input records.

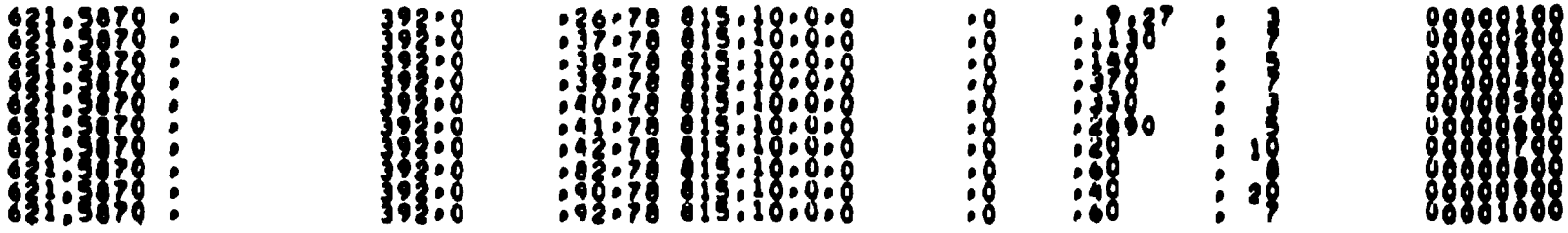

Example 4: Energy dispersive X-ray fluorscence (EDX-PLU).

One observation is composed of 13 input records.

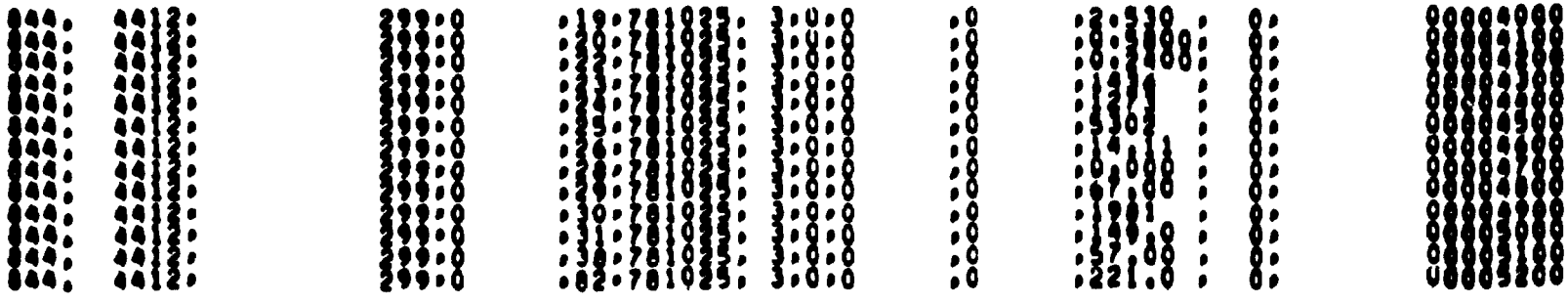

Example 5: Gamma-spectrometer analyses of drill core samples (GAM-SPEC).

Drill hole	top	bottom	GEO	K %	σ(K)	U ppm	σ(U)	Th ppm	σ(Th)	
64	42.00	43.00	299	2.04	0.12	127.0	0.7	216.0	1.6	06402200
64	44.00	45.00	299	2.07	0.12	147.0	0.7	174.0	1.5	06402300
64	46.00	47.00	299	2.21	0.12	145.0	0.7	149.0	1.5	06402400
64	48.00	49.00	299	2.14	0.12	172.0	0.8	160.0	1.6	06402500
64	50.00	51.00	299	1.79	0.13	160.0	0.8	154.0	1.6	06402600
64	52.00	53.00	299	1.72	0.12	185.0	0.8	173.0	1.6	06402700
64	54.00	55.00	299	2.33	0.13	189.0	0.8	171.0	1.7	06402800
64	56.00	57.00	299	2.16	0.13	188.0	0.9	188.0	1.7	06402900
64	58.00	59.00	299	2.26	0.13	152.0	0.8	143.0	1.6	06403000
64	60.00	61.00	299	1.95	0.12	131.0	0.7	138.0	1.5	06403100
64	62.00	63.00	299	1.87	0.12	122.0	0.7	138.0	1.5	06403200

Example 6: Gamma-spectrometer values, surface data.

Codes: Amount of A: outcrop, B: scree, C: sand, soil, D: vegetation and E: snow, water.

Area	X	Y	GEO	K %	σ(K)	U ppm	σ(U)	Th ppm	σ(Th)	A	B	C	D	E	
1	160.00	120.00	0	0.00	0.00	206.4	0.2	550.9	0.1	0	2	5	3	0	00002100
1	150.00	120.00	294	0.00	0.00	198.1	0.2	532.4	0.1	2	0	8	0	0	00002200
1	150.00	90.00	429	0.00	0.00	126.9	0.4	646.8	0.1	0	9	1	0	0	00002300
1	140.00	90.00	234	0.00	0.00	188.3	0.2	541.6	0.1	0	9	1	0	0	00002400
1	130.00	90.00	293	0.00	0.00	269.3	0.2	743.1	0.1	0	3	0	7	0	00002500
1	120.00	90.00	293	0.00	0.00	398.7	0.2	1048.4	0.1	5	2	3	0	0	00002600
1	110.00	90.00	293	0.00	0.00	351.3	0.2	1126.9	0.1	0	4	6	0	0	00002700
1	110.00	70.00	293	0.00	0.00	375.9	0.2	1114.4	0.1	4	2	3	1	0	00002800
1	120.00	70.00	240	0.00	0.00	326.0	0.2	839.8	0.1	5	3	1	1	0	00002900
1	130.00	70.00	299	0.00	0.00	337.3	0.2	629.4	0.1	0	5	5	0	0	00003000
1	140.00	70.00	293	0.00	0.00	271.5	0.2	709.4	0.1	0	7	0	3	0	00003100
1	150.00	70.00	0	0.00	0.00	131.8	0.3	407.3	0.1	0	1	0	9	0	00003200

Example 7: X-ray fluorscence analyses (XRF).

```
4460,249,13,1998,291,34,896,133,182,134,1[illegible],315
4462,296,13,2359,272,27,647,59,114,127,696,193
4464,296,13,2657,290,32,713,45,[illegible],139,926,174
4466,296,13,3484,370,32,759,68,158,159,1754,163
4468,296,13,4135,450,34,875,77,147,165,1443,211
4470,296,13,4414,503,31,854,112,157,169,1812,228
4472,296,13,2779,368,40,835,143,115,156,1649,192
4474,296,13,3290,533,38,835,145,156,170,1963,180
4476,296,13,2722,498,30,727,113,121,145,1108,224
4478,296,13,2179,368,25,679,78,98,129,833,226
```

Example 8: Logging data.

```
BOREHOLE 59 LOGGING RESULTS:

ST     = 0.6381
SU     = 1.9211
BU     = 32
ALPHA  = 2.2213

 METERS    PPM U    PPM TH    TH/U

  1-  2      361       996    2.76
  2-  3      400      1336    3.34
  3-  4      367      1159    3.16
  4-  5      363      1777    4.90
  5-  6      132       311    2.36
  6-  7       92       194    2.12
  7-  8      214       869    4.07
  8-  9      352      1148    3.26
  9- 10      390      1104    2.83
 10- 11      407      1225    3.01
 11- 12      378      1021    2.70
 12- 13      334       868    2.60
 13- 14      351       615    1.75
 14- 15      403      1187    2.94
 15- 16      414      1159    2.80
 16- 17      281      1645    5.85
 17- 18      119       302    2.53
 18- 19      263      1130    4.30
 19- 20      359      1466    4.08
 20- 21      370      1545    4.17
```

Example 9: Neutron activation analyses (ENAA).

One observation is composed of 16 input records.

```
55.002          FE886I
0   3 .000      .00 .000     11 .161+06 4.80 .153+05 19 .000     .00 .000
0  20 .000      .00 .138+06  21 .000     .00 .450-01 24 .000    9.07 .798+01
0  25 .000      .00 .000     26 .962+05 1.21 .901+03 27 .000     .00 .991+00
0  30 .241+04 1.27 .285+02  31 .000     .00 .000    33 .000     .00 .764+02
0  34 .000      .00 .574+01  35 .000     .00 .318+02 37 .000    2.62 .590+02
0  38 .000      .00 .313+03  40 .000     .00 .370+03 41 .000     .00 .412+03
0  42 .000      .00 .194+04  47 .000     .00 .436+01 48 .000     .00 .536+03
0  50 .000      .00 .712+03  51 .000     .00 .267+01 53 .000     .00 .000
0  55 .161+02 2.51 .763+00  56 .000    3.41 .462+03 57 .170+04 1.55 .663+01
0  58 .306+04 1.04 .554+01  59 .000     .00 .109+05 60 .702+03 5.47 .846+02
0  62 .141+03 1.12 .967-02  63 .683+01 3.14 .431+00 64 .000     .00 .826+01
0  65 .124+02 2.23 .497+00  66 .000     .00 .722+03 67 .000     .00 .000
0  70 .638+02 1.42 .131+01  71 .914+01 2.42 .377+00 72 .362+02 1.32 .524+00
0  73 .126+02 4.60 .125+01  74 .000     .00 .187+03 79 .000     .00 .118+00
1  80 .000      .00 .203+01  90 .612+03 1.04 .889+00 92 .000    5.48 .441+02
```

APPENDIX C2

Coding-sheet used for chip samples

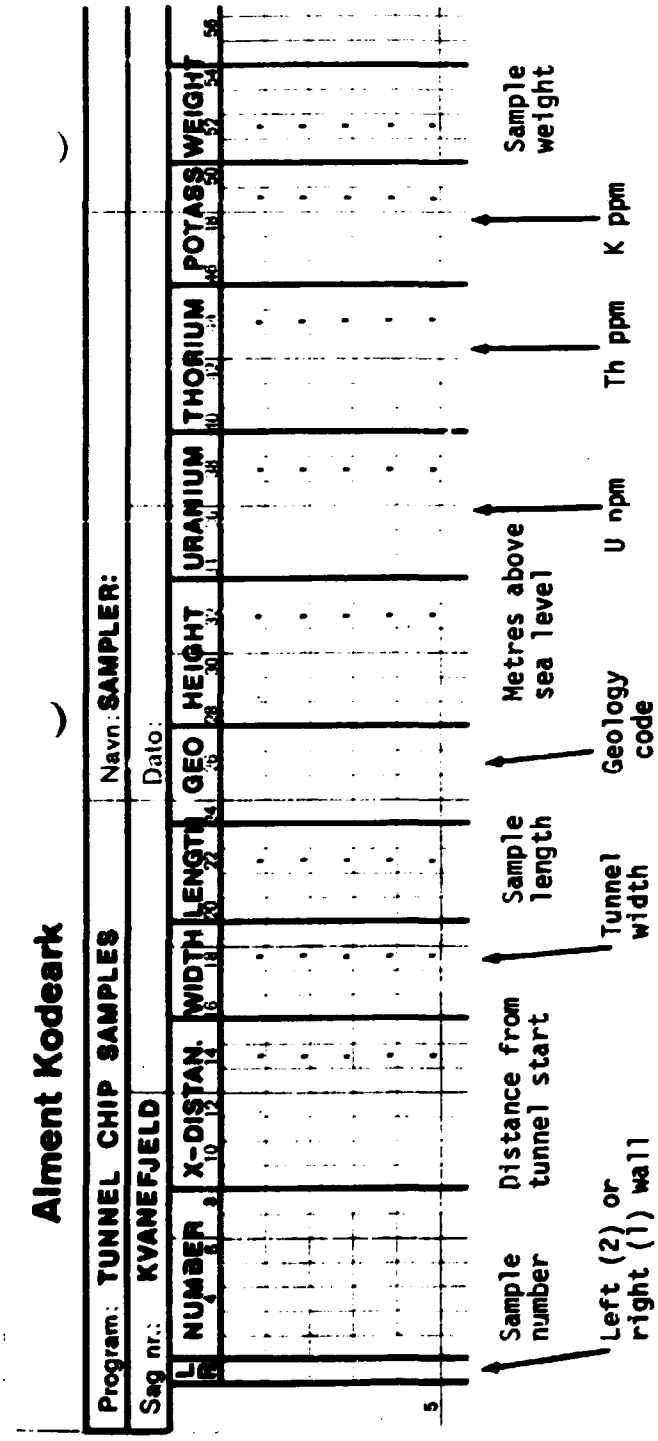

APPENDIX D

List of symbols used.

A	Block to be estimated
a	Range of influence
$\hat{a},\hat{b}$	Regression parameters
α,β	Log-normal distribution parameters
b_o	Orthogonal regression coefficient
C	Sill value
C_o	Nugget effect
c_{ti}	Classification coefficient
$cov(h)$	Covariogram function
COG	Cutoff grade
$D^2_{m\ell}$	Mahalanobis distance
d	distance
$d_{j\ell}$	Euclidian distance
$D_t(\underline{X})$	Discriminant function
$D(x,h)$	Difference in grades
Δ	Confidence level
$E\{Z(x)\}$	Expectation of the RV $Z(x)$
$F(\ell)$	Variance of grades within a line
$F(\ell,b,d)$	Variance of grades within a 3-D block
F_1,F_2,f	Variance factors
$\Phi(z)$	Probability that a Standard Normal variate is less than z
g_i	A sample
$\gamma(h)$	The semi-variogram
$2\gamma(h)$	The variogram
$\hat{\gamma}$	Estimator for γ
$\gamma^*(h)$	Experimental point semi-variogram
$\gamma_\ell(h)$	Experimental regularised semi-variogram
$\bar{\gamma}(g_i,g_j)$	Mean semi-variogram value between sample g_i and sample g_j
$\bar{\gamma}(g_i,A)$	Mean semi-variogram value between sample g_i and the block A

$\bar{\gamma}(A,A)$	The within-block semi-variogram value
h	Distance, lag
k	Exponent, number of groups
L, ℓ	Lengths of samples
λ	Lagrangian Multiplier
$m(x)$	Drift at point x
M	Diagonal variance matrix
n', n''	Points within samples
n, $n(h)$	Number of samples or sample pairs
p	Slope of a linear semi-variogram, number of variables
P_1, P_2, p_1, p_2	Proportions
S_x, S_y, S_{xy}	Sum of squared differences
σ^2_ϵ	Estimation variance
σ^2_k	Kriging variance
σ^2	A priori variance of Z(x)
$V\{Z(x)\}$	Variance of the RV Z(x)
w_i	Sample weights
x,y,z	Spatial coordinates
X,Y	Regression variables
X_{ij}	Stochastic multi-variable
$\bar{x}_{ci}$	Average grade above cutoff
$Y(x)$	Residual at point x
Z	Regionalised variable, Standard Normal deviate
Z^*	Estimator formed from the sample values
$Z(x)$	Grade at point x

APPENDIX E1

Table of drill hole parameters.

Drill hole	X	Y	Z	Azimuth	Dip	No. of Samples
1	544.2	-772.4	629.0			154
2	538.7	-716.0	638.0			38
3	513.4	-673.6	652.0			79
4	466.4	-641.8	668.0			67
5	498.6	-614.0	658.0			110
6	594.0	-738.8	624.0			90
7	570.0	-656.0	638.0			103
8	494.0	-801.2	624.0			31
9	454.6	-801.8	617.0			108
10	426.0	-746.4	626.0			34
11	425.6	-604.0	678.0			52
12	390.0	-688.7	647.0			39
13	460.2	-569.0	658.0			26
14	426.0	-665.0	657.0			23
15	650.0	-775.8	622.0			96
16	487.2	-768.6	636.0			95
17	470.0	-700.6	645.0			89
18	626.2	-806.4	623.0			88
19	811.4	-645.6	600.0			39
20	664.4	-832.8	619.0			92
21	512.0	-750.6	635.0			98
22	696.2	-854.0	611.0			144
23	540.2	-860.6	611.0			109
24	828.0	-704.0	600.0			41
25	730.0	-879.0	602.0			84
26	589.6	-854.0	617.0			179
27	759.2	-919.6	603.0			69
28	881.0	-745.6	595.0			84
29	764.4	-854.2	607.0			65
30	699.6	-805.4	612.0			77
31	562.0	-807.0	617.0			78
32	942.2	-837.6	570.0			32
33	656.6	-698.2	615.0			103
34	159.8	-1018.0	378.0			0
35	1069.0	-1066.8	547.0			0
36	196.2	-998.0	397.0			0
37	490.0	-894.8	595.0	0.0	70.0	166
38	133.4	-393.0	667.0	62.0	70.0	0
39	0.0	0.0	666.0	180.0	85.0	173
40	9.0	2.0	660.0	0.0	70.0	164
41	414.0	-490.0	637.0	140.0	75.0	0
42	492.4	-586.8	657.0	280.0	70.0	119
43	744.0	-768.0	593.0	180.0	70.0	205
44	-1386.7	279.8	612.0	85.0	44.1	115
45	196.4	0.5	652.0			27

46	97.2	-98.2	622.0	180.0	90.0	73
47	201.8	17.0	652.0			24
48	189.3	-193.0	602.0	29.0	88.7	95
49	303.8	-102.9	620.0	209.0	89.1	112
50	514.1	-89.8	608.0	204.0	89.7	101
51	-1400.7	207.2	596.0	327.0	88.4	48
52	-1003.2	190.0	573.0	89.0	37.9	121
53	-1036.0	118.0	550.0	248.0	89.1	81
54	10.0	-205.3	618.0	21.0	89.3	67
55	383.3	-18.4	608.0	192.0	89.1	100
56	309.4	-294.9	602.0	68.0	88.6	86
57	404.3	-195.7	604.0	108.0	89.2	102
58	506.1	-305.0	590.0	242.0	89.7	77
59	606.5	-191.8	584.0	172.0	89.2	100
60	375.3	-388.8	608.0	234.0	89.2	98
61	605.9	-410.2	574.0	313.0	89.2	99
62	806.3	-390.4	544.0	222.0	89.1	98
63	900.0	-505.9	558.0	166.0	89.5	68
64	537.0	72.3	626.0	21.0	89.5	99
65	636.8	-274.5	558.0	196.0	82.2	83
66	717.5	-147.8	574.0	275.0	89.1	100
67	797.5	-202.7	546.0	258.0	89.6	29
68	896.2	-294.7	524.0	105.0	89.6	57
69	976.9	-400.4	522.0	314.0	89.5	60
70	182.6	20.5	652.0	324.0	89.1	83

X and Y coordinates according to CSI.

APPENDIX E2

Table of analyses available from drill cores

Drill hole	GAM-SPEC	XRF	EDX-CD	F	OPSPEC	ENAA	EDX-PLU
1-33	x						
34							
35							
36							
37	x						
38							
39	x						
40	x						
41							
42	x						
43	x						
44	x	x		x	x	x	x
45	x				x	x	
46	x	x		x	x	x	x
47	x						
48	x	x	x	x	x	x	x
49	x	x	x	x	x	x	x
50	x		x	x	x	x	
51	x	x	x	x	x	x	x
52	x			x	x	x	
53	x			x	x	x	
54	x						
55	x	x	x	x	x	x	x
56	x		x	x	x	x	
57	x		x	x	x	x	
58	x		x	x			
59	x	x	x	x	x	x	x
60	x		x	x	x		
61	x		x	x			
62	x		x	x			
63	x		x	x			
64	x			x			
65	x		x	x			
66	x		x	x			
67	x			x			
68	x		x	x			
69	x		x	x			
70	x		x	x			
Number of samples analysed:							
	5658	614	234	570	107	833	573

APPENDIX E3

List of variables included in the drill core database KVANE

Variable Name	Analytical method	Comment/Laboratory
PR_NR		Sample number
GEOLOGI		Geology code
BH		Drill hole number
AZIMUTH		
DIP		
DYBDE1		Depth to sample top
DYBDE2		Depth to sample bottom
X		Coordinates of the top of each drill core sample according to CSI
Y		
Z		
XTR		Coordinates according to system CSII
YTR		
ZTR		
U_PPM1	GAM-SPEC	Automatic operating gamma-spectrometer or core scanning. RISØ.
TH_PPM1	"	
K_PCT1	"	
ZR_PPM2	XRF	Institute of Petrology, The University of Copenhagen
Y_PPM2	"	
SR_PPM2	"	
RB_PPM2	"	
TH_PPM2	"	
PB_PPM2	"	
GA_PPM2	"	
ZN_PPM2	"	
NB_PPM2	"	
FE_PCT3	EDX-CD	RISØ
RB_PPM3	"	
SR_PPM3	"	

Y_PPM3	EDX-CD	
ZR_PPM3	"	
NB_PPM3	"	
MO_PPM3	"	RISØ
PB_PPM3	"	
TH_PPM3	"	
U_PPM3	"	
F_PCT4	FLOUR	Below detection limit F_PCT4 = -99.0
BE_PPM5	OP-SPEC	Institute of Petrology, The University of Copenhagen
LI_PPM5	"	
NA_PPM6	ENAA	
K_PPM6	"	
SC_PPM6	"	
CR_PPM6	"	
MN_PPM6	"	
FE_PPM6	"	
CO_PPM6	"	
ZN_PPM6	"	
RB_PPM6	"	
ZR_PPM6	"	
SN_PPM6	"	
SB_PPM6	"	
CS_PPM6	"	
BA_PPM6	"	RISØ
LA_PPM6	"	
CE_PPM6	"	
ND_PPM6	"	
SM_PPM6	"	
EU_PPM6	"	
GD_PPM6	"	
TB_PPM6	"	
YB_PPM6	"	
LU_PPM6	"	
HF_PPM6	"	
TA_PPM6	"	
TH_PPM	"	

K_PCT7	EDX-PLU	
CA_PCT7	"	
TI_PCT7	"	
MN_PPM7	"	
FE_PPM7	"	
NI_PPM7	"	
CU_PPM7	"	RISØ
ZN_PPM7	"	
GA_PPM7	"	
SR_PPM7	"	
PB_PPM7	"	

APPENDIX E4

Table of geological coding

Samples from the Kvanefjeld area have been coded according to the geology of the sample. The code consists of three digits:

geology code = ABC

where:

- A defines the primary rock type, i.e. more than 50% of the sample consists of this rock type
- B defines the secondary rock type, if any. The amount of B is less than 50%
- C defines other characteristics associated with the primary rock type.

The following codes are available:

DIGIT	CODE	DEFINITION
A or B	0	Unspecified
	1	MC-lujavrite
	2	Fine-grained lujavrite
	3	Lava or gabbro
	4	Naujaite
	5	Syenite
	6	Anorthosite
C	0	Unspecified
	1	Shearing
	2	Shearing with Nb-minerals
	3	Analcime-steenstrupine vein
	4	Aegirine (concerning lujavrite)
	5	Naujakasite (concerning lujavrite)
	6	Villiaumite
	7	Villiaumite plus naujakasite
	8	Naujakasite/aegirine with steenstrupine vein

APPENDIX E5

Table of batch samples from the Kvanefjeld tunnel

The table gives a full listing of the batch samples taken in the Kvanefjeld tunnel. Some batch samples have been merged to forme composite samples (i.e. 17, 44, 45, 51 and 52).

The rock type of each batch is given by the geology code defined in appendix E4.

Uranium values are given in ppm. The column denoted 'Gamma-spec.' gives the uranium and thorium values obtained by on-site gamma-spectrometry. The columns '3D-estimates' and '3D-std.err.' give the estimates and kriging standard error when the uranium and thorium values are estimated by a three dimensional kriging procedure. For uranium a +1 search area has been used, for thorium a 0 search area (see chap. 5). In both cases an overall semi-vaiogram model was used.

The batch tonnage has been calculated using a rock density of 2.8 tons/m^3 and a fixed tunnel cross section of 9 m^2.

The calculation of the amount of uranium in each batch sample was based on the 3D-kriging estimate of the grade.

Batch no.	centre of batch from tunnel start	Metres above sea level	Tonnage (tons)	Rock type	Gamma-spec.		3D -estimates		3D -std.err.		Kilograms of uranium
					U	Th	U	Th	U	Th	
7	277.9	479.7	129	297	415	1270	401	860	10.6	33.1	51.7
8	285.5	479.9	126	297	360	1320	349	861	16.7	92.0	44.0
9	293.3	480.2	134	297	442	1220	429	820	10.6	37.5	57.5
10	301.2	480.5	136	297	518	995	508	681	10.5	36.5	69.1
11	309.2	480.8	134	297	513	895	424	616	11.6	38.9	56.8
12	317.1	481.1	268	297	386	910	332	724	18.8	64.7	89.0
13	323.7	481.3	131	297	347	1285	425	1219	13.4	45.8	55.7
14	331.4	481.5	219	297	359	1465	404	1206	9.3	33.9	88.5
15	341.1	481.9	134	297	406	1535	518	1631	10.3	35.5	69.4
16	349.1	482.2	136	297	489	1975	461	994	10.2	35.8	62.7
(17a	355.9	482.4	68	297			434	561	12.2	42.8	29.5)
(17b	361.3	482.6	68	297			418	554	12.5	39.4	28.4)
17			136	297	423	870	426	558			57.9
18	368.0	482.8	136	297	442	820	397	551	9.7	30.2	54.0
19	373.4	483.0	136	297	386	775	415	530	10.0	31.8	56.4
20	383.8	483.4	134	297	391	870	380	576	9.9	30.8	50.9
21	391.7	483.7	136	297	434	880	373	562	8.9	28.0	50.7
22	400.0	483.9	139	297	370	670	363	487	9.5	29.6	50.5
23	408.2	484.2	141	297	409	675	440	540	9.0	28.1	62.0
24	416.5	484.5	139	297	605	840	498	513	10.1	32.0	69.2

25	424.8	484.8	139	297	531	790	458	517	10.9	34.7	63.7
26	433.3	485.1	144	207	371	570	328	695	13.7	43.5	47.2
27	441.8	485.4	144	297	307	930	284	740	11.4	35.8	40.9
28	450.2	485.7	136	237	299	1035	221	604	11.4	35.4	30.1
29	458.3	486.0	136	237	422	1310	325	917	12.3	38.6	44.2
30	598.8	491.5	257	207	370	1280	341	655	8.7	30.8	87.6
31	606.6	492.0	136	297	375	1225	367	755	11.1	35.0	49.9
32	612.0	492.4	136	237	330	1260	310	661	10.9	34.1	42.2
33	618.8	492.9	204	237	320	1200	323	618	9.2	29.0	65.9
34	626.9	493.4	204	237	350	1280	304	705	9.1	28.4	62.0
35	633.6	493.8	136	247	330	1595	261	910	10.7	33.6	35.5
36	654.9	495.0	219	129	290	1240	234	617	14.3	46.4	51.2
38	664.9	495.4	282	149	248	686	296	686	12.4	40.0	83.5
39	698.4	495.6	209	297	275	825	243	720	8.8	28.6	50.8
40	706.6	495.9	207	297	290	940	239	707	9.7	33.9	49.5
41	713.4	497.2	136	297	265	815	239	617	10.6	33.7	32.5
42	721.6	497.5	136	297	320	1100	242	548	11.1	34.9	32.9
43	729.6	497.9	129	237	330	1020	145	363	10.6	33.3	18.7
(44a	736.2	498.2	68	237			217	632	13.9	47.4	14.8)
(44b	758.3	499.2	76	237			256	752	13.3	48.8	19.5)
44			144		252	1185	238	695			34.2
(45a	762.6	499.4	141	237			253	637	10.7	33.7	35.7)
(45b	769.6	499.7	71	297			363	743	13.4	50.6	25.8)
45			212		295	1185	290	673			61.4

46	775.2	500.0	212	297	394	1330	374	758	9.5	30.0	79.3
47	786.3	500.6	217	297	447	1335	412	874	8.7	27.2	89.4
48	795.0	501.1	219	237	449	1285	433	974	8.9	27.9	94.8
49	803.7	501.6	219	237	451	1455	439	1035	9.3	31.0	96.1
50	812.4	502.0	219	237	410	1410	431	953	9.1	28.5	94.4
(51a	818.2	502.4	73	297			442	1058	12.9	45.9	32.3)
(51b	824.0	502.9	73	297			361	711	13.1	45.4	26.4)
(51c	832.7	503.9	73	237			407	846	11.9	37.4	29.7)
51			219		394	1110	403	872			88.3
(52a	850.3	505.7	76	297			481	1120	12.8	47.0	36.6)
(52b	859.3	506.6	76	297			497	1195	12.3	38.4	37.8)
(52c	868.3	507.5	76	297			426	1036	12.5	47.0	32.4)
52			227		542	1830	468	1117			106.7
53	874.2	508.1	222	237	457	1690	246	652	9.2	29.3	54.6
Total			7844								2783.5

APPENDIX E6

List of lujavrite samples included in the multivariate study

DRILL HOLE	SAMPLE NUMBER	299	296	295	297
44	44012	x			
	44070		x		
	44080		x		
	44100		x		
	44128		x		
	44180		x		
46	46008			x	
	46012			x	
	46034			x	
	46038			x	
	46050			x	
	46054			x	
	46056			x	
	46058			x	
	46070			x	
	46072			x	
	46074			x	
	46094			x	
	46096			x	
	46146		x		
	46150		x		
48	48142				x
	48160				x
	48162				x
	48168				x
	48170				x
	48176				x
	48180				x
	48182				x
	48186				x
	48190				x

DRILL HOLE	SAMPLE NUMBER	299	296	295	297
48	48192				x
49	49002			x	
	49028			x	
	49030			x	
	49032			x	
	49034			x	
	49036			x	
	49068				x
	49074				x
	49078				x
	49084				x
	49106		x		
	49120		x		
	49130		x		
	49140		x		
	49150		x		
51	51016	x			
	51032	x			
	51040	x			
	51046	x			
	51062	x			
	51070	x			
55	55010	x			
	55050	x			
	55086		x		
	55094		x		
	55110	x			
	55140	x			
59	59050	x			
	59060	x			
	59062	x			
	59070	x			
	59100		x		
	59110		x		
	59130		x		
	59140		x		

DRILL HOLE	SAMPLE NUMBER	299	296	295	297
59	59150		x		
TOTAL NUMBER OF SAMPLES:		15	19	19	15

Geology codes according to GGU-system (appendix E4):

299	Arfvedsonite lujavrite
296	Arfvedsonite lujavrite plus villiaumite
295	Naujakasite lujavrite
297	Naujakasite lujavrite plus villiaumite

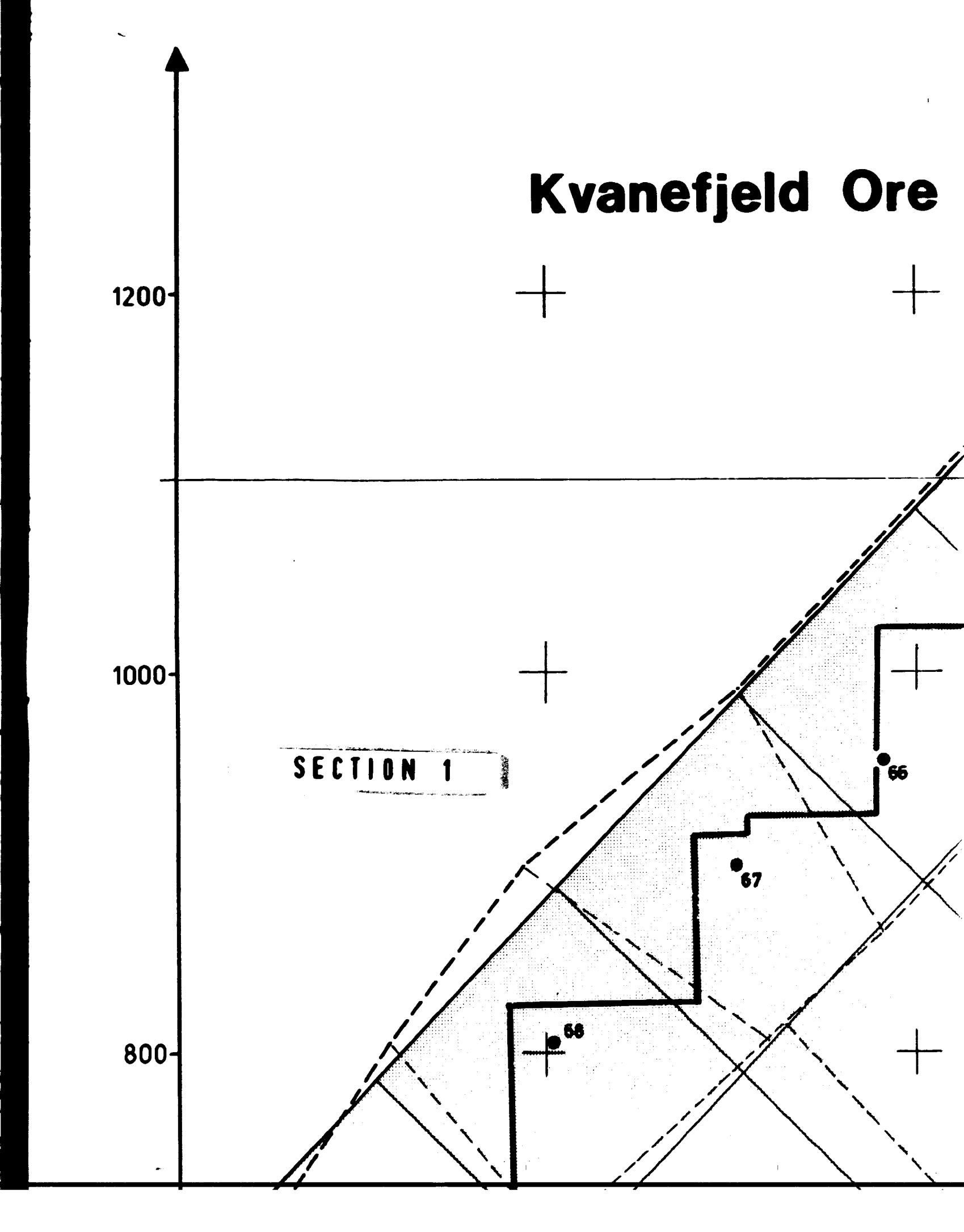
Kvanefjeld Ore
1200
1000
800
SECTION 1
66
67
68

re Reserve Study (block pattern)

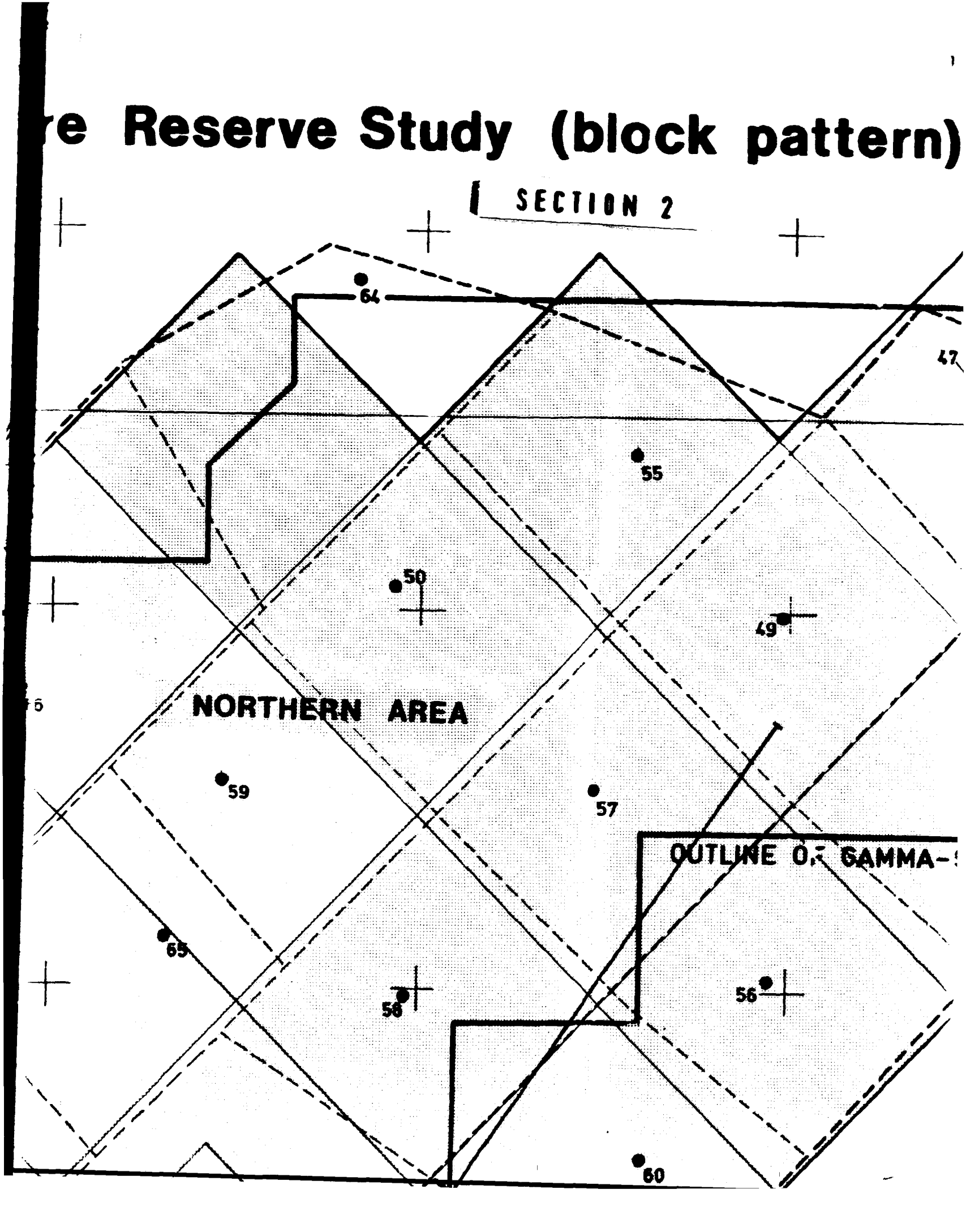

PLATE I

Fl. Lund Clausen:

A geostatistical study of the uranium deposit at Kvanefjeld, The Ilímaussaq intrusion, South Greenland. 1982.

k pattern)

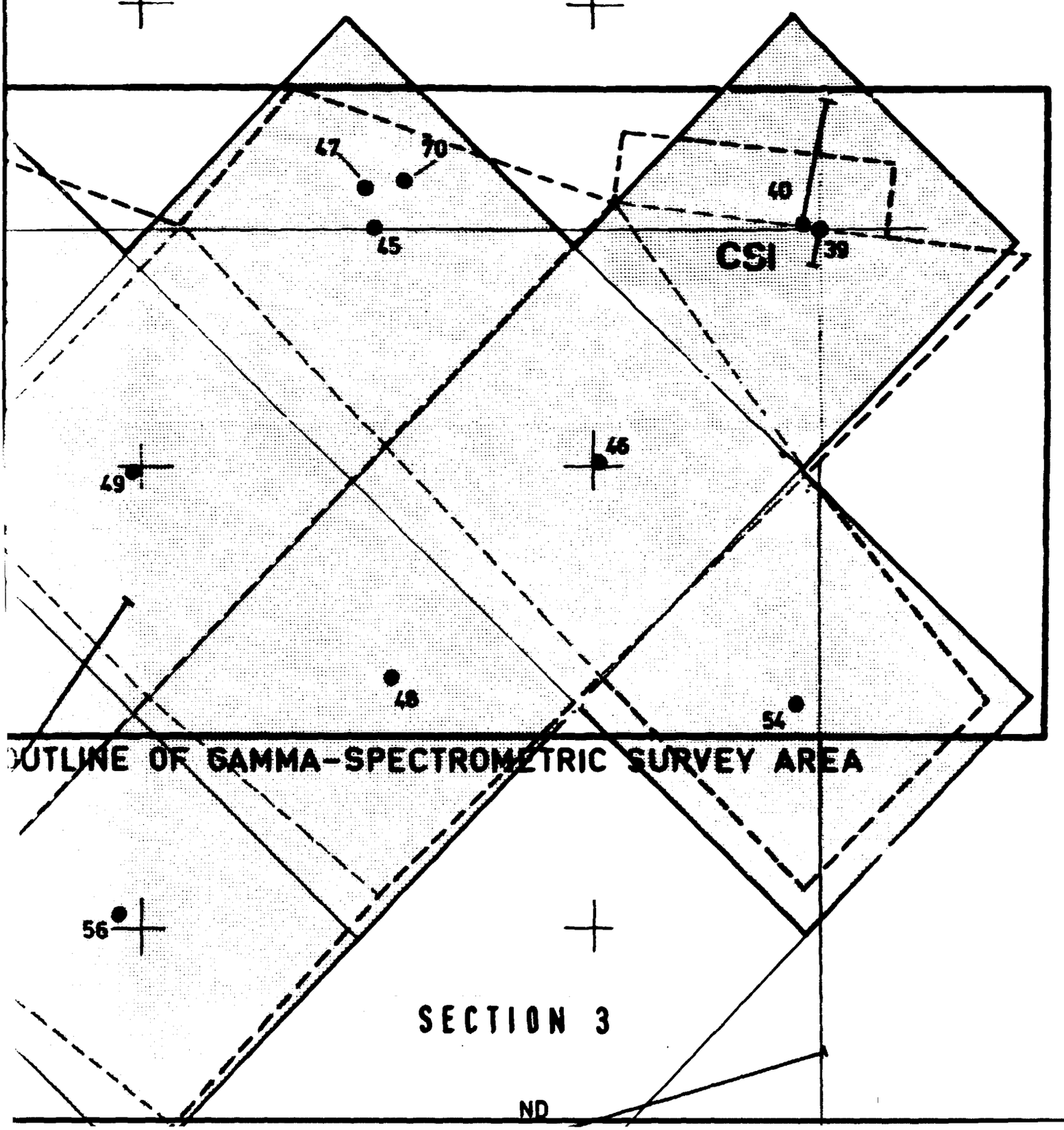

OUTLINE OF GAMMA-SPECTROMETRIC SURVEY AREA

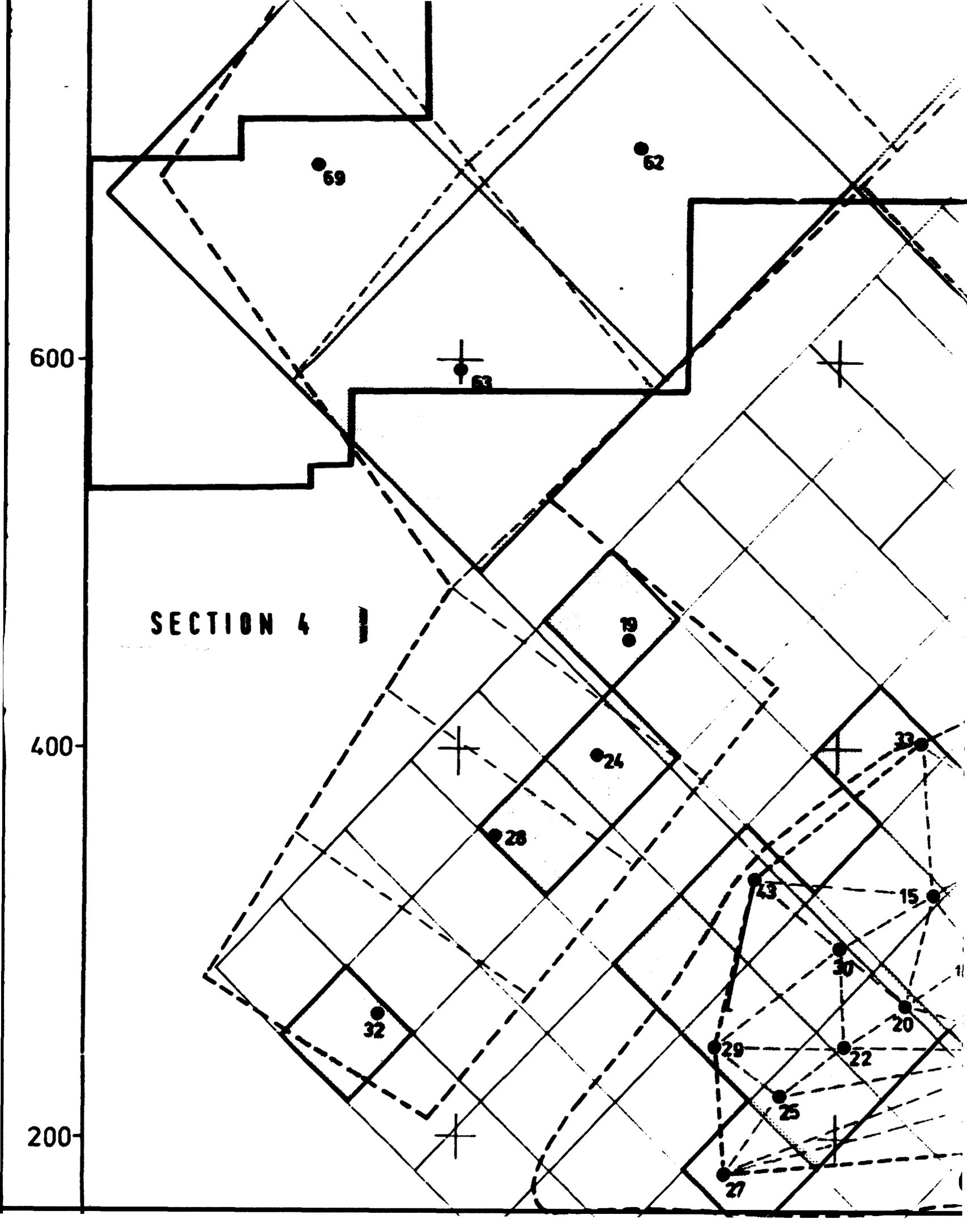
600
400
200
SECTION 4
69
62
63
19
24
28
32
33
43
15
30
20
29
22
25
27

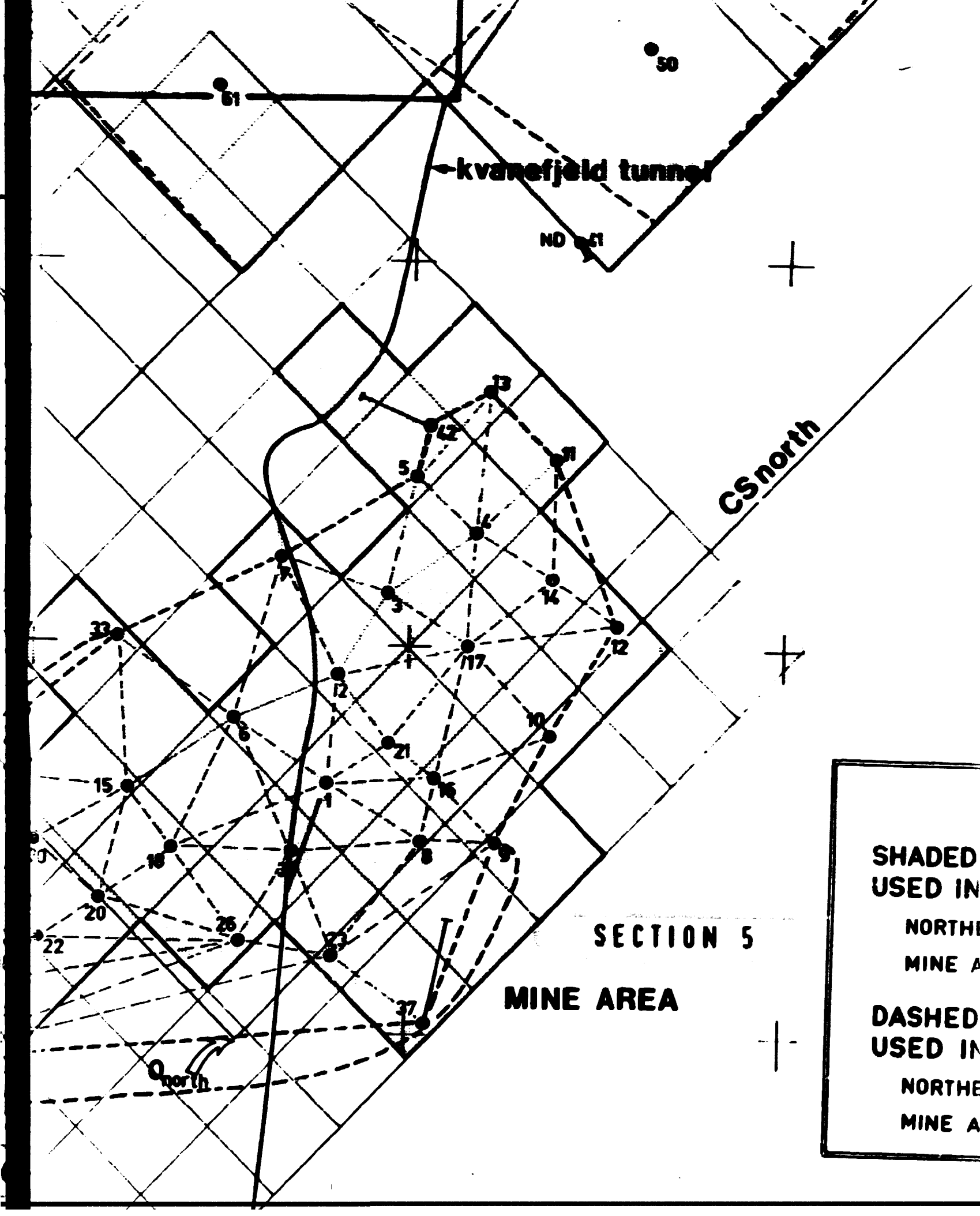
50
61
kvanefjeld tunnel
ND 51
CSnorth
33
15
16
20
22
26
37
SECTION 5
MINE AREA
SHADED
USED IN
NORTHE
MINE A
DASHED
USED IN
NORTHE
MINE A

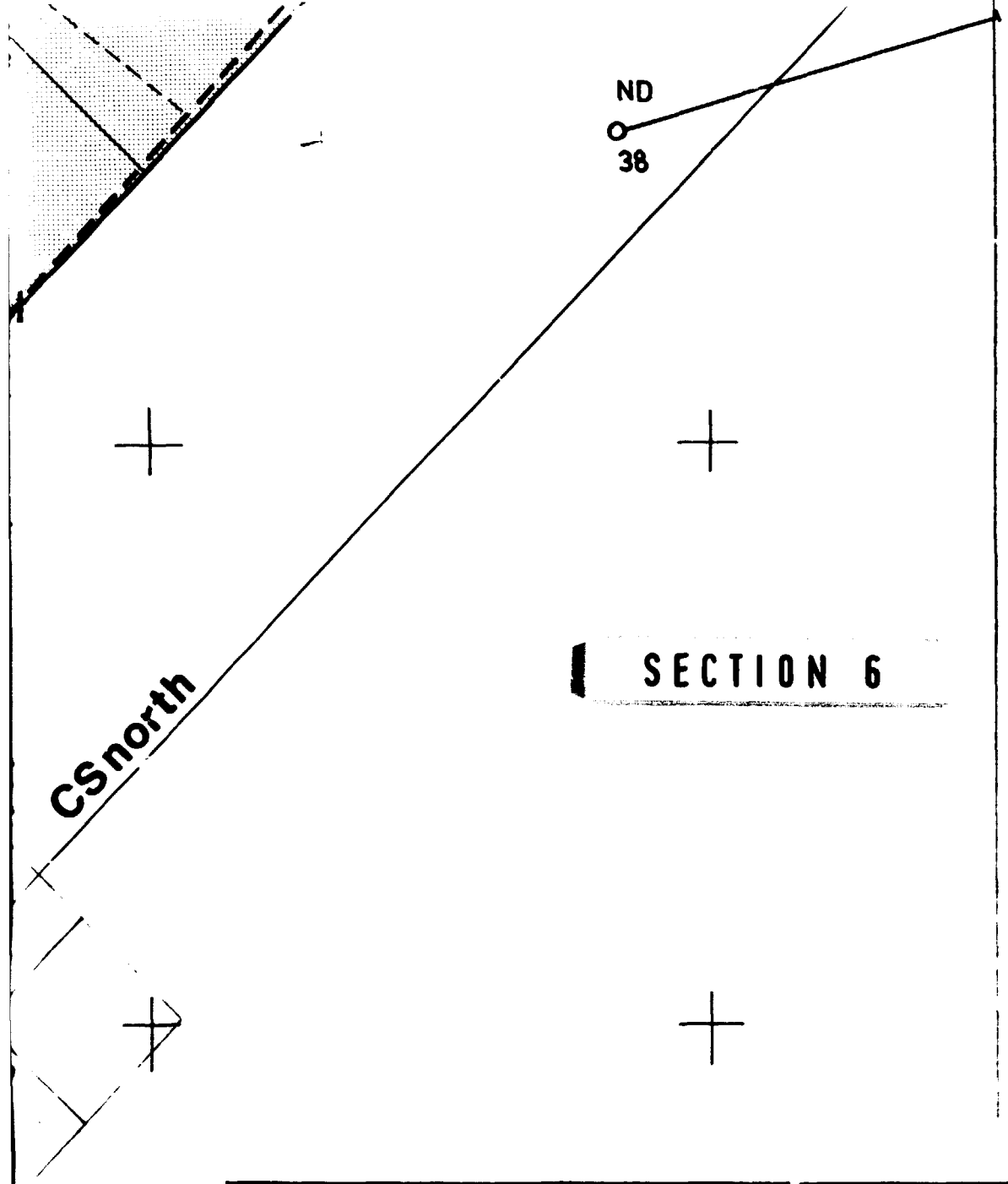

PLATE I

1:2000

SHADED AREAS INDICATE BLOCK PATTERNS USED IN GEOSTATISTICAL CALCULATIONS

NORTHERN AREA BLOCKS : 140 x 140 m.

MINE AREA BLOCKS : 50 x 50 m.

DASHED LINES INDICATE BLOCK PATTERNS USED IN CONVENTIONAL CALCULATIONS

NORTHERN AREA : Nyegaard et al. (1977)

MINE AREA : Sørensen et al. (1974)

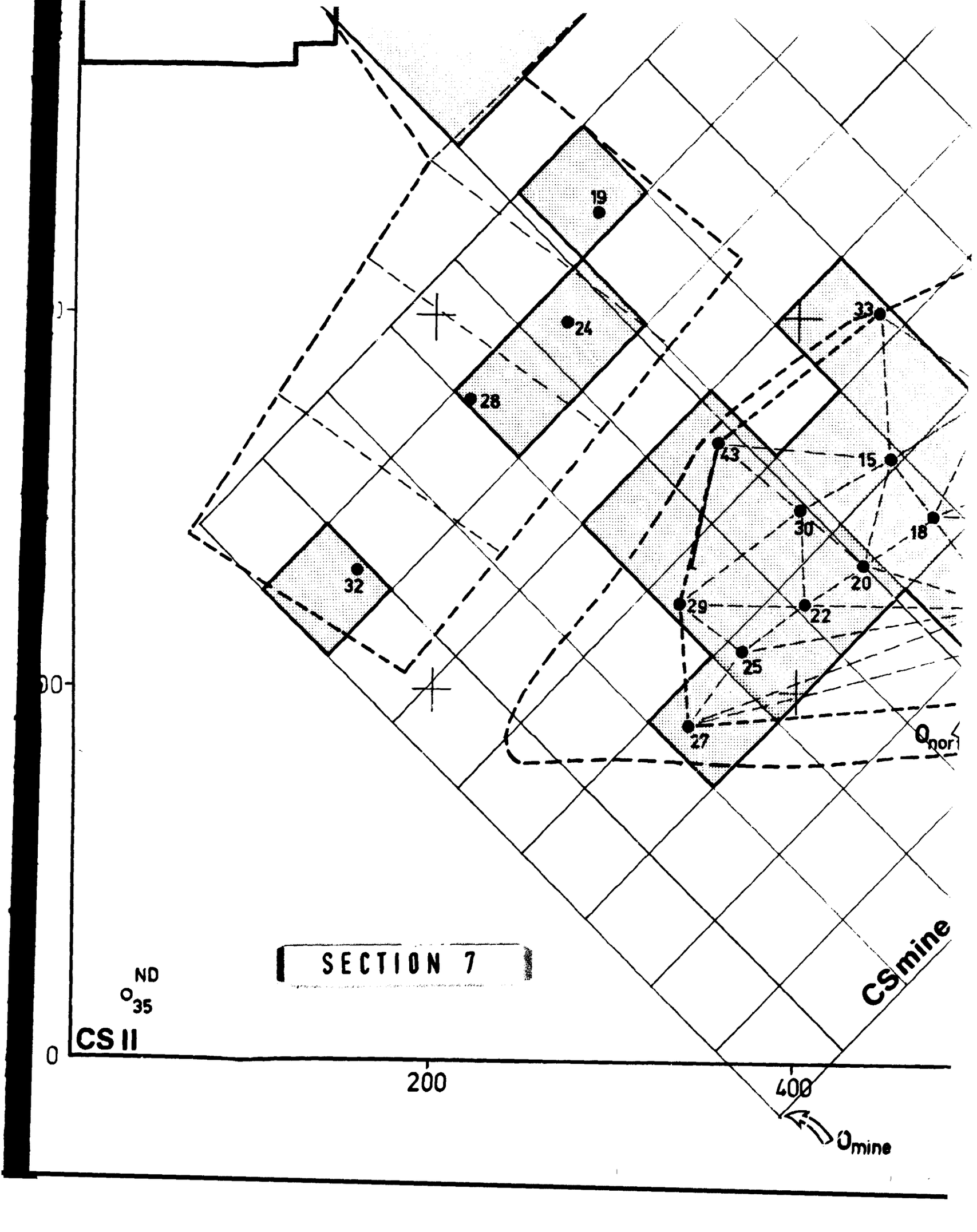
19
24
28
33
43
15
30
18
32
20
29
22
25
27
Q_{nor}
SECTION 7
ND
O_{35}
CS II
CS mine
Q_{mine}
0
200
400

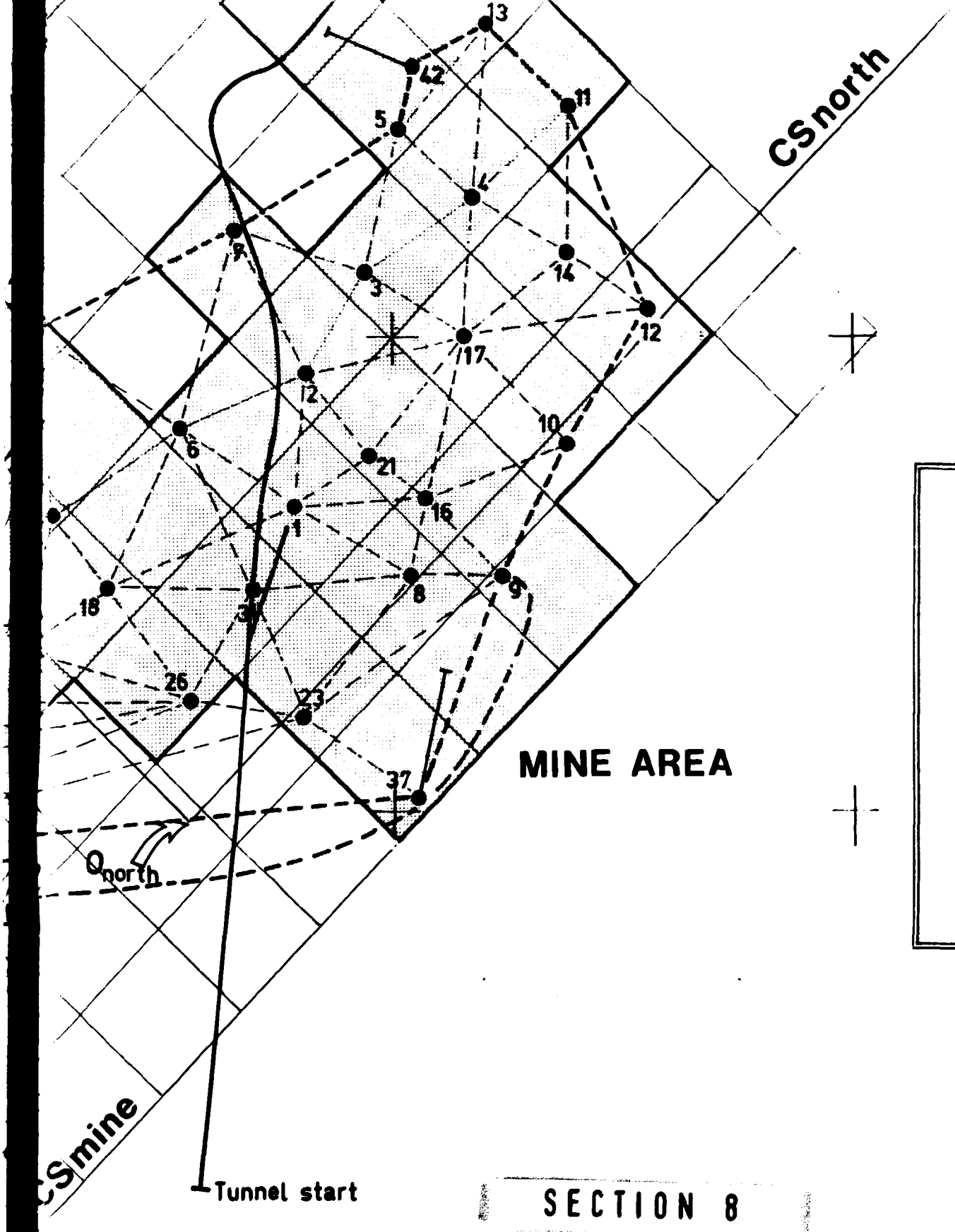

SHADED AREAS
USED IN GEOS
NORTHERN ARE
MINE AREA BL

DASHED LINES
USED IN CONV
NORTHERN AR
MINE AREA

ND
36

SECTION 8

600

800

ine

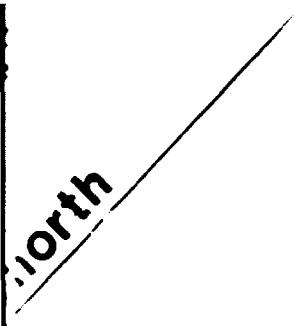

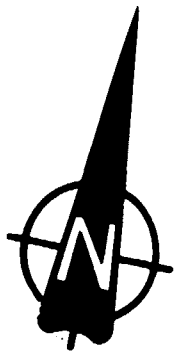

PLATE 1

1:2000

SHADED AREAS INDICATE BLOCK PATTERNS USED IN GEOSTATISTICAL CALCULATIONS

NORTHERN AREA BLOCKS : 140 x 140 m.

MINE AREA BLOCKS : 50 x 50 m.

DASHED LINES INDICATE BLOCK PATTERNS USED IN CONVENTIONAL CALCULATIONS

NORTHERN AREA : Nyegaard et al. (1977)

MINE AREA : Sørensen et al. (1974)

ND
36

ND
34

SECTION 9

800

1000

Compiled by: Fl. Lund Clausen 1982